Novel Functions for the BAF180 Tumour Suppressor: Insights from Mammalian and Yeast Systems

Peter Moore Brownlee

Thesis submitted for the degree of Doctor of Philosophy

University of Sussex

May 2014

Statement

I hereby declare that this thesis has not been and will not be, submitted in whole or in part to another University for the award of any other degree.

Signature:……

Acknowledgments

I would first like to thank my supervisor, Jessica A. Downs, who has unwaveringly supported me for the duration of this work. I am also extremely grateful to Anna L. Chambers, who contributed substantially to the experimental work presented here, and with whom I worked closely. I owe much to Anna's motivation and efficiency in the lab as both a colleague and a friend. My second supervisor, Matt Neale, has also provided support and useful discussion throughout. I thank Ross Cloney, who performed the FISH analyses, Penny Jeggo, Alessandro Bianchi, Andreas Kakarougkas and Amani Ishmail for advice and support, and Suzanna Hopkins for creating the stable shRNA U2OS cell lines. We thank John Spencer and members of the Spencer lab for providing HDAC inhibitors and information, and Peter Schmidt and Alice Shia for providing breast cancer cell line material. Finally, I would like to thank Sarah Phelps, Hanan Al'Atwi, and Sarah Pinder for help and friendship.

This work was funded by Cancer Research UK

Publications

Brownlee, P. M., Chambers, A. L., Cloney, R., Bianchi, A., Downs, J. A. BAF180 Promotes Cohesion and Prevents Genome Instability and Aneuploidy. *Cell Rep.* **6**: 973-981 (2014)

Brownlee, P. M., Chambers, A. L., Oliver, A. W., Downs, J. A. Cancer and the bromodomains of BAF180. *Biochem. Soc. Trans.* **40**: 364-369 (2012)

Chambers, A. L., **Brownlee, P. M**., Durley, S. C., Beacham, T., Kent, N. A., Downs, J. A. The two different isoforms of the RSC chromatin remodeling complex play distinct roles in DNA damage responses. *PLoS One*. **7**: e32016 (2012)

University of Sussex

Peter Moore Brownlee

Doctor of Philosophy (Genome Damage and Stability)

Novel Functions for the BAF180 Tumour Suppressor: Insights from Mammalian and Yeast Systems

Summary

Genomic DNA is compacted into a protein-DNA complex known as chromatin, which regulates diverse cellular processes including transcription, DNA replication, recombination, DNA repair and the maintenance of genome integrity. The structure and activity of chromatin is regulated by DNA sequences, histone variants, post-translational histone modifications and chromatin remodelling complexes. Chromatin remodelling complexes are multi-subunit entities that contain a single core catalytic ATPase subunit able to generate an array of nucleosome-related outputs. Importantly, recent studies have revealed that genes of the SWI/SNF family of chromatin remodeling complexes are frequently mutated in diverse cancers; however, their functional contributions in tumourigenesis are largely unclear.

This work is comprised of four major results chapters, examining the roles of targeting subunits of the RSC SWI/SNF complex in budding yeast and the homologous BAF180 tumour suppressor protein in mammalian cells. We identify novel functions for these proteins that are directly relevant to tumourigenesis. In the first section we explored the contributions of the two isoforms of the RSC SWI/SNF complex in DNA repair. We found that the two isoforms provide both overlapping and distinct functions in this process. In the second section we identify a novel function for BAF180 in promoting centromeric sister chromatid cohesion. Importantly, this defect was transcription-independent and represents a paradigm shift in the field of chromatin remodeling and cancer. In the third section we show that *PBRM1* missense mutations identified in cancer samples specifically impair a cohesion-related subset of functions when expressed in budding yeast. Moreover, these mutations completely ablated centromeric cohesion in human cells. In the final section we report the findings that novel HDAC inhibitors, which constitute a promising class of anticancer drugs, selectively sensitize cells lacking BAF180. These significant results suggest that HDAC inhibitors could be important tools for the treatment of BAF180-deficient tumours.

Table of contents

Title……i
Statement……..ii
Acknowledgments and publications……iii
Summary……..iv
Table of contents……v
List of tables and figures…..……vi
CHAPTER 1: INTRODUCTION……1
1.1. Chromatin structure and organization…….....1
1.2. DNA double-strand break repair……...31
1.3. Cohesin……..56
1.4. The BAF180 tumour suppressor……85
1.5. Synthetic lethality and HDAC inhibitors in cancer therapy……....91
1.6. Thesis experimental research goals……97
CHAPTER 2: MATERIALS AND METHODS……...98
2.1. DNA manipulations……..98
2.2. Antibodies and immunoblotting……..99
2.3. Yeast experiments……100
2.4. Mammalian cell experiments……104
CHAPTER 3: RSC1 AND RSC2 DIFFERENTIALLY MEDIATE DNA DAMAGE RESPONSES……109
3.1. Results……109
3.2. Discussion……...126
CHAPTER 4: BAF180 PROMOTES COHESION AND PREVENTS GENOME INSTABILITY AND ANEUPLOIDY……...130
4.1. Results……130
4.2. Discussion……...154
CHAPTER 5: MUTATIONS IDENTIFIED IN BAF180 FROM CANCER SAMPLES IMPAIR COHESIN-DEPENDENT FUNCTIONS IN YEAST AND MAMMALS…….163
5.1. Results……163
5.2. Discussion……...172
CHAPTER 6: NOVEL HDAC INHIBITORS SENSITIZE CELLS LACKING BAF180...177
6.1. Results……177
6.2. Discussion……...181
APPENDIX I: HDAC INHIBITOR VIABILITY ASSAYS……186
REFERENCES……190

List of tables and figures

Tables

Table 1.1. Subunit composition of RSC and SWI/SNF complexes……..12
Table 1.2. Gene and protein names of human SWI/SNF subunits……...19
Table 1.3. Functional domains and properties of cohesin proteins……..57
Table 2.1. Plasmids used in this study……..98
Table 2.2. Primers used in this study……99
Table 2.3. Yeast strains used in this study……100
Table 3.1. Summary of phenotypes associated with loss of *RSC1* and *RSC2*…….126
Table 4.1. Average number and range per cell of chromosomal aberrations in mESCs following MMC exposure……154
Table 5.1. Analysis of cancer-associated in-frame missense mutations found in *PBRM1*……...165
Table 6.1. Profile of HDAC inhibitors and their effects on BAF180 +/+ and BAF180 -/- mESCs……...182

Figures

Figure 1.1. Domain organization of the RSC subunits Rsc1, Rsc2 and Rsc4……14
Figure 1.2. BAF180 is homologous to a fusion of the RSC subunits Rsc1, Rsc2 and Rsc4, containing 6 homologous bromodomains and 2 bromo-adjacent homology domains……86
Figure 3.1. Rsc1 and Rsc2 define two separate isoforms of the RSC complex……...111
Figure 3.2. Neither Rsc1 nor Rsc2 are required for DNA damage checkpoint responses……113
Figure 3.3. Both Rsc1 and Rsc2 contribute to wild-type levels of NHEJ and show a similar spectrum of repair junctions……..115
Figure 3.4. Rsc1 and Rsc2 have distinct roles in mediating DNA damage hypersensitivity……118
Figure 3.5. Loss of Rsc1 function, but not that of Rsc2, abolishes DSB-dependent nucleosome sliding at an HO site within the *LEU2* gene……..119
Figure 3.6. Rsc1 domains can functionally compensate for Rsc2 domains in DNA damage survival assays……121

Figure 3.7. Replacing the BAH domain of Rsc2 with the Rsc1 BAH domain allows Rsc2 to remodel chromatin at DNA DSB……..123
Figure 3.8. Cells lacking *RSC2* display elevated rates of marker loss by unequal sister chromatid exchange and direct-repeat recombination…….125
Figure 4.1. BAF180 promotes centromeric sister chromatid cohesion in mESCs……132
Figure 4.2. siRNA-mediated depletion of BAF180 in 1BR-hTERT cells results in defective centromeric cohesion……133
Figure 4.3. siRNA-mediated depletion of BAF180 in 1BR-hTERT cells does not cause defective cohesion at chromosome arms……135
Figure 4.4. siRNA-mediated depletion of BAF180 in 1BR-hTERT cells does not cause defective cohesion at telomeres……...137
Figure 4.5. Stable shBAF180-depleted U2OS cells show defective centromeric cohesion……138
Figure 4.6. Depletion of BAF180 and SA2 results in a comparable defect in centromeric cohesion……139
Figure 4.7. BAF180 is not required for transcription of cohesin genes and has tissue-specific roles in regulating p53-dependent p21 transcription……...141
Figure 4.8. The cohesion defect in BAF180-depleted U2OS cells is not due to reduced levels of total chromatin-bound cohesin……..144
Figure 4.9. siRNA-mediated depletion of BAF180 in MRC5CV1 cells leads to altered chromosome morphology……...145
Figure 4.10. Loss of BAF180 results in aneuploidy, increased frequencies of micronuclei and abnormal anaphase events……147
Figure 4.11. Loss of BAF180 leads to hypersensitivity to MMC……..150
Figure 4.12. BAF180-deficient mESC and U2OS cells show increased frequencies of structural chromosomal aberrations after treatment with MMC.....152
Figure 4.13. BAF180-deficient mESCs show increased frequencies of micronuclei and dynamic chromosomal instability following treatment with MMC……..153
Figure 4.14. Model describing the consequences of BAF180 inactivation and the drive towards tumourigenesis……...156
Figure 5.1. Conservation and expression of BAF180 renal cell carcinoma missense mutations in yeast Rsc2……166
Figure 5.2. BAF180 missense cancer mutations expressed in yeast do not compromise a transcription-related subset of Rsc2 functions……168
Figure 5.3. BAF180 missense cancer mutations expressed in yeast result in impaired cohesin-dependent Rsc2 functions……..170

Figure 5.4. Complementation of BAF180-depleted U2OS cells with BAF180 missense cancer mutations……171
Figure 5.5. BAF180 missense mutations expressed in human cells result in a defect in centromeric cohesion……173
Figure 6.1. BAF180 protein expression is lost or reduced in breast cancer cells at high frequency……..178
Figure 6.2. Novel HDAC inhibitors specifically sensitize BAF180 -/- mESCs……...180

CHAPTER 1: INTRODUCTION

1.1. Chromatin structure and organization

Genomic DNA is compacted into a protein-DNA complex known as chromatin. 147bp of DNA tightly wrapped in ~1.7 superhelical turns around an octomeric core of two histone H2A-H2B dimers and a H3-H4 tetramer constitutes the canonical nucleosome, the basic unit of chromatin (Richmond & Davey 2003). In yeast, nucleosomes are separated by ~20bp of linker DNA, and the primary chromatin structure of a polynucleosomal tract resembles 'beads on a string' when observed using electron microscopy. The linker histone H1 stabilizes further condensation of nucleosomes into 30nm chromatin fibres, at least in vitro (Horn & Peterson 2002). The regulation of higher order chromatin structure beyond the level of the 30nm fibre through to the level of the mitotic chromosome is largely unknown. Compaction of genomic DNA into chromatin regulates access of DNA-binding proteins to nucleosomal DNA (Clapier & Cairns 2009). DNA transactions including transcription, replication, recombination, repair and the maintenance of genome integrity are consequently regulated by nucleosomes and chromatin. In this section we consider the major factors that specify and organize chromatin structure, including DNA sequence, histone variants, post-translational histone modifications and chromatin remodelling complexes.

1.1.1. DNA sequences

DNA sequences strongly determine the *in vivo* positioning of nucleosomes and provide binding sites for specific DNA-binding proteins (Rando & Chang 2009). The DNA sequence-dependent positioning of nucleosomes is particularly important for sculpting the chromatin structure of a gene to facilitate its regulation. A typical yeast promoter contains a nucleosome-free region (NFR) upstream of the transcription start site (TSS), which contains poly-A and poly-T tracts that intrinsically repel nucleosomes (Rando & Chang 2009). The promoter NFR is the site at which the majority of transcription factors bind and is flanked by two well-positioned nucleosomes, termed +1 and -1. NFRs also frequently occur at the 3' termination site. The coding regions of genes typically contain DNA sequences that favour the positioning of nucleosomes, such as AT-rich dinucleotides, particularly around the +1, +2 and +3 nucleosomes (Rando & Chang 2009). In mammalian cells NFRs also occur upstream of TSSs, but in contrast to yeast genes, additional nucleosome-depleted, DNAase hypersensitive sites (DHS)

occur that provide further transcriptional control. Enhancer DHSs are often found up to hundreds of kilobases distal to TSSs, and insulator DHSs function to disrupt communications between promoters and enhancers (Rando & Chang 2009).

Another specialised region of chromatin in which DNA sequence plays an important regulatory role is at the centromere. The centromere is a unique region of the chromosome that mediates the attachment of chromosomes via the kinetochore to the mitotic spindle and is essential for chromosome segregation. In budding yeast the centromere consists of three conserved sequences that together span 116-120bp (Verdaasdonk & Bloom 2011). CDEI is a non-essential 8bp palindromic sequence that is required for high-fidelity chromosome segregation and serves as a binding site for the centromere protein and transcription factor Cbf1 (Hemmerich *et al.* 2000). CDEII is an essential AT-rich sequence 78-86bp in length that is required for chromosome segregation. CDEIII is an imperfect 26bp palindromic sequence to which the four-protein CBF3 complex binds, a step that is essential for the subsequent assembly of the ~60 unique proteins that constitute the kinetochore (Lechner & Carbon 1991, Doheny *et al.* 1993, Strunnikov *et al.* 1995, McAinsh *et al.* 2003, Cohen *et al.* 2008). In contrast, human centromeres are substantially larger (up to 5Mb in length) and more complex owing to the presence of large tracts of repetitive 171-bp α-satellite sequences (Verdaasdonk & Bloom 2011). In addition to their repetitive occurrence, the similarity between α-satellite sequences has made the assignment of centromere competency to individual sequences difficult.

1.1.2. Histone variants

The core histones H2A, H2B, H3 and H4 all share a common structural architecture of a core domain, which is composed of three α-helices connected by short loops, and an unstructured N-terminal tail domain (Luger *et al.* 1997). The tetramer of two H3-H4 dimers is formed through a strong 4-helix bundle (4-HB) between the two H3 molecules along the H3-H4 tetramer. Additionally, the C-terminal docking domain of H2A interacts with H3 and H4, and L1 loops from each H2A molecule interact to stabilize the association of the two H2A-H2B dimers within the nucleosome (Luger *et al.* 1997, Bönisch & Hake 2012). Histone variants differ from canonical histones in their primary structure and expression timing. They are incorporated to create specialized nucleosomes that provide further levels of chromatin regulation. Three major histone variants will be considered here: H2A.Z, which is implicated in transcription, DNA repair, heterochromatin formation and chromosome segregation, H2A.X, which has a

fundamental role in the DNA damage response, and Cse4 (CENPA in vertebrates), which is required for the formation of a fully functional kinetochore at the centromere.

H2A.Z

H2A.Z is ~60% identical to canonical H2A in any one species and is essential in many organisms but not in *S. cerevisiae* or *S. pombe*, in which H2A.Z deletion leads to a severe growth phenotype (Zlatanova & Thakar 2008, Jackson & Gorovsky 2000, Carr *et al.* 1994, Bönisch & Hake 2012). The C-terminus of canonical H2A is an important regulatory domain for the protein because it occurs at the DNA entry/exit site of the nucleosome (Bönisch & Hake 2012). The C-terminus harbours an acidic patch that interacts with DNA, the linker histone H1, and the H4 N-terminal tail; the latter two of which are involved in establishing higher order chromatin structure. H2A.Z contains an extended acidic patch that alters the behaviour of the protein and confers unique properties (Bönisch & Hake 2012). The M6 region of the H2A.Z C-terminus is an important binding site for the chromatin remodelling complex SWR1, which exchanges H2A-H2B dimers for free H2A.Z-H2B dimers (Luk *et al.* 2010). The extended acidic patch of H2A.Z also fosters the formation of a more compact secondary chromatin structure due to stronger H4-H2A.Z inter-nucleosomal electrostatic interactions. Interestingly, the heterochromatin-associated protein HP1α preferentially binds highly condensed H2A.Z-containing chromatin and further enhances intrafibre folding (Fan *et al.* 2004). H2A.Z is present at centromeres and is likely to have important roles in organizing centromere structure and function (Greaves *et al.* 2007). H2A.Z also occurs in +1 and -1 nucleosomes at promoters in plants, mammals and in *S. cerevisiae,* as well as at enhancers and insulators in mammalian cells (Bönisch & Hake 2012). H2A.Z incorporation at promoters is known to have both repressive and activating roles in transcription due to its ability to alter nucleosome mobility and positioning. The incorporation of H2A.Z into euchromatin forms a boundary to adjacent heterochromatin by antagonizing the spread of Sir-dependent silencing (Bönisch & Hake 2012)

H2A.X has a specific role in the DNA damage response (DDR)

The minor histone variant H2A.X is rapidly phosphorylated at S129 across ~50kb either side of a DNA DSB in *S. cerevisiae* and S139 for several Mb in *H. sapiens* (Tsaber & Haber 2013). This phosphorylation is an early event in the DDR and is necessary for DNA damage checkpoint activation, HR and NHEJ. The role of H2A.X phosphorylation in these processes will be discussed in more detail in the DNA repair pathways section.

Cse4 (human CENPA) is a centromere-specific H3 variant

The H3 variant Cse4, known as CENPA in human cells, is unique to the centromere and is essential for recruiting kinetochore components (Van Hooser *et al.* 2001). Both canonical H3 and CENPA histones contain a histone fold domain in the N-terminus that consists of four α-helices termed N1, α1, α2 and α3. The loop between α1 and α2 in CENPA harbours the CENPA-targeting domain (CATD) that is required for centromere targeting and function (Black *et al.* 2004, Black *et al.* 2007). An interaction between the CATD and the CENPA chaperone HJURP is required for the deposition of CENPA during early G1 (Jansen *et al.* 2007, Foltz *et al.* 2009, Dunleavy *et al.* 2009). HJURP recruitment requires the Mis18 complex, which is recruited to centromeres during telophase (Barnhart *et al.* 2011, Moree *et al.* 2011). The CATD also serves as a docking site in conjunction with acidic patches on H2A and H2B for CENPN (Guse *et al.* 2011, Kato *et al.* 2013). The C-terminus of CENPA serves as a binding site for CENPC, which functions with CENPN to recruit other kinetochore components (Carroll *et al.* 2009, Carroll *et al.* 2010). CENPB also contributes to kinetochore integrity and binds directly to mammalian centromere repeats. This binding is stabilized via interaction with the N-terminus of CENPA (Fachinetti *et al.* 2013). The N1 α-helical domain of CENPA is shorter than that of H3, and CENPA-containing nucleosomes are wrapped by only 121bp of DNA and therefore protect less DNA (Hasson *et al.* 2013).

In budding yeast a single Cse4 nucleosome forms the core of a point centromere, whilst regional centromeres found in mammalian cells contain multiple CENPA nucleosomes interspersed with canonical nucleosomes (Furuyama and Biggins 2007, Blower *et al.* 2002). CENPA-H4 tetrasomes are structurally distinct from H3-H4 tetrasomes in that they are more rigid, and CENPA nucleosomes are more prone to unwrapping and releasing H2A-H2B dimers than canonical nucleosomes (Black *et al.* 2004, Sekulic *et al.* 2010, Conde e Silva *et al.* 2007). *Drosophila* and human CENPA nucleosomes also have reduced height relative to H3 nucleosomes, and the height varies with the cell cycle (Dalal *et al.* 2007, Dimitriadis *et al.* 2010, Bui *et al.* 2012). This height difference forms the basis for the proposed existence of alternative CENPA nucleosome structures, including hemisomes (half-nucleosomes). However, recent reports strongly support the idea that CENPA-containing nucleosomes are indeed homotypic octamers (with two CENPA proteins) (Miell *et al.* 2013, Zhang *et al.* 2012, Padeganeh *et al.* 2013, Catania & Allshire 2014).

CENPA specifies regional centromeres in higher organisms

Fascinating recent studies have shed some light on how complex regional centromeres found in higher organisms are specified and assembled. Unlike budding yeast point centromeres, in which specific DNA sequences are sufficient to initiate kinetochore assembly, the repetitive DNA sequences found at the centromeres of higher organisms display a lack of common features. Thus, it has been suggested that regional centromeres are largely specified epigenetically (Catania & Allshire 2014). Deletion of a 127kb DNA sequence containing the centromere of chromosome Z in DT40 cells initiated the formation of neocentromeres that retained the Z-chromosome (Shang *et al.* 2013). Peaks of CENPA at neocentromeres did not preferentially occur in association with repetitive DNA sequences, and predominantly arose flanking the original Z centromere. This suggests that residual CENPA at these sites dictates the seeding of neocentromeres. Artificial tethering of CID (*Drosophila* CENPA) to DNA recruited kinetochore components and mediated microtubule association (Mendiburo *et al.* 2011), suggesting that CENPA alone is sufficient to direct kinetochore assembly. In addition, tethering of HJURP in human cells led to CENPA deposition and kinetochore assembly (Barnhart *et al.* 2011).

In *Drospohila* and *S. pombe* centromere formation requires the presence of heterochromatin (Folco *et al.* 2008, Kagansky *et al.* 2009, Olszack *et al.* 2011). In contrast, neocentromere formation does not appear to rely on the presence of methylated H3K9 in DT40 (Shang *et al.* 2013), or HP1 in *C. elegans* (Gassman *et al.* 2012, Yuen *et al.* 2011), suggesting that centromere formation in these organisms is heterochromatin-independent. Instead, CENPA deposition might rely on the activity of factors involved in histone deacetylation, chromatin remodelling, replication initiation and DNA repair, which reside in heterochromatin at high density (Grewal 2010, Catania & Allshire 2014). Interestingly, forced induction of dicentric chromosomes in *S. pombe* leads to inactivation of one of the centromeres (Sato *et al.* 2012). This was accompanied by loss of CENPA and the engulfment of the intact centromeric chromatin by flanking heterochromatin, which prevented subsequent centromere activation. These data indicate that a context-dependent interplay exists between regions of CENPA chromatin and flanking heterochromatin. This appears to determine the influence of heterochromatin on CENPA and kinetochore assembly (Catania & Allshire 2014).

1.1.3. Histone post-translational modifications (PTMs)

Recent intense research has focused on identifying and mapping an ever-growing, bewildering array of histone post-translational modifications. Functional characterization of PTMs has led to their implication in various all chromatin-templated processes, particularly transcription, DNA repair, and genome stability. Importantly, factors responsible for performing or recognising PTMs are often misregulated in cancer. PTMs predominantly occur on histone N-terminal tails and affect chromatin structure and regulation in two major ways. First, they can alter nucleosomal net charges that lead to changes in histone-DNA and internucleosomal contacts. Second, they serve as recognition sites for various chromatin-binding factors that influence downstream processes (Musselman *et al.* 2012). PTMs are thought to constitute a 'histone code' that is read in a combinatorial manner by such effector proteins, leading to a tailored array of outputs (Jenuwein & Allis 2001, Strahl & Allis 2000). In this section an overview of the diversity of currently known PTMs will be given, with a focus on methylation, acetylation and phosphorylation modifications and their roles in transcription and mitosis. A more detailed overview of PTMs involved in the DNA damage response is provided in the DNA repair pathways section.

Histone methylation

Histone methylation occurs on lysine and arginine residues, which can be mono- di- or trimethylated. Methylation does not alter the net charge of the residue but alters its size and hydrophobic properties. Canonical methylated lysine residues include K4, K9, K26, K27, K36 and K79 of H3, K20 of H4, and K26 of H1 (Musselman *et al.* 2012). Proteins that bind methyllysine residues typically do so via an aromatic cage that contains two to four aromatic residues. The composition of residues that constitute the cage and the size of the pocket determine the specificity of the protein for the mono- di- or trimethylated state of the lysine. Protein modules that are known to recognise methyllysine include ATRX-DNMT3-DNMT3L (ADD), ankyrin, bromo-adjacent homology (BAH), chromobarrel, chromodomain, double chromodomain, malignant brain tumour (MBT), plant homeodomain (PHD), Pro-Trp-Trp-Pro (PWWP), tandem tudour domain (TTD), Tudour, WD40 and the zinc finger CW (zf-CW) (Musselman *et al.* 2012). Some 'readers' of methyllysine are highly specific to a certain lysine residue, whilst others are selective for a particular methylation state (mono- di- or tri-), and are therefore promiscuous binders.

Lysine tri-methylation at the 5' end of actively transcribed genes is conserved from yeast to higher eukaryotes and highlights the role of lysine methylation in transcription. H3K4 is methylated by the SET1 family of methyltransferases and functions largely as a gene activation mark; however the transcriptional output is highly context dependent (Schneider *et al.* 2004, Bernstein *et al.* 2002, Liang *et al.* 2004). For example, binding of the PHD finger of TAF3, which is part of the TFIID basal transcription complex, to H3K4me3 is associated with gene activation (Vermeulen *et al.* 2007). In contrast, binding of the PHD finger of ING2, a subunit of the mSin3a histone deacetylase complex to the same mark is associated with gene repression (Shi *et al.* 2006). H3K4me1 is a marker of active enhancer elements, and recognition of this mark by the chromo-barrel domain of the acetyltransferase TIP60 facilitates estrogen-induced transcription (Jeong *et al.* 2011). H3K4me2 is associated with an active or potentially active 'permissive' chromatin state, whilst H3K4me3 occurs with active transcription (Bernstein *et al.* 2002, Schneider *et al.* 2004). H3K36 is another methylated lysine involved in transcription, displaying a progressive shift from mono- to trimethylation between the 5' and 3' ends of genes (Bannister *et al.* 2005). Set2, which methylates H3K36 recognises H3K36me and binds elongating RNA polymerase II, which recruits the Rpd3S histone deacetylase complex (Carrozza *et al.* 2005, Joshi *et al.* 2005, Keogh *et al.* 2005). The histone deacetylase activity of Rpd3S is necessary to prevent spurious intragenic transcription in the wake of RNA polymerase II (Venkatesh *et al.* 2012). H3K36me is also implicated in the DNA damage response, replication, as well as mRNA alternative splicing and dosage compensation gene upregulation in *D. melanogaster* (Musselman *et al.* 2012).

H4K20 is di-methylated by Suv4-20H1/Suv4-20H2 and binds to the BAH domain of Orc1 to regulate replication licensing (Kuo *et al.* 2012). In yeast the Orc1 BAH domain also interacts with the silent information regulator 1 (Sir1) protein (Hsu *et al.* 2005), a component of the Sir complex with structural roles in silencing at *HM* loci and telomeres (Norris & Boeke 2010). H4K20me2 is also involved in the DDR via interaction with the TTD of 53BP1, which competes with the DDR-external binding by the demethylases JMJD2A and JMJD2B to this residue (Botuyan *et al.* 2006, Mallette *et al.* 2012) (discussed in more detail later). H3K9 and H3K27 methylation marks are largely associated with the formation of constitutive and facultative heterochromatin and silencing (Musselman *et al.* 2012). H3K27me1 and H3K9me3 are located in pericentric heterochromatin (Peters *et al.* 2003, Rice *et al.* 2003), whilst H3K27me3 and H3K9me2 are found together in transcriptionally repressed euchromatin. K27me recruits Polycomb proteins to repressed chromatin (Fischle *et al.* 2003, Min *et al.* 2003), and K9me recruits heterochromatin protein 1 (HP1) for heterochromatin

formation and spreading (Jacobs *et al.* 2002, Lachner *et al.* 2001, Canzio *et al.* 2011), via their chromobarrel domains. Competition between the silent information regulator 3 (Sir3) BAH domain and the methytransferase Dot1 for binding to methylated H3K79 constitutes an important regulatory mechanism for silencing at *HM* loci and telomeres in yeast (Norris & Boeke 2010).

Arginine residues can also be mono- or dimethylated, the latter of which occurs in symmetrical (Rme2s) or asymmetrical (Rme2a) conformations. Currently identified arginine methylation sites include H3R2, H3R8, H3R17, H3R26, H4R3, H2AR11, and H2AR29. Methylarginine residues are recognised by aromatic cages present in ADD, Tudour and WD40 domains (Musselman *et al.* 2012). The Tudour domain of the TDRD3 transcription co-activator recognises H3R17me2a and H4R3me2a to facilitate gene activation (Yang *et al.* 2010). H4R3me2s is bound by the ADD domain of the DNA methyltransferase DNMT3a and has a role in silencing of the β-globin gene (Zhao *et al.* 2009). Symmetric dimethylation of H3R2 by PRMT5 and PRMT7 is recognised by the WD40 domain of the co-activator complex component WDR5, which is required for euchromatin maintenance (Migliori *et al.* 2012).

Histone acetylation

Acetylation of lysine results in charge neutralization of the residue and changes the electrostatic properties of histones. Lysine acetylation induces a more relaxed chromatin structure by weakening the interaction with negatively charged DNA, and is largely associated with active transcription. Lysine is acetylated on H3 (K4, 9, 14, 18, 23, 27, 36 and 56), H4 (K5, 8, 12, 16, 20, 91), H2A (K5 and 9) and H2B (K5, 12, 15, 16, 20 and 120) (Musselman *et al.* 2012). Three protein binding modules recognise acetylated lysine: the bromodomain, PHD domain and PH domain. Bromodomains are ~110 amino acid residue structures that bind acetylated lysine and several flanking residues (Hudson *et al.* 2000, Mujtaba *et al.* 2002). Bromodomains fold into a highly conserved four-helix bundle that consists of αA, αB, αC and αZ α-helices. Acetyllysine residues insert into a deep hydrophobic cavity created by inter-helical ZA and BC loops and contact several hydrophobic residues; often two conserved tyrosines, with stabilization achieved through hydrogen bonding to a highly conserved asparagine (Musselman *et al.* 2012).

The binding affinity of individual bromodomains to single acetyllysine residues is often very weak, but binding can be substantially strengthened when multiply acetylated residues are recognised by covalently linked tandem bromodomains. For

example, the tandem bromodomains of TAF1, the largest subunit and core scaffold of the TFIID basal transcription factor complex, together form a V-shaped structure, with each bromodomain separated by 25Å and angled in the same direction (Jacobson *et al.* 2000). The protein has a much higher affinity for H4K5ac H4K12ac and H4K8ac H4K16ac doubly acetylated H4 tails than mono-acetylated peptides, with each bromodomain separately binding to one acetyllysine in the same H4 peptide. The first bromodomain of the bromodomain testes-specific protein (Brdt), which is involved in spermatogenesis, has a wider hydrophobic cavity that accommodates two acetyllysines, namely H4K5ac and H4K8ac. The second bromodomain of Brdt binds to H3K18ac (Mornière *et al.* 2009).

The double PHD finger of Ppf3b, which functions with the SWI/SNF chromatin remodelling complex BAF in transcriptional programs associated with heart and muscle development, is also known to associate with acetylated histone peptides (Lange *et al.* 2008, Zeng *et al.* 2010). The first PHD finger of Ppf3b binds to H3K14ac, whilst the second PHD finger binds to several N-terminal residues in the H3 tail. The double PH domain of the histone chaperone Rtt106 binds to H3K56ac and is involved in gene silencing and the DDR (Su *et al.* 2012). Histone acetylation is also important in the DDR through recruitment of SWI/SNF chromatin remodelling complexes (discussed in more detail later). Recognition of H4Kac by the double bromodomain-containing proteins Bdf1 and Bdf2 in yeast is important for the regulation of transcription, chromatin dynamics, replication-coupled DNA repair and mRNA splicing (Albulescu *et al.* 2012, Koerber *et al.* 2009, Garabedian *et al.* 2012, Matangkasombut & Buratowski 2003). The bromodomain-containing protein ACF7 is enriched in replicating pericentromeric heterochromatin and is required for normal cell cycle progression (Collins *et al.* 2002).

Histone phosphorylation

Histone phosphorylation adds a large, negatively charged group to residues and similarly changes the electrostatic and topographic properties of the histone (Musselman *et al.* 2012). Serine and threonine residues are phosphorylated at T3, T6, S10, T11, S28 and T45 of H3, S1 of H4, S1 and T120 of H2A, S139 (human) and S129 (yeast) of H2A.X and S14 of H2B (Musselman *et al.* 2012). S129 and S139 are phosphorylated by the phosphoinositide 3-kinase-like kinases (PIKKs) Mec1-Ddc2 in *S. cerevisiae* and ATR, ATM and DNA-PK in *H. sapiens* as an important signal transduction step following DNA DSB formation. Phosphorylated H2A.X (γ-H2A.X) plays a critical role in recruiting numerous DNA damage response proteins to the DSB.

Mitosis and transcription are also regulated by serine and threonine phosphorylation. Phosphorylation of H3S10 by Aurora B kinase during mitosis regulates chromosome condensation and segregation by disrupting the interaction between the HP1 chromodomain and H3K9me3, resulting in the release of HP1 from chromatin (Hirota *et al.* 2005, Fischle *et al.* 2005). Aurora B kinase activity at the centromere requires binding of Survivin to H3T3ph (Jeyaprakash *et al.* 2011, Wang *et al.* 2010). Finally, recognition of H3S10ph and H3S28ph by 14-3-3 protein family isoforms (Bmh1 and Bmh2 in yeast) is important for *GAL1* and *HDAC1* gene transcription (Walter *et al.* 2008, Winter *et al.* 2008).

Patterns of histone modifications at mammalian centromeres

Mammalian centromeres are comprised of distinct chromatin regions characterized by the presence of CENP-A, H3K9me2/3 and H3K4me2. These regions regulate the unique properties of the centromere and the flanking pericentromeric regions. A discrete chromatin domain adjacent to the outer kinetochore contains CENP-A nucleosomes that regulate kinetochore function. Adjacent to this is a section of chromatin containing H3K4me2, which is thought to contribute to the physical organization of the centromere (Dunleavy *et al.* 2005). Surrounding these domains is a large pericentromeric region characterized by H3K9me2- and H3K9me3-enriched chromatin in addition to H4K20me3 (Sullivan & Karpen *et al.* 2004). These modifications function to recruit proteins such as cohesin and HP1, which are required for the structural maintenance and function of the pericentromeric heterochromatin (Nonaka *et al.* 2002, Verdaasdonk & Bloom 2011).

A number of modifications have been identified that occur specifically on the N-terminal tail of Cse4/CENPA. In budding yeast, Cse4 is methylated on R37, acetylated on K49, and phosphorylated on S22, S33, S40 and S105. (Boeckmann *et al.* 2013). These serine residues are phosphorylated by the Aurora B kinase Ipl1 and appear to regulate sister kinetochore bio-orientation (Boeckmann *et al.* 2013). Mutation of R37 to alanine impaired the association of kinetochore components with centromeres (Samel *et al.* 2012). In human cells, CENPA is phosphorylated on S7 by Aurora kinase and regulates kinetochore function and cytokinesis (Zeitlin *et al.* 2001). CENPA phosphorylation appears to be important during mitosis by facilitating the binding of 14-3-3 proteins, which stabilize the association of CENPC (Goutte-Gattat *et al.* 2013). Phosphorylated S16 and S18 also occur on CENPA and affect kinetochore integrity, although a relationship with 14-3-3 or other proteins has not been identified (Catania & Allshire 2014).

1.1.4. Chromatin remodelling complexes

In addition to DNA sequence, histone variants and posttranslational histone modifications, chromatin is regulated by chromatin remodelling complexes. These complexes have widespread roles in establishing chromatin architecture, regulation of transcription, silencing, chromosome segregation, DNA replication and DNA repair (Clapier & Cairns 2009). Chromatin remodelling complexes are multi-subunit complexes that contain a single core catalytic ATPase subunit able to generate an array of nucleosome-related outputs. These include nucleosome sliding or repositioning, ejection, DNA unwrapping, transfer of H2A/H2B dimers and histone octamers between nucleosomes and to histone chaperones or other DNA molecules (Clapier & Cairns 2009). Central to these processes is the generation of force provided by ATP hydrolysis that breaks histone-DNA contacts and translocates DNA. How the ATPase translocates DNA and generates force and how translocation and force generation are coupled on nucleosomes is fundamental to understanding the remodelling process (Sirinakis *et al.* 2011).

Chromatin remodelling complexes function during DNA replication to eject and chaperone histone octamers in the path of DNA polymerases, as well as deposit and reposition them after replication (Clapier & Cairns 2009). Similarly, chromatin remodelling complexes replace and reposition nucleosomes ejected during transcription. They control the exposure of regulatory DNA sequences and DNA break sites to allow access for DNA binding proteins and the DNA repair machinery. There are four families of chromatin remodelling complexes, namely SWI/SNF, ISWI, CHD and INO80, which are specialized for particular biological functions and contexts (Clapier & Cairns 2009). This section focuses on SWI/SNF chromatin remodelling complexes, reviewing their subunit composition and summarising their known roles in various chromatin-related activities from yeast to humans.

Subunit composition of SWI/SNF chromatin remodelling complexes

SWI/SNF (switching defective/sucrose non-fermentable) chromatin remodelling complexes are composed of between 8 and 14 subunits (Clapier & Cairns 2009). In most eukaryotes two related complexes that contain related ATPase catalytic subunits are found. The catalytic ATPase subunits contain an N-terminal HSA (helicase-SANT) domain, an ATPase domain that is split into two parts termed DExx and HELICc, and a single C-terminal bromodomain. Various other conserved subunits that harbour

conserved domains are found in both complexes, in addition to subunits that are unique to each complex and provide functional specificity.

In yeast, the two SWI/SNF complexes are known as SWI/SNF and RSC (remodels the structure of chromatin). RSC is an abundant (~1000-2000 molecules per cell), essential chromatin remodelling complex (Cairns *et al.* 1996) from which 17 subunits have been identified, namely Sth1, Rsc1, Rsc2, Rsc3, Rsc4, Rsc6, Rsc7/Npl6, Rsc8, Rsc9, Sfh1, Arp7, Arp9, Rsc30, Htl1, Rtt102, Rsc58 and Ldb7. Sth1, which is essential for viability, provides the ATPase catalytic activity and is closely related to the Swi2/Snf2 catalytic subunit of the SWI/SNF complex. Rtt102, Arp7 and Arp9 are found in both RSC and SWI/SNF complexes, and Sfh1, Rsc8 and Rsc6 are homologous to subunits found in SWI/SNF (Table 1.1)

Table 1.1 Subunit compostion of RSC and SWI/SNF complexes

S. cerevisiae		Human	
RSC	SWI/SNF	PBAF (hSWI/SNF-B)	BAF (hSWI/SNF-A)
Sth1	**Snf2**	**BRG1**	**BRM or BRG1**
Arp7	Arp7	β-actin	β-actin
Arp9	Arp9	BAF53	BAF53
Rtt102	Rtt102		
Rsc6	Swp73	BAF60	BAF60
Sfh1	Snf5	SNF5	SNF5
Rsc8	Swi3	BAF170 and BAF155	BAF170 and BAF155
Rsc3			
Rsc30			
Rsc1, Rsc2 and Rsc4		BAF180	
		BRD7	
		BAF200	
	Swi1		BAF250
Rsc7			
Rsc9			
Ldb7			
Htl1			
Rsc58			
		BAF45	BAF45
		BAF57	BAF57
	Snf6		
	Snf1		
	Swp29		
	Swp82		

Table adapted from Chambers *et al.* 2012. Catalytic subunits are shown in bold. Rows show homologous subunits. RSC and SWI/SNF share Arp7, Arp9 and Rtt102, and four other homologous subunits. RSC is homologous to the human PBAF complex, and SWI/SNF is homologous to the human BAF complex. BAF180, BRD7 and BAF200 are specific to PBAF, and BAF250 is specific to BAF

Domain architecture of the RSC complex subunits Rsc1, Rsc2 and Rsc4

At least two isoforms of the complex occur, containing either Rsc1 or Rsc2 (Cairns *et al.* 1999). Deletion of both *RSC1* and *RSC2* is lethal, whilst single deletion retains viability, suggesting that there is some degree of functional redundancy. Rsc2 is approximately 10-fold more abundant than Rsc1 but both proteins have highly similar domain organization with 46% amino acid sequence identity and 62% similarity (Cairns *et al.* 1999) (Figure 1.1). Both proteins contain two bromodomains, the first of which is largely dispensable whilst the second is important for protein function (Cairns *et al.* 1999). They also contain an AT hook, a bromo-adjacent homology (BAH) domain and a C-terminal region (Figure 1.1). AT hooks are short DNA-binding motifs that preferentially bind to the minor groove of AT-rich DNA (Cairns *et al.* 1999). Although the AT hook is only necessary for Rsc1-specific functions, an AT hook must be present in either Rsc1 or Rsc2 for viability (Cairns *et al.* 1999). The C-terminal regions of Rsc1 and Rsc2 are necessary and sufficient for incorporation into the rest of the RSC complex (Cairns *et al.* 1999).

Rsc4 contains two bromodomains in tandem (Figure 1.1); the first (BD1) binds acetylated lysine 25 (K25ac) of Rsc4 itself and the second (BD2) binds acetylated lysine 14 of histone H3 (H3K14ac) (VanDemark *et al.* 2007). Gcn5 acetylates both Rsc4 K25 and H3K14, and binding of Rsc4 K25ac to BD1 prevents binding of BD2 to H3K14ac, indicating an autoregulation mechanism for histone modification recognition (VanDemark *et al.* 2007). A specific role for H3K25ac in promoting resistance to replication stress was discovered more recently (Charles *et al.* 2011). Less is known about the binding targets of the Rsc1 and Rsc2 bromodomains. Whilst the first bromodomain (BD1) of each protein is largely dispensable, the second bromodomain is important for function (Cairns *et al.* 1999). One study has examined the *in vitro* binding ability of the individual bromodomains of Rsc1 and Rsc2. Interestingly, all four bromodomains displayed extremely weak binding to the selection of acetyl-lysine-containing histone peptides tested and were classed as ‘non-binders’ (Zhang *et al.* 2010). It is therefore possible that these bromodomains in fact bind other non-histone acetylproteins.

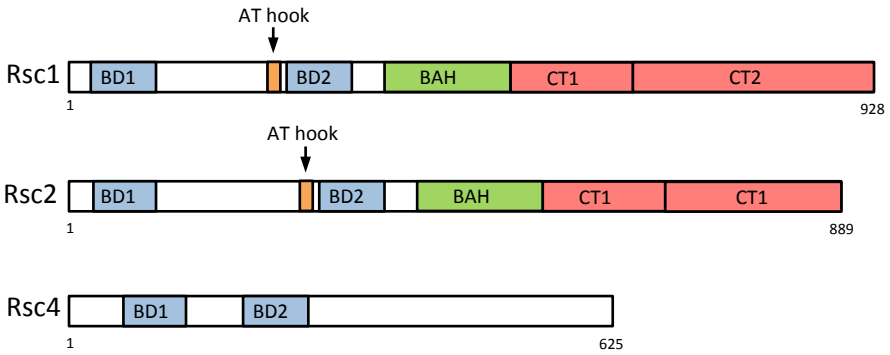

Figure 1.1. Domain organization of the RSC subunits Rsc1, Rsc2 and Rsc4. BD; bromodomain, BAH; bromo-adjacent homology, CT1; C-terminal region 1, CT2; C-terminal region 2

Bromo-adjacent homology (BAH) domains are ~200 amino acid residue structures found in several chromatin-associated proteins (Goodwin & Nicolas 2001, Callebaut *et al.* 1999). BAH domains fall into two classes based on amino acid sequence (Callebaut *et al.* 1999, Oliver *et al.* 2005). The 'RSC-like' class includes the BAH domains of Rsc1, Rsc2 and the two BAH domains found in the homologous BAF180 protein, as well as those of the transcription factor Ash1 and the CpG-DNA methyltransferase DNMT1 (DNA (cytosine-5) methyltransferase 1). The 'Sir3-like' class includes the BAH domains of Orc1 (origin recognition complex 1) and Sir3 (silent information regulator 3), which arose through a duplication of Orc1 in *S. cerevisiae* (Hickman & Rusche 2010, Chambers *et al.* 2013).

Transcriptional silencing by Orc1 and Sir3 at telomeres and the *HML/R* loci in budding yeast is critically dependent on their BAH domains (Norris & Boeke 2010). The BAH domain of Orc1 interacts with Sir1 (silent information regulator 1) (Hsu *et al.* 2005), and in higher eukaryotes an interaction exists between Orc1 and HP1 (heterochromatin protein 1) (Duncker *et al.* 2009). The BAH domain of Orc1 also mediates an interaction with nucleosomes (Noguchi *et al.* 2006, Muller *et al.* 2010). In higher eukaryotes this interaction is via H4K20me2 and is important for replication licensing (Kuo *et al.* 2012). In yeast the Sir3 BAH domain also binds to nucleosomes (Norris *et al.* 2008, Onishi *et al.* 2007) via the LRS (loss of ribosomal silencing) region, which includes sequences from H3 and H4, and also makes extensive contacts with all four core histones (Armache *et al.* 2011).

Recently, work in our lab identified a role for the Rsc2 BAH domain in rDNA silencing and nucleosome binding, which in contrast to the Sir3 BAH domain interacts specifically with H3 (Chambers *et al.* 2013). Furthermore, resolution of the Rsc2 BAH crystal structure at 2.4A revealed major differences between the structure of Rsc2 BAH

compared to those of Orc1 and Sir3. The canonical BAH domain is comprised of a distorted B-barrel core with additional N- and C-terminal B-strand and 3_{10} elements (Callebaut *et al.* 1999, Oliver *et al.* 2005). The core fold of all three BAH domains is highly conserved, and the Orc1 and Sir3 BAH domains contain an inserted H-domain (involved in protein-partner interactions) as well as a C-terminal helix-turn-helix motif (involved in specific nucleosome interactions). Notably, both of these additional structural motifs are absent in the Rsc2 BAH domain, presenting a unique and distinct interface for H3 binding. The study also showed that the Rsc1 and homologous proximal BAF180 BAH domain similarly display H3-specific binding. In addition, a novel Rsc2 BAH domain motif was identified that when mutated abrogates H3 binding *in vitro* and causes defective Rsc2 function *in vivo* (Chambers et al. 2013).

1.1.5. Properties of the RSC complex

Structural conformations of the RSC complex

Studies utilizing cryo-electron microscopy to visualize the structure of the RSC complex revealed a central cavity that appears able to accommodate a nucleosome. Addition of nucleosomes resulted in an increased density within the central cavity, suggesting that it indeed constitutes a nucleosome-binding cavity (Leschziner *et al.* 2007, Chaban *et al.* 2008, Asturias *et al.* 2002). Two different conformations of the complex were observed when Rsc2-RSC (Leschziner *et al.* 2007) and mixtures of the Rsc1-RSC and Rsc2-RSC (Chaban *et al.* 2008, Skiniotis *et al.* 2007) complexes were analysed, termed ‘open’ and ‘closed’. The predominant difference between the conformations was the positioning of the lower arm part of the complex. The ‘closed’ conformation was stabilized when acetylated H3 N-terminal peptides were incubated with the complexes (Skiniotis *et al.* 2007). A third conformation was also observed in ~16% of complexes in which part of the lower arm was absent or had reduced density. This might represent a conformation specific to Rsc1-RSC since this complex is known to account for ~10% of all RSC (Skiniotis *et al.* 2007, Chambers & Downs 2012). Addition of nucleosomes did not result in any major changes to RSC structure, however changes to the nucleosome were observed, including loss of H2A-H2B dimers (Chaban *et al.* 2008). In support of RSC-induced changes to nucleosomes the sensitivity of nucleosomal DNA to degradation by exonuclease III and DNase I was found to increase upon RSC binding (Lorch *et al.* 2010, Lorch *et al.* 1998).

Biochemical activity of the RSC complex

The RSC complex has been shown *in vitro* to perform nucleosome remodelling, repositioning, disassembly and octamer transfer. Its ATPase activity can be stimulated by at least 25bp of DNA but was not stimulated further upon addition of nucleosomes. A maximal turnover rate of ~7.5 ATP molecules per second was also observed (Cairns *et al.* 1996, Boyer *et al.* 2000, Saha *et al.* 2002). By itself, Sth1 was found to have ~2.5 times lower ATPase activity compared to the intact Rsc2-RSC complex (Saha *et al.* 2002). ATP hydrolysis by Sth1/RSC was also coupled to 3'-5' translocase activity as shown by DNA length-dependent stimulation, as well as stimulation by DNA minicircles and triplex displacement activity (Saha *et al.* 2002, Saha *et al.* 2005).

RSC has been shown to bind DNA and nucleosomes with comparable affinity, and incubation with nucleosomes and ATP induces a slower migrating 'activated' form of the complex. This form of RSC renders nucleosomal DNA more sensitive to DNase I and suggests RSC is able to alter the structure of the nucleosome (Lorch *et al.* 1998). In a different assay an inaccessible restriction site on the surface of the nucleosome was rendered accessible to digestion after ATP-dependent remodelling by RSC (Cairns *et al.* 1996, Lorch *et al.* 1998, Saha *et al.* 2002). Additional RSC functions include nucleosome repositioning, histone octamer transfer onto naked DNA and nucleosome disassembly in the presence of histone chaperones (Lorch *et al.* 2006, Lorch *et al.* 1999, Ferreira *et al.* 2007).

Other RSC subunits are important for maximal RSC activity because Sth1 alone was found to be five to six-fold less active than RSC in nucleosome mobilization (Saha *et al.* 2002). These auxiliary subunits might function to increase the affinity of RSC for nucleosomes. Tetra-acetylated H3-containing nucleosomes were remodelled by RSC ~16 times faster than unmodified nucleosomes due to preferential binding to the acetylated nucleosomes (Ferreira *et al.* 2007). In addition, RSC binds to nucleosomes acetylated by NuA4 with greater affinity (Ferreira *et al.* 2007), suggesting a possible role for the bromodomain-containing subunits (Rsc1, Rsc2, Rsc4 and Sth1) in RSC recruitment to chromatin and maximal remodelling activity (Chambers & Downs 2012). It is unclear as to whether the Rsc1- and Rsc2-containing isoforms of RSC possess different biochemical properties. This is because the *in vitro* assays described above have largely used either Rsc2-RSC alone or a mixture of Rsc1-RSC and Rsc2-RSC.

Studies have examined the molecular mechanism of nucleosome remodelling by RSC using single molecule approaches. RSC formed relaxed supercoiled DNA loops between 400 and 700bp in length in an ATP-dependent manner on DNA tethered

and stretched at low force with a magnetic trap (Lia *et al.* 2006). Loop formation of sizes between 20 and 1200bp (averaging ~100bp) was also observed on nucleosomal DNA templates, but these loops could not form at higher tensions (Zhang *et al.* 2006). Loop slippage was observed on both DNA templates, however the highest rate of translocation occurred on naked DNA (>500bp per second) compared to nucleosomal DNA (12bp per second). Together these data suggest a mechanism for remodelling that first sees the formation of a DNA bulge on the surface of the nucleosome. This bulge is then extended to generate a larger bulge, which upon dissipation can lead to reversal of the translocation, a jump in the position of the nucleosome, or nucleosome sliding (Chambers & Downs 2012).

In vivo *functions of the RSC complex*

RSC is known to regulate the transcription of many genes and co-immunoprecipitates with all three RNA polymerases (Angus-Hill *et al.* 2001, Soutourina *et al.* 2006, Ng *et al.* 2002). RSC activates and represses transcription of a group of genes that are distinct from those regulated by SWI/SNF (Du *et al.* 1998, Angus-Hill *et al.* 2001, Floer *et al.* 2010). Binding of RSC was observed at ~700 promoters (~11% of genes) when assayed by ChIP-on-ChIP, and there was no difference in the binding profiles between Rsc1 and Rsc2 (Ng *et al.* 2002). Furthermore, in a *rsc4* mutant strain ~12% of RNA polymerase II-transcribed genes were up- or down-regulated by at least 2-fold (Soutourina *et al.* 2006). RSC was also present at a number of tRNA promoters transcribed by RNA polymerase III and enriched at numerous genes involved in mitochondrial function, nitrogen and carbon metabolism as well histone gene promoters. Several *rsc* mutants display misregulated gene transcripts affecting cell wall integrity, cell cycle control and spindle pole body formation, yet RSC was not enriched at their corresponding promoters. Conversely, some transcripts from promoters at which RSC is enriched were not misregulated in *rsc* mutants (Angus-Hill *et al.* 2001), indicating that there is not a straightforward correlation between RSC occupancy at promoters and transcriptional activity.

RSC is also involved in kinetochore function. Mutations in Sth1 and Sfh1 were found to interact genetically and biochemically with mutants of various kinetochore components, the centromere-specific histone H3 variant Cse4 and mutated centromeric DNA elements (Hsu *et al.* 2003). In addition, RSC localized to centromeric and centromere-proximal chromatin. Sth1 and Sfh1 mutants displayed an altered centromeric chromatin structure, yet kinetochore components, including Cse4, remained associated with the centromere. This suggests that RSC functions in a post-

recruitment step to assemble or maintain centromeric chromatin structure, which in turn leads to the correct configuration of the kinetochore. Consistent with kinetochore dysfunction the Sth1 and Sfh1 mutants missegregated authentic chromosomes at a higher frequency than wild-type strains (Hsu *et al.* 2003).

Other functions of RSC include adaptation to the spindle assembly checkpoint (Rossio *et al.* 2010), nuclear pore complex localization (Titus *et al.* 2010) and sister chromatid cohesion (Baetz *et al.* 2004, Huang *et al.* 2004) (discussed later). Several *rsc* mutants also affect cell cycle progression and strains harbouring deletions, temperature sensitive alleles or degron alleles of genes encoding various RSC subunits (namely Sth1, Sfh1, Rsc3, Rsc4, Rsc6, Rsc8, Rsc9 and Rsc58) activate the G2/M DNA damage checkpoint (Chambers & Downs 2012).

1.1.6. Mammalian SWI/SNF complexes

Mammalian cells contain two closely related SWI/SNF complexes known as BAF (BRG1- or hBRM-associated factor) and PBAF (polybromo-BAF) (Wilson & Roberts 2011) (Table 1.1). PBAF (also called SWI/SNF-B) is the mammalian orthologue of the yeast RSC complex and contains twelve subunits, four of which constitute a highly conserved core including BRG1, the catalytic ATPase, BAF155, BAF170 and SNF5 (Table 1.1). Five subunits are classed as variant subunits, including β-actin, BAF53A/B, BAF60A/B/C, BAF57 and BAF45A/B/C/D. These core and variant subunits are also found in the BAF complex, which is orthologous to the yeast SWI/SNF complex (Table1.1). BAF contains either the ATPase subunit BRG1 or hBRM, which are mutually exclusive, as well as the BAF-specific subunit BAF250A/B, whilst BAF180, BAF200 and BRD7 are unique to PBAF (Wilson & Roberts 2011). Table 1.2 shows the gene and protein names for the complete list of SWI/SNF subunits.

Mammalian SWI/SNF complexes are highly diverse owing to the differential lineage-restricted expression timing of the variant subunits. Along with the differential inclusion of subcomplex-specific subunits it is thought that several hundred variant SWI/SNF complexes might exist (Wu *et al.* 2009). A major role of mammalian SWI/SNF complexes is the regulation of lineage-specific differentiation during neurogenesis, myogenesis, apipogenesis, osteogenesis and haematopoiesis (Kaeser *et al.* 2008, Lickert *et al.* 2004, Wu *et al.* 2009, Lessard *et al.* 2007, Yan *et al.* 2008). This appears to be achieved through interaction with tissue-specific transcription factors to regulate tissue-specific gene activation and repression. The differentially expressed variant subunits might modulate this activity by interacting with the tissue-specific factors to direct the complex's remodelling activity to specific loci (Wilson & Roberts 2011).

Table 1.2. Gene and protein names of human SWI/SNF subunits

Gene	Protein
SMARCA4	BRG1
SMARCA2	BRM
ACTB	β-actin
ACTL6A	BAF53
SMARCB1	SNF5
SMARCC1	BAF155
SMARCC2	BAF170
SMARCD1	BAF60
PBRM1	BAF180
BRD7	BRD7
ARID2	BAF200
ARID1A	BAF250

SWI/SNF subunits are frequently mutated in diverse cancers

Recent whole-exome sequencing studies have identified frequent mutations in subunits of SWI/SNF chromatin remodelling complexes in a diverse range of cancers. Most of these studies have analysed one tumour type, often reporting a strikingly high frequency of mutation in one specific SWI/SNF subunit. However, these studies have largely focused on the 'top hits' as the most frequently mutated genes. In an effort to systematically define the frequency and spectrum of SWI/SNF mutations across a broad range of human cancers, Shain and Pollack analysed mutational datasets from 24 studies, covering 18 cancer types. The authors revealed that the cancer types most frequently harbouring SWI/SNF mutations were ovarian clear-cell carcinoma (75%), clear cell renal cell carcinoma (57%), hepatocellular carcinoma (40%), gastric cancer (36%), melanoma (34%), and pancreatic cancer (26%). Strikingly, across all cancer types analysed, the average frequency of SWI/SNF mutation was 19%, approaching that of p53 at 26% (Shain & Pollack 2013).

The size of SWI/SNF's collective genomic 'footprint' might account for a high frequency of passenger mutations that could explain such mutation frequencies in cancer. In argument against this, it was found that the vast majority of mutations (72%) were predicted to be deleterious (38.8% frameshift, nonsense, rearrangement and splice-site, and 33.2% missense damaging). This suggests that most SWI/SNF mutations are likely to be driver mutations in cancer. Reports suggest that alternative mechanisms, including genomic DNA deletions, rearrangements and epigenetic silencing might contribute to SWI/SNF subunit inactivation (Shain *et al.* 2012, Delbove

et al. 2011). Therefore, these sequencing results might actually underestimate the true frequency of SWI/SNF inactivation (Shain & Pollack 2013).

The enzymatic and targeting subunits of SWI/SNF are preferentially mutated in cancer

SWI/SNF subunits can be roughly grouped as enzymatic subunits (Brg1 and hBRM), targeting subunits that confer functional specificity to each complex (BAF250A/B for BAF, BAF180, BAF200 and BRD7 for PBAF), and the remaining core and variant subunits, termed scaffolding subunits (Shain & Pollack 2013). Intriguingly, the majority of SWI/SNF mutations were found to occur in the genes of the enzymatic or targeting subunits. Specifically, the five most frequently mutated genes were *ARID1A* (9% of SWI/SNF nonsynonymous mutations), *PBRM1* (4%), *SMARCA4* (3%), *ARID1B* (2%) and *ARID2* (2%). However, mutations were found in the scaffolding subunits albeit at a noticeably lower frequency (none exceeded a frequency of 0.6%). The fact that mutations are found in a range of subunits suggests that they impact in part or whole the functional activity of the complex. That the enzymatic and targeting subunits are mutated more frequently might suggest that they are particularly critical for SWI/SNF function.

Certain cancer types often exhibit mutations predominantly in a single SWI/SNF subunit

Analysis of individual cancer types often reveals that a single SWI/SNF subunit is mutated. The most striking cases include *SMARCB1*, which is mutated in all malignant rhabdoid tumours (Roberts *et al.* 2000), and *PBRM1*, which is mutated in 41% of all renal cell clear cell carcinomas (Varela *et al.* 2011). However, most other cancer types, including melanoma, pancreatic cancer and diffuse large B-cell lymphoma (DLBCL) display a more balanced spectrum of mutations across the most commonly mutated subunits. An interesting question is therefore why do certain cancer types harbour mutations of single SWI/SNF subunits? It is possible that the affected subunit (and complex containing it) has cell- or tissue-type specific functions. Another possibility is that cell- and tissue-type specific mutational processes that preferentially affect a certain SWI/SNF gene or genomic locus might be operational (Shain & Pollack 2013).

Another interesting question is whether SWI/SNF mutations preferentially occur within certain subunit domains or structural motifs. Shain & Pollack report that no obvious mutation ‘hotspots’ were apparent from the exome data analysed as a whole. However, they note that the data appears too sparse to draw any firm conclusions in

this regard. Nevertheless, a few validation studies that analysed specific subunits (including *ARID1B*) in much larger cohorts similarly reported a lack of mutation 'hotspots' (Wang *et al.* 2011, Wiegand *et al.* 2010). The authors also investigated whether mutations in different SWI/SNF subunits were mutually exclusive of each other. They revealed that two mutations in different subunits occurred in the same tumour at roughly the same frequency as that expected by chance. This suggests that mutational 'hits' in two different subunits are not functionally redundant, and that individual mutations might incrementally impair the function of the complex (Shain & Pollack 2013).

Mutations in SWI/SNF are not mutually exclusive of other cancer gene mutations

The tumour suppressive role of SWI/SNF complexes is widely thought to operate by transcriptionally regulating the activity and expression of key tumour suppressor genes and pathways. These include Rb, p53, Polycomb, sonic hedgehog, Myc, stem cell programs and nuclear hormone receptor signalling (discussed later) (Wilson & Roberts 2011). Shain & Pollack performed a mutual exclusivity analysis on the exome sequencing data in an effort to identify key SWI/SNF tumour suppressor pathways. The rationale follows that one particular linear pathway in a tumour is unlikely to harbour multiple components with a mutation because these mutations would be functionally redundant. Thus, identifying components of a pathway that are only mutated when SWI/SNF mutations are not present could indicate a shared pathway. Similarly, identifying components that are always found mutated with SWI/SNF mutations in the same tumour might indicate a necessary cooperating pathway (Shain & Pollack 2013).

Mutual exclusivity has been previously reported with *ARID1A* and p53 mutations in both ovarian clear cell carcinoma and gastric cancer (Wang *et al.* 2011, Guan *et al.* 2011). Shain & Pollack similarly concluded from the datasets available that a trend towards mutual exclusivity occurs with SWI/SNF and p53 mutations in these cancers, although only gastric cancer reached statistical significance (P=0.018; Fisher's exact test). The authors highlight a need for caution when interpreting these trends, however, because of histological and genetic diversity amongst these two cancer types. Thus, mutual exclusivity might actually correlate with a cancer subtype rather than a mechanistic relationship. In contrast, mutual exclusivity was not observed between SWI/SNF and p53 in pancreatic cancer, melanoma, hepatocellular carcinoma and DLBCL. In fact, in pancreatic cancer all cases harbouring SWI/SNF mutations actually had a p53 mutation, indicating a trend towards mutual inclusivity (P=0.085; Fisher's exact test) (Shain & Pollack 2013).

SWI/SNF complexes are also thought to contribute to tumour suppression by antagonizing the oncogenic activity of polycomb repressive complex 2 (PRC2) (Shain *et al.* 2012, Wilson *et al.* 2010). *EZH2* is the enzymatic component of PRC2 and harbours activating mutations in ~15% of DLBCL. The study by Shain & Pollack revealed several cases of DLBCL containing a mutation in both SWI/SNF and *EZH2*, suggesting that mutual exclusivity does not occur with these mutations (Shain & Pollack 2013). In an effort to more systematically identify cancer gene mutations that display mutual exclusivity with SWI/SNF mutations, the authors analysed the top 189 mutated genes (those with $\geq$13 mutations) from the entire exome sequencing dataset from all 24 studies. These genes included many well-established tumour suppressor genes (e.g. *KRAS, BRAF, CDKN2A, PTEN, NF1, APC, SMAD4*) that function in canonical cancer signalling pathways, including Ras, PI3K, Wnt and Notch. However, no significant mutual exclusivity (or inclusivity) was observed with SWI/SNF mutations. As a favoured explanation for this the authors suggest that SWI/SNF impacts many of the aforementioned pathways simultaneously, which might obscure any mutually exclusive relationships (Shain & Pollack 2013). In support of this, the fact that SWI/SNF mutations are found in such a broad range of cancers in diverse tissue types implies that SWI/SNF impacts upon processes that are largely conserved. In addition, recent studies have identified between 5,000 and 10,000 SWI/SNF binding sites within the genome (Ho *et al.* 2009, Euskirchen *et al.* 2011), suggesting that SWI/SNF transcriptionally regulates many genes. Finally, and as mentioned previously, the orthologous SWI/SNF-related complexes in yeast are known to transcriptionally regulate diverse biological processes, including mitochondrial function, nitrogen and carbon metabolism, and cell cycle regulation. Deregulation of the equivalent processes in human cells (perhaps relating to growth, survival and metabolism) might also contribute to tumourigenesis (Shain & Pollack 2013).

1.1.7. Transcriptional regulation as a potential SWI/SNF tumour suppressor mechanism

Regulation of p21

Cellular senescence is an irreversible cell cycle arrest that serves to restrain the proliferation and transformation that results from oncogene activation. A unifying feature of oncogene-induced senescence is the activation of a robust DNA damage response (DDR) (Di Micco *et al.* 2006, Bartkova *et al.* 2006, Mallette *et al.* 2007), indicating that DNA damage is an important senescence stimulus. p53 is a transcription

factor with diverse roles in cell cycle control, DNA repair, apoptosis and stress responses, and is a major component of the senescence pathway. p53 is activated in response to several oncogenes, including RasV12, STAT5, E2F1, Mos and Cdc6, and is dependent on the DDR kinases ATM, ATR, Chk1 and Chk2 (Di Micco *et al.* 2006, Bartkova *et al.* 2006, Mallette *et al.* 2007). Activated p53 induces the expression of the CDK inhibitor p21, which effects cell cycle arrest (Rufini *et al.* 2013).

As mentioned previously, the gene encoding the PBAF-specific subunit BAF180 *(PBRM1)* is mutated in many cancers. *PBRM1* was first identified as harbouring multiple truncating mutations in breast cancer in a screen for novel breast cancer tumour suppressor genes (Xia *et al.* 2008). Specifically, 3 out of 26 breast cancer cell lines harboured truncating mutations that abolished protein expression and showed strong evidence of loss of heterozygosity (LOH). In addition, mutational screening of 52 primary breast tumours identified one other truncating mutation, and 25 of these samples (48.1%) showed BAF180 LOH without a mutation. Interestingly, all four of the identified mutations occurred in the bromodomains of BAF180 (Xia *et al.* 2008).

To investigate a potential tumour suppressor role the authors showed that re-expressing exogenous BAF180 in a mutant BAF180 breast cancer cell line reduced colony number and size. In addition, the BAF180-expressing cells were significantly enriched in G1, suggesting a role in regulating the transition from G1- to S-phase (Xia *et al.* 2008). This was found to correlate with increased expression of p21 in these cells, and siRNA depletion of BAF180 in a normal breast epithelial cell line led to reduced p21 protein levels. Furthermore, BAF180 depletion led to a reduction in p21 mRNA and BAF180 was found to reside at the p21 promoter when analysed by ChIP in a BAF180-expressing breast cancer cell line (Xia *et al.* 2008). In addition to p53, other signal-regulated transcription factors are known to activate the p21 promoter, including SMAD2/3/4, signal transducer and activator of transcription 3 (STAT3), vitamin D3 receptor, retinoid X receptor α, and peroxisome proliferator-activated receptor γ (Xia *et al.* 2008). The effects of γ-radiation-induced p53-dependent and TGF-β-induced SMAD-dependent p21 activation in the absence of BAF180 were also tested. The authors found that in response to these extracellular stimuli the induction of p21 and G1 cell cycle arrest were attenuated in the BAF180 siRNA-depleted breast cancer cells. Together, these data indicate that BAF180 functions as a regulator of cell cycle exit at G1, at least in part via p21 regulation, in response to various environmental stimuli (Xia *et al.* 2008).

A subsequent study by Burrows *et al.* similarly identified BAF180, as well as another PBAF-specific subunit, BRD7, as being unique regulators of replicative senescence in

human cells (Burrows *et al.* 2010). The authors performed a whole-genome shRNA screen in primary BJ fibroblasts and found that BRD7-depleted cells were largely unable to senesce compared to the control cells. BRD7-depleted BJ fibroblasts significantly delayed senescence and showed increased proliferation under normal conditions as well as in cells expressing the HPV E7 oncoprotein, which binds and inhibits Rb. This suggests that BRD7 regulates senescence independently of Rb. In addition, RasV12D-induced p53-dependent senescence was reduced in BRD7-depleted cells, suggesting a role for BRD7 in both replicative and oncogenic senescence (Burrows *et al.* 2010).

The authors next examined p53-dependent p21 induction in cells lacking BRD7, and found that basal p21 mRNA levels were reduced in BRD7 shRNA-treated cells. In addition, treatment with nutlin-3a, an inhibitor of MDM2 that results in p53 stabilization, similarly led to reduced p21 mRNA levels in the absence of BRD7. Stabilization of p53 after nutlin-3a treatment was found to be normal in the BRD7 shRNA-treated cells, consistent with a role of BRD7 downstream of p53. Interestingly, *MDM2* mRNA levels were also reduced, indicating that p21 is not the only p53 target gene regulated by BRD7. Both p21 and Mdm2 basal mRNA levels were also reduced in BRD7-depleted cells transduced with RasV12D compared to control cells, implicating BRD7 in the expression of several p53 target genes following replicative and oncogenic stress senescence induction (Burrows *et al.* 2010).

To further analyse the involvement of BRD7 in p53-mediated gene expression the authors performed gene expression profiling on control and BRD7 shRNA-depleted cells after nutlin-3a treatment. The genes found to be most differentially expressed between the control and BRD7 shRNA-treated cells were then compared with a list of previously identified p53 target genes (Riley *et al.* 2008). A number of additional p53 target genes were found to be down-regulated in BRD7-depleted cells, including *DcR1, TRIM22, NDRG1* and *PLYCARD*. However, expression of other p53 target genes, such as *Bax,* did not require BRD7, suggesting that BRD7 is required for expression of only a subset of p53 target genes (Burrows *et al.* 2010). BRD7 was found to co-immunoprecipitate with p53, suggesting that the two proteins physically interact. BRD7 contains a single bromodomain that is known to bind H3K14ac (Peng *et al.* 2006). To determine whether the BRD7 bromodomain is also required for the interaction between BRD7 and p53, a strain harbouring a deletion of the bromodomain was created. The BRD7-p53 interaction was found to remain in this strain, indicating that the bromodomain is dispensable for this interaction (Burrows *et al.* 2010).

BAF180 was similarly found to be required for replicative senescence, consistent with the findings by Xia *et al.* BAF180 depletion led to delayed senescence

and proliferation, decreased basal and nutlin-3a-induced p21 expression, and decreased nutlin-3a-induced Mdm2 and DcR1 expression. This suggests that BAF180 is also required for expression of a subset of p53 target genes (Burrows *et al.* 2010).

Wild-type BRD7 overexpression in BJ fibroblasts led to premature senescence and elevated p21 expression, whilst overexpression of the BRD7 bromodomain mutant did not slow proliferation or increase p21 to the same level. In response to nutlin-3a reduced p21 was also observed in the mutant-expressing cells compared to wild-type BRD7-expressing cells. This suggests that the BRD7 bromodomain has a functional role in mediating p21 expression, and might function to bridge p53 to chromatin for its transcriptional activity (Burrows *et al.* 2010). In a database consisting of 3,131 samples and cell lines from 54 cancer subtypes (Beroukhim *et al.* 2010) BRD7 was deleted at a statistically significant frequency, supporting a tumour suppressor function. Again, the scale of involvement of this subunit in tumour suppression might be underestimated by mutation frequency alone, because BRD7 expression was silenced by promoter methylation in samples of nasopharyngeal carcinoma (Liu *et al.* 2008).

Finally, the authors showed that BRD7 also affects p53-independent p21 transcription. BRD7 was found to be required for TGF-β-induced SMAD-dependent p21 activation in HCT116 cells, similar to findings by Xia *et al.* with BAF180, as well as for p21 induction by $1\alpha,25(OH)_2D_3$ (vitamin D) in human mammary epithelial cells (Burrows *et al.* 2010).

Regulation of pluripotency and differentiation

In embryonic stem (ES) cells a unique subset of variant SWI/SNF complexes cooperate with various ES cell-associated factors to regulate pluripotency and self-renewal (Yan *et al.* 2008, Ho *et al.* 2009, Kidder *et al.* 2009, Gao *et al.* 2009). Mouse embryos lacking BRG1, SNF5, BAF155 or BAF250A die around the peri-implantation stage of development, soon after the formation of ES cells (Roberts *et al.* 2000, Klochendler-Yeivin *et al.* 2000, Guidi *et al.* 2001), and BRG1 or BAF250A deficiency results in self-renewal defects and increased differentiation (Bultman *et al.* 2000, Gao *et al.* 2009). A variant complex in which BAF170 is replaced by a second BAF155 subunit interacts with ES cell-specific transcription factors such as OCT4, SOX2 and NANOG at ES-specific target promoters (Ho *et al.* 2009). Overexpression of BRG1 and/or BAF155 results in the reprogramming of fibroblasts into induced pluripotent stem (iPS) cells (Singhal *et al.* 2010). In addition, upregulation of stem cell-associated signatures occurs following SNF5 inactivation in primary embryonic fibroblasts as well as in SNF5-mutated malignant rhabdoid tumours, which are characteristically poorly

differentiated (Wilson *et al.* 2010). Thus, the regulation of pluripotency and differentiation might represent one possible mechanism for SWI/SNF's tumour suppressor activity (Wilson & Roberts 2011).

Antagonism of PRC2 oncogenic activity

Studies in *D. melanogaster* revealed that SWI/SNF mutations suppressed defects associated with mutated PcG (Polycomb Group) proteins (Kennison & Tamkun 1988, Tamkun *et al.* 1992). *EZH2* is the enzymatic subunit of PRC2 (polycomb repressive complex 2) and has a key role in lineage-specific developmental silencing by facilitating the trimethylation of H3K27 (Cao & Zang 2004). Whilst PcG proteins were shown to repress *Hox* gene expression, SWI/SNF complexes were required for *Hox* gene activation (Kennison 1995), suggesting an antagonistic relationship. As mentioned previously, *EZH2* expression is often elevated in various cancers, including breast cancers, prostate cancers and lymphomas, and correlates with advanced disease progression and poor prognosis (Simon & Lange 2008). A mechanistic relationship between PcG and SWI/SNF in cancer was suggested after finding that SNF5 re-expression in an SNF5-deficient rhabdoid tumour cell line resulted in PcG eviction at the *CDKN2A* locus (encoding the CDK inhibitor $p16^{INK4A}$) (Kia *et al.* 2008). Supportively, primary SNF5-deficient tumours and primary cells with inactivated SNF5 display elevated *EZH2* expression (Wilson *et al.* 2010), the latter indicating that it is a primary effect and not a secondary consequence of oncogenic transformation. PRC2 target genes are repressed in SNF5-deficient tumours and SNF5-inactivated mouse embryonic fibroblasts (MEFs) (Wilson *et al.* 2010, Kia *et al.* 2008), consistent with increased PRC2 activity. In addition, levels of H3K27me3 are increased in the absence of SNF5, and tumour formation is prevented in an SNF5-deficient mouse model after conditionally inactivating *EZH2* (Wilson *et al.* 2010). Finally, *EZH2* overexpression has been associated with the pathogenesis of other cancer types, in which SWI/SNF mutations frequently occur, including ovarian and renal cell carcinomas (Lu *et al.* 2010, Wagener *et al.* 2008). Together, these findings suggest that the antagonistic relationship between SWI/SNF and PcG complexes is an important tumour suppressor mechanism.

Regulation of cell cycle progression and aneuploidy via the Rb pathway

Rb is a multifunctional protein with diverse roles that might variously contribute to tumour suppression. These include G1 checkpoint regulation, cell cycle exit control

(relating to differentiation, senescence and quiescence), and regulation of autophagy, apoptosis, angiogenesis and metastasis (Burkhart & Sage 2008). The impact of Rb on these processes is thought to be due to transcriptional regulation of key target gene pathways. More recently, however, loss of Rb has been shown to increase genomic instability, likely stemming from defects in mitosis, and probably represents an important tumour suppressive function (Manning & Dyson 2012) (discussed later).

The most intensely researched role of Rb is its ability to transcriptionally repress E2F-regulated genes (Manning & Dyson 2012). These include genes involved in regulating cell cycle progression at G1/S and proliferation, as well as DNA synthesis, DNA repair, mitosis, the spindle assembly checkpoint (SAC), G2/M control, apoptosis and differentiation. Hence, the Rb-E2F pathway constitutes an important coupling between cell cycle progression and the SAC (Stevaux & Dyson 2002, Hernando *et al.* 2004). Rb is negatively regulated by the cyclin-dependent kinase (CDK) inhibitor $p16^{INK4A}$, which inhibits cyclin D1-CDK4-mediated phosphorylation of Rb (Lowe & Sherr 2003). Hyperphosphorylated Rb leads to its dissociation from E2F genes, thereby relieving its antiproliferative effect. SWI/SNF is implicated in controlling this pathway because SNF5 inactivation leads to reduced $p16^{INK4A}$ expression (Isakoff *et al.* 2005, Oruetxebarria *et al.* 2004). SWI/SNF and Rb also cooperate directly to transcriptionally repress E2F-regulated genes during differentiation (Trouche *et al.* 1997). Interestingly, E2F target genes are upregulated in SNF5-mutated rhabdoid tumour cells as well as SNF5-deficient MEFs (Isakoff *et al.* 2005, Versteege *et al.* 2002). Co-inactivation of Rb or $p16^{INK4A}$ and SNF5 does not result in accelerated tumour formation (Isakoff *et al.* 2005), and loss of SNF5 can replace the loss of Rb in pituitary tumour generation (Guidi *et al.* 2006). These observations suggest that SWI/SNF and Rb have redundant functions in tumourigenesis. However, tumours arising after SNF5 inactivation occur more rapidly and in different tissue types than those caused by Rb or $p16^{INK4A}$ inactivation, suggesting the involvement of other tumour suppressor pathways.

A fascinating study by Vries *et al.* showed that four cancer-associated point mutations in SNF5 from MRTs were fully able to initiate $p16^{INK4A}$-depedent G1 arrest, senescence and apoptosis. This suggests that other processes other than proliferation might underlie the cancer association of these mutations (Vries *et al.* 2005). Expression of the S284L SNF5 mutation in a predominantly diploid SNF5-deficient MRT cell line (harbouring multiple structural chromosome aberrations) led to multilobed nuclei, aneuploidy, polyploidy and spindle and centrosome amplifications. Expression of wild-type SNF5 in these cells did not result in this phenotype, and after 96 hours of expression the ~10% of cells in this cell line that were near tetraploid became almost

perfectly diploid (Vries *et al.* 2005). This suggests a role for SNF5 in the mitotic (SAC) checkpoint. Furthermore, aborted anaphases in S284L expressing cells appeared to be caused by failed kinetochore-microtubule attachment. Strikingly, whilst wild-type SNF5 re-expression rapidly purged aneuploid cells to become diploid, two cancer-associated SNF5 mutations (P48S and R127G) were unable to generate a diploid population. The other two mutations (S284L and S289A) strongly promoted further aneuploidy (Vries *et al.* 2005).

Previously it was shown that SNF5-induced senescence was achieved by activating $p16^{INK4A}$, which inhibits CDK4-mediated phosphorylation of Rb (Oruetxebarria *et al.* 2004). Therefore, the authors tested whether SNF5-dependent ploidy control is exerted via $p16^{INK4A}$. Expression of a $p16^{INK4A}$-insenstivie $CDK4^{R24C}$ mutant in parallel with SNF5 expression could not revert the aneuploidy, suggesting that disruption of the Rb pathway prevents SNF5-dependent ploidy control (Vries *et al.* 2005). Re-expression of SNF5 led to altered expression of multiple E2F target genes, including those involved in mitotic control, including strong downregulation of *MAD2* and *E2F1*. Overexpression of *MAD2* and *E2F1* is observed in many MRTs and can lead to aneuploidy (Hernando *et al.* 2004). Furthermore, expression of $CDK4^{R24C}$ abolished the SNF5-mediated downregulation of these genes. The authors conclude that regulation of the $p16^{INK4A}$-cyclinD/CDK4-Rb-E2F pathway by SNF5 is important for ploidy control in MRTs. However, it is noted that additional structural roles of SNF5 (and SWI/SNF), such as regulation of centromere structure and/or cohesion, could also contribute to aneuploidy with high importance in tumourigenesis (Vries *et al.* 2005).

SWI/SNF appears to regulate cyclin D1 expression levels, which might also contribute to tumourigenesis. Firstly, cyclin D1 levels are increased in SNF5-deficent rhabdoid tumour cells, and SNF5 re-expression resulted in binding if SNF5 to the cyclin D1 promoter, reduced cyclin D1 expression and cell cycle arrest (Zhang *et al.* 2002, McKenna *et al.* 2008). Secondly, in cyclin D1-deficient mice SNF5 loss does not result in tumour formation (Tsikitis *et al.* 2005). Contrary to a role of elevated cyclin D1 expression in tumourigenesis is the observation that in kidney rhabdoid tumours cyclin D1 levels are reduced (Gadd *et al.* 2010). However, cyclin D1 inhibitors attenuate the growth of rhabdoid tumour cells (in which all are currently known to contain an SNF5 mutation) *in vitro* and *in vivo.* These inhibitors might therefore offer a therapeutic approach to the treatment of SNF5-deficient tumours (Lunenberger *et al.* 2010, Alarcon-Vargas *et al.* 2006, Smith *et al.* 2011).

Interaction with MYC

The MYC oncogene is often overexpressed in cancer and functions to regulate the transcription of genes involved in cell cycle control, apoptosis and differentiation. MYC interacts directly with SNF5 to effect MYC target gene activation *in vitro* (Cheng *et al.* 1999), yet SWI/SNF complexes are also known to repress *MYC* expression during differentiation-associated cell cycle arrest (Nagl *et al.* 2006). Interestingly, BAF complexes containing BAF250A repress *Myc* transcription, whilst BAF complexes containing BAF250B promote *Myc* transcription (Nagl *et al.* 2007). MYC is consistently overexpressed in malignant rhabdoid tumours, all of which harbour SNF5 mutations (McKenna *et al.* 2008, Gadd *et al.* 2010). Thus, MYC deregulation may have important implications in the suppression of SWI/SNF-mutant cancers

Interaction with nuclear hormone receptors (NHRs)

SWI/SNF complexes interact with a range of nuclear hormone receptors (NHRs), including glucocorticoid, oestrogen, vitamin D3 and retinoic acid receptors (Trotter *et al.* 2008). These receptors transduce hormonal stimuli to regulate the expression of genes associated with proliferation and differentiation, and many are implicated in oncogenic transformation. In acute lymphoblastic leukaemia (ALL) reduced expression of several SWI/SNF subunits was found to be associated with increased glucocorticoid resistance (Pottier *et al.* 2008). Specific SWI/SNF complexes appear to regulate specific NHR gene targets, as PBAF, but not BAF, interacted with the retinoic acid receptor-α (RXRA), vitamin D3 receptor (VDR) and peroxisome proliferator-activated receptor-γ (PPARG) to facilitate transcription, at least *in vitro* (Lemon *et al.* 2001). In contrast, BAF is necessary and sufficient for *in vivo* glucocorticoid receptor-mediated transcription (Chen *et al.* 2005, Trotter *et al.* 2004).

Regulation of Hedgehog (HH) pathway signalling

Misregulation of the Hedgehog (HH) pathway, particularly through mutation of upstream pathway components, occurs in several types of cancer. Several SWI/SNF subunits interact with GLI1, an important effector of the HH pathway involved in differentiation and patterning, and reside at GLI1-regulated promoters (Jagani *et al.* 2010). SNF5 inactivation resulted in enhanced HH signalling and was found to be essential for growth of rhabdoid tumour cells *in vivo,* raising the possibility that GLI1 targeting may be beneficial as a therapeutic strategy in treating this cancer (Jagani *et*

al. 2010). In addition, repression of HH signalling in neural stem cells requires the function of BRG1 in a neural stem-cell specific variant complex (Lessard *et al.* 2007).

Transcriptional regulation of genes involved in cellular motility

SWI/SNF complexes regulate the transcription of actin cytoskeleton genes, and misregulation of these pathways is observed in SNF5-deficent rhabdoid tumours. Specifically, SNF5 controls cytoskeletal structure and cell migration by regulating the RHOA pathway, which is upregulated following SNF5 loss (Caramel *et al.* 2008). RHOA functions to stimulate contractility and the formation of stress fibres, and overexpression in cancer correlates with poor prognosis (Karlsson *et al.* 2009). Cancer cells lacking BRG1 also display altered cytoskeleton structures, and reduction of BRG1 levels in a BRG1-expressing pancreatic carcinoma cell line increased the number of actin stress bundles (Rosson *et al.* 2005). In contrast, re-expression of BRG1 in a BRG1-deficent cervix carcinoma cell line induced the formation of stress fibre-like actin filament bundles. This was found to be due to increased expression of the RHOA component RHO-associated protein kinase 1 (ROCK1) (Asp *et al.* 2002). SWI/SNF dysfunction correlated with aberrant expression of the CD44 transmembrane glycoprotein, which is also associated with metastasis. Loss of BRG1 or hBRM resulted in CD44 downregulation, and CD44 re-expression was achieved when BRG1 or hBRM were re-expressed in doubly deficient cells lines (Strobeck *et al.* 2001, Reisman *et al.* 2002).

1.2. DNA double-strand break repair

1.2.1. DNA double-strand breaks

DNA lesions are continuously generated in eukaryotic cells from endogenous and exogenous sources. The most dangerous lesion is a DNA double-strand break (DSB) (Kanna & Jackson 2001), generated through replication fork stalling, oxidative metabolism-generated reactive oxygen species (ROS), ionizing radiation (IR) and chemotherapeutic agents. An unrepaired or misrepaired DNA DSB can initiate cellular senescence and apoptosis, in addition the generation of chromosome fragments and rearrangements. Importantly, these can result in loss of heterozygosity and genome instability, which in higher eukaryotes is associated with tumourigenesis. It is therefore imperative that the cell is able to correctly repair a DNA DSB in a timely manner in order to retain viability and fitness. Two conserved, major pathways are utilised to perform DNA DSB repair: non-homologous end-joining (NHEJ) and homologous recombination (HR). In this section a review of these pathways in budding yeast and mammalian cells will be provided.

1.2.2 Non-homologous end-joining

Non-homologous end-joining (NHEJ) is the process by which the two broken DNA molecules of a DNA DSB are directly religated. NHEJ is an error-prone DSB repair mechanism that operates throughout the cell cycle. In mammalian cells, NHEJ represents the major DNA repair pathway (Rothkamm *et al.* 2003), and ~80% of IR-induced DNA DSBs are repaired with fast kinetics by NHEJ in G2 (Beucher *et al.* 2009). There are several sequential steps involved in NHEJ that are currently thought to occur in a stepwise manner (Williams *et al.* 2014). Firstly, the two DNA ends are recognized and the NHEJ protein components are assembled and stabilized. Next, the ends are tethered together, positionally stabilized, and processed. Finally, the ends are ligated and the protein components are dissipated (Davis & Chen 2013).

DSB end recognition by Ku

Recognition of the DNA DSB is performed by the Ku heterodimer, which is composed of the Ku70 and Ku80 subunits. Both subunits contain an N-terminal von Willebrand A (vWA) domain, a core domain and a C-terminal region (Downs & Jackson 2004). The

vWA and core domain are involved in heterodimerization of the Ku complex. The C-terminal region of Ku70 contains SAF-A/B, Acinus and PIAS (SAP) domains, the latter of which is likely to bind DNA (Aravind & Koonin 2000, Zhang *et al.* 2001). The Ku80 C-terminal region folds into a flexible arm structure that resembles a common scaffold involved in protein-protein interactions (Zhang *et al.* 2004). Ku localizes to laser-induced DNA DSBs within seconds of creation (Mari *et al.* 2006). Such rapid localization is thought to be due to its high abundance (~400,000 molecules per cell), its ability to bind DNA in a sequence independent manner (via sugar-backbone binding), and its extremely high binding affinity for DNA ends (equilibrium dissociation constant of $2X10^{9}$ M^{-1}) (Downs & Jackson 2004, Mimori *et al.* 1986, Walker *et al.* 2001, Blier *et al.* 1993). Binding of the Ku heterodimer to DNA is achieved by sliding of the DSB end through its central *β*-barrel ring structure (Walker *et al.* 2001). In mammalian cells, Ku is thought to bind to all double-ended DNA DSBs and initiates a first attempt at repair by NHEJ, regardless of cell cycle phase (Beucher *et al.* 2009, Shibata *et al.* 2011).

Assembly and stabilization of NHEJ factors

Ku is unquestionably the first NHEJ factor to localize to a DSB. The order of recruitment of factors following Ku is likely to be flexible and dependent on the complexity of the break (Davis & Chen 2013). Break complexity is also likely to define which factors are necessary for the completion of the NHEJ process. For example, a break that shares a microhomology consisting of two perfectly complementary 4bp overhangs can be repaired by XRCC4 and DNA ligase IV alone, without Ku, at least *in vitro* (Gu *et al.* 2007). However, such perfect microhomologies are very rare in nature, and efficient NHEJ typically requires an orchestrated use of many factors that are able to function alone as well as synergistically (Davis & Chen 2013). Many of these factors play important roles in several of the steps involved in NHEJ, as will be discussed below.

The Ku-DNA complex is thought to function as a scaffold to which multiple NHEJ proteins can bind (Davis & Chen 2013). In vertebrates Ku is able to directly recruit the phosphatidylinositol 3' kinase-like kinase (PIKK) DNA-PK_{cs} in the presence of DNA (Gottlieb & Jackson 1993). DNA-PK_{cs} forms a complex with Artemis, and together have important functions in the processing of DSB termini (Lieber 2010). Recruitment of the XRCC4-DNA Ligase IV-XLF complex (corresponding to Lif1-Dnl4-Nej1 in budding yeast) is also dependent on Ku. Ku70 physically interacts with XRCC4 (Mari *et al.* 2006) and the Ku heterodimer physically interacts with the tandem BRCA1

C-terminal (BRCT) domains in the C-terminus of DNA Ligase IV (Costantini *et al.* 2007, Hsu *et al.* 2002). An interaction between the Ku heterodimer and the C-terminus of XLF recruits XLF to the DNA end in a DNA-dependent manner (Yano *et al.* 2008, Yano *et al.* 2011). Aprataxin-and-PNK-like factor (APLF) is known to bind the Ku80 vWA domain via a conserved peptide in the protein's MID domain (Grundy *et al.* 2013).

XRCC4 is thought to function as a second NHEJ scaffold with complex roles in NHEJ such as securing the ability of processing enzymes and accessory proteins to interact with the DSB (Davis & Chen 2013). XRCC4 has no known enzymatic activity and contains a globular head, alpha-helical stalk and a C-terminal tail domain (Junop *et al.* 2000). DNA ligase IV interacts with the XRCC4 alpha-helical stalk via the linker region between its tandem C-terminal BRCT domains (Sibanda *et al.* 2001, Wu et al. 2009). Polynucleotide kinase-phosphatase (PNKP), Aprataxin (APTX) and APLF also interact with XRCC4 via their FHA domains in a manner dependent on casein kinase 2 (CK2) phosphorylation of XRCC4 (Koch *et al.* 2004, Kanno *et al.* 2007, Macrae *et al.* 2008, Iles *et al* 2007, Clements *et al.* 2004). Several proteins involved in processing require both Ku and XRCC4 for recruitment to the DNA DSB, including the DNA polymerase u and the RecQ helicase family member Werner (WRN) (Mahajan *et al.* 2002, Cooper *et al.* 2000, Karmakar *et al.* 2002, Kusumoto *et al.* 2008). The NHEJ complex assembled thus far is stabilized by Ku, DNA-PK_{cs} and XRCC4 (Yano *et al.* 2009). APLF has also been implicated in assembling NHEJ components and appears to have a major role in retaining XRCC4, DNA ligase IV and XLF at the DSB (Grundy *et al.* 2013).

Positional stabilization and tethering of DSB termini

Ku has an important role in protecting the DSB ends from spurious processing that could result in the generation of chromosomal aberrations (Davis & Chen 2013). This is likely due to its ability to draw and hold the DSB ends together in a synaptic complex (Pang *et al.* 1997). Another protective role of Ku arises from the ability of Ku80 to prevent DSB ends from 'roaming' the nucleus. A positionally stabilized DSB is unable to locate other breaks in the nucleus, which might lead to a damaging translocation. This positional stabilization was found to be independent of DNA repair factors, H2A.X, MRN and the cohesin complex (Soutoglou *et al.* 2007). DNA-PK_{cs} forms a distinct structure at the DSB after its recruitment by Ku and is thought to form a synaptic complex that tethers DSB termini (Cary *et al.* 1997, Weterings & van Gent 2004). Recent structural insights indicate that the DNA-PK_{cs} HEAT repeats function as compressible macromolecular springs (Williams *et al.* 2014). These are thought to

regulate the transfer of energy within the NHEJ flexing scaffold to control its overall conformation (Williams *et al.* 2014). The globular head domain residues Arg54, Leu65 and Leu115 of XRCC4 interact with the globular head of XLF, which through alternating head domain interfaces form super helical filaments that bridge DSB termini (Hammel *et al.* 2010, Andres *et al.* 2012). These filaments might function as an additional or alternative bridging and tethering mechanism. However, the co-ordination between bridging and tethering by Ku-DNA-PK_{cs} and XRCC4-XLF is unknown (Davis & Chen 2013).

Processing of the DSB termini

Processing is necessary to transform a break that cannot be ligated into a ligatable substrate. Numerous proteins are implicated in processing, including Artemis, PNKP, APLF, the DNA polymerases u and y, WRN, APTX and Ku (Davis & Chen 2013). These proteins can variously perform the removal of blocking end groups, resection, and gap filling. Again, the precise nature of the DSB determines which factors are required to produce a ligatable substrate.

The proteins PNKP and APTX have been shown to remove blocking end groups from DSB termini (Bernstein *et al.* 2005, Ahel *et al.* 2006). PNKP has dual kinase and phosphatase activity; its kinase domain can add phosphate groups to 5' hydroxyls and the phosphatase removes 3' phosphate groups (Bernstein *et al.* 2005). APTX belongs to the histidine triad family of nucleotide hydrolases and transferases and removes adenylate groups covalently linked to the termini of 5' phosphates (Ahel *et al.* 2006).

DNA-PK_{cs} exists in complex with Artemis, which together perform the majority of the short-range resection in NHEJ by utilizing a diverse array of nuclease activities (Lieber 2010). Upon DNA binding DNA-PK_{cs} acquires serine/threonine phosphatase activity (Hartley *et al.* 1995). Phosphorylation of Artemis by DNA-PK_{cs} stimulates 5' endonuclease, 3' endonuclease and hairpin opening nuclease activities (Ma *et al.* 2002), allowing the resection of a wide range of damaged DNA overhang types (Ma *et al.* 2005, Yannone *et al.* 2008). WRN has 3' to 5' exonuclease activity that is dependent on its interaction with Ku and XRCC4, whilst its 3' helicase activity is not (Cooper *et al.* 2000, Kusomoto *et al.* 2008, Perry *et al.* 2006). APLF has endonuclease and 3' to 5' exonuclease activity that is not dependent on any other NHEJ factors. However, resection of 3' overhangs by APLF is required *in vitro* for the subsequent ligation step by DNA ligase IV-XRCC4 (Kanno *et al.* 2007, Li *et al.* 2011).

Nucleotide gap filling is performed by the Pol X family polymerases mu and lambda. Polymerase mu is an error-prone polymerase that reduces the incidence of deletion events and is capable of template-dependent synthesis with dNTPs and rNTPs, as well as template-independent synthesis (Moon *et al.* 2007). The incorporation of uracil at the break site is thought to be important in G1 NHEJ when levels of rNTPs are high and dNTPs low. The uracil can possibly then be altered at a later time after base removal by uracil glycosylases (Nick McElhinny & Ramsden 2003). Polymerase mu can polymerize across a discontinuous template strand in the presence of Ku and DNA ligase IV-XRCC4 to effectively cross the two ends of DSB (Nick McElhinny *et al.* 2005, Davis *et al.* 2008). In addition, by adding nucleotides to the 3' ends of the break polymerase-generated microhomology can be achieved to increase the efficiency of ligation (Gu *et al.* 2007). Polymerase lambda also has known roles in NHEJ gap filling, including template-dependent functions in magnesium buffers and template-independent activity in manganese buffers (Bertocci *et al.* 2006, Lee *et al.* 2004, Ramadan *et al.* 2004, Moon *et al.* 2007).

The MRX (Mre11-Rad50-Xrs2) complex performs the comparable resection and tethering roles of DNA-PKcs in budding yeast

In yeast, MRX (Mre11-Rad50-Xrs2) localizes to the DNA DSB in a temporally similar manner to that of Ku and has roles in the detection, signaling, protecting NHEJ, HR and DNA damage checkpoint activation (Daley *et al.* 2005). MRX is critical for some of the resection in NHEJ and is also likely to facilitate the tethering and synapsis of DSB ends (Daley *et al.* 2005). It appears that in vertebrates the DNA-PK_{cs}-Artemis nuclease system evolved to replace that of MRX during the inception of V(D)J recombination (a B or T cell-specific physiological system that makes intentional DSBs for generating antigen receptor genes) at the vertebrate/invertebrate transition (Falck *et al.* 2005, Lieber 2010).

Mre11 has critical roles in the detection, signalling, protection and repair of DNA DSBs (Stracker & Petrini 2011, Williams *et al.* 2007, Wyman & Kanaar 2006). Mre11 is an SbcCD family nuclease capable of DNA binding, 3' to 5' dsDNA exonuclease, ssDNA structure-specific endonuclease, hairpin nuclease and strand-annealing activities (Paull & Gellert 1998, Trujillo *et al.* 1998, Hopfner *et al.* 2000, Lim *et al.* 2011). Two Rad50 proteins each contribute a split ABC ATPase domain that associate to form a functional Rad50 ABC ATPase. The resulting Rad50 dimer is stabilised by Mre11, which additionally locks residues around the ATP-binding site and facilitates efficient Rad50 ATP hydrolysis (Lim *et al.* 2011). This drives a substantial conformational

change in both Rad50 and Mre11 that dislocates Rad50 from the Mre11 nuclease domain and subsequently exposes its active site (Lim *et al.* 2011). This is thought to be necessary for critical MRX functions, including tethering of DSB ends, Mre11 endonuclease activity and DNA-unwinding activity (Trujillo & Sung 2001, Lim *et al.* 2011). One hypothesis for a tethering mechanism follows that two Rad50 proteins bound to each DSB end interact through association of Zn hook structures present at the tips of a long looped coiled coil region. This reduces the volume and entropy for the ensuing NHEJ reaction (Hopfner *et al.* 2002, Daley *et al.* 2005).

Xrs2 has intrinsic DNA binding affinity and is required for binding MRX to DNA and bridging DSB ends (Trujillo *et al.* 2003). The protein contains N-terminal forkhead-associated (FHA) domains that interact with phosphorylated threonine residues in Lif1, highlighting an NHEJ-specific function of Xrs2 (Chen *et al.* 2001, Matsuzaki *et al.* 2008, Palmbos *et al.* 2008). The C-terminus of Xrs2 contains BRCT domains that interact with the phosphatidylinositol 3' kinase-like kinase (PIKK) Tel1, highlighting a critical role of MRX in DNA damage checkpoint activation, discussed later (Daley *et al.* 2005, Falck *et al.* 2005, Becker *et al.* 2006, Palmbos *et al.* 2008).

1.2.3. Homologous recombination

In contrast to NHEJ homologous recombination (HR) is an error-free DSB repair mechanism that relies on the availability of an intact sister chromatid, and therefore is restricted to late S and G2 phases of the cell cycle. In mammalian cells, HR overlaps with NHEJ in the repair of two-ended DSBs, and also promotes replication fork stabilization and one-ended DSB repair (Jeggo *et al.* 2011, Schlacher *et al.* 2011). HR can proceed via several distinct pathways: double-strand break-repair (DSBR), synthesis-dependent strand annealing (SDSA), single-strand annealing (SSA) and break-induced replication (BIR) (San Filippo *et al.* 2008). Correctly regulating the choice of pathway and their activities is important for maintaining genome integrity, since some forms of HR can lead to detrimental rearrangements. In this section an overview of these various HR mechanisms, the steps involved in each and their regulation will be provided.

The DSBR model involves the following steps: nucleolytic 5' to 3' resection of DSB ends to yield single-stranded DNA (ssDNA) termini, formation of a recombinase filament on the ssDNA, strand invasion into a homologous DNA sequence to form a D-loop, extension of the invading strand from the 3' end by DNA polymerase, capture of the second DSB end by annealing to the extended D-loop, formation of two Holliday junctions (HJs), and finally HJ resolution to yield crossover or noncrossover products

(San Filippo *et al.* 2008). SDSA differs from the DSBR model in that it envisages a migrating D-loop that does not result in capture of the second DSB end. After resection, strand invasion and DNA synthesis the invading strand is displaced and anneals to the second resected DSB end; no HJ is formed and thus only crossover products result (San Filippo *et al.* 2008). SSA is a deletion process that involves annealing of resected ssDNA strands to each other instead of engaging a homologous template, and occurs when a DSB is flanked by direct repeats (San Filippo *et al.* 2008). Single-ended DSBs that occur at telomeres and replication forks are repaired by BIR, which involves invasion of a single ssDNA strand into a donor DNA sequence (Lydeard *et al.* 2007).

DNA resection

The first stage in HR is 5' to 3' resection of the DSB ends. This is a complex and tightly regulated process involving redundant pathways containing nucleases, DNA helicases and other associated proteins (Niu *et al.* 2010). The MRX complex (human MRN; MRE11-RAD50-NBS1) and Sae2/CtIP) can directly initiate resection by generating short 3' ssDNA tails, or indirectly by recruiting the 5'-3' exonuclease Exo1/EXO1, the helicase Sgs1/BLM, and the endonuclease Dna2/DNA2 (Mimitou & Symington 2008, Mimitou & Symington 2010, Shim *et al.* 2010, Zhu *et al.* 2008). The generation of long 3' tails through long-range resection requires Exo1 or Sgs1-Top3-Rmi1 (STR complex) in association with Dna2 (Gravel *et al.* 2008, Mimitou & Symington 2008, Zhu *et al.* 2008). As described previously, Mre11 possesses endonuclease and exonuclease activity. A fascinating recent study showed that specific inhibition of MRE11 endonuclease activity promoted NHEJ in lieu of HR in IR-treated G2 cells, whilst inhibiting the exonuclease activity led to a DNA repair defect (Shibata *et al.* 2014). These findings indicate that the endonuclease activity is required to initiate resection, thus licensing repair via HR. The subsequent exonuclease activity in concert with EXO1/BLM promotes long-range resection that results in commitment to HR (Shibata *et al.* 2014).

The Fun30 (human SMARCAD1) Snf2-family ATPase chromatin remodeller was recently found to promote Exo1/EXO1- and Sgs1/BLM-dependent resection in *S. cerevisiae* and human cells (Costelloe *et al.* 2012, Chen *et al.* 2012). As discussed later, the differential regulation of resection during the cell cycle is a critical determinant of DNA pathway choice in mammalian cells (Symington & Gautier 2011).

RPA and Rad51 binding to ssDNA

The heterotrimeric replication protein A (RPA) is the first protein to bind ssDNA and has various regulatory roles in HR (Krejci *et al.* 2012). Firstly, RPA has several roles in resection itself: it stimulates Sgs1 helicase activity, enhances 5' strand incision by Dna2 and protects the 3' strand from its degradation (Cejka *et al.* 2010, Niu *et al.* 2010). RPA also removes secondary structure in ssDNA to facilitate the assembly of multiple Rad51 recombinase proteins (Sung *et al.* 2003), which in the presence of ATP forms a right-handed helical polymer, known as a presynaptic filament (San Filippo *et al.* 2008). Once a Rad51-mediated D-loop has formed RPA prevents its reversal by sequestering and scavenging ssDNA. This serves to prevent DNA from entering Rad51's second DNA-binding site (Eggler *et al.* 2002, Van Komen *et al.* 2002). RPA can also inhibit Rad51 association and thus has stimulatory and inhibitory roles in HR. RPA has a higher binding affinity for ssDNA than Rad51 and is recruited earlier, yet for HR to proceed correctly RPA must be displaced by Rad51, aided by various mediator proteins (Krejci *et al.* 2012).

RPA is SUMOylated in both yeast and humans upon DNA damage, and RPA70 SUMOylation in human cells facilitates RAD51 foci formation, promotes HR and DNA damage resistance (Burgess *et al.* 2007, Dou *et al.* 2010). RPA SUMOylation is also required for the recruitment of RPA to DNA damage sites (Galanty *et al.* 2009, Morris *et al.* 2009). Disruption of the SUMO pathway also leads to defective RAD51 trafficking and impaired RAD51 foci formation in human cells (Saitoh *et al.* 2002). RPA is phosphorylated by the DNA damage checkpoint kinase Mec1 (ATM in humans) and cell cycle cyclin-dependent kinases (CDKs). RPA phosphorylation is critical for recruitment of Rad51 to DSBs and increases the affinity of Rad52 for ssDNA (Zou & Elledge 2003, Shi *et al.* 2010). Rad51 is also phosphorylated by various kinases with several regulatory effects on the protein. These include enhanced DSB repair and drug resistance in the case of Try315 phosphorylation by BCR/ABL, inhibition of Rad51 binding and ATPase-dependent strand-exchange in the case of Tyr54 phosphorylation by c-ABL (Slupianek *et al.* 2011, Yuan *et al.* 1998), and enhanced ATPase and DNA binding activity in the case of Ser192 phosphorylation by Mec1 (Flott *et al.* 2011). Phosphorylation of human RAD51 at Ser14 by PLK1 triggers adjacent Ser13 phosphorylation by casein kinase 2 (CK2), to which NBS1 (MRN complex) then binds to facilitate Rad51 recruitment (Yata *et al.* 2012).

Human cells contain the two additional ssDNA binding proteins SSB1 and SSB2 that are part of the DSB sensing complex. These proteins are required for ATM signalling, and loss of either results in defective DNA damage checkpoint activation

and impaired HR (Richard *et al.* 2008, Huang *et al.* 2009, Li *et al.* 2009). SSB1 also has a role in DSB processing by stimulating MRN activity via interaction with NBS1 (Richard *et al.* 2011).

Mediators of Rad51

Proteins referred to as Rad51 mediators are able to overcome RPA's inhibitory effect on Rad51 and include Rad52, paralogues of Rad51, Rad55 and Rad57. They function to facilitate Rad51 loading onto ssDNA, stabilize the presynaptic filament and protect Rad51 from removal by various factors (Krejci *et al.* 2012). Rad52 interacts with Rad51 as well as ssDNA-bound RPA (Seong *et al.* 2008, Shinohara *et al.* 1992). Rad52 binding to Rad51 is required for efficient recruitment and nucleation of Rad51 onto ssDNA (Krejci *et al.* 2002, Shinohara & Ogawa 1998). However, the concomitant displacement of RPA during Rad51 filament assembly is not conducted directly by Rad52, but rather by the action of Rad51 polymerization along the ssDNA (Song & Sung 2000, Sugiyama *et al.* 1998). The C-terminus of Rad52 is responsible for Rad51 and DNA binding, whilst its central region interacts with RPA and is important for repair foci localization (Seong *et al.* 2008, Plate *et al.* 2008). The N-terminus is involved in oligomerization, DNA binding and annealing, and interacts with the homologous Rad59 protein (Shinohara & Ogawa 1998, Davis & Symington 2001, Mortensen *et al.* 1996). Both Rad52 and Rad59 promote second end capture during DSBR as well as strand annealing during SSA (McIlwraith & West 2008, Nimonkar *et al.* 2009. Human RAD52 does not possess mediator activity lacks the C-terminal regions of yeast Rad52 involved in Rad51 and RPA interactions; in this regard it is more similar to yeast Rad59 (Seong *et al.* 2008, Krejci *et al.* 2012). Human RAD52 can perform strand annealing and acts in parallel with BRCA2 (discussed below) (Feng *et al.* 2011, Singleton *et al.* 2002, Van Dyck *et al.* 2001). RAD52 also has a late role in HR at stalled forks not shared by BRCA2.

In budding yeast Rad52 is SUMOylated on lysines 10, 11 and 220 after DNA damage in S-phase, with diverse outcomes that are dependent on the DNA substrate (Ohuchi *et al.* 2008, Ohuchi *et al.* 2009, Krejci *et al.* 2012). In human cells, SUMOylation of RAD52 is not induced upon DNA damage but instead alters RAD52 subcellular localization (Saito *et al.* 2010). Rad52 is constitutively phosphorylated in yeast and occurs at Try104 following DNA damage in humans (Antunez de Mayolo *et al.* 2006, Kitao & Yuan 2002). This modification might direct RAD52 to DNA repair intermediates that undergo strand annealing (Honda *et al.* 2011).

Rad55 and Rad57 both have ATPase activity like Rad51, and assemble as a heterodimeric ssDNA-binding complex, however they cannot stimulate strand exchange (Hays *et al* 1995, Johnson & Symington 1995, Sung 1997). Rad55-Rad57 interacts with Rad51 to facilitate its loading onto RPA-coated ssDNA. The heterodimer also forms co-filaments with Rad51 that resists the anti-recombinase action of Srs2 (discussed later) (Liu *et al.* 2011). Rad55 is phosphorylated at Ser2, 8 and 14 by DNA damage checkpoint kinases to promote Rad51 function (Herzberg *et al.* 2006). The Shu complex, consisting of Shu1, Psy3, Shu2 and Csm2 is a poorly understood positive regulator of Rad51 that appears to have specialized roles in HR during replication stress (Mankouri *et al.* 2007).

In human cells several paralogues of RAD51 function as RAD51 mediators and share 20-30% sequence identity to RAD51. Two RAD51 paralogue complexes exist: the first consists of RAD51B, RAD51C, RAD51D and XRCC2 and has a high affinity for branched DNA damage substrates such as stalled replication forks (Masson *et al.* 2001, Badie *et al.* 2009, Henry-Mowatt *et al.* 2003, Petermann *et al.* 2010, Yokoyama *et al.* 2004); the second consists of RAD51C and XRCC3 and associates with HJ resolution activity (Kuznetsov *et al.* 2007, Liu *et al.* 2007).

BRCA2 fulfils Rad52 mediator roles in mammalian HR and is regulated by several proteins

BRAC2 functions as the central RAD51 mediator in human cells despite the presence of RAD52 and has no homology to RAD52. As the central mediator BRCA2 controls RAD51 nucleofilament assembly (San Filippo *et al.* 2008, Thorslund & West 2007) and contains two types of BRC repeat domains that interact with RAD51. The first type targets RAD51 to ssDNA and stabilizes the RAD51 nucleofilament in its active form by down-regulating its ATPase activity. The second type prevents RAD51 necleation onto dsDNA (Carreira *et al.* 2009, Carreira & Kowalczykowski 2011, Pellegrini *et al.* 2002, Shivji *et al.* 2009). An additional interaction with RAD51 in its filament form exists with the C-terminus of BRCA2. This interaction is under cell cycle control and appears to be important for nucleofilament and replication fork stability (Davies & Pellegrini 2007, Esashi *et al.* 2007, Ayoub *et al.* 2009, Shlacher *et al.* 2011).

The proteins DSS1, PALB2 and MCPH1 function as regulators of BRCA2. DSS1 interacts with the C-terminal DNA-binding domain (DBD) of BRCA2 and facilitates BRCA2-mediated RAD51 filament formation (Yang *et al.* 2002, Sonoda *et al.* 1998). PALB2 interacts with the N-terminus of BRCA2 and has several roles in HR, including stabilizing BRCA2 by promoting its chromatin association and by possibly

affecting RAD51 function directly. PALB2 oligomerization is also known to promote the delivery and stabilization of RAD51 at DSBs (Xia *et al.* 2006, Sy *et al.* 2009). MCPH1 (microcephalin) is another BRCA2-interacting protein that negatively regulates BRCA2 by reducing levels of BRCA2 and RAD51 at DSBs (Wu *et al.* 2009).

Rad54 and Rdh54 have multiple roles in regulating Rad51

The Snf2/Swi2 family DNA-dependent ATPase helicases Rad54 and Rdh54 are able to translocate along duplex DNA and have multiple roles in HR (Krejci *et al.* 2012). They can positively regulate Rad51 by stabilizing pre-synaptic filaments, stimulating Rad51-mediated strand invasion, and at least in the case of Rad54 enhance D-loop branch migration. Rad54 and Rdh54 also function as negative Rad51 regulators by limiting the non-specific binding of Rad51 to dsDNA, as well as by removing Rad51 to allow access to 3'-OH primer termini for DNA replication (Krejci *et al.* 2012). Rad54 activity is regulated by ubiquitination and phosphorylation. Ubiquitin-mediated proteolysis controls Rad54 activity in G1-phase *S. pombe* cells (Trickey *et al.* 2008), and Rad54 is phosphorylated by Rad53, suggesting its activity is regulated by the DNA damage checkpoint (Chen *et al.* 2010).

Negative regulators of Rad51

Srs2 is a 3'-5' SF1 helicase able to dismantle Rad51 presynaptic filaments in budding yeast (Aboussekhra *et al.* 1989, Krejci *et al.* 2003, Veaute *et al.* 2003), an activity that requires its translocase function and interaction with Rad51. This activity is further enhanced in the presence of RPA, which prevents Rad51 re-nucleation (Krejci *et al.* 2003, Veaute *et al.* 2003, Colavito *et al.* 2009, Krejci *et al.* 2004, Seong *et al.* 2009). Null mutants of *srs2* are characterized by increased rates of spontaneous recombination (Aguilera & Klein 1988), synthetic lethality with deletion of the RecQ helicase *sgs1* (Lee *et al.* 1999, Wang *et al.* 2001), and hypersensitivity to various sources of DNA damage (Bennett *et al.* 2001, Aboussekhra *et al.* 1992, Birrell *et al.* 2002). Srs2 is phosphorylated in a Cdk1-dependent manner and this modification promotes the use of the SDSA pathway (Saponaro *et al.* 2010). Srs2 is also SUMOylated but the function of this is less clear (Krejci *et al.* 2012).

A functional analogue of Srs2 was first identified in *C. elegans,* known as SPAR-1, and subsequently in vertebrates, known as RTEL1 (regulator of telomere length 1) (Barber *et al.* 2008). Deletion of *spar-1* in *C. elegans* resulted in synthetic lethality with deletion of the RecQ helicases *him-6* (human *BLM)* and *rcq-5* (human

RECQ5). The synthetic lethality was accompanied by a massive accumulation of recombination intermediates, and *spar-1* single mutants displayed elevated meiotic recombination and hypersensitivity to DNA damage that specifically affects replication fork progression (Barber *et al.* 2008). Moreover, depletion of human RTEL1 led to increased recombination and hypersensitivity to mitomycin C (MMC), but not IR (Barber *et al.* 2008). RTEL1 was also found to prevent D-loop formation *in vitro,* but rather than disassembling presynaptic filaments this activity was due to disrupting pre-formed D-loops (Barber *et al.* 2008). Collectively, these findings indicate that RTEL1 is critical for supressing HR, which is likely to have importance for preventing genome instability and cancer.

More recent studies have further revealed that RTEL1 functions as a prominent genome stability factor, with key roles in DNA replication, recombination, DNA repair and maintenance of telomere integrity (Vannier *et al.* 2012, Uringa *et al.* 2012, Vannier *et al.* 2013, Vannier *et al.* 2014). RTEL1 removes telomeric DNA secondary structures, such as T-loops and G-quadruplex (G4) DNA, to prevent telomere fragility and loss (Vannier *et al.* 2012). In mouse cells, loss of Rtel1 leads to misregulated recombination, defective telomere replication, and facilitates telomere elongation by telomerase (Uringa *et al.* 2012). RTEL1 has also been linked to global replication through an interaction with PCNA (proliferating cell nuclear antigen) (Vannier *et al.* 2013). Disruption of the RTEL1-PCNA interaction led to accelerated senescence, replication fork instability and reduced fork extension (Vannier *et al.* 2013). Furthermore, tumourigenesis onset was accelerated in p53-deficient mice compromised for the RTEL1-PCNA interaction (Vannier *et al.* 2013). Intriguingly, significance-associated SNPs within *RTEL1* introns 15 and 17 have been identified in cases of glioma and astrocytoma (Wrensch *et al.* 2009, Shete *et al.* 2009), suggesting that that the various roles of RTEL1 in maintaining genome stability represent important tumour suppressor activities.

The Mph1 translocase (FANCM in humans) is also able to disrupt Rad51-coated D-loops, stimulate branch migration and displace the extended primer in D-loop-associated DNA synthesis (Gari *et al.* 2008, Prakash *et al.* 2009, Sun *et al.* 2008, Zheng *et al.* 2011, Sebesta *et al.* 2011). Consequently, a prominent role of Mph1 is in channelling HR into the SDSA pathway over DSBR to supress potentially deleterious crossovers in mitotic cells (Prakash *et al.* 2009). The RecQ family helicase Sgs1 forms a complex with Top3 and Rmi1 in yeast (Ahmad & Stewart 2005, Chang *et al.* 2005) and is homologous to BLM in mammalian cells. Like BLM, Sgs1 might directly

dismantle presynaptic filaments (Bugreev *et al.* 2007, Ira *et al.* 2003, Mankouri *et al.* 2002). Addition roles include the elimination of aberrant invasion events, resolution of recombination intermediates (Oh *et al.* 2007, Oh *et al.* 2008), dissolution of dHJs to yield non-crossovers (Cejka *et al.* 2010, Wu & Hickson 2003), and possibly direction of D-loop intermediates away from DSBR and into SDSA (Krejci *et al.* 2012). SUMOylation of Sgs1 is known to promote recombination at telomeres at least in yeast (Lu *et al.* 2010), whilst SUMOylation of BLM in human cells leads to increased Rad51 binding and promotes HR at stalled replication forks (Ouyang *et al.* 2009).

1.2.4. The DNA damage response in budding yeast

The DNA damage checkpoints trigger cell cycle arrest in response to a DSB or defective replication fork to provide time for the cell to deal with the problem. Without this mechanism damaged or mutated DNA will be segregated and can lead to genome instability or cell death. In budding yeast Mec1 and Tel1 represent the two major upstream 'sensor' phosphatidylinositol 3' kinase-like kinases (PIKKs) (Tsaber & Haber 2013). These are recruited to the site of damage by interaction with other DNA damage response (DDR) proteins, and promote checkpoint activation through two interrelated processes. Firstly, they phosphorylate S129 on H2A.X that triggers a signalling cascade and recruits many additional DDR factors. Secondly, they activate the downstream 'effector' kinases Rad53 and Chk1, which have multiple targets involved in enforcing an appropriate cellular response to the problem.

Recruitment of the sensor kinases Mec1 and Tel1

Tel1 is directly recruited to MRX-bound DSBs through interaction with the C-terminus of Xrs2 (Nakada *et al.* 2003). Tel1 phosphorylates H2A.X S129 but cannot spread this modification far beyond the DSB due to its restrictive association with MRX (Tsaber & Haber 2013). Because DSBs in G1 cells remain relatively unresected Tel1 alone phosphorylates H2A.X at S129 to become γ-H2A.X. Recruitment of Mec1 to a DSB is indirectly dependent on MRX, which initiates resection upon binding to the DSB to yield ssDNA that is coated by RPA (Tsaber & Haber 2013). Mec1-Ddc2 is recruited to the DSB via an interaction between RPA and Ddc2. Mec1 also phosphorylates H2AX at S129, which initially spreads over a range of ~50kb on either side of the DSB within 15-30 minutes (Shroff *et al.* 2004). Continued resection along the length of the chromosome at a slower rate facilitates further spreading of γ-H2A.X as Mec1-Ddc2 binds to the newly recruited RPA (Kim *et al.* 2007).

γ-H2A.X is required in conjunction with H3K79 methylation for the adapter protein Rad9's recruitment to the DSB (Shroff *et al.* 2004, Javaheri *et al.* 2006). Mec1 also phosphorylates Rad9 at multiple S/TQ motifs, which subsequently interact with Rad53 FHA domains. This activates Rad53 and induces extensive Rad53 autophosphorylation (Sun *et al.* 1998). Phosphorylated Rad9 and Rad53 then dissociate in a complex that subsequently multimerizes, resulting in further trans-autophosphorylation of Rad53 (Harrison & Haber 2006). Fully activated Rad53 then dissociates from the complex before interacting with and/or phosphorylating a myriad of effector proteins involved in cell cycle arrest and/or DSB repair (Harrison & Haber 2006)

1.2.5. The DNA damage response in human cells

Activation of ATM and H2AX phosphorylation

In mammalian cells H2A.X phosphorylation at S139 occurs within one minute following DSB induction (Bewersdorf *et al.* 2006, Celeste *et al.* 2002, Rogakou *et al.* 1998, Rogakou *et al.* 1999) and is largely dependent on the Mec1 homologue Ataxia-Telangiectasia Mutated (ATM). In NHEJ DNA-PK_{cs} mediates H2A.X phosphorylation downstream of ATM, whilst the Tel1 homologue ATM- and Rad3-related (ATR) in association with ATRIP (Ddc2 homologue) appear to promote H2A.X phosphorylation once recruited to ssDNA after DNA processing at replication forks (Pinto & Flaus 2010). ATM and ATR phosphorylate CHK2, and CHK1, respectively, which leads to their activation (Jazayeri *et al.* 2006). The maintenance of IR-induced checkpoint arrest in G2 requires sustained ATM-CHK2 activation as well as resection-dependent ATR-CHK1 activation (Shibata *et al* 2010). Phosphorylated CHK1 and CHK2 target CDC25, which inactivates cyclin-dependent kinases (CDKs), leading to cell cycle arrest (Jazayeri *et al.* 2006)

Activation and recruitment of ATM as a consequence of ATM-mediated autophosphorylation is proposed to be dependent on local DNA conformational changes, the presence of MRE11-RAD50-NBS1 (MRN) (Lee & Paull 2007), and the activity of the histone acetyltransferases (HATs) MOF1 and TIP60 (Gupta *et al.* 2005, Sun *et al.* 2005). Depletion of MOF1, which acetylates H4K16 leading to abrogated 30nm fibre formation and global chromatin compaction, results in impaired ATM activity (Shogren-Knaak *et al.* 2006). Indeed, γ-H2AX formation occurs preferentially in euchromatin (Kim *et al.* 2007), suggesting that a more condensed chromatin structure attenuates ATM activity. Binding of TIP60 to H3K9me3 via its chromodomain promotes

acetylation of ATM by TIP60, leading to ATM activation (Sun *et al.* 2009). Recently, DNA damage-dependent phosphorylation of TIP60 on T44 was shown to increase the binding of TIP60 to H3K9me3, leading to ATM activation (Kaidi & Jackson 2013).

Recruitment of factors required for amplification of the DDR

Mediator of DNA damage checkpoint protein 1 (MDC1) binds to γ-H2A.X via its BRCT domain, and MDC1 recruitment is essential for ionizing radiation-induced foci (IRIF) and G2 checkpoint maintenance (Jungmichel & Stucki 2010, Stucki *et al.* 2005, Shibata *et al.* 2010). MDC1 recruitment initiates a positive-feedback loop that perpetuates the expansion of γ-H2A.X by recruiting more ATM (Lou *et al.* 2006, Stucki *et al.* 2005). MDC1 is phosphorylated by casein kinase 2 (CK2) at several repeated motifs and is required for an interaction between MDC1 and NBS1 that retains MRN at IRIFs (Chapman & Jackson 2008, Melander *et al.* 2008, Spycher *et al.* 2008, Wu *et al.* 2008). Subsequent DNA end processing by MRN stimulates the recruitment of additional ATM (Lee & Paull 2007). Binding of MDC1 to γ-H2A.X directly or indirectly requires MOF1-dependent acetylation of H4K16 (Li *et al.* 2010) and is also negatively regulated by phosphorylated H2A Y142 (Cook *et al.* 2009, Xiao *et al.* 2009).

γ-H2A.X appears to stimulate the binding of the HATs GCN5, p300, CBP and TIP60 that acetylate various lysine residues on H3 and H4 of DSB-flanking nucleosomes (Deem *et al.* 2012). These acetylation marks are required for the recruitment of SWI/SNF chromatin remodeling complexes (discussed later) and various other DDR proteins. TIP60 mediates H4 acetylation that can extend for several kilobases flanking the DSB and promotes the recruitment of MDC1, 53BP1, BRCA1 and RAD51 (Murr *et al.* 2006).

Recruitment and activity of the DDR mediator and effector 53BP1

53BP1 (Rad9 homologue) is a core component of the DNA DSB response, functioning as a scaffold for other DSB factors, a DNA damage checkpoint mediator, and a critical determinant of DNA repair pathway choice (Panier & Boulton 2014). The DSB proteins 53BP1 exerts its critical checkpoint function by stimulating ATM activity via an interaction between its C-terminal BRCT domains and the RAD50 component of MRN, which recruits ATM (Lee & Paull 2007).

Recent studies have shed light on how several histone PTMs direct 53BP1 recruitment specifically to chromatin adjacent to DNA DSBs. The E3 ubiquitin ligase ring finger 8 (RNF8), in association with the E2 conjugating enzyme UBC13 (and other

E2 enzymes), is recruited to the DSB via direct interaction with phosphorylated MDC1 (Huen *et al.* 2007, Kolas *et al.* 2007, Mailand *et al.* 2007). RNF8 then ubiquitinates an unknown substrate, which serves as a binding site for a second E3 ubiquitin ligase RNF168, which ubiquitinates H2AK13 and/or K15 in association with UBC13 (Gatti *et al.* 2012, Mattiroli *et al.* 2012). Recruitment of 53BP1 to sites of DNA damage requires the simultaneous recognition of H4K20me2 and RNF168-dependent H2AK13/15ub (Fradett-Turcotte *et al.* 2013). 53BP1 binds H4K20me2 via its tandem TUDOR domains (Botuyan *et al.* 2006, Huyen *et al.* 2004), and binds H2AK13/15ub via a small ubiquitination-dependent recruitment (UDR) motif (Fradett-Turcotte *et al.* 2013).

Generation of H4K20me2 occurs in a stepwise manner beginning with SETD8 (SET domain-containing protein 8)-dependent monomethylation of H4K20, which is required for MMSET (multiple myeloma SET domain-containing protein)-dependent generation of H4K20me2 (Hajdu *et al.* 2011, Oda *et al.* 2010, Pei *et al.* 2011). Proteins including the histone demethylase JMJD2A and the Polycomb protein L3MBTL1 also bind to H4K20me2 independently of DNA damage (Acs *et al.* 2011, Mallette *et al.* 2012). A current model for 53BP1 binding to DNA damage sites follows that JMJD2A and L3MBTL1 are released from chromatin adjacent to the DSB in an RNF8- and RNF168-dependent manner (Acs *et al.* 2011, Mallette *et al.* 2012). As a result, H3K20me2 is exposed, triggering 53BP1 recruitment.

53BP1 recruitment to DNA DSBs is also regulated by DNA damage-induced acetylation. Acetylation of H4K16 by TIP60 reduces the affinity of the 53BP1 Tudour domain for binding to H4K20me2 (Hsiao & Mizzen 2013, Tang *et al.* 2013). In addition, the histone deacetylases HDAC1 and HDAC2 are implicated in positively regulating 53BP1 recruitment by deacetylating H4K16 (Hsiao & Mizzen 2013, Tang *et al.* 2013, Miller *et al.* 2010).

53BP1 regulates DNA repair pathway choice and antagonizes BRCA1

The regulation of 53BP1 binding at DNA DSBs dictates whether NHEJ or HR is utilized for repair (Panier & Boulton 2014). The recently identified association of 53BP1 with the RIF1 (RAP1-interacting factor 1) effector protein appears to be crucial for blocking resection in G1, thus inhibiting HR and channeling DNA repair into the NHEJ pathway (Panier & Boulton 2014). RIF1 interacts (directly or indirectly) with multiple ATM-phosphorylated Ser/Thr-Gln sites in the N-terminus of 53BP1 (Chapman *et al.* 2013, Escribano-Diaz *et al.* 2013, Zimmerman *et al.* 2013, Di Virgilio *et al.* 2013). Another effector protein, PTIP, contains BRCT repeats that interact with phosphorylated Ser25 on 53BP1 in an ATM-dependent manner (Munoz *et al.* 2007). 53BP1 and RIF1 appear

to impact physiological DSB repair, such as class-switch recombination (CSR), and pathological DSB repair, such as joining dysfunctional telomeres (Panier & Boulton 2014). In contrast, PTIP only seems to influence the repair of pathological DSBs. Precisely how 53BP1, RIF1 and PTIP cooperate to inhibit resection during G1 remains largely speculative.

A currently held model follows that during G1, 53BP1-RIF1 bound to the DSB blocks the association of BRCA1 (Escribano-Diaz *et al.* 2013, Feng *et al.* 2013). Through an unclear mechanism, CDK-dependent phosphorylation of MRN-bound CtIP and BRCA1 is prevented, which ultimately blocks resection (Panier & Boulton 2014). During S and G2 phases, TIP60-dependent acetylation of H4K16 reduces the affinity of 53BP1-RIF1 for DSB-flanking chromatin, and CtIP and BRCA1 are phosphorylated by CDK. The subsequent assembly of a CtIP-BRCA1 complex promotes resection, which is enhanced by the SIRT6-dependent removal of a CtIP acetylation mark, thus committing the cell to repair via HR (Panier & Boulton 2014).

1.2.6. The RSC complex in the DNA damage response

RSC was first implicated in the DNA damage response (DDR) after the findings that deletion of several RSC subunits (Rsc1, Rsc2, Rsc7, Rsc30 and Htl1), and a temperature sensitive mutant of Sth1 conferred sensitivity to various DNA damaging agents, including methyl methane sulphonate (MMS), phleomycin, bleomycin, hydroxyurea (HU), UV and IR (Wilson *et al.* 2006, Cairns *et al.* 1999, Bennett *et al.* 2001, Koyama *et al.* 2002, Chai *et al.* 2005). Major advances in understanding how RSC functions in the DDR have been made using the mating-type switching HO system. Mating-type switching in *S. cerevisiae* involves induction of a DNA DSB at the *MAT* locus by HO endonuclease. Repair of this break and switching is achieved by intrachromosomal recombination between one of two silent donor cassettes termed *MAT***α** and *MAT***a**. The HO system relies on the ability to induce HO expression in a strain background in which the donor cassettes have been deleted. Thus, upon HO induction a persistent DSB is generated at a specific locus that can only be finally repaired by an error-prone NHEJ mechanism. Nevertheless, central HR and DNA damage checkpoint proteins are still recruited, along with the associated histone modifications. This allows the temporal and spatial accumulation of DNA repair factors and nucleosome remodelling activity to be monitored at the break by techniques such as ChIP and nucleosome accessibility experiments.

Recruitment of RSC to DNA DSBs

Recruitment of RSC to an HO-induced DSB was first monitored by ChIP using TAP-tagged Sth1. Enrichment of Sth1 relative to an uninduced sample was detected on both sides of the break after 10 minutes, placing RSC recruitment very early in the DNA damage response (Chai *et al.* 2005, Shim *et al.* 2005). Sth1 had returned to basal levels 2hrs after HO induction was terminated (Shim *et al.* 2005). Rsc8 and Rsc1 were also enriched in a temporally similar manner, suggesting that the entire RSC complex was recruited (Shim *et al.* 2005, Shim *et al.* 2007). In contrast, enrichment of the Snf5 subunit of SWI/SNF was only detected after 40 minutes following induction, indicating temporally distinct recruitment profiles between the two complexes (Chai *et al.* 2005). In a strain in which H2A S129 cannot be phosphorylated Sth1 and Rsc1 recruitment was found to be normal. Also, recruitment was not affected by cell cycle phase (Shim *et al.* 2007, Liang *et al.* 2007).

Sth1 enrichment was not detected in the absence of Mre11 and was slightly delayed in the absence of Ku70 (Shim *et al.* 2005). Furthermore, Rsc1 and Rsc2 were found to physically interact with Mre11 and Ku80 in a yeast two-hybrid assay (Shim *et al.* 2005). However, chromatin remodelling by RSC was still observed at the break in the absence of Mre11 (discussed later), indicating that some RSC must be present. Importantly, these ChIP assays calculated the enrichment of RSC relative to an uninduced sample. Therefore the absolute level of RSC present before induction is not revealed and a lack of enrichment does not equate to an absence of RSC (Chambers & Downs 2012). Consistent with prior association before DSB formation, work in our lab showed that Rsc2 and Rsc7 function to establish a normal chromatin structure at *MAT* in the absence of a DSB (Kent *et al.* 2007).

Nucleosome remodelling by RSC at DSBs

DNA DSBs induce a rapid change in the surrounding chromatin structure. Changes in the positions of nucleosomes in chromatin extracted from MNase-treated permeabilized yeast can be visualized using indirect end labelling. Using this technique, the repositioning of 6 proximal nucleosomes away from the break and a slight increase in MNase cleavage efficiency immediately distal to a break at *MAT* was observed (Shim *et al.* 2007, Kent *et al.* 2007). Also, chromatin derived from cross-linked nuclei and subject to MNase digestion was more efficiently cleaved after DSB induction as measured by qPCR (Shim *et al.* 2007). This is consistent with enhanced accessibility of nucleosomal DNA after break induction (Shim *et al.* 2007). These

changes were observed within 30 minutes of DSB formation, are independent of Mre11 (as mentioned previously), and occur in G1, indicating that the event is distinct from subsequent histone eviction by MRX. Furthermore, this nucleosome repositioning is not restricted to the *MAT* locus; its also occurs at HO DSBs present in *URA3* and *LEU2* loci (Kent *et al.* 2007).

The chromatin remodelling event described above was found to be dependent on RSC but not on the other chromatin remodelling complexes SWI/SNF, INO80 or Rad54 (Kent *et al.* 2007). A strain in which Sth1 was conditionally repressed and an *rsc2* null strain did not display significantly increased MNase sensitivity after break induction, suggesting that Sth1 and Rsc2 are important for the remodelling (Shim *et al.* 2007). Conversely, indirect end labelling showed that nucleosome repositioning occurred normally in an *rsc2* null strain (as well as *rsc7* and *rsc30* null strains), but as mentioned previously these cells display altered chromatin structure prior to break induction (Kent *et al.* 2007). However, a defect in remodelling after break induction is observed in an *rsc1* null strain in this assay. It is unclear where the discrepancy in Rsc2 remodelling in these two assays used arises. The MNase sensitivity assay might be more sensitive to occupancy changes within a population, whilst the end labeling might be more sensitive to positional changes. Thus, both Rsc1 and Rsc2 might be involved in break-induced remodelling. It should also be noted that *rsc1* and *rsc2* null strains both retain some RSC function. The relative contributions of each RSC isoform might depend on cell cycle, chromatin context or genomic location (Chambers & Downs 2012).

The effects of RSC on H2A S129 phosphorylation and resection

The very early recruitment of RSC to a DSB parallels that seen for phosphorylation of H2A S129, perhaps indicating that the two events are connected. Rsc1 recruitment was normal in a strain in which H2A S129 cannot be phosphorylated, but defective phosphorylation after a HO-induced DSB or MMS treatment is observed in *rsc* mutants. This places RSC upstream of H2A S129 phosphorylation in the DNA damage response (Shim *et al.* 2007, Liang *et al.* 2007, Kent *et al.* 2007). Consistent with reduced H2A S129 is the observations that Mec1 and Tel1 recruitment are reduced by ~2-fold in an *rsc2* null strain (Liang *et al.* 2007). RSC is also required for efficient DSB-dependent methylation of H3K4 by Set1 (Faucher & Wellinger 2010), indicating that remodelling by RSC is important for downstream chromatin modifications.

Repression of Sth1 leads to reduced Mre11 and Ku70 accumulation at a DSB, suggesting that RSC-dependent remodelling facilitates their binding (Shim *et al.* 2007).

Reduced Mre11 at the break might lead to impaired MRX-stimulated resection. Consistently, a slight reduction in resection is observed in *rsc* mutants as measured by quantitative amplification of ssDNA (QAOS) and restriction site cleavage in dsDNA (Tsuchiya *et al.* 1992, Kent *et al.* 2007). In addition, enrichment of RPA adjacent to a DSB is reduced in Sth1-repressed or *rsc2* null strains, whilst Rad51 recruitment was slightly delayed (Shim *et al.* 2007, Liang *et al.* 2007).

Together these data suggest a model for RSC action at a DSB. Upon break induction a small amount of Ku and Mre11 bind to the DSB ends, which facilitates RSC recruitment. RSC then remodels the chromatin adjacent to the break, which allows further enrichment of Ku and Mre11 and generates a positive feedback loop to achieve maximal accumulation of these repair factors.

The involvement of RSC in NHEJ

Rsc8 and Rsc30 were first identified in a genetic screen as factors required for wild-type levels of NHEJ activity in the error-prone repair of HO-induced DNA DSBs (Shim *et al.* 2005). *rsc30* null cells also displayed DSB repair joint sequence alterations characteristic of other NHEJ mutants (Shim *et al.* 2005). In addition, *rsc30* and *htl1* null strains were also defective in NHEJ of a transformed linearised plasmid (Florio *et al.* 2007, Shim *et al.* 2005, Moscariello *et al.* 2010). In contrast, another study reported substantially elevated plasmid repair by NHEJ in *rsc1* and *rsc2* null and *sth1* mutant strains (Chai *et al.* 2005). Nevertheless, these findings, along with the impaired recruitment of RSC in the absence of Mre11 and Ku70 (Shim *et al.* 2005), indicate that RSC is necessary for efficient NHEJ.

The involvement of RSC in HR

Defective DSB repair by HR in a plasmid gap repair assay has been reported in *rsc1*, *rsc2,* and *htl1* null strains as well as *sth1* mutant strains (Chai *et al.* 2005, Moscariello *et al.* 2010). Whilst an *snf5* null mutant (Swi/Snf complex) was severely defective in synapsis during DSB repair via mating type switch gene conversion, *rsc2* null cells were proficient in this step. Instead, the *rsc2* null strain was found to be slightly defective in the post-synaptic ligation of DNA DSBs, suggesting a late role of RSC in the HR reaction (Chai *et al.* 2005). More recently, the RSC subunits Rsc2 and Rsc7 were found to be involved specifically in Rad59-dependent, Rad51-independent HR. In addition, Rsc1 and Rsc2 physically interacted with Rad59 in a yeast two-hybrid assay, whilst recruitment of Rad59 to a DSB was normal in the absence of *RSC2* as shown by

ChIP (Oum *et al.* 2011). Deletion of *RSC2* or *RSC7* did not impair mating type switch gene conversion, in contrast to that reported by Chai *et al.* Furthermore, RSC was dispensable for non-allelic or heteroallelic recombination, SSA and BIR, however formation of SSA and BIR recombination intermediates was delayed in the *rsc2* mutants. This might reflect the substantial growth defect reported in this strain and could explain the reduced post-synaptic ligation reported by Chai *et al.* (Oum *et al.* 2011).

In a spontaneous direct-repeat recombination assay using tandem repeats of the *FLO1* gene deletion of *RSC7* resulted in a highly elevated rate of recombination but *rsc2* was not tested. Recombination in this assay can occur via replication slippage, unequal sister chromatid exchange or SSA. RSC was also shown to be required for recombination between sister chromatids. Firstly, *rsc2* and *rsc7* mutants were more severely defective in repair of MMS-induced DNA damage during G2 than G1. Second, *rsc7* cells displayed a reduced rate of spontaneous unequal sister chromatid exchange, whilst again the rate in a *rsc2* mutant was not shown. Finally, in the absence of *RSC2* or *RSC7* recruitment of the cohesin subunits Smc1 and Scc1 to a DSB was severely compromised (Oum *et al.* 2011).

1.2.7. Mammalian SWI/SNF complexes in the DNA damage response

H2A.X phosphorylation

Mammalian SWI/SNF complexes are recruited to sites of DNA DSBs (Park *et al.* 2006, Peng *et al.* 2009, Ogiwara *et al.* 2011), suggesting that mammalian SWI/SNF complexes play a role in DNA DSB repair like their yeast counterparts. Park *et al.* showed that tetracycline-induced expression of an ATPase-defective dominant-negative version of BRG1 (which compromises PBAF function and a subset of BAF complexes) resulted in reduced cell survival after IR, as well as reduced DNA repair as shown by comet assay (Park *et al.* 2006). The authors also reported that H2A.X phosphorylation was defective in these cells following IR, despite normal ATM activation. However, as discussed below, the finding that BRG1 is required for γ-H2A.X induction is contentious, and the subsequent follow-up studies by the Kwon lab made on this basis should be treated skeptically.

ATPase-defective BRG1-expressing cells and cells depleted of BRG1 and hBRM by siRNA did not show a gross defect in G2/M checkpoint activation after IR or treatment with adriamycin. Furthermore, defective activation of the S-phase checkpoint was also not observed in ATPase-defective BRG1-expressing cells after IR and

Adriamycin treatment. Interestingly, S-phase checkpoint activation was defective in these cells after treatment with the DNA interstrand crosslinking agent cisplatin, suggesting distinct roles for SWI/SNF S-phase checkpoint activation in response to different drugs (Park *et al.* 2006).

In support of a role of SWI/SNF in γ-H2A.X induction, Ray *et al.* found that siRNA depletion of SNF5 (a subunit found in all SWI/SNF complexes) led to reduced levels of γ-H2A.X after UV (Ray *et al.* 2009). Somewhat in contrast, however, were the findings that SNF5 depletion led to reduced phosphorylation of ATM (but not ATR) and reduced ATM recruitment (as measured by foci number) after UV, providing an explanation for the reduced γ-H2A.X levels. The authors similarly found that DNA damage checkpoint activation was intact after UV in SNF5-deficient cells, despite reduced γ-H2A.X, by showing that ATM/ATR-mediated phosphorylation of CHK1/CHK2 was normal (Ray *et al.* 2009).

In contrast to the report by Park *et al.*, McKenna and co-workers reported that SNF5 did not co-localize with γ-H2A.X foci or relocalize within the nucleus following IR in MEFs (McKenna *et al.* 2008). In addition, they found that the affinity of SNF5 for chromatin remained unchanged after DNA damage by UV, IR and doxorubicin when comparing protein levels in soluble and chromatin-bound fractions. SNF5 depletion did not result in reduced γ-H2A.X foci formation (measuring % γ-H2AX positive cells rather than number of foci per cell) or total levels of γ-H2A.X after 5Gy IR. SNF5 depletion also did not lead to sensitivity to cisplatin, etoposide or UV, however the methodology used in these assays seems questionable. Firstly, proliferation (WST-1 absorption) was only measured 24 hours after addition of cisplatin, which seems early to measure an effect of this drug. Second, and more importantly, the positive control Rad18-/- MEFs did not show increased sensitivity to this drug compared to wild-type cells as has been previously reported (e.g. Wagner & Karnitz 2009) (McKenna *et al.* 2008).

Consistent with the report by Park *et al.* are the findings that following IR SNF5 deficiency led to normal ATM activation, and consequently p53 and CHK1 were also normally activated (McKenna *et al.* 2008). Activation of the G2/M DNA damage checkpoint (measured using phosphorylated H3 as a marker of mitotic cells) in response to IR was not defective in the SNF5-depleted cells. In addition, p53-dependent p21 expression (as measured by Western blot) was normal in the absence of SNF5, which is somewhat in contrast to the findings by Xia *et al.* and Burrows *et al.*, in which BAF180 and BRD7 depletion leads to reduced p21 activation (McKenna *et al.* 2008, Xia *et al.* 2008, Burrows *et al.* 2010).

Notably, no independent data has been published that recapitulates the findings by Park *et al.* made eight years ago, in which BRG1 was reported to be necessary for γ-H2A.X induction. In addition, we do not see loss of γ-H2A.X following depletion of BRG1 or BAF180 (Q. Riballo, P. A. Jeggo, J. A. Downs and P. M. Brownlee, unpublished data). Together with the findings that another SWI/SNF subunit, SNF5, does not impair γ-H2A.X induction (McKenna *et al.* 2008), we conclude that mammalian SWI/SNF complexes are dispensable for γ-H2A.X induction.

Regulation of SWI/SNF recruitment to DSBs by histone acetylation

In the first of a series of contentious follow-up studies, the Kwon lab reported that BRG1 associates with γ-H2A.X nucleosomes via interaction between its bromodomain and acetylated H3 (Lee *et al.* 2010). In support for a role of histone acetylation in the recruitment of SWI/SNF complexes for efficient DNA repair Ogiwara *et al.* independently identified the HATs CBP and p300 as being important for NHEJ (Ogiwara *et al.* 2011). Depletion of these HATs using siRNA led to impaired repair of IR-induced DSBs as well as etoposide sensitivity in lung cancer cells. The authors showed that CBP and p300 were recruited to DSBs and were required for DSB-dependent acetylation of H3K18, as well as H4K5, 8, 12 and 16. Furthermore, Ku70 and Ku80 recruitment to the DSB site were reduced in the absence of these HATs, providing an explanation for the reduced NHEJ activity. As well as reduced Ku70 and Ku80 recruitment, CBP and p300 depletion led to reduced recruitment of the SWI/SNF ATPase hBRM (restricted to a subset of BAF complexes) (Ogiwara *et al.* 2011).

ATM-mediated phosphorylation of BRG1

More recently, a third study by the Kwon lab reported that phosphorylation of BRG1 by ATM serves as a critical modification to promote BRG1-dependent DNA repair (Kwon *et al.* 2014). Rapid and transient phosphorylation of BRG1 at S721 occurred in response to IR-induced DNA DSB induction. BRG1 bound to acetylated H3 peptides with a much greater affinity when S721 was phosphorylated after DNA damage, whilst the transcriptional and ATPase activity of BRG1 were not significantly altered by this modification (Kwon *et al.* 2014).

Regulation of SWI/SNF recruitment to DSBs by BRIT1 (MCPH1)

BRIT1 (also known as microcephalin, MCPH1) is a transcriptional repressor of human telomerase reverse transcriptase (hTERT), with additional roles in the early DDR and recruitment of DNA repair proteins to DNA lesions (Rai *et al.* 2006). Multiple core subunits of SWI/SNF, including BRG1, hBRM, BAF170, BAF155 and SNF5 were identified by mass spectrometry as BRIT1 binding partners. This BRIT1-SWI/SNF interaction was entirely abolished when BAF170 was depleted and was significantly reduced after BAF155 depletion (Peng *et al.* 2009). Upon DNA damage the interaction between BRIT1 and SWI/SNF was enhanced. Interestingly, this enhanced binding upon DNA damage, but not the basal level of binding, was reduced upon ATM and ATR depletion. BAF170 was found to contain S/TQ motifs common to ATM/ATR substrates, and could be pulled down with a phospho-S/TQ (p-S/TQ) antibody in a manner dependent on ATM/ATR. Mutation of BAF170 S969 specifically blocked the DNA-damage enhanced binding of BAF170 to BRIT1, suggesting that this enhanced binding is mediated by ATM/ATR-dependent phosphorylation of BAF170 (Peng *et al.* 2009).

The authors next examined the importance of the BRIT1-SWI/SNF interaction in DNA repair. BRIT1 depletion led to a significant repair defect in a comet assay, as well as a defect in DNA repair of an I-*Sce*I-induced DSB by both HR and NHEJ mechanisms. In addition, BRIT1 depletion significantly reduced the levels of chromatin-bound BRG1, hBRM, BAF170, Rad51 and Ku70 in both undamaged cells and cells irradiated with 10Gy IR. Basal BRG1 localization to an I-*Sce*I restriction site before break induction was reduced in the absence of BRIT1 as shown by ChIP. Furthermore, DNA damage-induced BRG1 and hBRM localization to an I-*Sce*I-induced DSB were also reduced in BRIT1-depleted cells. In contrast, depletion of SWI/SNF subunits did not impair the recruitment of BRIT1 to chromatin or to the site of a DSB, placing SWI/SNF function downstream of BRIT1 (Peng *et al.* 2009).

BRIT1 and SWI/SNF depleted cells exhibited increased resistance to MNase digestion in the presence and absence of DNA damage, consistent with a role of SWI/SNF in chromatin relaxation to facilitate DNA repair factor recruitment. The role of BRIT1 in recruiting SWI/SNF for this purpose was confirmed using a version of BRIT1 in which a small (aa1-48) N-terminal deletion was made. This abolished the interaction with SWI/SNF but retains the ability of BRIT1 to form foci. The cells expressing this BRIT1 deletion were unable to restore the chromatin relaxation defect, indicating that SWI/SNF recruitment by BRIT1 is important for chromatin remodeling. Furthermore, RAD51 and phosphorylated-RPA (p-RPA) foci formation were impaired in BRIT1-depleted cells, and treatment of BRIT1-depleted cells with the chromatin relaxation

agent TSA reversed the defect in RPA foci formation and increased DSB repair efficiency by HR (Peng *et al.* 2009).

Finally, lymphoblastoid cell lines (LCLs) harbouring loss-of-function mutations in *BRIT1* were found to be defective in DNA repair by comet assay, more sensitive to camptothecin and etoposide (which generate DSBs in S-phase and are repaired predominantly by HR), and more sensitive to IR in G1 phase (readout of NHEJ repair). In addition, RAD51 and RPA foci formation and recruitment after UV were reduced in the BRIT1-defective cells compared to the corresponding controls. Furthermore, SWI/SNF binding to chromatin was substantially reduced in these cells, which also did not undergo chromatin relaxation after DNA damage (Peng *et al.* 2009).

1.3. Cohesin

1.3.1. The cohesin complex, cohesin loading, and cohesion establishment

Cohesin is a four-subunit, highly conserved complex that is able to entrap two DNA segments (Remeseiro & Losada 2013). Sister chromatid cohesion is when the two DNA segments are sister chromatids, and is essential for correct chromosome segregation during mitosis and DNA repair by homologous recombination. Two segments of DNA within the same sister chromatid can be held together by cohesin to form a loop. This looping is emerging as an important mechanism controlling interactions between promoters and enhancers to regulate transcription, in addition to organizing replication factories, recombination and chromosome condensation. Moreover, mutations in cohesin and regulatory factors are associated with cancer and developmental disorders, known as cohesinopathies (Remeseiro & Losada 2013).

Structure of the cohesin complex

Cohesin is a ring-shaped complex that consists of Smc1, Smc3, Scc1/Mcd1 and Scc3 in budding yeast (Remeseiro & Losada 2013) (Table 1.3). Smc1 and Smc3 are members of the structural maintenance of chromosomes (SMC) family, which also incudes the condensin subunits Smc2 and Smc4, and the Smc5/6 subunits Smc5 and Smc6. Smc1 and Smc3 are long polypeptides that fold back upon themselves by intramolecular 50nm antiparallel coiled-coil interactions to yield a protein with a globular ATPase ‘head’ domain at one end and a dimerization ‘hinge’ domain at the other (Haering *et al.* 2002, Carretero *et al.* 2010). Heterotypic dimerization between the Smc1 and Smc3 hinge domains results in the formation of a large V-shaped structure. A bipartite cohesin ring is formed, at least transiently, when the two halves of the ABC-type ATPase ‘heads’ from Smc1 and Smc3 are bound in the presence of ATP. The Smc1 head domain binds ATP via its Walker A and Walker B motifs, which binds motifs in the Smc3 head domain. A second ATP molecule binds in a vice-versa manner between the two proteins. Interaction between the Smc1 and Smc3 head domains is stabilised through interaction with the Scc1/Mcd1 C- and N-terminal domains, respectively (Losada *et al.* 2000). An interaction between Scc3 and Scc1/Mcd1 reinforces the cohesin ring (Gruber *et al.* 2003).

A number of models have been proposed to explain the topological linkage of DNA molecules achieved by cohesin. A widely depicted, but perhaps speculative

presumption is that the SMC arms of a single cohesin complex embrace two DNA molecules. Support for this is lacking from DNA-protein mapping studies, and the observation that Smc1 and Smc3 heads remain closely apposed during anaphase (McIntyre *et al.* 2007, Rudra & Skibbens 2013). In addition, SMC heads are observed to reside near SMC hinges (Sakai *et al.* 2003, McIntyre *et al.* 2007), and cohesins have been shown to bind each sister chromatid oddly, at least at the *HMR* locus in budding yeast (Chang *et al.* 2005). Thus, an alternative scenario sees individual cohesins bound to individual DNA molecules being modified to stabilize inter-cohesin assemblies (Rudra & Skibbens 2013).

Table 1.3. Functional domains and properties of cohesin proteins

	S. cerevisiae	*H. sapiens*	Domains and properties
Cohesin core complex	Smc1	SMC1α	Forms heterodimer with Smc3 via interaction between hinge domains, head domain constitues one half of a split ATPase domain
	Smc3	SMC3	Forms heterodimer with Smc1 via interaction between hinge domains, head domain constitues one half of a split ATPase domain
	Scc1/Mcd1	RAD21	Stabilizes Smc1-Smc3 heterodimer; C-terminus binds Smc1 head domain, N-terminus binds Smc3 head domain
Cohesin loader components	Scc2	NIPBL	Forms heterodimer with Scc4, required for efficient topological loading of core complex onto DNA, stimulates Smc1-Smc3 ATPase activity
	Scc4	MAU2	Forms heterodimer with Scc2, required for efficient topological loading of core complex onto DNA, stimulates Smc1-Smc3 ATPase activity
Establishment factors	Eco1/Ctf7	ESCO1 and ESCO2	Acetylates Smc3 on K112 and K113 (K105 and K106 in mammlian cells) during S-phase to establish cohesion; Esco2 specifically acetylates SMC3 in pericentric regions
	-	Sororin	No yeast homolgue, FGF motifs compete with Wapl FGF motifs for binding to Pds5 to counter anti-establishment
	Sgo1	SGO1	Protects centromeric cohesion from the prophase pathway until anaphase in mammalian cells
Anti-establishment factors	Scc3	SA1 and SA2	Component of anti-establishment complex; recruited to cohesin ring via interaction with Scc1, SA1 regulates cohesion at telomeres and is involved in transcriptional regulation, SA2 regulates centromere cohesion and DNA repair; both proteins are phosphorylated by Polo during execution of the prophase pathway in mammalian cells
	Wapl/Rad61	WAPL	Component of anti-establishment complex; binds Pds5 via N-terminal FGF motifs, which are absent in yeast Wapl
	Pds5	PDS5A and PDS5B/APRIN	Component of anti-establishment complex; contains HEAT-repeats, recruited to cohesin ring via interaction with Scc1, Pds5B specifically regulates centromeric cohesion and promotes DNA repair via interaction with BRCA2

Cohesin loading dynamics

Cohesin loading occurs on unreplicated chromatin in G1, whilst a substantial increase in the residence time of a proportion of the cohesin pool is observed during replication (Gerlich *et al.* 2006). During G1, a roughly equal proportion of soluble and dynamically bound cohesin (with a high dissociation constant) is found in the cell. The dynamically cycling pool of cohesin is present throughout interphase but not after late prophase, and might have important implications in replication and transcription (Terret *et al.* 2009, Fay *et al.* 2011). This cycling process is dependent on the cohesin regulatory proteins Wapl (also known as Rad61) and Pds5, which have a cohesin unloading (anti-establishment) function (discussed later) (Gandhi *et al.* 2006, Kueng *et al.* 2006, Tedeschi *et al.* 2013). A steady increase in stably bound cohesin (with a

low dissociation constant) occurs concomitantly with replication, peaking at S/G2 and remaining until anaphase (Gerlich *et al.* 2006). This stably bound cohesin is thought to function in the process of sister chromatid cohesion and is achieved through a process known as establishment (discussed later).

The mechanism of cohesin loading

The heterodimeric cohesin loader components Scc2 and Scc4 are required for cohesin to associate with DNA (Table 1.3) (Kogut *et al.* 2009, Bernard *et al.* 2006, Ciosk *et al.* 2000, Furuya *et al.* 1998, Rollins *et al.* 2004, Seitan *et al.* 2006). Cohesin loading also depends on ATP hydrolysis by the Smc head domains (Arumugam *et al.* 2003, Weitzer *et al.* 2003) and a transient separation of the Smc hinge domains (Gruber *et al.* 2006). This latter observation is proposed to function as the DNA 'entry' gate and provides strong evidence that DNA becomes trapped within a single cohesin ring (Chan *et al.* 2012). Nevertheless, the molecular mechanism of action for how these events are coordinated to promote cohesin loading remains poorly understood. In addition, it is largely unclear where the sites of cohesin loading are. Once loaded cohesin is found at discrete sites along chromosome arms known as cohesin-associated regions (CARs) and is particularly enriched at pericentric regions (Onn *et al.* 2008). Cohesin loading is dependent on the formation of pre-replication factories in *Xenopus*, to which Scc2-Scc4 is recruited (Takahashi *et al.* 2008). However, in somatic cells Scc2-Scc4 is not recruited to pre-RCs and loading of cohesin occurs independently of pre-RC formation, suggesting alternative loading mechanisms (Guillou *et al.* 2010, MacAlpine *et al.* 2010). Interestingly, in budding yeast the cohesin complex does not colocalize with Scc2-Scc4, perhaps due to the ability of cohesin to translocate along the chromain fibre following loading (Hu *et al.* 2011, Ocampo-Hafalla & Uhlmann 2011). In *Drosophila* and mouse embryonic stem cells cohesin and Scc2 are found together at transcriptionally active sites (Misulovin *et al.* 2008, Kagey *et al.* 2010). Thus, the open state of active euchromatin might facilitate cohesin loading, or cohesin might be more dynamically bound at these sites and requires more frequent reloading (Remeseiro & Losada 2013).

Recently, cohesin loading onto DNA in *S. pombe* was reconstituted using purified cohesin and Scc2-Scc4 (Murayama & Uhlmann 2014). Incubation of cohesin with DNA alone resulted in inefficient spontaneous topological loading. Incubation of the Scc2-Scc4 loader stimulated the ATPase activity of cohesin to improve the efficiency of topological loading. In addition, Scc2-Scc4 was found to contact the

cohesin ring at multiple sites, including via interaction with the enigmatic Scc3 component (Murayama & Uhlmann 2014).

Cohesion establishment and anti-establishment

Cohesion establishment is the process that converts chromatin bound cohesin into a state that is tethering-competent, or cohesive. Mechanistically this process is poorly understood and appears to be highly complex (Sherwood *et al.* 2010, Skibbens *et al.* 2011). Establishment of cohesion occurs during DNA replication and is critically dependent on the cohesin acetyltransferase Eco1 (also known as Ctf7) (Table 1.3). Eco1 interacts with a multitude of DNA replication factors in S-phase, including the clamp-like proliferating cell nuclear antigen (PCNA), replication factor C (RFC), the Chl1 helicase and the Okazaki fragment maturation flap endonuclease I Rad27 (also known as Fen1). Indeed, a widely held model is that cohesion is established immediately once nascent sister chromatids emerge behind the replication fork (Skibbens 2000, Rudra & Skibbens 2013). Establishment is also regulated by at least three other proteins known as Scc3, Pds5 and Wapl (Table 1.3). These three proteins have an important function in the prophase pathway (in mammalian cells), which serves to release cohesin from chromosome arms during mitosis (discussed later). Wapl binds to Pds5, which is a large HEAT-repeat-containing protein, and Pds5 and Scc3 are recruited to the cohesin ring via interaction with Scc1 (Hartman *et al.* 2000, Panizza *et al.* 2000, Shintomi & Hirano 2009). Wapl, Pds5 and Scc3 form a stable complex thought to promote ‘anti-establishment’ (Rowland *et al.* 2009).

During S-phase in budding yeast Eco1 acetylates Smc3 on two lysine residues, K112 and K113, located within the ATPase head domain. Individually mutating lysine 112 to a similar but non-acetylatable arginine does not impair viability or cohesion, in contrast to mutating lysine 113 to the same residue, which causes a cohesion establishment defect and inviability (Zhang *et al.* 2008, Unal *et al.* 2008, Rolef Ben-Shahar *et al.* 2008, Rowland *et al.* 2009). This suggests that acetylation of K113 is most crucial in this regard, however K112 acetylation does appear to regulate the cohesin-dependent process of chromosome condensation (discussed later). Strikingly, deletion of *WAPL* supresses the inviability conferred by the K113R mutation. K113R inviability is also suppressed by several *pds5* and *scc3* mutations, which cluster within specific domains within the N- and C-terminal regions of these two proteins (Rolef Ben-Shahar *et al.* 2008, Rowland *et al.* 2009, Unal *et al.* 2008, Zhang *et al.* 2008). Thus, a proposed model for the function of Smc3 acetylation is to counter the ‘anti-establishment’ activity of the Wapl-Pds5-Scc3 complex.

A critical issue is whether anti-establishment prevents the actual formation of cohesive cohesin during S-phase or destroys it after its establishment following S-phase. Chan *et al.* revealed that in cells lacking Eco1 destruction of cohesin upon Wapl expression occurred long after replication, providing support for the latter hypothesis (Chan *et al.* 2012). Importantly, Wapl was not able to destroy this post-replicative cohesion when Smc3 was acetylated. Using GFP-tagged proteins, Wapl was found to be ~4-fold less abundant than Pds5 and showed ~4-fold lower association with pericentric chromatin. Expression of Wapl-GFP in a *wapl* null haploid strain led to conditional lethality in an *eco1-1* strain. This lethality was even observed when Wapl-GFP was heterozygous over *wapl* deletion in a diploid strain. Together, these results indicate that Wapl is able to destroy all cohesion in an Smc3 acetylation-compromised scenario despite its low abundance and substoichiometric chromatin association (Chan *et al.* 2012).

Wapl was found to very rapidly exchange between cohesin complexes located at different pericentric regions as measured by iFRAP in a manner largely independent of Eco1. In contrast, Pds5, which interacts with Wapl via its N-terminal domain, as well as Scc1 cycled much more slowly, and their cycling was increased in the absence of Eco1. Furthermore, in a *wapl* null strain Scc1 turnover was largely abolished, as was Smc3 turnover in a *wapl eco1-1* strain incubated at the permissive temperature, indicating that cohesin turnover depends on Wapl. Strikingly, mutations in *smc3, pds5 and scc3*, which had been previously identified as suppressors of *eco1* inviability, led to reduced cohesin turnover. Interestingly, only a subset of *pds5* mutations, which were previously shown to disrupt the interaction between Pds5 and Wapl, reduced Wapl recruitment (Chan *et al.* 2012).

Collectively, these results indicate that unacetylated cohesin has an intrinsic ‘releasing activity’ that promotes its turnover on chromatin and promotes its anti-establishment by Wapl, Pds5 and Scc3. The ring model, in which two DNA molecules are entrapped within one cohesin ring, provides the simplest mechanistic explanation for this. If the ‘entry’ gate for cohesin loading occurs at the Smc1/Smc3 hinge domain, as described by Gruber *et al.,* an ‘exit’ gate might be present at the Smc1/Smc3/Scc1 interface. The releasing activity of unacetylated cohesin, facilitated by Wapl, Pds5 and Scc3, might involve a transient dissociation of Scc1 from the Smc1/Smc3 interface to allow DNA exit. In support of this, Chan *et al.* showed that fusion of Scc1 to Smc3, but not to Smc1, suppressed *eco1* null and *eco1-1* conditional lethality. This was accompanied by reduced cohesin turnover and occurred despite normal Wapl recruitment. The authors propose that the function of Smc3 acetylation is to lock

cohesin onto DNA by stabilizing the interaction between Smc3 and Scc1 (Chan *et al.* 2012).

The model described above does not account for the observation that in Xenopus Smc3 can be readily acetylated *after* DNA replication and when replication is inhibited (Song *et al.* 2012). In addition, acetylation occurring outside of S-phase is unable to generate cohesion, suggesting that although Smc3 acetylation is critical for cohesion it must occur in context amongst other replication-associated factors (Song *et al.* 2012, Rudra & Skibbens 2013). In yeast, four alternative RFC complexes exist in yeast in which the large Rfc1 subunit can be replaced with Elg1, Ctf18 or Rad24. Interestingly, whilst most DNA replication components promote establishment, the Elg1-containing RFC complex antagonises Eco1 function (Maradeo & Skibbens 2009, Maradeo & Skibbens 2010, Parnas *et al.* 2009). This supports the notion that there exits a complex network of cohesion establishment regulation during S-phase. There are likely to be additional yet to be identified replication factors with roles in cohesion establishment. Notably, this might include proteins harbouring bromodomains (Rudra & Skibbens 2013), which bind acetylated lysine residues, such as BAF180 in mammalian cells.

Smc3 acetylation as a precursor to the 'cohesin code'

Several studies have shown that the inviability of an *eco1* null strain is rescued by deletion of Wapl (Feytout *et al.* 2011, Rowland *et al.* 2009, Skibbens *et al.* 1999, Sutani *et al.* 2009, Tanaka *et al.* 2001, Tóth *et al.* 1999). This would be predicted to be due to restoration of sister chromatid cohesion, but in fact *eco1 wapl* cells display a severe cohesion defect that is comparable to an *eco1* single null strain (Guacci & Koshland 2012, Rowland *et al.* 2009, Sutani *et al.* 2009, Feytout *et al.* 2011). Expression of an Smc3 acetyl-mimic mutant, in which lysine 113 is mutated to glutamine (K113Q) in an *smc3-42* ts strain, results in a severe cohesion establishment defect and inviability at the restrictive temperature. The same phenotype is observed when K112 and K113 together are mutated to glutamine (K112Q K113Q). Intriguingly, in an *smc3-42* strain expressing K112R (rendering the residue non-acetylatable) together with K113, viability is restored, but the severe cohesion establishment defect remains.

The severe cohesion establishment defect in these strains did not severely impair accurate chromosome segregation, as would be predicted in cohesion-defective cells due to failed bipolar microtubule attachment. This is likely due to a

feature unique to yeast whereby a bipolar spindle forms in early S-phase and sister kinetochores achieve stable attachment during replication (McCarrol & Fangman 1988, Kitamura *et al.* 2007). Specifically, 75% of *smc3-42* cells, ~74% of K113Q and ~82% of K112R K113Q cells exhibited disjunction of most chromatids. For comparison, ~98% of wild-type cells exhibited disjunction. This suggests that an alternative cohesin-mediated process exists to promote viability in these cells (Guachi & Koshland 2012). The authors found that whilst *smc3-42* and K113Q cells were unable to perform condensation at the rDNA locus into discrete loops, the K112R K113Q and *eco1 wapl* double null cells were able to condense these structures, and that the degree of condensation correlated with viability. Therefore, the levels of Smc3 acetylation at K112 and K113 appear to represent a critical bifurcation step that dictates whether cohesin is utilized for cohesive or condensive purposes (Guachi & Koshland 2012). On this basis Rudra & Skibbens propose that Smc3 acetylation represents the beginning of a 'cohesin code' that is analogous to the familiar histone code (Rudra & Skibbens 2013). In addition to Smc3 acetylation, many other cohesin subunits are subject to numerous acetylation, phosphorylation and SUMOylation modifications. Deciphering such a code might provide essential insight into the increasingly diverse roles of cohesin in various cellular processes including ribosome biogenesis, transcription, cohesion, condensation and DNA repair (Rudra & Skibbens 2013).

1.3.2. Vertebrate cohesin

In vertebrates several cohesin proteins have undergone duplication and divergence and appear to regulate cohesion at specific chromosomal regions. These include the two versions of Scc3 known as SA1 and SA2, two versions of Eco1 known as ESCO1 and ESCO2, and two versions of Pds5 known as PDS5A and PDS5B (Table 1.3). In addition, SMC3 acetylation in mammalian cells is accompanied by binding of another protein known as Sororin, which might interact with cohesin through binding to PDS5 via its FGF motifs (Shintomi & Hirano *et al.* 2009, Nishiyama *et al.* 2010) (Table 1.3). Binding of Sororin is proposed to displace the binding of WAPL, which might also bind to PDS5 via its 3 N-terminal FGF motifs, to counter its anti-establishment activity (Dreier *et al.* 2011, Liu *et al.* 2013).

In vertebrate cells the bulk of cohesin along chromosome arms is removed during execution of the prophase pathway (Gandhi *et al.* 2006, Kueng *et al.* 2006). This requires polo-like kinase 1 (PLK1)-dependent phosphorylation of the SA subunit and the anti-establishment activity of WAPL and PDS5 (Shintomi & Hirano 2010).

This activity is enhanced once Sororin is removed upon phosphorylation of CDK1 (Nishiyama *et al.* 2010, Dreier *et al.* 2011). Disruption of the prophase pathway prevents chromosome resolution, most likely because the persistence of cohesin inhibits topoisomerase II-dependent processing of replication-generated DNA catenations (Farcas *et al.* 2011). A small population of cohesin is protected from the prophase pathway at pericentromeric regions until anaphase. This is dependent on Shugosin (SGO1) and the protein phosphatase 2A (PP2A), which removes the phosphorylation on SA to counter the activity of PLK1 (Gutierrez-Caballero *et al.* 2012) (Table 1.3). This pericentromeric cohesion has an essential role in chromosome biorientation and segregation.

The spindle assembly checkpoint (SAC) in metaphase prevents cell cycle entry into anaphase until all chromosomes have aligned with their kinetochores attached to the mitotic spindle (Nezi & Musacchio 2009, Musacchio & Salmon 2007, Kops 2008, Lara-Gonzalez *et al.* 2012). Aurora B plays an important role in sensing incorrect microtubule-kinetochore interactions and selectively destabilizing them, which results in SAC activation. This gives the cell an opportunity to correct the attachment (Lampson & Cheeseman 2011). Aurora B achieves this activity by phosphorylating a range of kinetochore substrates, and its localization to kinetochores depends on BUB1-mediated H2A threonine 120 phosphorylation and Haspin-mediated H3 threonine 3 phosphorylation at the inner centromere (Kelly *et al.* 2010, Wang *et al.* 2010, Wang *et al.* 2012, De Antoni *et al.* 2012). The mitotic checkpoint complex (MCC), consisting of BUB1, BUB3, MAD2 and CDC20, blocks the activation of APC/C until the SAC is satisfied. Once the SAC is satisfied the MCC is no longer generated and activated APC/C uniquitilates Securin, which is bound to Separase. Ubiquitilated Securin is targeted for proteolytic cleavage, releasing active Separase that cleaves RAD21 present in the remaining pericentromeric population of cohesin (Lara-Gonzalez *et al.* 2012). This allows full separation of sister chromatids in concert with topoisomerase II activity (Shamu *et al.* 1992, Oliveira *et al.* 2010, Toyoda *et al.* 2006).

SA1 and SA2 differentially mediate telomeric and centromeric cohesion

The two versions of the Scc3 homologue in vertebrates, known as SA1 and SA2, share 75% sequence identity along the central region of the proteins and differ only in short regions of the C- and N-termini (Table 1.3). Despite displaying similar cell cycle loading and dissociation regulation (Losada *et al.* 2000), and both being expressed in all mouse tissues (Remeseiro *et al.* 2012), SA1 and SA2 do not function equivalently.

In human cells SA2 is several times more abundant than SA1, whilst in Xenopus eggs SA1 is the major form (Losada *et al.* 2000, Sumara *et al.* 2000). SA1, but not SA2, is known to bind to the telomeric Shelterin complex components TRF1 and TIN2 (Canudas *et al.* 2007). Shelterin negatively regulates telomere length by restricting the access of telomerase (van Steensel & de Lange 1997, Kim *et al.* 1999, Ancelin *et al.* 2002). Association of TRF1 and TIN2 with telomeres is negatively regulated by the activity of poly (ADP-ribose) polymerase tankyrase 1 (Smith *et al.* 1998), which when overexpressed dissociates TRF1 and TIN2 and allows telomere elongation by telomerase (Smith & de Lange 2000, Houghtaling *et al.* 2004). Tankyrase 1 is involved in the correct separation of sister chromatids after replication, and in tankyrase 1-depleted cells remain tethered at telomeres and suffer prolonged mitosis (Dynek *et al.* 2004). This prolonged telomeric association can be rescued by depletion of TIN2 or SA1 and is due to protein-protein interactions (Canudas *et al.* 2007, Hsiao & Smith 2009). This indicates that sister telomere association and separation is regulated by a unique mechanism.

Canudas and Smith addressed whether SA1 might play a role in regulating telomere cohesion. First, TIN2, SA1 or SA2 were singly depleted using siRNA in HeLa cells and mitotic cells were isolated using mitotic shake-off. These cells were subject to fluorescent *in situ* hybridization (FISH) with a probe specific to the subtelomeric region of chromosome 16p (Canudas & Smith 2009). The distances between the two signals from each sister chromatid were then measured. Control cells transfected using GFP and SA2 siRNA showed comparable distributions of distances between the signals. In contrast, TIN2 and SA1-depleted cells showed substantial increases in the distances compared to the control cells. Therefore, depletion of TIN2 and SA1, but not SA2, leads to a substantial increase in the separation of sister chromatids at telomeres, consistent with a telomeric cohesion defect. Next, cells were subject to FISH using a probe specific to the centromere of chromosome 6. Whilst GFP, TIN2 and SA1-depelted cells showed comparable distributions of distances between the signals, the SA2-depleted cells showed substantial increases in the distances compared to the control cells. This suggests that SA2 specifically regulates cohesion at centromeres. Using a probe specific to the arm of chromosome 20 (20p12) revealed similar results to that shown with the telomere probe, in that TIN2 and SA1 depletion led to a cohesion defect, whilst SA2-depletion did not. This suggests that compromised telomere cohesion can influence arm cohesion (Canudas & Smith 2009).

FISH labeling of telomeres in BrdU-positive S-phase cells revealed that the telomere cohesion defect in TIN2 and SA1-depleted cells was evident in this phase of

the cell cycle. In addition, FISH analysis on cells synchronized in late S-phase using a double thymidine block revealed a similar defect. This suggests that there is a defect in either the establishment or maintenance of telomere cohesion after replication in TIN2 and SA1-depleted cells. Further analysis of metaphase chromosome spreads showed that TIN2 and SA1 depletion led to an increased frequency of cells showing an arm/telomere cohesion defect consistent with the FISH data. SA2-depleted cells did not show this defect in arm cohesion and instead showed a clear increase in the frequency of cells showing a centromere cohesion defect (Canudas & Smith 2009).

SA1, but not SA2, plays a role in gene regulation and development

Cohesin has an important function in transcriptional regulation by facilitating chromatin looping in concert with other factors including CTCF (Toyoda *et al.* 2006, Hou *et al.* 2010), estrogen receptor (ER) (Shmidt *et al.* 2010), Mediator (Miyanari *et al.* 2012) and Polycomb (Strubbe *et al.* 2011). SA1 null mouse embryos were found to exhibit several features characteristic of the cohesinopathy Cornelia de Lange syndrome (CdLS). These included reduced body size and various developmental abnormalities but no obvious cohesion defect (Kawauchi *et al.* 2009, Remeseiro *et al.* 2012). Analysis of SA1 and SA2 genome-wide binding revealed 25,737 SA1 binding sites and 7,741 SA2 binding sites. More importantly, SA1 was highly enriched ~1kb upstream from TSSs and within gene bodies, whilst SA2 enrichment largely occurred at intergenic regions (Remeseiro *et al.* 2012). In addition, SA1 was predominantly responsible for cohesin enrichment at promoters and at CTCF-bound sites. SA1 was required for regulating the expression of various development-associated genes that could not be compensated for by SA2. Thus, SA1 function in gene expression appears to underlie the molecular aetiology of CdLS (Remeseiro *et al.* 2012).

A specific role of SA1 in transcriptional regulation is supported by findings that in three isogenic sets of *STAG2*-corrected and *STAG2* knockout tumour-derived cell lines the gene expression profiles between STAG2-proficient and –deficient cells were strikingly similar (Solomon *et al.* 2011). Specifically, only 16 of 28,869 genes (0.06%) were found to be modulated >1.5-fold in the *STAG2*-corrected glioblastoma cells compared to the *STAG2*-deficient control. In addition, the few genes that were misregulated by STAG2 were not misregulated in more than one cell line. Therefore STAG2 does not appear to be an important regulator of global gene expression (Solomon *et al.* 2011).

ESCO2 specifically regulates pericentromeric cohesion

Mammalian cells encode two forms of Eco1, known as ESCO1 and ESCO2, which both contain a divergent N-terminus, a C2H2 zinc finger and a highly conserved acetyltransferase domain (Hou & Zou 2005) (Table 1.3). Acetylation of human SMC3 on K105 and K106 (Zhang *et al.* 2008) and Sororin binding requires both ESCO1 and ESCO2 (Nishiyama *et al.* 2010), suggesting that they might function redundantly. Recently, homozygous Esco2 -/- mouse embryos were found to have terminated development at pre- and post-implantation stages, indicating a non-redundant role for Esco2 (Whelan *et al.* 2012). Cells from these embryos showed a marked centromeric cohesion and chromosome segregation defect (discussed later) that likely underlies the loss of viability phenotype. Esco2 was expressed transiently during mid to late S-phase and specifically localized to pericentromeric heterochromatin (PCH) as shown by immunofluorescence and ChIP. The localization and distribution of cohesin, Aurora B, Incenp and Sgo1, which are normally enriched in metaphase PCH, was disrupted in the absence of Esco2. Finally, levels of acetylated Smc3 were reduced from S-phase through to prometaphase, and Sororin levels at PCH were significantly reduced in Esco2 depleted cells. Taken together, it appears that Esco2 has a unique role in acetylating Smc3 and establishing and maintaining cohesion specifically at pericentromeric regions (Whelan *et al.* 2012).

PDS5B specifically regulates cohesion at centromeres

Two versions of Pds5 exist in mammalian cells, PDS5A and PDS5B (Sumara *et al.* 2000, Losada *et al.* 2005), which are both ~1400 amino acids in length and share ~72% sequence homology, including two HEAT repeat clusters (Table 1.3) The proteins differ in their C-terminal 300 amino acids. Both PDS5A and PDS5B associate with either SA1 or SA2 (Losada *et al.* 2005), and knockout Pds5A -/- and Pds5B -/- mice die perinatally with various developmental defects reminiscent of Cornelia de Lange Syndrome (CdLS) (Zhang *et al.* 2007, Zhang *et al.* 2009).

In a more recent study, efforts to generate Pds5A -/- and Pds5B -/- knockout mice similarly resulted in embryonic lethality at late post-implantation stages. Whilst Pds5A -/- embryos that survived to E16.5 and 18.5 were considerably smaller than wild-type mice the Pds5B -/- showed less severe defects. Primary MEFs from both Pds5A -/- and Pds5B -/- also showed a proliferation defect (Carretero *et al.* 2013). Pds5A -/- and Pds5B -/- MEFs did not individually show altered levels of chromatin bound Rad21, Stag1 or Stag2. However, depletion of Pds5A and Pds5B using siRNA

in Pds5B -/- and Pds5A -/- MEFs resulted in a moderate but significant increase in the levels of chromatin bound cohesin as measured by IF, consistent with a role of Pds5 proteins in anti-establishment/unloading. The absence of both Pds5 proteins in metaphase cells similarly resulted in increased cohesin binding to chromatin. This indicates that Pds5A and Pds5B contribute to cohesin anti-establishment/unloading in interphase and mitosis (Carretero *et al.* 2013).

Levels of chromatin bound Wapl and acetylated Smc3, but not Sororin, were moderately reduced in Pds5A -/- MEFs. Pds5B -/- MEFs displayed similarly reduced levels of Wapl, unaffected levels of Sororin, and more severely reduced levels of acetylated Smc3. Double depletion of Pds5 proteins severely compromised the association of Wapl, acetylated Smc3 (consistent with recent yeast reports) (Vaur *et al.* 2012, Chan *et al.* 2013) and Sororin to chromatin. Next, the authors examined telomeric cohesion by measuring the frequency of telomere fragility using a telomeric FISH probe. Telomere fragility is visualized as an irregularly shaped or multimeric signal and results from defective telomere replication, which is dependent on telomere cohesion. Individually, Pds5A -/- and Pds5B -/- MEFs did not show increased telomere fragility, but depletion of both proteins slightly increased telomere fragility, suggesting that they are both required for telomere cohesion. In contrast, analysis of metaphase spreads showed a clear centromeric cohesion defect that was only apparent in the Pds5B -/- MEFs. Because of this centromere-specific cohesion defect, the recruitment of Esco2 (which is recruited to pericentromeric heterochromatin (PCH) in mid to late S-phase), and Sororin to PCH was monitored by IF. Reduced Esco2 accumulation at sites of PCH (labelled using PCNA IF) was observed in Pds5B -/- cells, and to a lesser extent in Pds5A -/- cells. In addition, Sororin levels at PCH foci in G2 cells and at the inner centromere were also strikingly reduced in Pds5B -/- cells. Thus, Pds5B appears to function in centromeric cohesion establishment or maintenance by promoting Esco2 and Sororin association at PCH. As a consequence, these cells were found have a chromosome segregation defect (discussed later) (Carretero *et al.* 2013).

Aurora B recruitment requires Bub1-mediated phosphorylation of H2A threonine 120 and Haspin-mediated phosphorylation of H3 threonine 3 (Kelly *et al.* 2010, Wang *et al.* 2010, 2012, De Antoni *et al.* 2012). Whilst Bub1 association was unaffected in the absence of Pds5B, H3 T3 phosphorylation and Aurora B enrichment was defective, suggesting impaired Haspin recruitment. As a consequence, correction of monastrol-induced syntelic attachments (Kapoor *et al.* 2010) was impaired in the Pds5B -/- cells. Furthermore, Pds5B -/- cells exited mitosis quicker than wild-type cells upon taxol treatment (microtubule destabilizing drug), suggesting a defect in

spindle assembly checkpoint (SAC) activation. Levels of activated Aurora B, which is phosphorylated at serine 232 (Yasui *et al.* 2004), were also reduced in the Pds5B-deficient cells. Therefore, Pds5B is required for centromere cohesion as well as the centromeric accumulation and activity of Aurora B (Carretero *et al.* 2013).

1.3.3. Cohesin in DNA repair

Cohesin in yeast DNA repair

A conserved role of cohesin in DNA repair is supported by studies from yeast to humans. Studies in yeast have indicated that deletion of cohesin genes results in reduced homologous recombination, leading to the hypothesis that cohesin promotes recombination through its ability to hold sister chromatids in proximity (Parisi *et al.* 1999, Klein *et al.* 1999, Nasmyth *et al.* 2001, Doll *et al.* 2008). The earliest study pointing to a role for a cohesin gene in DNA repair revealed that *S. pombe* cells containing an I67T mutation in Scc1/Mdc1 were rendered highly sensitive to IR (Birkenbihl & Subramani 1992). The first evidence that cohesin between sister chromatids is essential for DSB repair in mitotic cells was provided by Sjögren & Nasmyth in 2001. They showed that the presence of cohesin at the time of DSB induction in S-phase is essential for repair of DSBs in G2, and requires Scc2 as well as Eco1 (Sjögren & Nasmyth 2001). Subsequently, a 100kb domain of cohesin enrichment was found to occur surrounding a single DSB in conjunction with H2A S129 phosphorylation in budding yeast. Cohesin enrichment at this domain was dependent on Mre11 and Scc2 and also functioned in postreplicative DNA repair (Unal *et al.* 2004).

Indeed, sister chromatid cohesion is established *de novo* following DNA damage at the break site as well as genome-wide, and can occur in a replication-independent manner. Furthermore, phosphorylation of Mdc1 at S83 by phosphorylated Chk1 in response to Mec1 activation was important for the establishment of DSB-induced cohesion (Unal *et al.* 2008). Interestingly, separase-mediated cleavage of cohesin is required for efficient cohesin-mediated DNA repair, possibly by removing break site-proximal cohesin or by promoting its relocation (Nagao *et al.* 2004).

Cohesin in vertebrate DNA repair

Evidence for a conserved role of cohesin in vertebrate DNA repair first came from the finding that deletion of *RAD21* in DT40 cells compromised the repair of spontaneous and IR-induced chromatid breaks (Sonoda *et al.* 2001). Recruitment of cohesin to laser-induced DNA DSBs was observed immediately after damage induction. This was dependent on MRE11 and RAD50 but not ATM and NBS1, and MRE11/RAD50 interacted with cohesin predominantly in S and G2 when cohesin was recruited to DNA damage sites (Kim *et al.* 2002). In human cells SMC1α is phosphorylated at S957 and S966 following IR in an ATM-dependent manner (Kim *et al.* 2002, Yazdi *et al.* 2002). Mutation of these serine residues to a non-phosphorylatable form of SMC1α causes a defect in the S-phase DNA damage checkpoint, reduced cell survival, and an increased prevalence of chromosomal aberrations after IR (Kitagawa *et al.* 2004). Depletion of SMC1α and SMC3 also causes a defect in the G2 DNA damage checkpoints (Watrin & Peters 2009). Control siRNA-treated metaphase HeLa cells irradiated in early S-phase contained few broken chromosomes and RPA foci, in contrast to SMC1α and SMC3 depleted cells, which nearly all contained frequent breaks and RPA foci. This was due to failures in activating CHK2 and recruiting 53BP1 to the sites of DNA damage (Watrin & Peters 2009).

Enhanced genome-wide binding of Smc1 and Smc3 at pre-existing cohesin binding sites also occurs in human cells after IR (Kim *et al.* 2010). ATM was shown to phosphorylate SMC3 at S1083, and this modification is important for the DNA damage-induced reinforcement of cohesin. The same study showed that acetylation of SMC3 at K105 and K106 after IR required ATM and ATR as well as ESCO1 ESCO1. Furthermore, SMC3 acetylation was necessary for for the IR-induced intra-S phase DNA damage checkpoint and viability. Despite both requiring ATM, SMC3 acetylation and phosphorylation can occur independently, and both are required for DNA damage-induced cohesin establishment (Kim *et al.* 2010). HeLa cells depleted of cohesin showed reduced survival after X-rays and slower DSB repair kinetics as measured by persistence of γ-H2AX and 53BP1 foci in G2. Cohesin recruitment to DNA damage sites occurred in G2 but not in G1, supportive of a specific role in homologous recombination (Bauerschmidt *et al.* 2010).

Cancer and cohesin-mediated DNA repair by HR

Defective or inappropriate homologous HR appears to underlie the generation of oncogenic chromosomal aberrations, loss of heterozygosity and various other

structural chromosome alterations including deletions, inversions and translocations. In addition to aneuploidy, discussed later, such alterations are hallmark features of the vast majority of cancers (Bishop *et al.* 2003, Reliene *et al.* 2007). Moreover, mutations in genes encoding proteins involved in HR are frequently mutated in various cancer types, exemplified by breast cancer associated *BRCA1* and *BRCA2* mutations (Hall *et al.* 1990, Wooster *et al.* 1994, Moynahan & Yasin 2010).

Rad21 +/- heterozygous mice show reduced frequencies of sister chromatid exchanges (Xu *et al.* 2010), and in human cells siRNA-mediated depletion of RAD21 increases intra-chromosomal recombination (Potts *et al.* 2006). In budding yeast a fourfold reduction in the dosage of Smc3 or Scc1/Mcd1 suppressed sister chromatid recombination but led to increased recombination between homologous chromosomes (Covo *et al.* 2010). Taken together, disruption of cohesin can lead to misregulation of physiological recombination pathways that might promote deleterious genomic instability (Xu *et al.* 2011).

1.3.4. Distinct roles for vertebrate centromere-specific cohesin variants in DNA repair

SA2 in DNA repair

Although not in response to induced DSBs STAG2 KO colorectal HCC116 cells recurrently harboured a unique structural chromosome karyotype that was not apparent in SA2 expressing control cells (Solomon *et al.* 2011). This suggests a role for SA2 in regulating structural chromosome stability. More recently, Kong *et al.* reported the intriguing finding that clustering of SMC1α to the sites of DNA damage is completely abolished in the absence of SA2 (Kong *et al.* 2014). Also, SA2 recruitment to these sites was abolished upon SMC1α or RAD21 depletion. Furthermore, a significant enrichment of SA2, but not SA1, was observed at both laser- and endonuclease-induced DSBs. Accumulation of NIPBL was abolished in the absence of SA2 but not in the absence of SA1. Together, these observations suggest that SA2-containing cohesin complexes, but not SA1-containing complexes are recruited to DNA DSBs (Kong *et al.* 2014). However, both SA1- and SA2-containing complexes co-immunoprecipitated with MRE11 in both undamaged and damaged cells, indicating that preferential SA2 association with DSBs is not due to a differential MRE11 interaction (Kong *et al.* 2014).

Both SA1 and SA2 contain an N-terminal Irr1 domain with >90% homology, within which the STAG domain is located. The central regions of the proteins share

70-90% homology, whilst the C-terminal regions share only 30-50% homology. Both full-length proteins, as well as the N-terminal and middle domains from each, interacted with RAD21. The N-terminal segments of the proteins that lacked the Irr1 domain weakly interacted with RAD21, whilst no interaction was observed with the SA1 and SA2 C-terminal regions. Therefore, the N-terminal Irr1/STAG domain is important for incorporation of both proteins into the cohesin complex (Kong *et al.* 2014). Interestingly, the nuclear localization signals (NLSs) of SA1 and SA2 are located in different domains of the proteins: the SA1 NLS is found in the N-terminus and contains the Irr1 region, and the SA2 NLS is found in the C-terminus. The critical differences in the SA1 and SA2 C-termini was highlighted by the finding that replacing the C-terminus of SA1 with the C-terminus of SA2 conferred damage site targeting ability to SA1 (Kong *et al.* 2014).

The SA2-specifc role in DNA DSB repair was further confirmed by showing that SA2 depletion, but not SA1 depletion, led to a decrease in the frequency of DNA damage induced SCEs. Also, SA2 depletion enhanced DSB repair by NHEJ as seen in RAD21-depleted cells, likely due to a shift in repair pathway choice (Potts *et al.* 2006, Kong *et al.* 2014). Finally, the authors investigated the roles of SA1 and SA2 in the G2 DNA damage checkpoint. In contrast to previous reports, no defect in checkpoint enforcement was observed in SA1 or SA2 depleted cells, as measured by mitotic index after DNA damage with and without caffeine. In contrast, SMC1α phosphorylation, which is required for the intra-S DNA damage checkpoint, was comparable in SA1- and SA2-containing complexes after DNA damage. Consistently, SA1- and SA2-depleted cells both displayed increased radioresistant DNA synthesis (RDS), which is indicative of an intra-S DNA damage checkpoint defect (Kim *et al.* 2002, Luo *et al.* 2008, Yazdi *et al.* 2002). Both SA1- and SA2-depleted cells show reduced survival after IR, indicating an important role of both proteins in the DNA damage response. Also, double depletion of SA1 and SA2 reduced survival to a level comparable with RAD21-depleted cells. In conclusion, this study identifies a separate role of SA2 in DNA repair that is distinct from a role of both SA1 and SA2 in the intra-S DNA damage checkpoint (Kong *et al.* 2014).

Pds5B interacts with BRCA2 and is required for genome stability

Drosophila BRCA2 was found to interact with human PDS5B far more strongly than with human PDS5A (Brough *et al.* 2012). A strong interaction between human BRCA2 and PDS5B was observed following IR exposure, suggesting a role for this interaction in DNA repair. This interaction was dependent on a fragment of BRCA2

encompassing amino acids 786-1909, and several BRCA2 missense variants identified from the Breast Cancer Information Core (BIC) impaired the BRCA2-PDS5B interaction and HR (Brough *et al.* 2012). Depletion of PDS5B using siRNA in 293T cells led to decreased survival in response to aphidicolin, hydroxyurea, mitomycin C, IR and PARP inhibitor. Furthermore, treatment with mitomycin C, which results in DSB formation after replication fork collapse in S-phase led to an increased prevalence of structural chromosome aberrations in PDS5B-depleted cells. Similarly, an increase in chromatid breaks after treatment with aphidicolin was observed in Pds5B -/- MEFs (Carretero *et al.* 2013). PDS5B silencing also reduced the number of IR-induced Rad51 and BRCA2 foci. In a GFP reporter assay PDS5B depletion led to reduced repair of an I-*Sce*I-induced DSB by HR comparable to BRCA2 depletion, suggesting a direct role for PDS5B in HR. Enrichment of PDS5B was also observed at the DSB as shown by ChIP. Collectively these data highlight a critical role of PDS5B in DSB repair by HR (Brough *et al.* 2012).

Further examination of the BRCA2-PDS5B interaction revealed that the two proteins preferentially interacted when the majority of cells were in the first half of S-phase. PDS5B also interacted with the BRCA2-interacting proteins RAD51 and PALB2 and in a temporally similar manner to the BRCA2-PDS5B interaction. These results are consistent with the hypothesis that PDS5B interaction with these proteins is associated with DSB formation generated by replication fork collapse. Treatment with an ATM inhibitor abolished the BRCA2-PDS5B interaction, supporting a function for ATM in the interaction. This is consistent with the identification of PDS5B as a potential ATM/ATR target (Matsuoka *et al.* 2007, Brough *et al.* 2012).

Like BRCA2, PDS5B was found to interact with the replication-associated proteins CDC45 (pre-replication complex component) and PCNA predominantly in S-phase. Both PDS5B and BRCA2 interacted with RAD21 and SMC3, and the association of BRCA2 with these replication and cohesin proteins in early S-phase required Pds5B. Depletion of PDS5B also reduced the binding of RAD51 and PALB2 to BRCA2. Collectively this suggests that PDS5B functions as a node for the interaction between replication and cohesin factors (Brough *et al.* 2012). Finally, PDS5B expression in a cohort of breast tumours revealed that 75/160 (46.9%) had reduced PDS5B expression, and six of these showed apparently no detectable expression. Furthermore, the frequency of low PDS5B expression correlated with histological grade as well as ER-negative and basal-like phenotypes. A statistically significant longer disease-free survival (DFS) was observed in low PDS5B expression ER-negative tumours treated with the DNA damage-inducing chemotherapeutic agent anthracycline. Altogether, these findings suggest that low PDS5B expression

correlates with chemotherapeutic outcome, at least in ER-negative breast tumours (Brough *et al.* 2012).

1.3.5. Disruption of centromeric cohesion as a cause of aneuploidy

Virtually all cancers are aneuploid, and in recent years the potential importance of aneuploidy as a driving mechanism in cancer has been exposed (discussed later). The mechanism whereby reduced centromere cohesion could lead to aneuploidy likely involves disruption of back-to-back sister kinetochore geometric constraint during metaphase alignment. This would in turn increase the frequency of erroneous kinetochore-microtubule attachment from opposing spindle poles, known as merotely (Compton 2011). Importantly, the SAC does not sense merotelic attachments because they do not compromise the total number of kinetochore-microtubule attachments (Cimini *et al.* 2001). Consequently, anaphase onset is not delayed and sister chromatids entering anaphase with uncorrected merotelic attachments become lagging chromosomes, which promote chromosome missegregation. Indeed, the most common cause of chromosome missegregation in CIN-positive cancer cells is lagging chromosomes (Thompson & Compton 2008). Lagging chromosomes and other chromosome segregation defects in mitosis could also cause cell-to-cell fusions and tetraploidy, which is thought to be a transitional state preceding the development of many near-tetraploid and triploid karyotypes (Ganem *et al.* 2007, Duelli & Lazebnik 2007).

An increasing number of studies point to a crucial role of centromeric cohesion in preventing aneuploidy in vertebrates. The frequency of aneuploidy in oocytes increases dramatically during maternal aging, suggesting an age-related reduction in oocyte quality (Hassold & Hunt 2001). More recently, ooyctes from older, but not young mice displayed compromised centromeric cohesion during meiosis I and aneuploidy, which correlated with reduced chromosome-associated Rec8 (meiotic Rad21) (Chiang *et al.* 2011). In mitotic cells, Rad21 +/- mice displayed an increased frequency of aneuploidy but were not prone to tumourigenesis, suggesting a requirement for additional mechanisms to promote aneuploid-related tumour progression (discussed later) (Xu *et al.* 2010).

SA2 and aneuploidy in human cancer

Depletion of SMC1α, SMC3 and SA2 using siRNA resulted in the development of tetraploid and octaploid populations in colon carcinoma cells (Barber *et al.* 2008).

Analysis of metaphase chromosome spreads revealed that knockdown of all three genes resulted in the premature release of sister chromatid cohesion, when primary constriction cohesion at the centromere was assayed (Barber *et al.* 2008).

Solomon *et al.* provided further evidence for SA2-mediated centromeric cohesion preventing aneuploidy in human cancer (Solomon *et al.* 2011). Scoring of primary constriction cohesion revealed that *STAG2*-deficient glioblastoma cells prematurely release sister chromatids compared to cells in which the *STAG2* mutation has been endogenously corrected. In addition, STAG2-deficient cells had an increased frequency of anaphase bridges, chromosomal translocations and displayed altered chromosome counts compared to the STAG2-proficient controls. Specifically, correction of the endogenous *STAG2* mutation in a glioblastoma cell line changed the modal chromosome number from 90 to 85. Cre-mediated knockout of *STAG2* in a colorectal cell line led to a modal chromosome increase of 1, from 45 to 46. Importantly, there are no details on how long after correction/depletion the karyotypes were analysed (Solomon *et al.* 2011).

More recently, 9 out of 12 urothelial carcinomas harbouring *STAG2* mutations had overt aneuploidy as measured using Affymetrix CytoScan HD Arrays (Solomon *et al.* 2013). In a single tumour up to 35 clonal chromosomal aberrations were observed, whilst 3 *STAG2*-mutated samples showed no detectable aberrations. Thus, the majority of *STAG2*-mutated urothelial cancers do display aneuploidy, further supporting a role of STAG2 in preventing aneuploidy in various cancers. Furthermore, depletion of STAG2 using shRNA in urothelial carcinoma cells clearly altered the modal chromosome number from 89 to 88. Again, the time after STAG2 depletion before measuring the chromosome number is not stated (Solomon *et al.* 2013). Supportively, Guo *et al.* reported that tumours with *STAG2* genetic alterations had significantly more aneuploidy (P = 0.01) from analysis of copy number changes on chromosome arms (Guo *et al.* 2013).

Contrary to these findings, Balbáz-Martinéz *et al.* found that loss of SA2 expression occurred predominantly in genomically stable, non-aggressive urothelial bladder cancers (UBCs). Amongst 11 tumours lacking SA2 expression 9 were karyotypically normal and 2 had lost one copy of chromosome 9. In addition, these authors found that shRNA-mediated depletion of SA2 in bladder cancer cells did not lead to aneuploidy (Balbáz-Martinéz *et al.* 2013). This is consistent with findings that frequent mutations in *STAG2, SMC3, SMC1A* and *RAD21* were not associated with aneuploidy in acute myeloid leukemia (Welch *et al.* 2012, Walter *et al.* 2009). Specifically, normal karyotypes were observed in 12 AML cases harbouring cohesin

gene mutations, and 6 cases contained 3 or fewer abnormalities. Only one case displayed complex cytogenetics (Welch *et al.* 2012). Somewhat contrary to a role of cohesin in preventing aneuploidy in cancer are findings that amongst 43 cases of myeloid neoplasm harbouring cohesin mutations only 10 were aneuploid, and a further ten showed chromosome aberrations without aneuploidy. Amongst the 29 cases with a *STAG2* mutation, 16 were karyotypically normal, 7 were aneuploidy, and 6 had chromosome aberrations without aneuploidy. Therefore, aneuploidy is not ubiquitous amongst cancers with mutations in *STAG2.* This is perhaps surprising, and might be due to different levels of tolerance to aneuploidy in different cell types (Balbáz-Martinéz *et al.* 2013).

Chromosome missegregation and aneuploidy in cells lacking components that regulate the centromere-specific cohesion pathway

Esco2 -/- MEFs show a centromeric cohesion defect and severe chromosome segregation defects (Whelan *et al.* 2012). These included lagging chromosomes, anaphase bridges and chromosomes located near spindle poles, all of which are consistent with a centromere cohesion defect. Interphase nuclei were frequently multilobed and contained micronuclei, which are typical of cells that have experienced chromosome missegregation in the previous mitosis (Whelan *et al.* 2012). Carretero *et al.* reported a centromeric cohesion defect in Pds5B -/- MEFs, as well as increased cytokinesis failure, cell death and statistically significant increases in aneuploidy (Carretero *et al.* 2013). Specifically, the aneuploidy manifest as an increased range of chromosome counts per cell, indicating relatively equal chromosome gains and losses (Carretero *et al.* 2013). Overexpression of Separase, which is frequently observed in numerous human tumour types, was found to result in a centromeric cohesion defect in mouse mammary epithelial cells (Zhang *et al.* 2008). Moreover, Separase overexpression led to an increased frequency of lagging chromosomes and anaphase bridges, and the formation of aneuploid tumours in an *in vivo* mouse mammary transplant model (Zhang *et al.* 2008).

The SWI/SNF-related Alpha thalassemia/mental retardation X linked (ATRX) ATPase is highly enriched at PCH and is required for centromeric cohesion and congression (Ritchie *et al.* 2010). Mutations in ATRX give rise to various mental retardation syndromes characterized by developmental delay, cognitive defects and microcephaly (Ritchie *et al.* 2010). Depletion of ATRX in human cells caused a delay in the prometaphase to metaphase transition, increased interkinetochore distance,

defective SAC, increased frequencies of anaphase bridges and micronuclei (Ritchie *et al.* 2010).

Cells in which the potent tumour suppressor Rb is lacking or inactivated are prone to aneuploidy (Hernando *et al.* 2004, Iovino *et al.* 2006, Isaac *et al.* 2006, Mayhew *et al.* 2007, Srinivasen *et al.* 2007, Amato *et al.* 2009), but until recently the exact involvement of the protein in preventing aneuploidy was unclear (Manning *et al.* 2010). Loss of Rb might cause aneuploidy via a number of distinct mechanisms. First, Rb transcriptionally regulates several genes involved in mitosis and the SAC, including Aurora A, Astrin, CDC20, MAD2, NEK2 and NDC80 (Iovino *et al.* 2006, Chakraborty *et al.* 2007). Indeed, overexpression of MAD2 can compromise the SAC and cause aneuploidy (Sotillo *et al.* 2007). However, MAD2 levels are found to decrease rather than increase in cells depleted of Rb (Amato *et al.* 2009).

Manning *et al.* made the important finding that loss of Rb results in substantially elevated rates of chromosome missegregation that is not associated with a defective SAC (Manning *et al.* 2010). Moreover, Rb-depleted cells showed a statistically significant increase in the distance between sister centromeres, reduced centromeric sister chromatid cohesion, impaired chromosome congression, and an increase in the number of chromosomes displaying a centromeric distortion pattern characteristic of merotely (Cimini *et al.* 2003, Draviam *et al.* 2006, Manning *et al.* 2010). Loss of Rb compromised mitotic progression, leading to increased multipolar spindles and increased anaphase bridges. A minor reduction in chromatin-bound RAD21 and SMC3 was observed in Rb-depleted cells. However, centromere-localized cohesin only represents ~10% of all chromatin bound cohesin (Peters *et al.* 2008). Thus, loss of all cohesin from the centromere might not be obvious in a chromatin fractionation experiment. Consistent with a specific reduction in chromatin bound cohesin at the centromere were findings that in mitotic Rb-depleted cells the punctate pattern of RAD21 localization was conspicuously reduced (Manning *et al.* 2010). This study identifies a novel, potent role for Rb in promoting centromeric cohesion and preventing aneuploidy that is independent of transcriptional regulation (Manning *et al.* 2010).

1.3.6. Aneuploidy as a driver of tumourigenesis

Chromosomal abnormalities, including translocations, deletions, amplifications and aneuploidy, were known to be associated with cancer over a century ago. Aneuploidy is common in cancer and correlates with poor prognosis in many situations (Carter *et*

al. 2006). Some cancers are karyotypically stable but all cancers at least harbor multiple mutations and/or structural chromosome aberrations. A long-standing debate has focused on whether such genetic alterations and aneuploidy are a cause or a consequence of tumourigenesis (Gordon *et al.* 2012, Kolodner *et al.* 2011). Cancer cells accumulate mutations, rearrangements and aneuploidy during their development and progression, but the order and mechanisms by which these occur are largely unclear (Kolodner *et al.* 2011).

The 'mutator' hypothesis envisions that cancer cells must somehow acquire a phenotype that results in elevated rates of mutation and genetic alterations that drives the development of further alterations required for progression (Loeb 2001). This hypothesis has gained substantial support in recent years from findings that frequent mutations in diverse cancers occur in pathways that (might) regulate genome stability, including cohesin and chromatin remodeling complexes. In addition, numerous familial cancer predisposition syndromes are caused by defects in DNA damage repair and response pathways (Kolodner *et al.* 2011).

The effects of aneuploidy in cancer are less clear. Although aneuploidy is considered a hallmark of most cancers, the gain of single chromosomes can result in reduced cell growth in human and mouse cells (Torres *et al.* 2010, Williams *et al.* 2008), and is usually lethal in many organisms from *Drosophila* to human (Torres *et al.* 2008). Indeed, aneuploidy confers severe disadvantages to cells due to increased stress burdens from altered protein homeostasis and metabolism (Torres *et al.* 2007, Torres *et al.* 2010, Williams *et al.* 2008). In addition, the progression of some cancers is attenuated by aneuploidy but enhanced in others in mice (Weaver *et al.* 2007). Studies in yeast suggest that the effects of aneuploidy are likely to be highly complex and dependent on the altered expression of many genes and pathways (Rancati *et al.* 2008). Cancer cell lines with gross chromosomal instability (CIN) missegregate chromosomes at a substantially higher frequency than nontransformed cells (Thompson *et al.* 2008, Lengauer *et al.* 1997). Thus, aneuploidy in this context might simply represent a by-product of pre-existing genome instability.

More recently, a fascinating study by Sheltzer *et al.* showed that the engineered gain of single chromosomes in yeast resulted in modest but statistically significant increases in the rate of point mutation, spontaneous mitotic recombination and further aneuploidy (chromosome loss), as well as sensitivity to DNA damaging agents and increased spontaneous Rad52 foci (Sheltzer *et al.* 2011). Furthermore, the increased genomic instability was found to be due to stoichiometric protein imbalances rather than increased DNA content. This study indicates that aneuploidy can drive genomic

instability at least in yeast, and has important implications for aneuploidy in cancer. Aneuploidy occurring as an early event in a nontransformed precursor cell could be sufficient to drive the genomic instability required for the cell's development and progression towards cancer. This has profound implications given the recent findings that a high frequency of mutations occur in genes known to prevent aneuploidy, including *STAG2* as a shining example.

1.3.7. Cohesin and cancer

Transcriptional misregulation as a functional *consequence of cohesin dysfunction in cancer*

Cohesin is important for transcriptional regulation by forming loops within DNA to regulate promoter-enhancer interactions. A number of transcriptional programs associated with tumourigenesis appear to be regulated by cohesin. The Drosophila homologue of RAD21, known as *vtd,* is a member of the trithorax group (TrxG) protein family (Hallson *et al.* 2008), which includes dominant suppressors of PcG and HH proteins. However, Drosophila *vtd* is not a known functional homologue of *RAD21,* and mutations in *SMC1* or *PDS5* did not mirror the TrxG phenotype (Xu *et al.* 2011).

Cohesin also closely interacts with the transcriptional repressor CCCTC-binding factor (CTCF), which regulates interactions between *trans*-acting factors with promoters and is a putative tumour suppressor (Wendt & Peters 2009, Nikolaev *et al.* 2009). Potential tumour suppressor activities of cohesin/CTCF include protection of tumour suppressor gene promoters from methylation-dependent silencing, maintenance of genomic imprinting, regulation of *MYC*, *IGF2* (imprinting gene), interleukin-3 (*IL-3),* granulocyte-macrophage colony stimulating factor 2 (*CSF2)* and *IFNG* transcription (Xu *et al.* 2011). Loss of imprinting is common in many tumours and is often one of the first abnormalities to be observed (Filippova *et al.* 2008). Cohesin-CTCF also appears to have a broad function in the global regulation of transcription, which if misregulated could lead to oncogene activation and tumour suppressor inactivation (Kagey *et al.* 2010, Miele & Dekker 2008, Xu *et al.* 2011).

Cancer-associated mutations in cohesin genes

Barber *et al.* performed a screen for mutations in human homologues of 102 known yeast chromosomal instability (CIN) genes in a panel of colorectal cancers and

identified four genes that regulate sister chromatid cohesion (Barber *et al.* 2008). Within the 132 cases analysed 10 mutations were identified, occurring in *SMC1A* (four mutations), *NIPBL* (four mutations), *SMC3* (1 mutation), *STAG3* (meiotic paralogue of yeast *SCC3,* 1 mutation). Collectively, cohesin mutations were identified in ~7.5% of all colorectal tumours analysed (Barber *et al.* 2008).

More recently, Soloman *et al.* performed single-nucleotide polymorphism (SNP) arrays on human glioblastoma cell lines to locate regions of DNA deletion and amplification (Solomon *et al.* 2011). One cell line (U138MG) contained a deletion at Xq25 that has been observed in other studies, and is a region that harbours the *STAG2* gene. Accordingly, STAG2 protein expression was absent in U138MG, as well as in 42MGBA and H4 cell lines, which were found to contain nonsense and frameshift mutations, respectively. Further sequencing of 68 glioblastoma cases identified four additional *STAG2* mutations, and ten cell lines from a panel of 168 various cancer types showed complete loss of STAG2 expression (Solomon *et al.* 2011). This suggests that *STAG2* represents an important tumour suppressor gene is various cancers types.

A very recent spate of exome sequencing studies revealed further frequent mutations in various cohesin genes in diverse cancer types (Welch *et al.* 2012, Solomon *et al.* 2013, Guo *et al.* 2013, Balbáz-Martinez *et al.* 2013, Kon *et al.* 2013, Kim *et al.* 2013). Four independent studies published together in *Nature Genetics* identified frequent truncating mutations in various cohesin genes, but particularly *STAG2*, in bladder cancer (Solomon *et al.* 2013, Guo *et al.* 2013, Balbáz-Martinéz *et al.* 2013) and myeloid neoplasms (Kon *et al.* 2013). Solomon *et al.* reported that 52 out of 295 urothelial carcinomas of the bladder (18%) showed complete loss of SA2 expression. Loss of SA2 expression was also occasionally observed in several other cancer types. In an independent cohort of 111 primary urothelial carcinomas 25 mutations were found in 23 cases. Amongst these, 21 mutations resulted in a truncated protein product, 5 of which were nonsense, 6 were splice-site and 10 were frameshift mutations. Three missense mutations were found to retain SA2 expression as shown by immunohistochemistry. 5 out of 32 urothelial carcinoma cells lines also harboured truncating mutations, and concurrent p53 overexpression or mutation was frequently found in tumours and cell lines with SA2 mutations (Solomon *et al.* 2013).

Balbáz-Martinéz *et al.* sequenced the exomes of 17 urothelial bladder cancer samples with matched normal leukocyte DNA. A total of 2,927 mutations were identified, of which 798 were predicted to be damaging (i.e. to have a functional effect). Importantly, the study identified recurrent, previously unreported mutations in

DNA repair genes, including *ATM, ERCC2 and FANCA*, and the cohesin subunit genes *STAG2, STAG1, SMC1A* and *SMC1B* (Balbáz-Martinéz *et al.* 2013)

The authors next focused on SA2 because of its high mutation rate in a collection of bladder cancer studies (damaging somatic mutations in 12 out of 77 tumours (15.6%)). Amongst these, 5 were nonsense, 4 were exon junction, 2 were missense and 1 was an insertion and deletion (indel) mutation. Expression of SA2 was reduced or not detected in 6 out of 7 (85%) urothelial bladder cancers with damaging mutations and 3 out of 34 (9%) tumours with wild-type SA2. Tissue microarray analysis of incident tumours found loss of SA2 expression (histoscore ≤50 with detectable stromal expression) in 197 of 671 tumours (29.3%). In these samples loss of SA2 expression correlated significantly with multicentricity, tumour size, low stage and low grade.

The third study to report frequent alterations in cohesin genes performed whole exome sequencing of 99 samples of transitional cell carcinoma (TCC, the predominant form of bladder cancer) (Guo *et al.* 2013). Amongst 13 newly identified TCC genes *STAG2* ranked most significantly mutated. Specifically, 11 cases (11%) had *STAG2* mutations, 9 of which were truncating (3 small frameshift indels, 4 nonsense, 2 splice-site). *STAG2* genomic deletions were observed in 5 of the 99 cases. Sequencing of a further 50 matched tumour samples revealed 5 somatic mutations in 4 tumours. Also, examination of the *STAG2* promoter in 30 TCCs showed hypermethylation in 7 cases (23%). Kaplan-Meier survival analysis showed that individuals with *STAG2* mutations had a much worse prognosis compared to wild-type *STAG2* individuals. Frequent genetic alterations were also observed in other cohesin genes, including *NIPBL* (4% of tumours), *SMC1A* (3%) and *SMC3* (2%). Interestingly, frequent mutations were also found in *ESPL1* (6%), which encodes separase (Guo *et al.* 2013).

Whole exome sequencing of 24 acute myeloid leukemia (AML) cancers identified a total of 19 mutations in *STAG2, SMC3, SMC1A* and *RAD21.* 11 of these were loss of function mutations (nonsense, splice site or gene deletion) (Welch *et al.* 2012). A more recent exome sequencing study of myeloid neoplasms found 54 recurrent, usually mutually exclusive mutations and deletions in *STAG2, SMC3, SMC1A* and *RAD21.* Again, the majority of the mutations (33; 61.1%) were found in *STAG2,* whilst 12 (22.2%), 5 (9.3%) and 4 (7.4%) occurred in *RAD21, SMC3 and SMC1A,* respectively (Kon *et al.* 2013). The authors showed that leukemic cells harbouring cohesin mutations had reduced levels of chromatin-bound cohesin proteins. In addition, forced expression of RAD21 and SA2 in leukemic cell lines with

reduced RAD21 and SA2 expression suppressed cell growth, suggesting an important role for reduced cohesin in myeloid leukemogenesis (Kon *et al.* 2013).

A study by Kim *et al.* sought to determine if the centromere cohesion-specific putative tumour suppressor genes *SGO1* and *PDS5B* were mutated or misexpressed in gastric and colorectal cancer (Kim *et al.* 2013). The genes encoding both proteins contain mononucleotide repeats in coding sequences that were considered possible mutation sites in microsatellite unstable cases of these cancers. Analysis of 91 gastric and 100 colorectal cancers identified a total of 21 *SGO1* frameshift mutations in 21 cases and 18 *PDS5B* frameshift mutations in 16 cases (Kim *et al.* 2013). Amongst 112 microsatellite unstable cancers 26.6% and 20.3% contained *SGO1* and *PDS5B* mutations, respectively. In addition, out of all cancers (microsatellite stable and unstable) 19% and 47% had lost expression of PDS5B and SGO1, respectively, as measured by immunohistochemistry. Thus, this study suggests that frameshift mutation and loss of expression of *PDS5B* and *SGO1* is a feature of gastric and colorectal cancer and might function in cancer pathogenesis (Kim *et al.* 2013).

Deregulated expression of cohesin genes in cancer

The studies described above provide fascinating new evidence that various cohesin genes are mutated at a previously unknown high frequency in diverse cancers. *STAG2* mutations appear to be particularly frequent. This might reflect a particularly critical role of SA2 in preventing tumourigenesis, or alternatively might be due to the fact that the *STAG2* gene resides on the X chromosome. Therefore, inactivation of *STAG2* would only require one mutational hit (Balbáz-Martinéz *et al.* 2013).

In addition to the high frequency of mutation, numerous cohesin subunits are misregulated in cancer. At present, the mechanisms underlying the cases of misregulation described below are largely unclear (Xu *et al.* 2011). In particular, RAD21 was consistently overexpressed preferentially in undifferentiated, usually aneuploid cancer types including ovarian, breast, brain, bladder, and lung cancers (Rhodes *et al.* 2004). More recently, in a large cohort of sporadic breast cancers RAD21 expression was elevated in high-grade tumours from various subtypes and was associated with poor prognosis (Xu *et al.* 2011, van ‘t Veer *et al.* 2002). Also, RAD21 is overexpressed in 30-40% of hormone-refractory prostate cancers (Porkka *et al.* 2004) and in mesothelioma (Roe *et al.* 2009). SMC3 overexpression has been observed in colon carcinoma tissue and adenomatous polyps and adenocarcinomas with β-catenin overexpression (Ghiselli & Iozzo 2000, Ghiselli *et al.* 2003).

Cohesin-associated proteins are also overexpressed in many cancers. *PTTG1,* which encodes Securin, is overexpressed in breast, thyroid, brain, oesophagus, and colon and hepatocellular cancers. This overexpression is correlated with tumour stage and survival in many of these cancers (Salehi *et al.* 2008). Other cohesin-associated proteins that are overexpressed include PDS5A in high-grade gliomas (Hagemann *et al.* 2011), Separase in prostate, 70% of breast cancers and osteosarcoma specimens (Zhang *et al.* 2008, Meyer *et al.* 2009), WAPL in cervical dysplasia and carcinoma (Oikawa *et al.* 2004), and ESCO2 in aggressive melanomas (Ryu *et al.* 2007).

Interestingly, depletion of many cohesin proteins in various cancers has an antiproliferative effect, including Securin (Salehi *et al.* 2008), and WAPL in cervical cancer (Oikawa *et al.* 2004), suggesting that cohesin might regulate proliferation. In grade III invasive breast ductal carcinomas genome-wide integrated analysis of array-based genomic hybridization and microarray expression profiling showed that RAD21 expression levels are correlated with DNA copy number (Xu *et al.* 2011). Therefore, copy number variation (CNV) might at least partially contribute to the altered cohesin protein expression levels in cancer (Xu *et al.* 2011). In summary, the mechanisms underlying the cases of misregulation described above are largely unclear (Xu *et al.* 2011). Many cohesin genes are upregulated in diverse cancers, however the importance of these changes in tumour progression remains to be determined.

1.3.8. Rsc1 and Rsc2 are required for establishing sister chromatin cohesion

In 2004 two studies published a month apart implicated RSC in sister chromatid cohesion. Baetz *et al.* employed a genomic haploinsufficiency modifier screen to identify genes that affect chromosome transmission (Baetz *et al.* 2004). A haploid *MAT*α deletion mutant array (DMA) was mated with wild-type *CTF13* and mutant *ctf13-30 MAT***a** haploids. *CTF13* encodes a subunit of the essential inner kinetochore protein CBF3, and the *ctf13-30* mutant is both temperature and microtubule destabilizing drug-sensitive (Doheny *et al.* 1993, Spencer *et al.* 1990). The resulting heterozygous deletion diploids that displayed altered temperature and/or drug sensitivity to the CTF13/*ctf13-30* heterozygous diploid were identified. Further screening isolated both *RSC1* and *RSC2* as mediators of chromosome segregation, however only the *rsc2* mutant had a detectable change in the rate of chromosome loss (Baetz *et al.* 2004). Deletion of *RSC2* was synthetically lethal with mutants of the inner kinetochore gene *NCD10*, as well as being conditionally synthetic lethal (CSL) (by increased temperature) with *cse4-1*, *okp1-5* and *ctf13-30* kinetochore mutants. In contrast, deletion of *RSC1* only resulted in CSL with the *NCD10* mutants (Baetz *et al.*

2004). Next, ChIP was used with tagged Ndc10, Cse4 (inner kinetochore) and Ctf3 (central kinetochore) to show that localization of these proteins to the centromere was normal in the *rsc2* mutant.

The possibility that the chromosome missegregation defect in *rsc2* might be due to a defect in sister chromatid cohesion was also tested. Deletion of *RSC2* caused CSL with *scc1-73*, *smc3-4* mutants and reduced the permissive growth temperature with *ctf8*, *ctf18* and *scc2-4* mutants. The *rsc2* mutant was then shown to have a defect in sister chromatid cohesion using a strain that expresses a Tet repressor-green fluorescent protein (GFP) fusion protein. Tet operator repeats were integrated 35kb from the centromere of chromomsome V (Michaelis *et al.* 1997), and by scoring the number of nocodazole-arrested cells that show two GFP signals readout of cohesion is given (Baetz *et al.* 2004). 7% of wild-type cells had two GFP signals whilst *rsc2* and *rsc1* had 22% and 14% respectively. Furthermore, the association of the cohesin subunits Smc3 and Scc1 with chromatin were not affected by deletion of *RSC2*, indicating that Rsc2 is involved in either the establishment or maintenance of sister chromatid cohesion. Finally, wild-type, *rsc2* and *scc1-73* cells were arrested in α-factor, released into nocodazole until >90% of cells had undergone DNA replication, before shifting to 37°C and scoring GFP signals over a time-course. Whilst the *scc1-73* mutant showed a steady increase in two GFP signals over time, both the wild-type and *rsc2* did not show an increase, indicating that establishment and not maintenance of cohesion is defective in *rsc2*.

Huang *et al.* also reported an involvement of RSC in sister chromatid cohesion. Initially, the authors reported that a temperature-sensitive bromodomain mutant of Sth1, *sth1L1346A*, was defective in 2μ plasmid maintenance but not *CEN* plasmid maintenance (Huang *et al.* 2004). Previously it had been shown that Rsc2 mutants are also defective in maintaining 2μ plasmids (Wong *et al.* 2002). The yeast 2μ plasmid is maintained at about 60 copies in a haploid cell and undergoes a process known as partitioning, important for high fidelity segregation the plasmid. Partitioning involves the localization of the proteins Rep1 and Rep2, which are encoded by the plasmid, to the *STB* (Malik 2006). It has since been shown that 2μ plasmid segregation depends on the recruitment Cse4 to the *STB* locus (Hajra *et al.* 2006). In the absence of Cse4 it was shown that Rep2 fails to localize to the *STB*, Rsc2-dependent remodelling of Cse4-containing nucleosomes does not occur, and consequently cohesin is not recruited (Hajra *et al.* 2006).

Next, it was shown that *rsc2* and *sth1L1346A* displayed an increased rate of minichromosome loss, whilst only the *sth1-3ts* mutant showed an increased rate of

minichromosome non-disjunction. The *sth1-3ts* mutant was previously shown to be defective in kinetochore function and *CEN* plasmid segregation (Hsu *et al.* 2003), highlighting separate chromosome transmission functions of *sth1L1346A* and *rsc2* compared to *sth1-3ts* (Huang *et al.* 2004). Consistently, both Sth1 and Rsc8 subunits localized only to the *STB* locus on 2μ plasmids and in a cell-cycle dependent manner similar to that of Mcd1 as shown by ChIP. Like Mcd1, recruitment of Sth1 occurred in late G1, before dissociating in late G2, however association and dissociation occurred 15 minutes preceding Mcd1 (Huang *et al.* 2004). An identical pattern of Sth1 recruitment was also observed at four chromosome arm loci, whilst its association with the centromere was constitutive.

Intriguingly, the temperature sensitivity of an *scc1-73* mutant was rescued by additionally mutating *sth1L1346A* or *rsc2*, whilst the *scc1-73 sth1-3ts* double mutant conferred no growth advantage, again separating the *sth1L1346A* and *rsc2* mutations from *sth1-3ts*. In addition, Sth1 co-immunoprecipated with Mcd1 and Scc3. Importantly, in the *sth1L1346A* and *rsc2* mutants Mcd1 failed to associate with chromosome arm loci and the *STB* locus but remained associated with centromeres. Furthermore, *rsc2* cells arrested in hydroxyurea also displayed this Mcd1 localization pattern, suggesting that the cohesion defect occurs before replication (Huang *et al.* 2004). Finally, the authors demonstrated that the *rsc2* and *sth1L1346A* mutants separate sister chromatids prematurely. Using the same Tet repressor-GFP reporter assay described previously, *rsc2* cells showed between 3 and 7-fold increases in the number of mother cells with separated sister chromatids (35kb from centromere) compared to wild-type cells. The *sth1L1346A* mutant showed premature release of sister chromatid cohesion at two arm loci (35 and 284kb from the centromere) but not at the centromere itself. Curiously, cohesion at the centromere in *rsc2* was not tested (Huang *et al.* 2004).

1.4. The BAF180 tumour suppressor

1.4.1. Binding and activity of the BAF180 tumour suppressor

BAF180 is one of three proteins that are unique to the PBAF (SWI/SNF-B) complex, along with BRD7 and ARID2, which distinguish the complex from the BAF (SWI/SNF-A) complex (Wilson & Roberts 2011) (Table 1.1). At present very little is known about the specific functions BAF180. Considerably more research has been done on subunits common to both BAF and PBAF. As described previously, these include SNF5, which is implicated in the transcriptional regulation of Rb and E2F target gene pathways, and BRG1, which has a role in DNA repair.

BAF180 is mutated at a strikingly high frequency in certain cancer types, but is also mutated at a lower frequency in an increasingly diverse range of other cancers. Thus, BAF180 is considered an important tumour suppressor, but only a few potential tumour suppressor functions have been identified. As described previously, the currently held belief is that BAF180 enforces its tumour suppressor activity by regulating the transcriptional activity of specific tumour suppressor genes, such as p21. However, the actual importance of this activity in tumour suppression has not been demonstrated. Valuable insight into other potential tumour suppressor functions of BAF180 can be gained from studies on the highly conserved yeast homologues of BAF180. These include Rsc1, Rsc2 and Rsc4, which have many well-characterized roles that might directly equate to tumour suppressor activities in mammalian cells. In this section we provide an overview of the binding targets, known functions, and current mutation spectrum of BAF180 in cancer.

Binding targets of the BAF180 bromodomains and BAH domains

BAF180 appears to be an evolutionarily conserved fusion of the RSC subunits Rsc1, Rsc2 and Rsc4, containing six bromodomains, two BAH domains and an HMG domain (involved in DNA binding) (Xue *et al.* 2000) (Figure 1.2). At present very little is known about the binding targets of the BAF180 bromodomains and BAH domains. Two studies have tested the ability of BAF180's six individually expressed and purified bromodomains to bind specific acetyl-lysine histone peptides, however each study came to very different conclusions. Chandrasekaran and Thompson generated dissociation constants using fluorescence anisotropy with H3 peptides acetylated at K4, K9, K14, K18 and K23. They found that the first five individual bromodomains

showed a distinct pattern of affinity for each different acetylated peptide. Specifically, BD1 preferentially bound to K4Ac, BD2 and BD3 bound to K9Ac, BD4 bound to K23Ac, and BD5 bound to K14Ac. Interestingly, BD6 showed no obvious preference for any of the acetylated H3 peptides tested (Chandrasekaran & Thompson 2007).

The second study by Charlop-Powers and co-workers used a dot-blot assay to assess binding of the six BAF180 bromodomains to monoacetylated peptides from all four core histones (Charlop-Powers *et al.* 2011). Again, each bromodomain showed a distinct pattern of binding preference to specific acetylated peptides, however none of the top 'hits' matched those found in the study by Chandrasekaran and Thompson. The acetylated peptides that scored as 'high' binding affinity were H3K36Ac for BD1, H3K14Ac and H2BK116Ac for BD2, H3K115Ac, H4K12Ac, H2BK15Ac and H2BK120Ac for BD3, H3K14Ac and H3K11Ac for BD4, H3K36Ac for BD5 and H2BK24Ac and H2BK116Ac for BD6. Notably, the entire top 'hits' from the previous study scored as 'negative' in terms of binding affinity (Charlop-Powers *et al.* 2011). Thus, the true binding targets of the BAF180 bromodomains are yet to be conclusively identified (Brownlee *et al.* 2012). Recent work in our lab showed that the BAH domain of Rsc2 and the homologous proximal BAF180 BAH domain (BAH2) bind to unmodified H3 (Chambers *et al.* 2013). Therefore it seems reasonable to assume that the BAF180 bromodomains recognise acetylated lysine residues on the same or neighbouring histones. It is also entirely possible that the bromodomains bind to other non-histone acetyl-lysine residues.

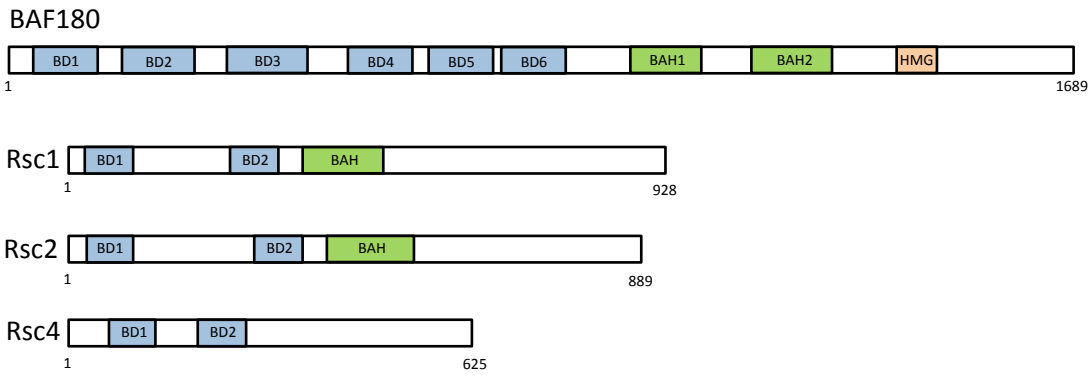

Figure 1.2. BAF180 is homologous to a fusion of the RSC subunits Rsc1, Rsc2 and Rsc4, containing 6 homologous bromodomains (BDs) and 2 bromo-adjacent homology (BAH) domains.

BAF180 is required for the replication of damaged DNA

A recent study by Niimi *et al.* identified a role for BAF180 and the yeast homologue Rsc2 in repriming stalled replication forks at site of DNA damage (Niimi *et al.* 2012). Replicative polymerases encountering a damaged base, such as cyclic pyrimidine dimers (CPDs) induced by UV, are unable to progress past the lesion. In this situation, the replicative polymerase is substituted by translesion synthesis (TLS) polymerases, which can bypass the lesion (Yang & Woodgate 2007, Lehmann *et al.* 2007). Proliferating cell nuclear antigen (PCNA) regulates the switch from replicative to TLS polymerase. PCNA is ubiquitinated by the E2 ubiquitin-conjugating enzyme Rad6 and the E3 ubiquitin ligase Rad18 in the presence of single-stranded DNA at the blocked replication fork (Hoege *et al.* 2002, Kannouche *et al.* 2004, Davies *et al.* 2008). TLS polymerases have a high affinity for uniquitinated PCNA, and therefore PCNA ubiquitination provides a mechanism for the polymerase switching (Bienko *et al.* 2005, Plosky *et al.* 2006, Kannouche *et al.* 2004).

Deletion of *RSC2*, but not *RSC1*, resulted in reduced PCNA ubiquitination after treatment with UV, MMS and HU. Similarly, depletion of BAF180 using siRNA resulted in a similar reduction of ubiquitinated PCNA after UV. Moreover, BAF180-depleted cells showed reduced levels of chromatin-bound unmodified PCNA and Rad18. Because PCNA ubiquitination is required for post-replicative DNA repair the authors next analysed fork progression after UV. Consistently, a modest reduction in fork progression was observed in the BAF180-depelted cells, however these cells did not show reduced survival after UV. In addition, untreated BAF180-depleted cells did not display any obvious alteration in cell cycle progression (Niimi *et al.* 2012). Rsc2 was recruited to replication forks during S-phase as shown by ChIP, and by extrapolation this was considered to be the case with BAF180.

A proposed model based on these observations follows that BAF180 promotes the repriming of replication downstream from blocked replication forks preceding TLS. Each repriming event at subsequent stalled forks involves recruitment of a new PCNA molecule, which requires BAF180. In the absence of BAF180 there is less PCNA loading and replication through damaged DNA is delayed (Niimi *et al.* 2012).

A role for BAF180 and PBAF at centromeres

Both the human BAF and PBAF complexes displayed ATP-dependent nucleosome disruption activity in a remodelling assay (Xue *et al.* 2000). In the same study the intracellular localization of human PBAF was analysed by immunofluorescence using a

BAF180 antibody. Interphase nuclei showed uniform BAF180 staining, whilst in prometaphase BAF180 co-stained with cytoplasmic dynein (kinetochore marker) at some kinetochores. This localization was only observed in prometaphase and not in metaphase, anaphase or telophase. Interestingly, BAF180 also localized to spindle poles, which persisted into metaphase. The localization of BAF180 to the kinetochores of mitotic chromosomes implies that BAF180 plays a role there during mitosis (Xue *et al.* 2000).

More recently, Bourgo *et al.* showed that Cre-mediated depletion of Brg1 in primary mouse adult fibroblasts (MAFs) led to a dramatic disruption of DAPI-dense heterochromatic domain structure (Bourgo *et al.* 2009). Importantly, depletion of Snf5 did not cause the same defect, indicating a phenomenon that is specific to the Brg1 ATPase subunit. Brg1-depleted cells also showed a disrupted nuclear pattern of H3K9me3 and H4K20me3, which are characteristic modifications in pericentromeric heterochromatin (Bourgo *et al.* 2009). Interestingly, these modifications are not required for the formation of these heterochromatin domains (Peters *et al.* 2001, Gonzalo *et al.* 2005). Therefore, the finding that Brg1 is required for correct heterochromatin structure and distribution of these modifications reveals that Brg1 underlies a hierarchical maintenance of heterochromatin function.

Brg1 depletion also resulted in a striking increase in micronuclei formation, dramatically reduced proliferation, and an increased number of cells with 4N and >4N DNA content, indicative of polyploidy (Bourgo *et al.* 2009). There was also a strong selection against Brg1 loss. Furthermore, >70% of Brg1-depleted mitotic cells displayed some form of abnormal mitotic division, and the few cells that entered anaphase frequently showed anaphase bridges, lagging chromosomes or mitotic catastrophe. In summary, this study identifies Brg1 as being important for the maintenance of pericentromeric heterochromatin and genome stability. However, the underlying mechanism was not identified, and it remains to be determined if other subunits of PBAF are similarly required for this unique function.

BAF180 mutation spectrum in human cancer

PBRM1 was first identified as harbouring multiple truncating mutations in breast cancer in a screen for novel breast cancer tumour suppressor genes (Xia *et al.* 2008). 3 out of 26 breast cancer cell lines harboured truncating mutations that abolished protein expression, and showed strong evidence of loss of heterozygosity (LOH). In addition, mutational screening of 52 primary breast tumours identified one other truncating

mutation, and 25 of these samples (48.1%) showed BAF180 LOH without a mutation (Xia *et al.* 2008).

An important study by Varela *et al.* initially sequenced the protein coding exomes of 7 clear cell renal cell carcinomas (ccRCCs) and found truncating *PBRM1* mutations in 4 cases (Varela *et al.* 2011). Sequencing of an additional 257 RCCs identified truncating mutations in a striking 34% of cases, as well as two in-frame deletions and nine missense mutations. These mutations are discussed in more detail in Chapter 5. In cases where SNP array data was available *PBRM1* mutations all occurred in the context of 3p21 loss of heterozygosity (LOH) (38/38 cases). Further sequencing of 727 cancer cell lines from various histologies identified 5 homozygous *PBRM1* truncating mutations. These included 3 frame-shifting deletions in a RCC, a small-cell lung cancer, and a gall bladder cell line, and 2 nonsense mutations in a squamous-cell lung cancer and a pancreatic adenocarcinoma cell line. In addition, 6 nonsense, 3 frameshift, 1 in frame deletion and 22 missense heterozygous *PBRM1* mutations were found in various other cell lines. Potentially more interesting is the identification of 6 homozygous missense mutations. These included an E1287Q mutation (BAH2) in a breast cancer cell line, Y893C mutation (BD6) in a lung cancer cell line, G340A in (occurs in region between BD2 and BD3) in a skin cancer cell line, I233T (BD2) in a kidney cancer cell line, R66G (BD1) in a colon cancer cell line, and T56A (BD1) in a central nervous system cancer cell line. Intriguingly, the Y893C mutation also occurred as a heterozygous mutation in a lymphoblastic leukemia cell line and a liver cancer cell line (Varela *et al.* 2011). These missense mutations are potentially of great interest because they might not disrupt protein stability, and predominantly occur in the bromodomains and BAH domains of BAF180. The finding that the Y893C homozygous mutation also occurs as a heterozygous mutation in two other cancer samples suggests that heterozygous *PBRM1* mutations are also important in tumourigenesis.

A significant enrichment of insertion events in mouse *Pbrm1* was observed from several transposon insertional mutatgenesis screens, providing further support that *PBRM1* can act as a tumour suppressor gene. Insertions were found in pancreatic dysplasia, intraductal, and high-grade invasive tumours, suggesting that inactivation of *Pbrm1* in this model is an early event (Varela *et al.* 2011). BAF180 depletion using siRNA in 4/5 RCC cell lines resulted in significantly increased proliferation, colony formation and cell migration, indicating an increase in transformed phenotype. Inspection of gene expression microarrays showed that BAF180 knockdown resulted in statistically significant changes ($P < 0.05$) in the expression of 62 genes in all three RCC cell lines analysed. Amongst these, only three genes associated with genome

stability and replication were significantly misregulated. These included ATM, which was upregulated following BAF180 loss (P = 0.011), GINS4 (GINS complex subunit 4, which is required for DNA replication initiation in budding yeast), was upregulated (P = 0.024), and SKA1 (spindle and kinetochore associated complex subunit 1, P = 0.038), which was also upregulated (Varela *et al.* 2011). Therefore, BAF180 depletion does not appear to result substantial downregulation of genes involved in genome stability. This is consistent with the findings that amongst the 371 genes found to be significantly misregulated following BRG1 depletion, only 2 of these were involved in DNA repair (NER and BER) (Park *et al.* 2006).

More recently, in a cohort of 68 diffuse large B-cell lymphomas 2 *PBRM1* mutations were identified (Lohr *et al.* 2012, Pasqualucci *et al.* 2011, Morin *et al.* 2011). A small number of *PBRM1* mutations have also been also found in head and neck cancers (Stransky *et al.* 2011, Agrawal *et al.* 2011), multiple myelomas (Chapman *et al.* 2011), chronic lymphocytic leukemia (Quesada *et al.* 2011, Wang *et al.* 2011), and pancreatic cancer (Jones *et al.* 2008). Even more recently, 5 truncating *PBRM1* mutations were identified in 5 out of 32 intrahepatic cholangiocarcinomas (17%), which consisted of 1 nonsense and 4 frameshift mutations (Jiao *et al.* 2013).

In summary, *PBRM1* mutations occur a frequency that is likely to represent an important tumour suppressor activity in diverse cancers. Certain cancer types harbour *PBRM1* mutations at a strikingly high frequency. Whilst the vast majority of mutations result in a truncated protein, many missense and a few in-frame deletion mutations have been identified. Intriguingly, most of these occur in the bromodomains or BAH domains of BAF180, and therefore might provide crucial insight into the mechanistic activity of these domains in BAF180 function.

1.5. Synthetic lethality and HDAC inhibitors in cancer therapy

1.5.1. Identifying and utilizing synthetic lethal interactions for anticancer therapy

Standard chemotherapies frequently result in side effects, including hair loss, nausea and immunosuppression. This is due to their relatively nonspecific inhibition of rapidly dividing normal cells in addition to cancer cells (Druker 2002, Hellman & Vokes 1996). Recent cancer research has led to the identification and targeting of traits characteristic of cancer cells, such as DNA repair deficiency and aberrant cell signaling. Much effort has subsequently been made to develop therapies that specifically target these pathways with fewer side effects, leading to some very promising treatments. Some of these treatments have received regulatory approval, and have led to increased survival in patients with previously intractable cancers (Chan & Giaccia 2011).

Exploitation of synthetic lethality in cancer cells

Exploiting synthetic lethal interactions in cancer cells is a particular promising strategy for developing tailored cancer therapies. The concept of synthetic lethality, originally described in yeast models, follows that mutating two cooperating genes in an essential process causes cell death, whilst the single mutations retain viability (Guarente 1993, Hartman *et al.* 2001, Chan & Giaccia 2011). Therefore, administering an inhibitor of a gene product in cancer cells that contain a mutation in an interacting gene would induce synthetic lethality specifically in those cells.

This forms the basis of one aspect of tailored cancer therapy, which requires prior identification and validation of the synthetic lethal interaction before developing a suitable targetting drug (Chan & Giaccia 2011). Predictions on synthetic lethal interactions can be made where sufficient data exists on the function of genes in an essential process, for example in DNA repair. However, unexpected and complex interactions exist that might hold great promise for cancer therapy. Such interactions can be identified using synthetic lethal screens, either using RNA interference libraries or small-molecule compound libraries (Chan & Giaccia 2011). Identifying synthetic lethal interaction with genes that are frequently mutated in cancer would prove most useful for developing tailored therapies.

Examples of clinically relevant synthetic lethal interactions

Inhibitors of (Poly (ADP-ribose) (PARP) are amongst the first class of small molecule inhibitors that have been developed to interact in a synthetic lethal manner with DNA repair factors (Rouleau *et al.* 2010). As described previously, BRCA1 and BRCA2 promote DNA DSB repair by HR, and mutations in *BRCA1* and *BRCA2* are associated with various hereditary breast and ovarian cancers (Hall *et al.* 1992, Casey *et al.* 1993, Wooster *et al.* 1994, Parikh & Advani 1996). PARP functions as a single-stranded DNA (ssDNA) break sensor and facilitates the recruitment of ssDNA break repair factors (Petermann *et al.* 2005). Synthetic lethality has been reported with *BRCA1* and *BRCA2* mutations and PARP inhibition in normal cells and breast cancer xenografts (Bryant *et al.* 2005, Farmer *et al.* 2005). Mechanistically, ssDNA lesions that cannot be repaired because of PARP inhibition lead to replication fork collapse and the generation of DNA DSBs. In the absence of *BRCA1* or *BRCA2* HR is defective, leading to unrepaired DSBs that trigger apoptosis. As a consequence of these studies PARP inhibitors are being evaluated in clinical trials with *BRCA*-deficient breast and ovarian cancer patients (Tutt *et al.* 2010, Fong *et al.* 2009, Hutchinson *et al.* 2010). This example demonstrates proof of principle regarding synthetic lethality in cancer therapy.

Another example of potential synthetic lethal interactions involving DNA repair factors includes colorectal carcinoma-associated mutations in *MSH1* and *MSH2,* which are involved in DNA mismatch repair, and silencing of Polymerase β and γ, involved in base excision repair (Martin *et al.* 2010, Martin *et al.* 2011). Thus, simultaneous inhibition of these mismatch repair and base excision repair proteins leads to DNA damage accumulation that ultimately leads to cell death (Chan & Giaccia 2011).

Several synthetic lethal interactions have also been identified in factors involved in cell signaling. Mutations in *VHL* occur frequently in a specific subset of cancers, particularly renal carcinomas. Strikingly, >80% of renal carcinoma cases show loss of *VHL* expression, either through mutation or epigenetic silencing (Gnarra *et al.* 1994, Herman *et al.* 1994, Young *et al.* 2009). In addition, renal cancers are particularly intractable because of a lack of symptoms preceding metastasis (Ritchie & Chisholm 1983). Thus, treatments that target *VHL* deficiency are likely to be of great importance for improving renal carcinoma therapy. *VHL* functions by targeting HIF (hypoxia-inducible factor) for degradation, and loss of *VHL* results in HIF accumulation and activation of hypoxia-inducible genes under normoxic conditions. Three kinases were identified as synthetic lethal *VHL* interaction partners in an shRNA library screen and included cyclin-dependent kinase 6 (CDK6), hepatocyte growth factor receptor (also known as MET),

and dual specificity mitogen-activated protein kinase (MAP2K1) (Bommi-Reddy *et al.* 2008). A small molecule screen found that STF-62247, involved in Golgi trafficking, induced synthetic lethality with *VHL* mutation (Turcotte *et al.* 2008). A synthetic lethal interaction between PTEN mutations and mTOR inhibition has also been demonstrated (Neshat *et al.* 2001, Podsypanina *et al.* 2001, Thomas *et al.* 2006). Several compounds have also been identified that selectively inhibit cells with activated *KRAS* (Torrance *et al.* 2001), in addition to a number of synthetic lethal interaction genes (Sarthy *et al.* 2007, Puyol *et al.* 2010). Synthetic lethal interactions with *MYC* overexpression have also been identified. In summary, these studies show that clinically relevant synthetic lethal interactions involving commonly mutated signaling factors can be discovered using small compound and RNA interference screens.

1.5.2. Histone deacetylase (HDAC) inhibitors in cancer therapy

HDACs represent a promising class of small molecules that display potent anti-tumour activity *in vitro.* Many of these of these inhibitors are in clinical trials with haematological and solid cancers, although results are mixed depending on the cancer type (Chan & Giaccia 2011). Nevertheless, two inhibitors, Vorinostat (suberoylanilide hydroxamic acid (SAHA)) and Depsipeptide (romidepsin), have been granted approval from the US FDA for the treatment of cutaneous T-cell lymphoma, and more recently Depsipeptide has been approved for treating peripheral T-cell lymphoma (Chan & Giaccia 2011). Despite these advances, there are major issues confounding our understanding of how HDAC inhibitors exert their anti-cancer effects. In particular, most HDAC inhibitors simultaneously inhibit multiple HDACs, which constitute a diverse group of proteins that regulate a myriad of cell processes. Therefore, the impacts of HDAC inhibition on cancer cells are likely to be highly complex and far-reaching. In addition, the *in vivo* targets of individual HDAC enzymes are largely unidentified. More systematic approaches aiming to identify the genetic and epigenetic interactions involved in HDAC-mediated tumour cytotoxicity are necessary. These might include synthetic lethal screens as described previously. Indeed, unidentified synthetic lethal interactions might actually underlie the efficacy observed for HDAC inhibitors in certain cancers.

Classification of mammalian HDACs

Human cells contain 18 HDACs that are grouped into four classes. Class I, II and IV HDACs represent the classic Zn^{2+}-dependent HDACs, whilst class III HDACs are

metal-independent. Class I HDACs are closely related to budding yeast Rpd3 (Yang & Seto 2008) and include HDAC1, HDAC2 HDAC3 and HDAC8. Class I HDACs are expressed ubiquitously and localize in the nucleus, where they regulate diverse processes including transcription and DNA repair. Class II HDACs are related to budding yeast Hda1 and are subdivided into two groups. Class IIa HDACs include HDAC4-7 and HDAC9, whilst class IIb HDACs includes HDAC6 and HDAC10. The class II HDACs display tissue-specific expression and localize predominantly to the cytoplasm, although class IIa HDACs can shuttle between the cytoplasm and the nucleus (Martin *et al.* 2007). Class III HDACs are NAD-dependent proteins known as Sirtuins and are closely related to budding yeast Sir2 (Haigis and Sinclair 2010). These include SIRT1-7, which can localize to the nucleus and cytoplasm and are involved in various processes including metabolism, transcription, DNA repair and cell cycle control (Haigis and Sinclair 2010). HDAC11 is the only member of class IV and has poorly understood functions.

Biological consequences of HDAC inhibition

HDACs remove acetylation marks on histone N-terminal tails made by histone acetyltransferases (HATs) (Smith and Denu 2009, Bernstein *et al.* 2007). Histone acetylation induces chromatin relaxation by weakening interactions with DNA, and is broadly associated with active transcription. Histone acetylation promotes the recruitment of transcription factors via interaction with domains such as bromodomains. Human cancers frequently display reduced histone acetylation, which is associated with cancer progression. In particular, loss of H4K16ac (and H4K20me3) is considered a hallmark of cancer (Fraga *et al.* 2005). Thus, the hyper-acetylation resulting from HDAC inhibition could restore the transcription of inappropriately silenced tumour suppressor genes, representing a potential mechanism for HDAC-mediated cancer cell cytotoxicity. However, a global increase in transcription does not necessarily result from HDAC inhibition, and amongst the small fraction of genes (20%) actually affected by HDAC inhibition around half are activated and half are repressed (Minucci & Pelicci 2006). Nevertheless, HDAC inhibitors are known to upregulate p21 transcription (Richon *et al.* 2001, Sandor *et al.* 2000) and reduce cyclin transcription in cancer cells, the latter of which results in Rb dephosphorylation to indirectly affect E2F transcription (Zhao *et al.* 2005). Therefore, HDAC inhibitor-mediated transcriptional modulation might explain some of the antiproliferative effects of these drugs on cancer cells.

In addition to regulating histone acetylation HATs and HDACs also affect more than 50 non-histone protein substrates, which extends their involvement beyond far transcriptional regulation (Ocker 2010). These include factors involved in transcription, signal transduction, DNA repair and chaperoning. The effects of acetylating these non-histone proteins range from altering DNA binding affinity, transcriptional activity, protein stability and protein-protein interactions (Ververis *et al.* 2013).

Relatively recent reports indicate that HDAC inhibitors enhance DNA damage caused by DNA damaging agents. One explanation is that the induction of a more relaxed chromatin structure increases the exposure and sensitivity of DNA to damage (Karagiannis *et al.* 2007). A study by Miller *et al.* demonstrated a specific function of HDAC1 and 2 in deacetylating H3K56, which is required for efficient DNA DSB repair principally via NHEJ (Miller *et al.* 2010). Therefore, HDAC inhibitors that target HDAC1 and 2 could exert anticancer activity by impairing DSB repair. Transcriptional down-regulation of various DNA repair proteins, including Ku80, BRCA1 and RAD51 has also been reported following HDAC inhibition (Adimoolam *et al.* 2007, Zhang *et al.* 2007). HDAC inhibitors are also known to induce apoptosis via transcription-dependent and –independent mechanisms (Minucci & Pelicci 2006, Bolden *et al.* 2006), as well as reducing angiogenesis by reducing HIF and VEGF expression (Kim *et al.* 2001). In summary, HDAC inhibitors target traits associated with cancer cells via multiple transcription-dependent and –independent mechanisms, which may have relevance to their anticancer activity.

HDAC3 is required for centromeric cohesion

A growing body of evidence indicates that HDAC inhibitors might exert a transcription-independent antiproliferative effect by disrupting centromeric cohesion. An intriguing study by Eot-Houllier *et al.* demonstrated a specific role for HDAC3 in promoting centromeric sister chromatid cohesion by deacetylating H3K4. Depletion of HDAC3 led to an increased mitotic index, chromosome congression defects and a pronounced centromeric cohesion defect, whilst SAC activity was unaffected (Eot-Houllier *et al.* 2008). Furthermore, HDAC3 depletion led to impaired centromeric Sgo1 localization and Haspin-mediated H3T3 phosphorylation. Mitotic centromeres show a distinct H3K4me2-enriched inner centromere domain adjacent to a CENP-A domain. Surrounding these domains is a large pericentromeric region characterized by H3K9me2-enriched chromatin (Sullivan & Karpen *et al.* 2004). HDAC3 was required for deacetylating H3K4 prior to mitosis in order to allow H3K4 methylation (Eot-Houllier *et al.* 2008). The authors propose that centromeric H3K4ac impairs Sgo1 recruitment,

which might be dependent on H3K4me2. This study reveals a novel transcription-independent function for a HDAC in promoting centromeric cohesion.

Another relationship between HDACs and cohesin exists between HDAC8 and SMC3. HDAC8 was found to be the HDAC responsible for deacetylating SMC3 once cohesion dissolution occurs after execution of the prophase pathway (Deardorff *et al.* 2012). Consequently, in the absence of HDAC8 cohesin renewal was impaired, which ultimately led to decreased cohesin loading. These findings might have potential implications for HDAC3- and HDAC8-specific inhibitors in targeting cancers with mutated cohesin genes.

Classification of HDAC inhibitors

HDAC inhibitors can be broadly classified into groups based on their chemical structure, and include hydroxamic acids, cyclic peptides, bibenzimides and short-chain fatty acids (Ververis *et al.* 2013). Most hydroxamic acids predominantly inhibit class I and II HDACs, and include Vorinostat (SAHA) and TSA. Cyclic peptides and benzimides such as Depsipeptide and Etinostat selectively inhibit class I HDACs, and fatty acids such as butyrate inhibit class I and II HDACs (Ververis *et al.* 2013). Inhibitors that target single HDAC enzymes are becoming increasingly available, and these would prove most useful for elucidating the functions of the individual proteins. There is substantial debate regarding whether enzyme- or class-specific inhibitors are more useful than broad-spectrum inhibitors from a clinical perspective. It is likely that inhibiting specific combinations of HDACs in different cancer types or genetic and epigenetic backgrounds leads to favoured outcomes. A major goal for the advancement of HDAC inhibitor-based cancer therapy is to integrate biological and genetic data with chemistry techniques to develop purpose-designed inhibitors.

1.6. Thesis experimental research goals

The work presented in the following sections comprises three broad research goals. First, we perform an investigation into the roles of the two isoforms of the RSC complex in the DNA damage response in budding yeast. Substantial literature has shown that RSC is involved in a range of DNA damage response processes, including DSB-induced chromatin remodelling, NHEJ, and HR. However, the differential involvement of the two isoforms of RSC in these processes has not been comprehensively tested.

A second major goal is to explore whether the BAF180 subunit of PBAF in mammalian cells functions to promote cohesion. There are several important reasons for addressing this question. Firstly, the homologous Rsc2 subunit of RSC is known to be important for cohesion establishment, thus in one respect we aim to determine if BAF180 shares a conserved function. Secondly, recent exome sequencing studies have revealed that the gene encoding BAF180 and various genes that regulate cohesion are frequently mutated in diverse cancers. Recent literature has also shown that defects in centromere cohesion causes aneuploidy in cancer, and that aneuploidy can drive genome instability. Taken together, a conserved role for BAF180 in cohesion might represent a novel and important tumour suppressive function. We then extend this investigation to assess the importance of the role of BAF180 in promoting cohesion with respect to tumourigenesis. We also set out to explore the possibility that this function is distinct from its well-characterized role in transcriptional regulation.

Finally, we test whether there is a conserved synthetic lethal interaction between BAF180 and HDACs, as has been demonstrated between Rsc2 and HDACs in budding yeast. Because BAF180 is frequently mutated in cancer, a conserved synthetic lethal interaction with HDAC loss could be exploited as a potential therapeutic strategy using HDAC inhibitors.

CHAPTER 2: MATERIALS AND METHODS

2.1. DNA manipulations

Yeast expression plasmids

All plasmids used in this study are shown in Table 2.1. pRSC2-myc was altered by site-directed mutagenesis to generate pRSC2-T67P-myc, pRSC2-M280I-myc, and pRSC2-H458P-myc.

Table 2.1. Plasmids used in this study

Plasmid	Name	Description	Source
pRS415	pRS415	Yeast expression vector, AMP^R, CEN/ARS, *LEU2,* F1 origin	Stratagene
pRSC1		Rsc1 coding sequence plus 700 bp upstream sequence and 200 bp downstream sequence in *Not*I site of pRS415	Chambers *et al.* 2012
pRSC2	pJD587	Rsc2 coding sequence plus 700 bp upstream sequence and 200 bp downstream sequence in *Not*I site of pRS415	Chambers *et al.* 2012
$pRSC2^{BD1}$	pJD588	BD1 from Rsc1 swapped into Rsc2 in pRSC2	Chambers *et al.* 2012
$pRSC2^{BD2}$	pJD589	BD2 from Rsc1 swapped into Rsc2 in pRSC2	Chambers *et al.* 2012
$pRSC2^{BAH}$	pJD590	BAH from Rsc1 swapped into Rsc2 in pRSC2	Chambers *et al.* 2012
pRS416	pRS416	Yeast expression vector, AMP^R, CEN/ARS, *URA3,* F1 origin	John Diffley
pRSC2-myc	pJD629	RSC2 with 13-myc C-terminal tag under the control of its own promoter with *TRP1* marker in pRS416 backbone	Chambers *et al.* 2013
pRSC2-T67P-myc	pJD750	As pJD629 with T67P substitution	Brownlee *et al.* 2014
pRSC2-M280I-myc	pJD751	As pJD629 with M280I substitution	Brownlee *et al.* 2014
pRSC2-H458P-myc	pJD752	As pJD629 with H458P substitution	Brownlee *et al.* 2014
pEGFP-C3	pJD775	Mammalian expression vector, EGFP under the control of the CMV promoter, KAN^R	
$pEGFP-BAF180^R$	pJD776	siRNA resistant BAF180 isoform 8 with EGFP N-terminal tag in pJD775 backbone	Brownlee *et al.* 2014
$pEGFP-BAF180^R$-T232P	pJD777	As pJD776 with T232P substitution	Brownlee *et al.* 2014
$pEGFP-BAF180^R$-M538I	pJD778	As pJD776 with M538I substitution	Brownlee *et al.* 2014

Mammalian expression plasmids

BAF180 complete cDNA (clone MGC:156155, IMAGE:40082629) was purchased from Source BioScience and cloned into the *Hind*III/*Kpn*I sites of pEGFP-C3 (Clontech) to generate pEGFP-BAF180 (performed by Queti Riballo). This clone contains a N122S substitution relative to the published sequence. To create the siRNA resistant construct $pEGFP-BAF180^R$ site-directed mutagenesis was performed using the primer BAF180-$RNAi^R$ (performed by Anna Chambers) Site-directed mutagenesis was performed on $pEGFP-BAF180^R$ to generate siRNA resistant plasmids expressing EGFP-tagged BAF180 containing substitutions identified in tumour samples: $pEGFP-BAF180^R$-T232P and $pEGFP-BAF180^R$-M538I (performed by Anna Chambers).

Primers

Primers used in this study for cloning, site-directed mutagenesis and yeast strain construction are shown in Table 2.2.

Table 2.2. Primers used in this study

Primer name	Sequence
Rsc2T67P-F	CCTGTATCTTTCAATCCATTAAAAAAGCGTATTC
Rsc2T67P-R	GAATACGCTTTTTTAATGGATTGAAAGATACAGG
Rsc2M280I-F	GTATATTCAAAGAATTAAAAATGTTATGAAAG
Rsc2M280I-R	CTTTCATAACATTTTTAATTCTTCTTTGAATATAC
Rsc2H458P-F	CGAACAAACTGTGCCAAGAGTGGATAGATTG
Rsc2H458P-R	CAATATCCACTCTTGGCACAGTTTGTTCG
Rsc2+1080	ACCTCTGTGCGAAATTCTAAAGTTG
Rsc2-588	CAACCACAGTATCAAAGCCGGCAGA
Rsc2-03	GAACCATAATATTTCACCC
Rsc2N76A-F	GAATGCCAAGACTTACGCAACAAGAGATTCAGGA
T232P-F	CCTATAGATCTCAAGCCAATTGCCCAGAGGATAC
T232P-R	GTATCCTCTGGGCAATTGGCTTGAGATCTATAGG
M538I-F	CATAAGAAAGCAGCGAATCAAAATCTTATTCAATG
M538I-R	CATTGAATAAGATTTTGATTCGCTGCTTTCTTATG
BAF180-R	CTTCTCCAGGATATGTGC
EGFP-C	CATGGTCCTGCTGGAGTTCGTG
BAF180-RNAi^{R}	GAGAAATCTTGAGACAGCCAAGAAA

2.2. Antibodies and immunoblotting

Custom made and commercially available antibodies used in this study are as follows: Myc (9E10 clone, CRUK), BAF180 (A301-590A, Universal Biologicals Cambridge), SMC1 (A300-055A, Universal Biologicals Cambridge), SMC3 (ab155587, Abcam), SA1 (ab4457, Abcam), SA2 (ab4463, Abcam), β-actin (ab8226, Abcam), H3 (Abcam), α-tubulin (ab7750, Abcam), CENPF (ab108483, Abcam), GFP (A6455, Life Technologies), H2A (Downs *et al.* 2000). Samples for Western blot analysis were prepared from yeast by glass-bead disruption and TCA precipitation. For mammalian cell samples, cells were lysed by resuspension in Laemmli buffer and sonicated using a Diagenode Bioruptor sonicating waterbath for 10 min using 30s on/30s off pulses. Samples were electrophoresed and immobilized on nitrocellulose membrane. Alice Shia provided breast cancer cell line pellets.

2.3. Yeast experiments

Yeast strains

Yeast strains used in this study are shown in table 2.3. *RSC2* was deleted in the DMY3010, W1479-11C and W1490-16A strains via standard gene-disruption methods using a cassette amplified by PCR.

Table 2.3. Yeast strains used in this study

Strain name	Genotype	Source
JKM179	Δ*ho* Δ*hml::ADE1* Δ*hmr::ADE1 ade1-100 leu2-3,112 trp1::hisG lys5 ura3-52 ade3::GAL::HO* MATα	Lee *et al.* 1998
YNK179-177	Δ*rsc1::KanMX* in JKM179	Kent *et al.* 2007
YNK179-191	Δ*rsc2::KanMX* in JKM179	Kent *et al.* 2007
YPF17	Δ*mata::hisG ade1 lys5 trp1::hisG ura3-52 leu2::HOcs* Δ*ho* Δ*hml::ADE1* Δ*hmr::ADE1 ade3::GAL::HO*	Paques *et al.* 1998
YNK17-20	Δ*rsc1::KanMX* in YPF17	Chambers *et al.* 2012
YNK17-24	Δ*rsc2::KanMX* in YPF17	Chambers *et al.* 2012
DMY2804	*RDN1-NTS1::mURA3* in W303a	Huang *et al.* 2006
JDY789	Δ*rsc1::KanMX* in DMY2804	Chambers *et al*. 2012
JDY790	Δ*rsc2::KanMX* in DMY2804	Chambers *et al*. 2012
DMY3010	*RAD5 RDN1::ADE2 in W303a*	Huang *et al.* 2006
JDY964	Δ*rsc2::KanMX* in DMY3010	Brownlee *et al.* 2014
W1479-11C	*MAT::HIS3 leu2*Δ*::Eco*RI*::URA3-HOcs::leu2*Δ*Bst*EII	Smith & Rothstein 1999
	Δ*rsc2::KanMX* in W1479-11C	This study
W1490-16A	*MAT::HIS3 RAD5 leu2*Δ*::Bst*EII*::URA3-HOcs::leu2*Δ*Eco*RI	Smith & Rothstein 1999
	Δ*rsc2::KanMX* in W1490-16A	This study

Analysis of Rsc1 and Rsc2 complex composition (Anna Chambers)

Rsc1-TAP and Rsc2-TAP were purified by two-step affinity purification. 1 litre of yeast was grown to mid-late log phase, pelleted and popcorn made in liquid nitrogen. Yeast were lysed by grinding and the powder was resuspended in 4 pellet volumes of IgG binding buffer (10 mM Tris-HCl pH8, 300 mM NaCl, 0.1% NP40, 100 µg/ml PMSF, 1 µM leupeptin, 1 µg/ml pepstatin A, 0.5 µg/ml aprotinin). Lysate was centrifuged at 15,000 rpm for 10 min at 4°C before the supernatant was incubated with 200 ul of IgG Sepharose beads for 2 hours at 4°C. Beads were washed with 3 X with 1 ml IgG binding buffer, followed by 2 X 1 ml TEV cleavage buffer (10 mM Tris-HCl pH8, 150 mM NaCl, 0.1% NP40, 0.5 mM EDTA, 1 mM DTT100 µg/ml PMSF, 1 µM leupeptin, 1 µg/ml pepstatin A, 0.5 µg/ml aprotinin). Beads were resuspended in 1 ml TEV cleavage buffer, 10 ul TEV protease were added to the samples, which were incubated overnight

at 4°C. 3 ml CaM binding buffer (10 mM Tris-HCl pH8, 150 mM NaCl, 10 mM beta-mercaptoethanol, 1 mM magnesium acetate, 1 mM imidazole, 2 mM CaCl2, 0.1% NP40, 100 µg/ml PMSF, 1 µM leupeptin, 1 µg/ml pepstatin A, 0.5 µg/ml aprotinin) and 3 µl 1 M CaCl2 were added, and beads collected by centrifugation. The supernatant was bound to 50 µl calmodulin beads for 1 hour at 4°C, washed with 4 X 1 ml CaM wash buffer (CaM binding buffer with 300 mM rather than 150 mM NaCl), and eluted in 1 ml elution buffer (10 mM Tris-HCl pH8, 150 mM NaCl, 10 mM beta-mercaptoethanol, 1 mM magnesium acetate, 1 mM imidazole, 2 mM CaCl2, 0.1% NP40, 30 mM EGTA, 100 µg/ml PMSF, 1 µM leupeptin, 1 µg/ml pepstatin A, 0.5 µg/ml aprotinin). 20% ice-cold acetone was used to precipitate proteins and the pellet was resuspended in 20 µl 10 mM Tris-HCl pH 7.5. A mock purification was performed from lysate created from an isogenic untagged strain. Gel slices were analyzed in the University of Sussex Proteomics Centre.

qPCR analysis of transcriptional induction (Anna Chambers)

For analysis of *RNR* induction, cultures of JKM179, *rsc1*, *rsc2* and *mec1* mutant strains were grown to mid-log in YPAD. Cultures were then incubated for a further 3 hours at 30°C in the absence or presence of 0.05% MMS. RNA was reverse transcribed using Qiagen QuantiTech RT kit. For each sample, qPCR reactions were performed using primers within *RNR2*, *RNR3* and results were normalized to the *ACT1* locus. The transcript level of the normalized wild type undamaged sample is set to 1 and all other values are shown relative to this. For analysis of *HXT7* transcription, cultures of *rsc2* DMY3010 containing cancer mutation plasmids were grown to mid-log phase in SC lacking tryptophan and RNA extracted using an RNeasy kit (Qiagen). 1µg of RNA was reverse transcribed into cDNA for analysis by qPCR using primers specific to the *HXT7* locus.

G2/M checkpoint analysis by fluorescence-activated cell sorting (FACS) (Anna Chambers)

Cultures of wild-type, *rsc1* and *rsc2* JKM179 cells were grown to mid-log in YPAD and an asynchronous sample taken at the outset of the assay. Cells were arrested in G2/M by incubation with 15mg/ml nocodazole for 1hr 45 minutes. Cultures were incubated for a further 45 minutes (with nocodazole still present) in the presence or absence of 0.1% MMS. Yeast were washed and resuspended in fresh YPAD and fixed in ethanol at 0, 30, 60, 90, 120, 150, 180 and 210 minutes after release. Cells were harvested and

incubated in 1mg/ml RNase A for 4 hours at 37°C, followed by incubation for 1 hour at 50°C in 2mg/ml proteinase K solution. Yeast cells were collected by centrifugation and resuspended in FACS buffer (200mM Tris-HCl pH7.5, 200mM NaCl, 78mM $MgCl_2$). Cells were added to 50µg/ml propidium iodide in 50mM Tris-HCl pH7.5, sonicated and analysed using a FACS Calibur.

G1 checkpoint analysis by fluorescence-activated cell sorting (FACS)

Cultures of wild-type, *rsc1* and *rsc2* DMY2804 cells were grown to mid-log in YPAD and an asynchronous sample taken at the outset of the assay. Cells were arrested in G1 by incubation with 4µg/ml α-factor for 1hr followed by an additional 2µg/ml for another hour. Cultures were incubated for a further 1hr with a final 2µg/ml dose of α-factor in the presence or absence of 0.1% MMS. Samples were taken at 0 and 30 minutes following addition of MMS and fixed in ethanol before washing and resuspending the remaining culture in fresh YPAD. Subsequent samples were taken at 60, 90, 120, 150, 180, 210, 240 and 270 minutes. Cells were harvested and incubated in 1mg/ml RNase A for 4 hours at 37°C, followed by incubation for 1 hour at 50°C in 2mg/ml proteinase K solution. Yeast cells were collected by centrifugation and resuspended in FACS buffer (200mM Tris-HCl pH7.5, 200mM NaCl, 78mM $MgCl_2$). Cells were added to 50µg/ml propidium iodide in 50mM Tris-HCl pH7.5, sonicated and analysed using a FACS Calibur.

Genomic NHEJ assays

Mid-log phase cultures of JKM179 or YPF17 were grown in YPAD or, when plasmids were used, SC lacking leucine, serially diluted and plated onto YPAD or SC lacking leucine containing both 2% glucose and 2% galactose. Colonies were counted after 4 days incubation at 30°C and repair efficiency was calculated as survival on galactose relative to survival on glucose. Experiments were performed at least in triplicate. Repair junctions of colonies surviving on galactose were analysed by sequencing.

Spot tests

Mid-log phase cultures of wild-type, *rsc1* and *rsc2* JKM179 containing plasmids were grown in SC lacking leucine, and cultures of *rsc2* DMY3010 containing plasmids were grown in SC lacking tryptophan. Cultures were diluted to OD_{600}=0.2 and 5-fold serial dilutions were spotted onto YPAD or YPAD containing the stated dose of drug. Cells

were grown for 2 days at 30°C and spot tests were performed multiple independent times.

Cell cycle survival assays

Exponentially growing cultures of wild-type, *rsc1, rsc2* and *rad52* JKM179 in YPAD were arrested in nocodazole, treated with MMS, centrifuged and resuspended in fresh YPAD as for G2 checkpoint analysis by FACS. Serial dilutions were plated onto YPAD and colonies were counted 3 days after incubation at 30°C. Experiments were performed in duplicate by Anna Chambers. For G1 survival assay, exponentially growing cultures of wild-type, *rsc1* and *rsc2* DMY2804 in YPAD were arrested in α-factor, treated with MMS, centrifuged and resuspended in fresh YPAD as for G1 checkpoint analysis by FACS. Serial dilutions were plated onto YPAD and colonies were counted 3 days after incubation at 30°C. Experiments were performed in triplicate.

Indirect end-label analysis (Sam Durley and Tracey Beacham)

Chromatin digestion using micrococcal nuclease (MNase) was performed exactly as described by *Kent et al.* 2007. Yeast cultures were grown in 1% peptone, 1% yeast extract plus 2% D(+)-raffinose. Cells were grown at 30 °C to densities of ~2.0×10^7 nucleated cells/ml (determined by hemocytometry). Cells were sampled just before ("HO 0 min" samples) and at time points after HO induction by the addition of D(+)-galactose to 2%. Spheroplasts were created by digestion in 1 ml of 10 mg/ml *Arthrobacter luteus* yeast lytic enzyme in 1M sorbitol, 5 mM β-mercaptoethanol for 4 min at 22 °C. Samples containing 2.0×10^8 nucleated cells were digested with between 75 and 300 units/ml MNase at 37 °C for 3 min or processed for purification of deproteinized DNA. Deproteinized DNA samples were digested with 5 units/ml MNase at 22 °C for 10 s to create "DNA" control digests. Purified DNA samples were digested to completion with *Bgl*II or *Bsp*EI (for analysis of the LEU2 and MAT loci, respectively) and separated on 1.5% agarose gels. Southern blots of the gels were hybridized to 400-bp indirect end label probes, which abut the relevant restriction sites.

Yeast survival and rDNA recombination assays

Wild-type and *rsc2* DMY3010 strains were grown to mid-log in YPAD before diluting to OD_{600}=0.2 and serial dilutions plated onto SC plates containing 10µg/ml adenine. *rsc2*

DMY3010 cells containing plasmids were grown in SC lacking tryptophan and plated onto SC plates lacking tryptophan containing 10µg/ml adenine. Plates were incubated at 30°C for 3-4 days before being placed at 4°C to intensify the red colouration. The percentage rate of ADE marker loss was calculated by dividing the number of half red/white sectored colonies with the total number of colonies per plate, excluding red colonies. Counts for each experiment were from six individual colonies per strain. Standard deviations are given ± the mean from three separate experiments. Between 10,000 and 20,000 colonies were counted for each strain in total.

LEU2 direct-repeat recombination assay

Wild-type and *rsc2* colonies from W1479-11A and W1490-16A strains grown on YPAD were resuspended in water and plated onto SC plates and SC plates lacking leucine. Colonies were counted after incubation at 30°C for 3-4 days. The rate of LEU+ prototroph formation in each experiment was calculated using the method of the median (Lea & Coulston 1949) from eight individual colonies. Standard deviations are given ± the mean from three separate experiments.

Yeast growth curves (Anna Chambers)

Cultures of *rsc2* DMY3010 containing cancer mutation plasmids were grown to mid-log phase in SC lacking tryptophan and diluted to OD_{600}=0.05 into fresh media. The OD_{600} was measured every hour for 9 hrs.

2.4. Mammalian cell experiments

Cell culture

Mouse ES cells (mESCs) were cultured at 37°C in a 5% CO_2 incubator in Knockout™ DMEM (Gibco), supplemented with 15% ES-Cult FBS (Stemcell Technologies), 1% penicillin/streptomycin, 1% NEAA, 1% L-glutamine, 0.1 µM β-mercaptoethanol and 1000 U/ml LIF (Millipore). Cells were seeded into gelatin-coated dishes. 1BR-hTERT and U2OS cells were cultured at 37°C in a 5% CO_2 incubator in DMEM (Gibco) supplemented with 15% FBS, 1% penicillin/streptomycin and 1% L-glutamine. MRC5 CV1 cells were cultured at 37°C in a 5% CO_2 incubator in MEM (Gibco), supplemented with 10% FBS, 1% penicillin/streptomycin and 1% L-glutamine.

siRNA knock-downs

1BR-hTERT and MRC5 CV1 cells were plated at $1x10^5$ cells per 6cm dish and knock-downs performed according to Niimi *et al.,* 2012. Cells were transfected with 20 nM BAF180, SA2 or non-targeting control siRNA (ON-TARGET plus SMART pool, Dharmacon) using HiPerFect transfection reagent (Qiagen), and then again with the same siRNAs 24h later. Cells were treated or sampled 72h after the first transfection.

Metaphase spreads

To arrest in metaphase, mES, 1BR-hTERT, MRC5 CV1 and U2OS cells were arrested in 0.1 µg/ml colcemid for 3hrs, trypsinized, swollen in 75 mM KCl for 30 min at room temperature and fixed in Carnoy's fixative (methanol:acetic acid 3:1). Cells were spotted onto a slide floating in a 37°C waterbath and dried overnight at room temperature. DNA staining was performed using ProLong® Gold Antifade Reagent with DAPI. For the mESC cohesion assays, 200 spreads were analyzed for each genotype. Centromeric cohesion was scored as 'normal' when fewer than three chromosomes showed gaps between sister chromatid centromeres, or 'defective' when more than two chromosomes showed gaps. Arm cohesion was scored as 'normal' when fewer than three chromosomes showed fully separated chromosome arms, or 'defective' when more than two chromosomes showed fully separated chromosome arms. For chromosome counts, 100 cells were analyzed for each cell type, with and without treatment with 0.04 µg/ml MMC for 40 hr prior to metaphase arrest. The same conditions were used for analysis of structural chromosome aberrations, with 2,033 and 2,133 chromosomes analyzed for +/+ and -/- mESCs, respectively. Stable U2OS cells were incubated with 0.04 µg/ml MMC for 48 hr prior to metaphase arrest, and a total of 2862 and 2741 chromosomes were analysed for shControl and shBAF180 cells, respectively.

Fluorescent in situ hybridization (FISH)

1BR-hTERT cells transfected with siControl or siBAF180 siRNA were treated with 0.1 µg/ml colcemid for 3h to arrest in metaphase before firmly tapping dishes against a bench 14 times to dislodge mitotic cells. Cells were washed with PBS and fixed in Carnoy's fixative. Cells were spotted onto a slide and dried overnight at room temperature. Ross Cloney performed FISH essentially as in Canudas & Smith 2009.

Cells were hybridized overnight with either DNA probes against arm and centromere regions of chromosome 10 (DiGeorge II probe, Cytocell LPU015) or subtelomeric region of chromosome 16 (Chromsome 16ptel05 probe, Cytocell LPT16R) as per the manufacturer's protocol. Nuclei were stained with ProLong® Gold Antifade Reagent with DAPI.

Transcript analysis

RNA was extracted from 1BR-hTERT and U2OS cells using an RNeasy kit (Qiagen). 1µg of RNA was reverse transcribed into cDNA for analysis by qPCR using primers specific to the indicated locus using QuantiTect Primer Mix (Qiagen) (performed by Anna Chambers). In experiments examining p21 induction nutlin-3a (Sigma) was added to 8µM for 6 hours prior to cell sampling.

Chromatin fractionation

U2OS cells were arrested in G1/S by incubation with 0.05 µg/ml aphidicolin for 16h, and released into fresh media following extensive washes with PBS. Cells were collected for chromatin fractionation 0, 3 and 6 hr after release into fresh media. An asynchronous sample was also taken for FACS. Cells were harvested and resusupended in 75 µl low salt lysis buffer (50 mM Tris-HCl pH 8, 2 mM EDTA, 2 mM EGTA, 150 mM NaCl, 0.2% Triton, 0.3% NP40, containing protease inhibitors) before incubation on ice for 5 min. Samples were spun at 3000 rpm at 4°C for 4 min and supernatant kept as the soluble fraction. The pellet was washed with ice-cold PBS before resuspension in 50 µl nuclease buffer (50 mM Tris-HCl pH 8, 20 mM NaCl, 2 mM MgCl2). 2.5 µl of benzonase (Novagen) was added and samples incubated on ice for 30 min. NaCl and Triton were adjusted to final concentrations of 1M NaCl and 0.2% Triton. Samples were sonicated in Diagenode Bioruptor sonicating waterbath for 15 min using 30s on/30s off pulses. Samples were spun at 13,000rpm at 4°C for 5 min and supernatant was taken as the chromatin fraction. Protein content of the fractions was measured by Bradford assay. Laemmli buffer was added to permit analysis of 50 µg of each fraction by Western blotting (fractionation and blotting performed by Anna Chambers).

Mammalian cell FACS

FACS was performed essentially as described by the Salk Institute for Biological

Sciences (http://www.salk.edu/fccf/protocols/cellcycle.php). Cells were harvested, washed twice in in PBS containing 0.1% BSA. 3ml ice-cold ethanol was added dropwise whilst vortexing gently to 1ml of suspension containing 1-2X10^6 cells and fixed overnight at 4°C. Cells were washed twice with PBS and resuspended in 1ml propidium iodide (PI) staining solution (3.8mM sodium citrate, 40µg/ml (PI) in PBS) containing 0.5µg/ml RNase A, and incubated at 37°C for 20 min. Cells were passaged through a fine-gauge needle immediately prior to FACS sampling on a FACS Canto.

Immunofluorescence (IF)-FISH

For IF-FISH, 4 X 10^5 U20S cells were plated onto glass coverslips and transfected with 40 nM BAF180 single siRNA (Invitrogen) or non-targeting control siRNA using HiPerFect transfection reagent (Qiagen). After 19 hr, cells were treated with 2.5 mM thymidine for 17 hr before being released. At 9 hr after release, cells were transfected with the siRNA-resistant plasmids using NanoJuice Core transfection reagent (Merck Chemicals). After 5 hr, the cells were washed with PBS and subjected to a second thymidine block using 2.5 mM thymidine for a further 17 hr. At 8 hr after release, the cells were fixed with 3% paraformaldehyde (PFA).

For IF, cells were blocked in blocking solution (3% BSA, 0.1% Triton X-100, 1 mM EDTA pH 8.0 in PBS) for 30 min at room temperature, and subjected to antibody incubation in blocking solution. Immunostained cells were fixed in 3% PFA for 10 min at room temperature. Ross Cloney performed the subsequent DNA FISH according to Chaumeil *et al.* 2008. Cells were washed twice in 2X SSC for 5 min, permeablized in 0.1M HCl/0.7% Triton for 10 min on ice, and washed twice in 2X SSC for 5 min. Cells were denatured in 50% formamide/2X SSC pH7.2 for 30 min at 80°C. Cells were washed several times in ice-cold 2X SSC before hybridization with the FISH probe overnight at 42°C in a dark, humid chamber with paper tissues soaked in 50% formamide/2X SSC. Cells were washed 3 times in 50% formamide/2X SSC pH7.2 for 5 min each at 42°C, washed three times in 2X SSC for 5 minnutes each at 42°C and mounted with ProLong Gold Antifade Reagent with DAPI.

Analysis of micronuclei and abnormal mitoses

For mESCs, spontaneous micronuclei were counted in interphase cells from two independent experiments (total counts=983 for WT, 1043 for BAF180-/-). For 1BR-hTERT cells, three separate knockdown experiments were analyzed (total counts=2629 for siControl, 2716 for siBAF180). 1324 and 1291 cells were counted for

shControl and shBAF180 lines, respectively. In experiments to analyze the effect of mitomycin C on micronuclei formation, 563 WT cells and 676 BAF180 -/- cells were counted 40 hr after treatment with 0.04 µg/ml MMC. 1596 and 1781 cells were counted for shControl and shBAF180 lines, respectively, 48 hr after treatment with 0.04 µg/ml MMC. DNA staining was performed using ProLong® Gold Antifade Reagent with DAPI. Analysis of aberrant mitoses in was performed on 183 WT and 207 BAF180-/- anaphase cells from two independent experiments.

Viability assays

Viability assays following drug treatments were performed in 96-well format in triplicate at the stated doses. $1x10^4$ mouse ES and $5x10^3$ 1BR-hTERT cells were plated per well. For mitomycin C viability was measured 4 days following treatment, and for HDAC inhibitors viability was measured 2 days following treatment using cell-titre glow reagent (Promega).

CHAPTER 3: RSC1 AND RSC2 DIFFERENTIALLY MEDIATE DNA DAMAGE RESPONSES

3.1. Results

Introduction

Cairns *et al.* reported that there are two separate isoforms of the RSC complex defined by the presence of either Rsc1 or Rsc2 (Cairns *et al.* 1999). A degree of functional redundancy is likely to exist between the two complexes because deletion of either *RSC1* or *RSC2* does not cause lethality, whilst deletion of both genes is lethal (Cairns *et al.* 1999). However, *rsc1* and *rsc2* mutant strains have overlapping but not identical cellular phenotypes, indicating that they do not act entirely redundantly (Cairns *et al.* 1999, Rossio *et al.* 2010, Baetz *et al.* 2004, Bungard *et al.* 2004). These differences might relate to differences in dosage of each protein, with Rsc2 being approximately ten-fold more abundant than Rsc1 (Cairns *et al.* 1999). Alternatively, Rsc1 and Rsc2 might display differences in transient and dynamic binding to chromatin.

Both Rsc1 and Rsc2 have been implicated in DNA repair. Strains lacking either *RSC1* or *RSC2* are hypersensitive to a range of DNA damaging agents (Kent *et al.* 2007, Chai *et al.* 2005, Shim *et al.* 2005) and have reported defects in HR (Chai *et al.* 2005). Strains lacking subunits common to both complexes also displayed impaired NHEJ (Shim *et al.* 2005), suggesting that at least one of the two RSC isoforms is important for this activity. In addition, the catalytic RSC subunit is enriched at DSB sites following induction as shown by ChIP (Chai *et al.* 2005, Shim *et al.* 2005), indicating that at least one of the isoforms is recruited to breaks.

Following DSB induction RSC activity is required for a chromatin remodeling event adjacent to the break (Kent *et al.* 2007, Shim *et al.* 2007). Previous work in our lab showed that this remodeling event is dependent on Rsc1, whilst Rsc2 is important for establishing the correct chromatin structure prior to break induction (Kent *et al.* 2007). In contrast, Shim *et al.* showed that the DSB-induced remodeling event is dependent on Rsc2, however the dependence of this on Rsc1 was not tested (Shim *et al.* 2007). Therefore, it is possible that both isoforms function in remodeling after DSB formation. No studies to date have comprehensively compared the contributions of the Rsc1- and Rsc2-containing isoforms of the RSC complex in DNA damage responses. Therefore, we sought to address whether Rsc1 and Rsc2 play distinct roles in mediating DNA damage responses.

Rsc1 and Rsc2 define two separate isoforms of RSC

Previously Cairns *et al.* reported the existence of two RSC isoforms that contain either Rsc1 or Rsc2, however the subunit composition of these two complexes was not determined (Cairns *et al.* 1999). To examine whether the subunit composition of the two complexes is otherwise identical, affinity purifications from cell extracts containing C-terminally TAP-tagged Rsc1, Rsc2 or an untagged wild-type control were performed (Figure 3.1A, Anna L. Chambers). The purified complexes were then analysed by mass spectroscopy (Figure 3.1B, Anna L. Chambers). Rsc2 was not identified in the Rsc1-TAP complex, and Rsc1 was not identified in the Rsc2-TAP complex, consistent with previous findings (Cairns *et al.* 1999). Furthermore, all of the other RSC subunits (except Htl1 and Ldb2, which are amongst the smallest RSC subunits at 9.1 and 19.7kDa, respectively) were identified in both complexes, indicating that the two complexes are otherwise identical in subunit composition (Chambers *et al.* 2012). However, it has been reported that the heterodimer-forming Rsc3 and Rsc30 subunits preferentially associate with Rsc1 (Campsteijn *et al.* 2007). This is consistent with our findings that fewer Rsc3 and Rsc30 peptides were recovered from the Rsc2-TAP purification compared to the Rsc1-TAP purification (Figure 3.1B), although Rsc3 and Rsc30 clearly associate with both complexes (Chambers *et al.* 2012).

Rsc1 and Rsc2 are dispensable for DNA damage checkpoint activation

DNA damage checkpoint activity had not yet been directly tested in any RSC mutants despite reported defects in resection, Mec1 recruitment and phosphorylation of H2A and Rad53 (Kent *et al.* 2007, Liang *et al.* 2007, Shim *et al.* 2007). We first tested the ability of *rsc1* and *rsc2* null mutant strains to induce the transcription of *RNR2* and *RNR3* genes, which is Mec1- and Rad53-dependent (Harrison & Haber 2006), in response to DNA damage. The levels of *RNR2* and *RNR3* mRNA relative to *ACT1* control mRNA were quantitated using qPCR after treatment with MMS. Whilst the *mec1* mutant strain was severely defective in *RNR2* and *RNR3* induction as expected, both the *rsc1* and *rsc2* strains were able to induce transcription of these genes to levels comparable to wild-type cells (Figure 3.2A, Anna L. Chambers). This suggests that Mec1-dependent DNA damage checkpoint activation is intact in these strains (Chambers *et al.* 2012).

To examine this further, we monitored cell cycle re-entry in wild-type, *rsc1* and *rsc2* strains arrested in G2/M or G1 after MMS treatment. Cells were arrested in G2/M

A

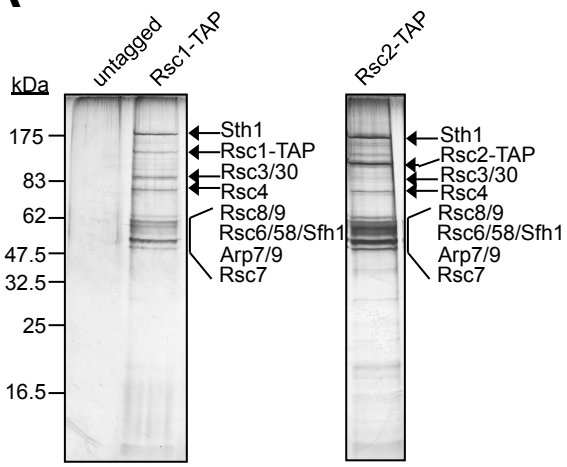

B

	Rsc1-TAP		Rsc2-TAP	
Subunit	No. peptides	%coverage	No. peptides	%coverage
Sth1	24	21	36	26
Rsc1	13	15	0	0
Rsc2	0	0	36	37
Rsc3	20	23	5	7.6
Rsc4	17	27	18	30
Rsc6	12	24	30	25
Rsc7	11	28	19	49
Rsc8	18	33	25	40
Rsc9	11	18	21	31
Sfh1	4	9.6	7	22
Arp7	13	26	14	24
Arp9	14	21	16	30
Rsc30	7	7	1	1
Htl1	0	0	0	0
Rtt102	3	27	5	27
Rsc58	18	33	28	46
Ldb7	0	0	0	0

Figure 3.1. Rsc1 and Rsc2 define two separate isoforms of the RSC complex. (A) Tandem-affinity purification from a strain containing TAP-tagged Rsc1, TAP-tagged Rsc2, or from an untagged strain were analysed by mass spectrometry. (B) Results from the mass spectroscopy analysis of the purified RSC complexes from (A).

using nocodazole, one set was treated with MMS, and the cultures were released into fresh media (performed by Anna L. Chambers). Cell cycle re-entry was monitored by FACS. In the wild-type strain treated with MMS cell cycle re-entry was delayed by 30-60 minutes compared to untreated cells (Figure 3.2B). The FACS profile of the *rsc1* strain closely resembled that of wild-type, indicating normal checkpoint activation in this strain (Figure 3.2B). The *rsc2* strain re-entered the cell cycle normally in the absence of DNA damage and also did not show premature cell-cycle re-entry after MMS treatment compared to wild-type, indicating a robust checkpoint response in these cells (Figure 3.2B). In fact, the *rsc2* cells were unable to subsequently re-enter the cell cycle following DNA damage in G2/M, indicating a prolonged G2/M arrest.

To determine whether *rsc1* and *rsc2* mutants are required for activation of the G1 DNA damage checkpoint cells were arrested in α-factor, one set was treated with MMS, and cultures were released into fresh media. In the wild-type strain treated with MMS cell cycle re-entry was delayed by approximately 180 minutes compared to unteated cells (Figure 3.2C). Similar to cells arrested in G2/M, premature cell cycle re-entry from G1 was not observed in either the *rsc1* or *rsc2* mutants after DNA damage, suggesting that neither strain is defective in G1 DNA damage checkpoint activation (Figure 3.2C). Altogether, these data demonstrate that despite defects in resection and H2A phosphorylation, sufficient Mec1 is recuited to allow robust activation of the G2/M and G1 DNA damage checkpoints in *rsc1* and *rsc2* mutants in response to MMS.

Both Rsc1 and Rsc2 facilitate NHEJ activity

We next sought to determine whether Rsc1 and Rsc2 make distinct contributions in DNA repair. Because RSC is known to function in the repair of DNA DSBs by non-homologous end-joining (NHEJ) (Shim *et al.* 2005), we first decided to examine the contributions of Rsc1 and Rsc2 in this pathway. We measured survival following an HO-induced DNA DSB at the *MAT* locus in a strain where the *HML* and *HMR* silent mating cassettes have been deleted. Survival is therefore a measure of NHEJ because the cells cannot repair the DSB by HR. *rsc2* cells had substantially decreased NHEJ activity relative to wild-type, whilst *rsc1* cells might be only slightly defective (Figure 3.3A). This suggests that Rsc2 has a greater role than Rsc1 in NHEJ at this locus.
NHEJ-defective mutants including *ku70*, *lig4*, *mre11, rad50* and *rsc30* exhibit large deletion repair events at DSB repair junctions that are a feature of NHEJ deficiency (Boulton *et al.* 1996, Moore *et al.* 1996, Wilson *et al.* 1997, Shim *et al.* 2005). Sequence analysis of the repair junctions from wild-type, *rsc1* and *rsc2* strains showed that both the *rsc1* and *rsc2* mutant strains had a very different pattern of repair events

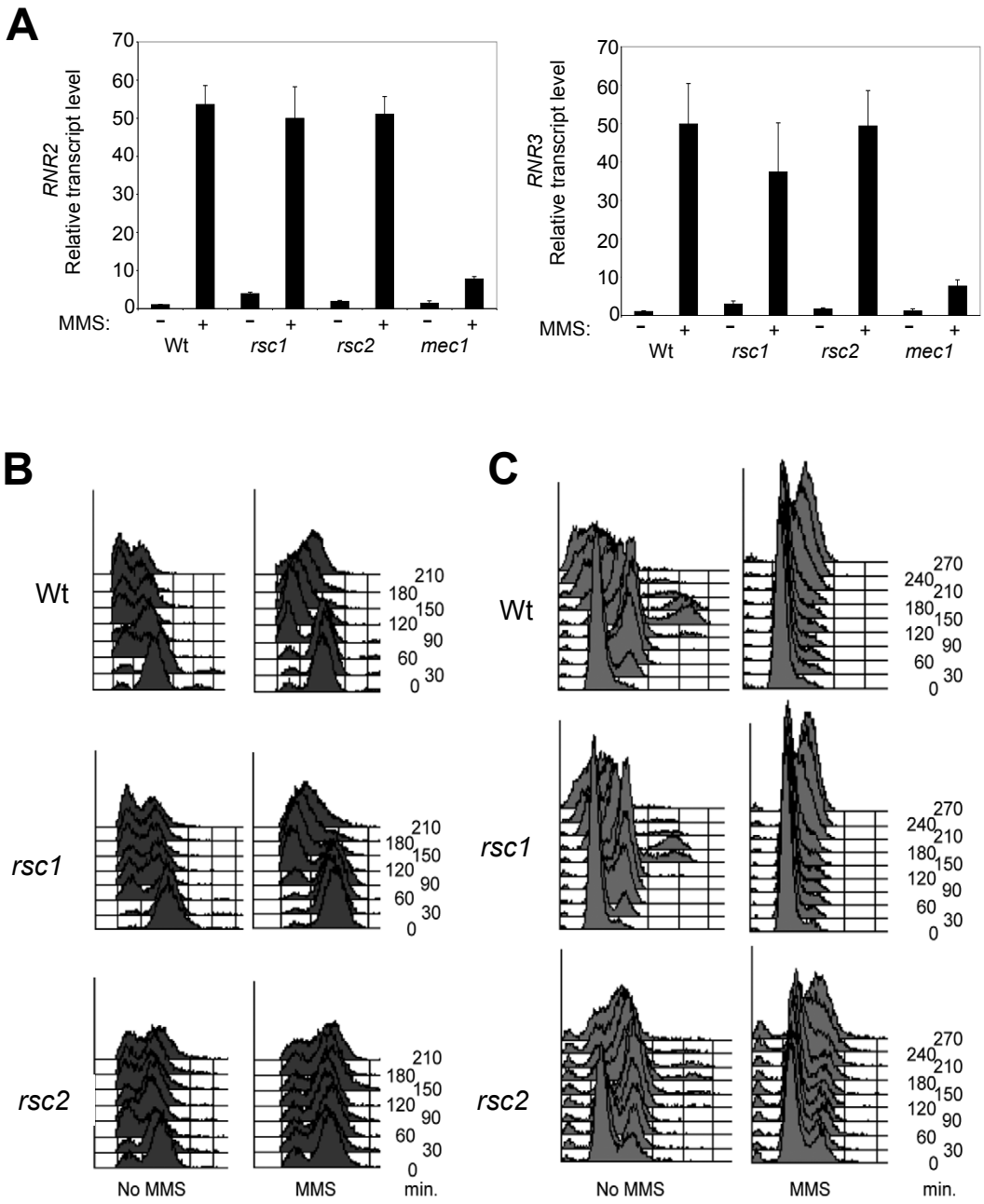

Figure 3.2. Neither Rsc1 nor Rsc2 are required for DNA damage checkpoint responses. (A) Transcriptional induction of *RNR2* and *RNR3* mRNA in response to MMS in the Wt, *rsc1* and *rsc2* strains as quantitated by qPCR. (B) FACS profiles of strains arrested in G2/M using nocodazole and treated with either no drug (left panel) or 0.1% MMS (right panel) for 1hr. Cells were collected every 30 minutes after release. (C) FACS profiles of strains arrested in G1 using α-factor and treated with either no drug (left panel) or 0.1% MMS (right panel) for 1hr. Cells were collected every 30 minutes after release.

compared to wild-type. Specifically, the majority of repair events in the wild-type strain had insertions (65.4%), whilst both *rsc1* and *rsc2* had fewer insertions (31.5% and 16.1%, respectively). In addition, there was an increased frequency of deletions in the *rsc1* and *rsc2* cells (61.4% and 68% respectively, compared to 32.7% for wild-type) (Figure 3.3B). Whilst the majority of wild-type deletion events were 1bp (56% of total deletions), the majority of *rsc1* and *rsc2* deletion events were 3bp (54% and 52% of total deletions, respectively) (Figure 3.3B). Interestingly, there were only very subtle differences in the pattern of repair events between *rsc1* and *rsc2* cells, suggesting that the two proteins contribute equally to NHEJ.

Defects due to loss of RSC1 or RSC2 cannot be rescued by additional copies of the other gene

The Rsc2 isoform of RSC is 10-fold more abundant than Rsc1, and it might be predicted that the relative hypersensitivity of the two mutants to DNA damaging agents is reflected by their relative abundance. Interestingly, whilst *rsc2* cells are more severely hypersensitive to MMS than *rsc1* cells, both mutants are similarly hypersensitive to phleomycin, CPT and 4NQO (Anna, L. Chambers, unpublished observations). To test whether Rsc1 and Rsc2 might function redundantly in DNA damage responses additional centromeric copies of *RSC1* and *RSC2* were transformed into the *rsc2* and *rsc1* mutants, respectively. These additional gene copies do not rescue the hypersensitivity of the strains to phleomycin, suggesting that the two proteins are unable to compensate for each other in the repair of phelomycin-induced DNA damage (Figure 3.4A, Anna L. Chambers). Importantly, plasmids expressing *RSC1* and *RSC2* do rescue the respective *rsc1* and *rsc2* hypersensitivities to this drug (Figure 3.4B, Anna L. Chambers).

Rsc1 and Rsc2 make distinct contributions to DNA repair

We noted that *rsc2* cells exhibit a prolonged G2/M arrest when treated with MMS in G2, whilst *rsc1* cells are able to re-enter the cell cycle after a short delay (Figure 3.2B). This raises the possibility that Rsc1 and Rsc2 might have cell cycle-specific roles in DNA damage repair. To test this, we assayed survival of wild-type, *rsc1* and *rsc2* strains in G1 and G2 phases of the cell cycle after treatment with MMS. When arrested in G2, the *rsc2* strain shows substantially reduced survival, whilst the *rsc1* strain shows survival levels comparable to wild-type (Figure 3.4C). In contrast, when arrested in G1, both the *rsc1* and *rsc2* strains show reduced survival compared to wild-type (Figure

A

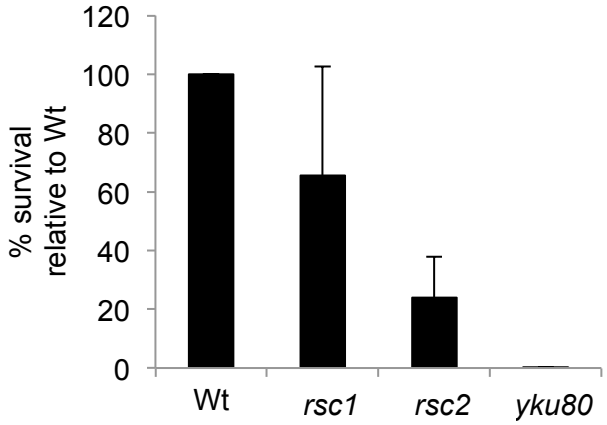

B

Change from Wt sequence	Wt	*rsc1*	*rsc2*
Total insertions	**36 (65.4%)**	**18 (31.5%)**	**5 (16.1%)**
+ 1 bp	0 (0%)	3 (5.2%)	0 (0%)
+ 2 bp	28 (51.5%)	12 (21%)	4 (13%)
+ 3 bp	8 (14.5%)	2 (3.5%)	1 (3.2%)
Total deletions	**18 (32.7%)**	**35 (61.4%)**	**21 (68%)**
- 1 bp	10 (18%)	10 (17.5%)	7 (22.5%)
- 2 bp	1 (1.8%)	2 (3.5%)	3 (9.7%)
- 3 bp	6 (10.9%)	19 (33.3%)	11 (35.4%)
- >3 bp	1 (1.8%)	4 (11.4%)	0 (0%)
Total base changes	**0 (0%)**	**2 (3.5%)**	**0 (0%)**
Total compound mutations	**1 (1.8%)**	**2 (3.5%)**	**5 (16%)**

Figure 3.3. Both Rsc1 and Rsc2 contribute to wild-type levels of NHEJ and show a similar spectrum of repair junctions. (A) Survival of wild-type wild-type, *rsc1* and *rsc2* following chronic HO endonuclease cleavage at the *MAT* locus. Survival is a measure of NHEJ activity as the *HML* and *HMR* donor cassettes have been deleted and is calculated as the number of colonies surviving in continued HO expression relative to conditions where HO is not expressed. Wild-type (wt) repair rates are set to 100% and mutant strains are shown relative to wt. Data are means ± s.d., $n > 3$. (B) Sequenced repair events of survivors from a HO-induced DSB break from Wt, *rsc1* and *rsc2* strains. Percent of total repair events shown in parenthesis.

3.4D). Together, these data suggest that Rsc1 has a greater role in promoting survival after MMS-induced DNA damage in G1 compared to in G2, and that Rsc2 is important for survival in both cell cycle phases.

Because the *MAT* locus is a highly specialized chromatin environment that functions to facilitate efficient gene conversion (Kent *et al.* 2007, Haber *et al.* 1998) we next tested NHEJ activity in a strain in which the HO cleavage site has been moved to the *LEU2* open reading frame. We find that the *rsc1* strain shows similar survival levels at this locus to the levels seen at *MAT* (Figure 3.4E). In contrast, *rsc2* cells display greater survival levels at *LEU2* compared to *MAT*, suggesting that the dependence on Rsc2 for promoting survival is context specific.

DSB-dependent nucleosome sliding requires Rsc1 but not Rsc2

Previous work showed that immediately following a HO-induced DNA DSB at the *MAT* locus six distal nucleosomes are repositioned away from the break in a manner dependent on Rsc1 (Kent *et al.* 2007). In contrast, *rsc2* cells exhibit a nucleosome-positioning defect at *MAT* before HO induction. This suggests that Rsc1 and Rsc2 provide distinct functions in DSB repair. To determine whether this isoform specificity also exists at DSBs at other loci we tested the ability of wild-type, *rsc1* and *rsc2* cells to remodel chromatin in a strain where the HO cleavage site exists in the *LEU2* gene. We found that 40 minutes after DSB induction there is a movement of nucleosomes away from the break in wild-type cells (Figure 3.5A; inferred nucleosome positions before and after break induction are shown as white circles in Figure 3.5B; assays performed by S. Durley & T. Beacham). This is similar to the remodelling event seen at the *MAT* locus in wild-type cells (Kent *et al.* 2007). Moreover, this remodelling is entirely dependent on Rsc1 as has been previously observed in this assay at the *MAT* locus (Kent *et al.* 2007). Thus, despite a requirement for both Rsc1 and Rsc2 for maximal NHEJ activity at *MAT* and *LEU2*, these data indicate that only Rsc1 is required for the nucleosome sliding observed at these loci. This supports the notion that Rsc1 and Rsc2 do not function redundantly in DNA DSB responses.

The BAH domain of Rsc1 is a critical determinant for the ability of Rsc1 to remodel nucleosomes

We next sought to investigate whether specific domains of Rsc1 and Rsc2 might be particularly important in dictating the specificity of these proteins in DNA damage responses. Plasmids where the two bromodomains (BDs) and bromo-adjacent

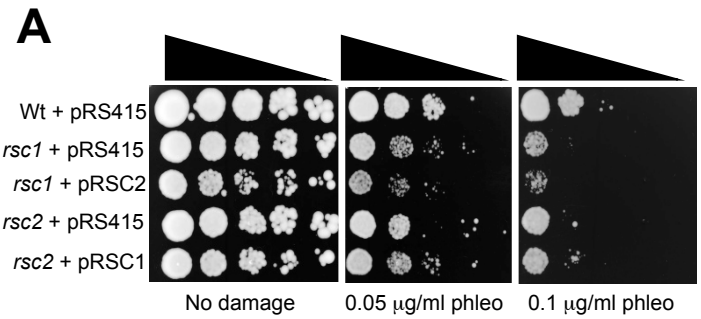
A
Wt + pRS415
rsc1 + pRS415
rsc1 + pRSC2
rsc2 + pRS415
rsc2 + pRSC1
No damage
0.05 μg/ml phleo
0.1 μg/ml phleo

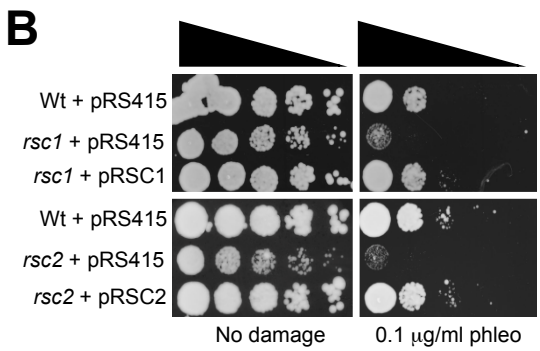
B
Wt + pRS415
rsc1 + pRS415
rsc1 + pRSC1
Wt + pRS415
rsc2 + pRS415
rsc2 + pRSC2
No damage
0.1 μg/ml phleo

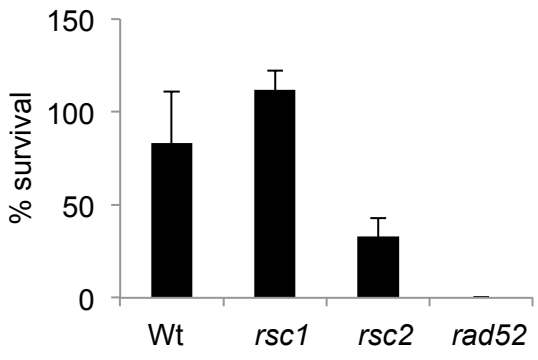
C
% survival
150
100
50
0
Wt
rsc1
rsc2
rad52

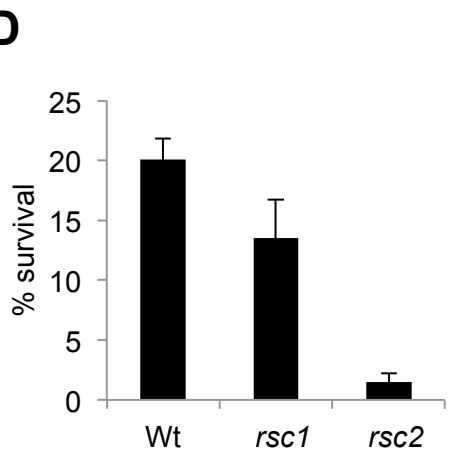
D
% survival
25
20
15
10
5
0
Wt
rsc1
rsc2

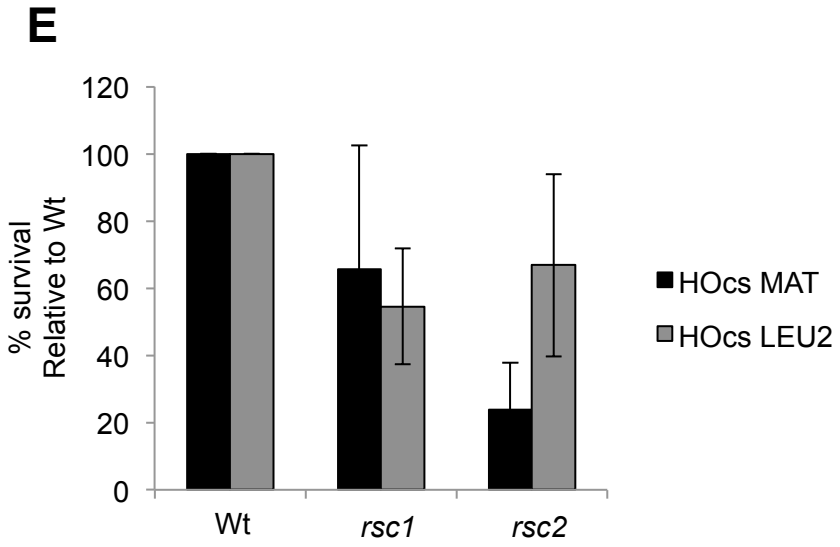
E
% survival
Relative to Wt
120
100
80
60
40
20
0
Wt
rsc1
rsc2
HOcs MAT
HOcs LEU2

Figure 3.4. Rsc1 and Rsc2 have distinct roles in mediating DNA damage hypersensitivity. (A) and (B) Serial dilutions of strains transformed with the indicated plasmids were plated onto YPAD or YPAD plates containing the indicated dose of phleomycin. (C) Wt, *rsc1, rsc2* or *rad52* strains arrested in G2/M using nocodazole and treated with 0.1% MMS for 1hr were plated onto YPAD. Survival is measured relative to untreated cells in G2/M. (D) Strains arrested in G1 using α-factor and treated with 0.1% MMS for 1hr were plated onto YPAD. Survival is measured relative to untreated cells in G1. (E) Survival of JKM179 (in which the HO cleavage site is in the *MAT* locus) and YPF17 strains (in which the HO cleavage site is in the *LEU2* locus) following chronic HO endonuclease cleavage. Wild-type (Wt) repair rates are set to 100% and mutant strains are shown relative to wt. Data are means ± s.d., $n > 3$

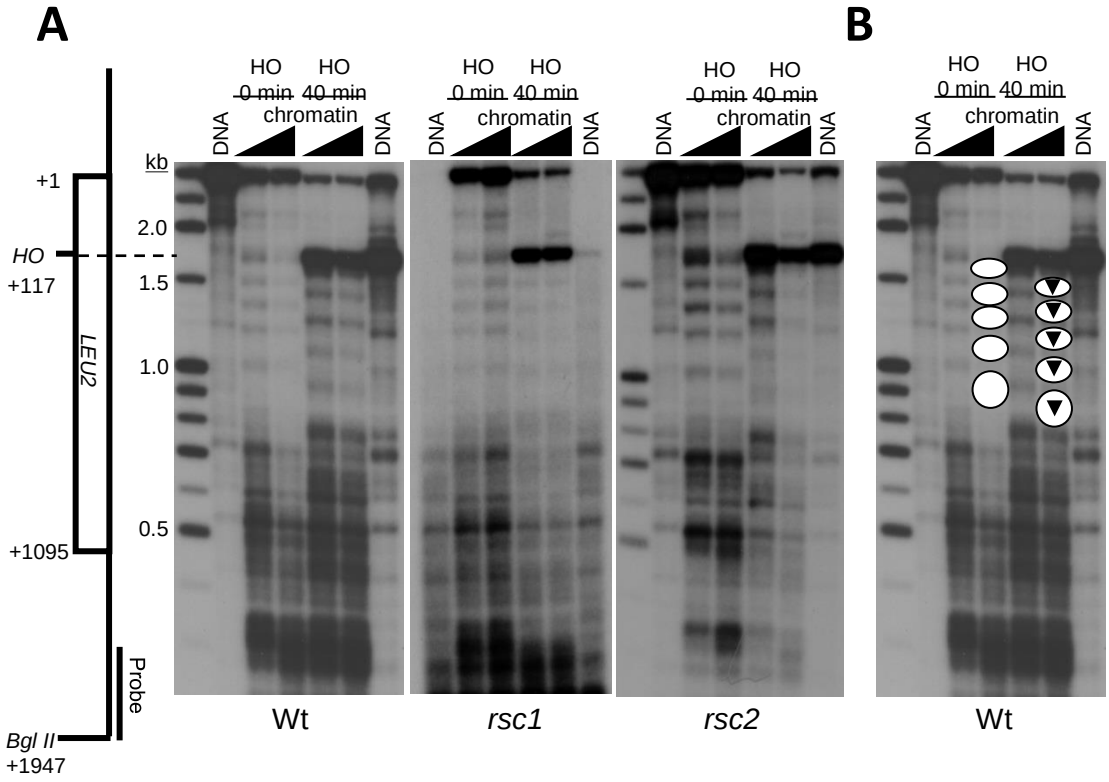

Figure 3.5. Loss of Rsc1 function, but not that of Rsc2, abolishes DSB-dependent nucleosome sliding at an HO site within the *LEU2* gene. (A) Indirect-end-label-analysis of MNase digested DNA from yeast strains of the YPF17 background using a probe abutting *Bgl*II site as shown. Deproteinized DNA and chromatin samples were analysed before (HO, 0 min) and 40 min after HO induction by addition of galactose to growth media. Wedges above chromatin samples indicate increasing amounts of MNase. Deproteinized DNA control samples show that that the banding patterns in the chromatin samples are representative of nucleosome positioning as opposed to DNA sequence-specific MNase cleavage. The lack of signal in the deproteinzed DNA samples in the *rsc1* gel of figure 3.5 is likely to reflect MNase over-incubation. The HO-induced DSB appears as the strong band in HO 40 min samples at 1830bp. (B) Inferred nucleosome positions superimposed over the wild-type MNase cleavage data from (A) to illustrate DSB-dependent nucleosome sliding associated with the HO cleavage site.

homology (BAH) domain from *RSC2* that have been individually replaced with the analogous domains from *RSC1* (Figure 3.6A) were transformed into *rsc2* and *rsc1/rsc2* strains. None of the three domain swap constructs confer DNA damage hypersensitivity to MMS compared to the wild-type *RSC2* construct in the *rsc2* background (Figure 3.6B, Anna L. Chambers). Similarly, none of the constructs confer DNA damage hypersensitivity to MMS compared to the wild-type *RSC2* construct in the *rsc1/rsc2* background (Figure 3.6C, Anna L. Chambers).

Furthermore, the same constructs were examined in our NHEJ assay at the *MAT* locus, and similarly no additional defects were observed in either the *rsc2* or *rsc1/rsc2* backgrounds compared to the wild-type *RSC2* construct (Figure 3.6D and E). Together, these data suggest that the analogous domains of Rsc1 and Rsc2 are interchangeable in DNA damage responses.

Rsc1 and Rsc2 have clearly distinct roles in DSB-dependent nucleosome sliding and establishing a nuclease-resistant chromatin structure at *MAT*, respectively. We therefore tested the ability of the domain swap constructs to perform these functions. Analysis of *MAT* before HO induction in wild-type cells revealed a normal nuclease-resistant chromatin structure upstream of the DSB site, consistent with previous results (Kent *et al.* 2007; Figure 3.7A, grey oval indicates nuclease-resistant region, assays performed by S. Durley & T. Beacham). In contrast, the *rsc1/rsc2* strain transformed with a pRSC1 plasmid displays increased nuclease sensitivity at this site but is able to remodel nucleosomes distal to the break upon HO induction (Figure 3.7B). The *rsc1/rsc2* strain transformed with the pRSC2^{BD1}, pRSC2^{BD2} or pRSC2^{BAH} domain swap constructs display normal *MAT* structure but defective remodelling, suggesting that all three of these Rsc2 domains are either dispensable for Rsc2 function or can be substituted with the analogous domains of Rsc1 (Figure 3.7C and data not shown). Strikingly, however, the pRSC2^{BAH} construct was able to perform some of the Rsc1-dependent remodelling after DSB-induction (Figure 3.7D). This suggests that the BAH domain of Rsc1 provides some of the specificity of Rsc1 in DSB-induced chromatin remodelling.

Cells lacking RSC2 display elevated rates of unequal sister chromatid exchange and direct-repeat recombination

The histone deacetylase Sir2 is required for silencing at all three heterochromatic loci, including at telomeres, *HML/R* loci, and at the rDNA repeats. At telomeres and *HML/R* loci Sir2 associates with the BAH-domain containing Sir3 protein, whilst at the rDNA it

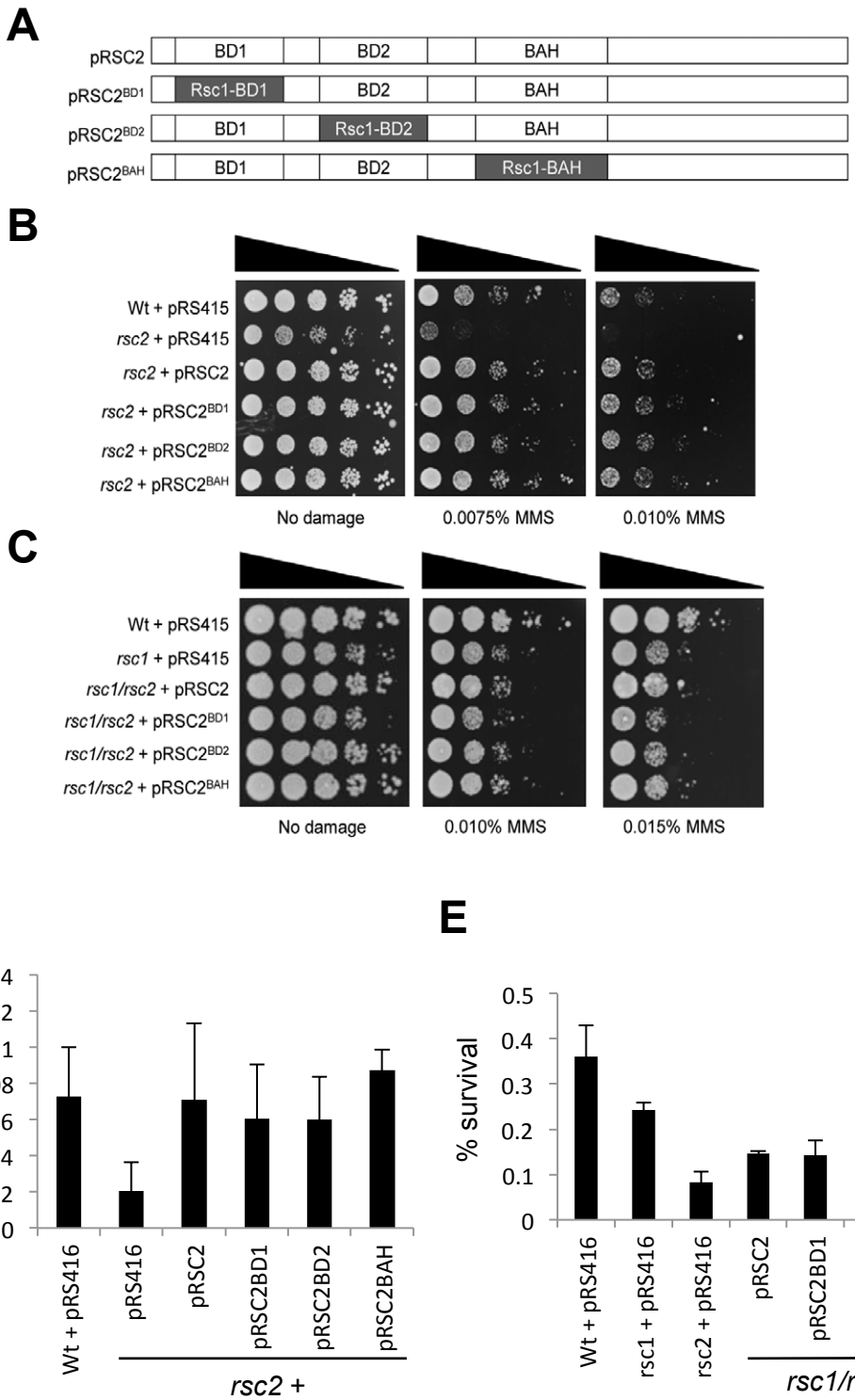
A
pRSC2
BD1
BD2
BAH
pRSC2BD1
Rsc1-BD1
pRSC2BD2
Rsc1-BD2
pRSC2BAH
Rsc1-BAH
B
Wt + pRS415
rsc2 + pRS415
rsc2 + pRSC2
rsc2 + pRSC2BD1
rsc2 + pRSC2BD2
rsc2 + pRSC2BAH
No damage
0.0075% MMS
0.010% MMS
C
Wt + pRS415
rsc1 + pRS415
rsc1/rsc2 + pRSC2
rsc1/rsc2 + pRSC2BD1
rsc1/rsc2 + pRSC2BD2
rsc1/rsc2 + pRSC2BAH
No damage
0.010% MMS
0.015% MMS
D
% survival
0.14
0.12
0.1
0.08
0.06
0.04
0.02
0
Wt + pRS416
pRS416
pRSC2
pRSC2BD1
pRSC2BD2
pRSC2BAH
rsc2 +
E
% survival
0.5
0.4
0.3
0.2
0.1
0
Wt + pRS416
rsc1 + pRS416
rsc2 + pRS416
pRSC2
pRSC2BD1
pRSC2BD2
pRSC2BAH
rsc1/rsc2 +

Fig. 3.6. Rsc1 domains can functionally compensate for Rsc2 domains in DNA damage survival assays. (A) Schematic of domain swap constructs used in the assays. Bromodomain 1 (BD1), bromodomain 2 (BD2) or the bromoadjacent homology (BAH) domain of Rsc2 was replaced with the analogous domain from Rsc1. (B) Serial dilutions of mid-log cultures of wild-type containing vector alone (pRS415) or *rsc2* mutant strain containing pRSC2 or domain swap expression plasmids were plated onto YPAD or YPAD plates containing the indicated dose of MMS. (C) Serial dilutions of mid-log cultures of wild-type containing vector alone (pRS415), *rsc1* with vector alone, or *rsc1/rsc2* mutant strain with pRSC2 or domain swap expression plasmids were plated onto YPAD or YPAD plates containing the indicated dose of MMS. (D) Survival of strains as in (B) following chronic HO endonuclease cleavage at the *MAT* locus. Survival is calculated as the number of colonies surviving in continued HO expression relative to conditions where HO is not expressed. Wild-type repair rates are set to 100% and mutant strains are shown relative to wild-type. Data are means ± s.d., *n*=3 (E) Survival of strains as in (C) following chronic HO endonuclease cleavage at the *MAT* locus. Survival is calculated as the number of colonies surviving in continued HO expression relative to conditions where HO is not expressed. Wild-type repair rates are set to 100% and mutant strains are shown relative to wild-type. Data are means ± s.d., *n*=3

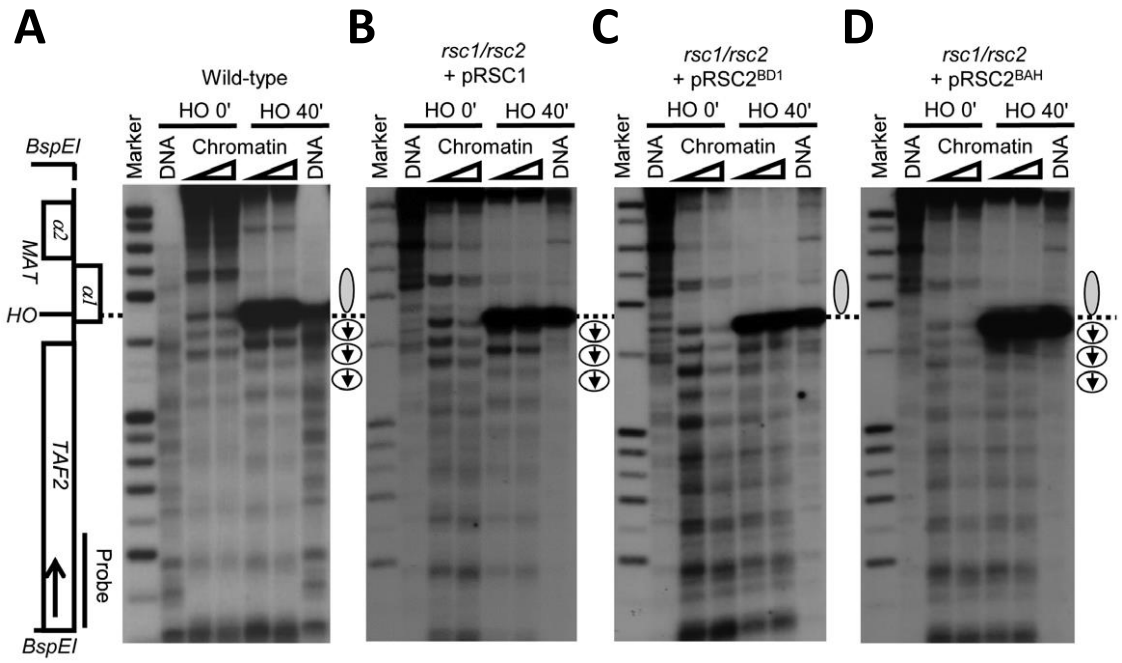

Figure 3.7. Replacing the BAH domain of Rsc2 with the Rsc1 BAH domain allows Rsc2 to remodel chromatin at DNA DSB. (A) Indirect-end-label-analysis of MNase digested DNA from wild-type JKM179 yeast using a probe abutting *Bsp*EI site as shown. Deproteinized DNA and chromatin samples were analysed before (HO, 0 min) and 40 min after HO induction by addition of galactose to growth media. Wedges above chromatin samples indicate increasing amounts of MNase. Deproteinized DNA control samples show that the banding pattern in the chromatin samples is representative of nucleosome positioning as opposed to DNA sequence-specific MNase cleavage. The lack of signal in the deproteinzed DNA HO 0min sample is likely to reflect MNase over-incubation. The position of the HO-induced DSB is marked on the gene map and across the figure with a dotted line. The nuclease-resistant structure characteristic of the normal *MAT*α locus on the *MAT*-proximal side of the HO site is marked with a grey oval to the right of the blot. The region of DSB-dependent nucleosome sliding in the region distal to the HO site is marked with circles (representing nucleosomes) and arrows (representing the apparent direction of sliding). (B) Indirect-end-label-analysis of the *rsc1/rsc2* strain containing pRSC1 showing normal DSB-dependent nucleosome sliding but loss of the nuclease-resistant structure on the *MAT*-proximal side of HO (characterized by MNase cleavage sites within this region). (C) Indirect-end-label-analysis of the *rsc1/rsc2* strain containing pRSC2BD1 showing that the Rsc2-dependent nucleosome-resistant structure is present as in normal cells normal DSB-dependent nucleosome sliding is defective. (D) Indirect-end-label-analysis of the *rsc1/rsc2* strain containing pRSC2BAH showing normal nuclease-resistant structure and normal DSB-dependent nucleosome sliding despite the absence of Rsc1.

is part of the RENT complex that comprises Sir2, Net1 and Cdc14 (Gartenberg 2000). Other work in our lab recently showed that an *rsc2* mutant is defective in rDNA silencing and appears to function in the same pathway as Sir2 (Chambers *et al.* 2013). The structure of transcriptionally silenced chromatin at the rDNA array is thought to suppress recombination because many rDNA silencing protein mutants, including *sir2*, have a hyper-recombination phenotype (Gottlieb & Esposito 1989, Huang *et al.* 2006). A proposed model links rDNA repeats to cohesin via a cohesin-associated clamp complex. Mutation of clamp complex components results in increased rates of marker loss by unequal sister chromatid exchange at the rDNA because of the consequent loss of sister chromatid cohesion (Huang *et al.* 2006).

Because *rsc2* is defective in rDNA silencing and cohesion (Huang *et al.* 2004, Baetz *et al.* 2004), we sought to test whether *rsc2* also has a hyper-recombination phenotype. *RSC2* was deleted in a strain that contains an *ADE2* marker in the rDNA array. Cells that have lost the *ADE2* marker by unequal sister chromatid exchange are red when grown on media with a low adenine concentration (Figure 3.8A). The rate of unequal sister chromatid exchange can be measured by counting the number of half red/white sectored colonies, which represent marker loss in the first division upon plating, compared to the total number of colonies (Kaerberlein *et al.* 1999). As predicted, the *rsc2* mutant shows a considerably higher rate of unequal sister chromatid exchange compared to wild-type (Figure 3.8B).

We also determined the rate of spontaneous direct-repeat recombination in the absence of Rsc2. The strain used in this assay contains a duplication of a mutated *LEU2* locus, and the two configurations of the strain, proximal and distal, differ only in the distance between the mutated sites (Smith & Rothstein 1999). Generation of *LEU*$^+$ prototrophs can result from replacement, deletion and triplication events via various intra- and interchromatid recombination mechanisms. Interestingly, the *rsc2* mutant shows a substantially elevated rate of *LEU*$^+$ prototroph formation in both configurations compared to wild-type (Figure 3.8C). Together, these data demonstrate that loss of Rsc2 results in increased rates of spontaneous recombination by unequal sister chromatid exchange and direct-repeat recombination. Altered rates of recombination might reflect the role of Rsc2 in sister chromatid cohesion and is likely to contribute to genome instability.

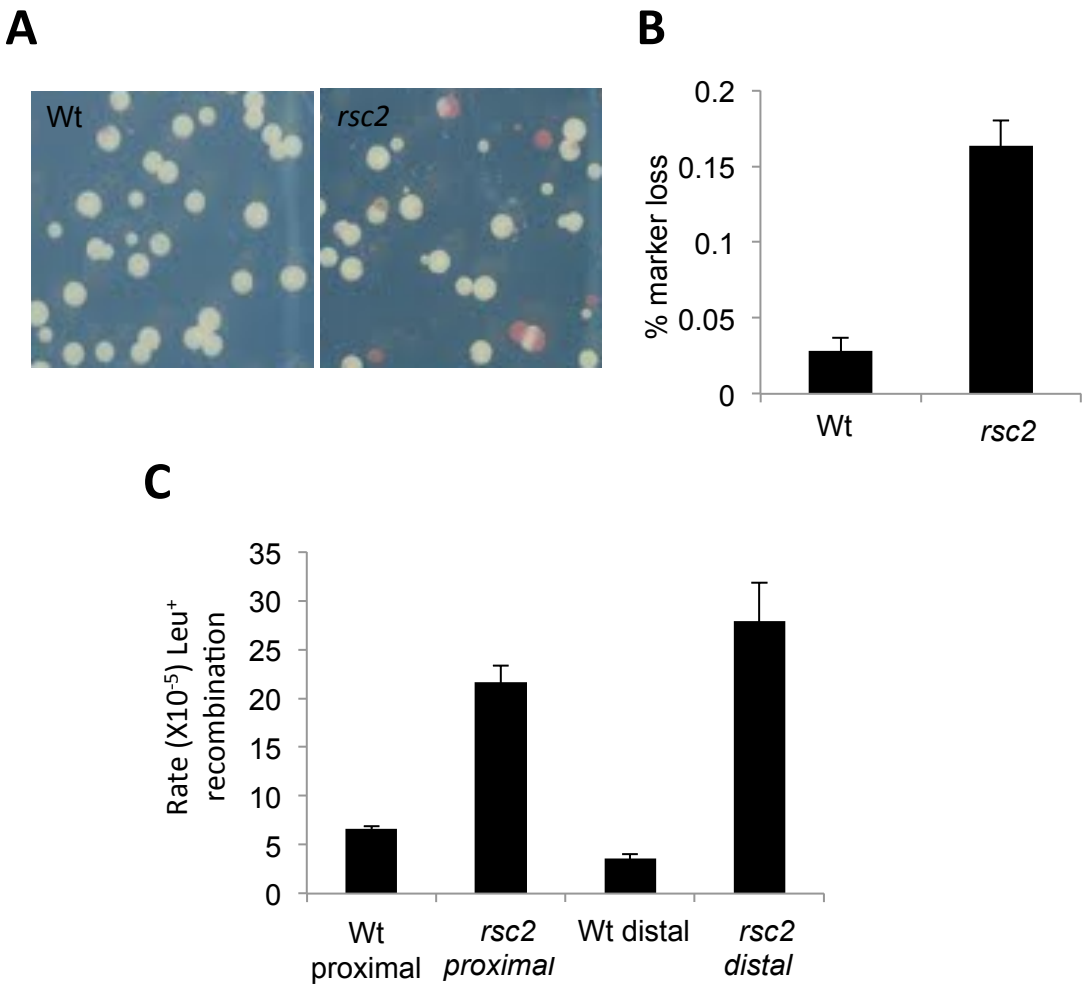

Figure. 3.8. Cells lacking *RSC2* display elevated rates of marker loss by unequal sister chromatid exchange and direct-repeat recombination. (A) Representative images of wild-type and *rsc2* colonies grown on SC media with low adenine. Cells that have lost the *ADE2* marker through unequal sister chromatid exchange give rise to red colonies, whilst *ADE2*-postivie cells are white. Half red/white sectored colonies represent marker loss during the first cell division upon plating. (B) Percent *ADE2* marker loss in wild-type and *rsc2* cells. Data are means ± s.d., *n* = 3 experiments. (D) Rates of spontaneous *LEU*$^+$ prototroph formation in wild-type and *rsc2* strains in the proximal and distal configurations. Data are means ± s.d., *n* = 3 experiments.

3.2. Discussion

In this section we showed that Rsc1 and Rsc2 exist in two separate isoforms of the RSC complex that are otherwise identical in subunit composition. We found that the two isoforms of the complex provide both overlapping and distinct functions in DNA repair, which is consistent with what has been found for other RSC-dependent cellular processes (Cairns *et al.* 1999, Baetz *et al.* 2004, Bungard *et al.* 2004). A summary of the phenotypes associated with loss of *RSC1* and *RSC2* is shown in Table 3.1.

Table 3.1. Phenotypes associated with the loss of *RSC1* and *RSC2*

Ceullular process/activity	Assay description	Δ*rsc1*	Δ*rsc2*	Reference
Growth	-	Normal		This work, unpublished observations
Temperature sensitivity (37°C)	-			Oum *et al.* 2011
DNA damage hypersensitivity	MMS			This work, unpublished observations
	Phleomycin			This work, unpublished observations
	CPT			This work, unpublished observations
	4NQO			This work, unpublished observations
	UV	Normal		Niimi *et al.* 2012
Checkpoint activity	MMS-induced G1 DNA damage checkpoint activation	Normal	Normal	Chambers *et al.* 2012
	MMS-induced G2/M DNA damage checkpoint activation	Normal	Normal	Chambers *et al.* 2012
	MMS-induced *RNR2* and *RNR3* expression	Normal	Normal	Chambers *et al.* 2012
Survival after DNA damage	MMS-induced DNA damage in G1	Normal		Chambers *et al.* 2012
	MMS-induced DNA damage in G2			Chambers *et al.* 2012
NHEJ activity	NHEJ activity at *MAT* locus			Chambers *et al.* 2012
	NHEJ activity at *LEU2* locus			Chambers *et al.* 2012
HR activity	Plasmid gap repair assay			Chai *et al.* 2005
DSB-induced nucleosome	HO-induced nucleosome sliding at *MAT* and *LEU2*		Normal	Chambers *et al.* 2012
remodeling	Basal nuclesome positioning at *MAT*	Normal		Chambers *et al.* 2012
Sister chromatid cohesion	-			Baetz *et al.* 2004
Replication of damaged DNA	PCNA ubiquitination (UV, MMS and HU)	Normal		Niimi *et al.* 2012

'Normal' indicates no defect, yellow indicates slight defect, orange indicates moderate defect, and red indicates severe defect

Overlapping and distinct roles for Rsc1 and Rsc2 in DNA damage responses

Directly comparing the phenotypes of *rsc1* and *rsc2* mutant strains reveals that they are very similar. Both are able to activate the G1 and G2/M DNA damage checkpoints, are hypersensitive to DNA damaging agents and have reduced NHEJ activity, and show a very similar spectrum of repair junctions in survivors of a sustained HO-induced DSB that is distinct from the wild-type repair spectrum. In addition, replacing either bromodomain or the BAH domain of Rsc2 with the analogous domains of Rsc1 does not impair the ability of Rsc2 to promote survival following DNA damage. This suggests that the domains are interchangeable for at least some functions.

However, the data presented here indicate that the two isoforms are not functionally redundant in DNA damage responses. Increasing the dosage of one of the two genes cannot compensate for loss of the other gene in DNA damage hypersensitivity assays with MMS. Moreover, we find that the dependence of NHEJ on the presence of either Rsc1 or Rsc2 appears to be context dependent, arguing for

distinct contributions. We also found that Rsc1 has a unique role in sliding DSB-distal nucleosomes away from HO-induced DSBs at two genomic loci. In contrast, Rsc2 has a specific role in establishing a nuclease-resistant DSB-proximal nucleosome arrangement at the *MAT* locus prior to DSB induction. Interestingly, Rsc2 has been implicated in organising chromatin adjacent to DSBs using other approaches (Shim *et al.* 2007). Taken together with the findings that both Rsc1 and Rsc2 contribute to DNA repair by NHEJ, and show a similar pattern of NHEJ repair junctions, these data suggest that Rsc1 and Rsc2 function at a DSB via two distinct remodelling events. These events might occur sequentially in the same linear pathway, and might be reflected by different recruitment timing to the DSB. The differential requirements for Rsc1 and Rsc2 in the repair of DNA lesions induced by different DNA damaging agents suggests that certain lesions are more dependent on one of these remodelling events than others for repair. The same might be true for lesions occurring at different genomic locations with different chromatin environments. Alternatively, Rsc1 and Rsc2 might be differentially enriched following DNA damage at different lesions or genomic locations.

Combinatorial binding of Rsc1 and Rsc2 bromodomains and BAH domains as a mechanism for regulating the DNA repair activity of the two proteins

Surprisingly, we found that replacing the BAH domain of Rsc2 with the BAH domain of Rsc1 allows Rsc2 to both establish chromatin structure at *MAT* and perform Rsc1-dependent chromatin remodelling. This suggests that the BAH domain dictates the specificity of Rsc1 in this chromatin remodelling events. Recently, other work in our lab established that the BAH domains of Rsc1 and Rsc2 both bind to unmodified H3 (Chambers *et al.* 2013). Therefore, it is unlikely that the differences in remodelling activity between Rsc1 and Rsc2 are due to different binding targets of their BAH domains. Instead, this specificity is likely to be dictated by combinatorial binding of the BAH domains and the bromodomains from both proteins. The idea that the domains of Rsc1 and Rsc2 bind in a combinatorial manner to mediate their activity seems likely, because in higher eukaryotes there are not two separate isoforms of the homologous complex, termed PBAF. Instead, the Rsc1, Rsc2 and Rsc4 subunits of RSC appear to have fused during evolution to produce the BAF180 subunit of PBAF, which contains 6 bromodomains and 2 BAH domains (Mohrmann & Verrijzer 2005). These numerous domains could contribute to the functional specificity of the protein in a modular fashion, and this might be particularly important because there are numerous

alternative splice transcripts of BAF180 that contain different combinations of domains (Horikawa & Barrett 2002).

Predictions made on the binding partners of the Rsc1 and Rsc2 bromodomains are currently speculative given data showing their extremely weak binding to a selection of acetyl-lysine-containing histone peptides (Zhang *et al.* 2010). It is therefore possible that these bromodomains in fact bind other non-histone acetylproteins. Alternatively, simultaneous binding of both bromodomains to their targets might be required to strengthen the interaction. Indeed, this is known to occur for the tandem bromodomains of TAF1, which has a much higher affinity for doubly acetylated H4 tails than mono-acetylated peptides (Jacobson *et al.* 2000). Identifying the true interaction partners of the Rsc1 and Rsc2 bromodomains is of high importance in order to fully understand the similarities and differences between the two proteins. Moreover, given the high conservation of these proteins with the mammalian BAF180 homologue, identifying the Rsc1 and Rsc2 bromodomain binding partners could shed light on how BAF180 functions as a tumour suppressor.

Rsc2 is important for maintaining repeat stability that likely reflects its role in cohesion

We showed that deletion of *RSC2* results in a ~4-fold increase in the rate of spontaneous unequal sister chromatid exchange at the rDNA repeats. This increase in unequal sister chromatid exchange is most likely to result from compromised cohesion in the *rsc2* null cells. This is somewhat in contrast to a study that reported substantially decreased unequal sister chromatid exchange in a *rsc7* null mutant, although a different assay was used (Oum *et al.* 2011). Rsc7 is a component of both isoforms of the RSC complex and therefore represents 100% of all RSC complexes. Because the Rsc2-containing complex represents ~90% of this total, it is perhaps difficult to reconcile how deleting subunits common to the vast majority of the RSC present can have such opposite effects on the same process. Perhaps Rsc2 and Rsc7 do indeed antagonise each other in RSC-mediated unequal sister chromatid exchange. Another alternative is that the increased rate of USCE that we observe in the *rsc2* null strain is a phenomenon unique to the association of RSC at the rDNA repeats. An ability of RSC to both repress and enhance recombination at different genomic loci might be analogous to its ability to both repress and activate the transcription of different genes. It would be useful to measure the effects of deleting *RSC2* and *RSC7* in the same unequal sister chromatid exchange assay to clarify this.

In contrast, our findings that a *rsc2* null mutant displays ~5-fold increase in the rate of direct-repeat recombination are in agreement with findings by Oum *et al.,* in

which an *rsc7* null strain showed a massively elevated rate of direct-repeat recombination (189-fold change in the rate of recombination compared to wild-type cells). Recombination in this assay can occur via replication slippage, unequal sister chromatid exchange or SSA. In our direct-repeat recombination assays recombination can occur via multiple intra- and interchromatid recombination mechanisms, including gene conversion, replication slippage, SSA, sister strand slippage, unequal sister chromatid exchange and intrachromatid crossovers. Therefore it is not appropriate to directly compare the differences between the two strains in the two assays. Nevertheless, these data collectively indicate that subunits of RSC play an important role in regulating appropriate levels of recombination in repetitive DNA sequences. Misregulated recombination is a known cause of genomic instability and loss of heterozygosity (LOH), which are important drivers of tumourigenesis. This has potentially important implications given that the mammalian homologue of Rsc2, BAF180, is a tumour suppressor gene.

CHAPTER 4: BAF180 PROMOTES COHESION AND PREVENTS GENOME INSTABILITY AND ANEUPLOIDY

4.1. Results

Introduction

A convergence of observations made in our lab with findings from a range of studies, both old and recent, prompted us to examine the possibility that BAF180 functions in sister chromatid cohesion. Firstly, the yeast homologues of BAF180, Rsc1 and in particular Rsc2, are required for sister chromatid cohesion (Huang *et al.* 2004, Baetz *et al.* 2004). Therefore BAF180 might play a conserved role in cohesion. Second, we observe an increased rate of unequal sister chromatid exchanges and direct-repeat recombination in *rsc2* null cells, suggesting that loss of Rsc2 results in misregulation of physiological recombination pathways (see chapter 3). Increased rates of unequal sister chromatid exchange is thought to be a consequence of impaired cohesion (Huang *et al.* 2006), and might also underlie an increased rate of direct-repeat recombination. Moreover, misregulation of homologous recombination pathways because of defective cohesion might be responsible for deleterious genomic instability, which is associated with tumourigenesis (Xu *et al.* 2011). Thirdly, a spate of exome sequencing studies revealed that numerous cohesin genes are frequently mutated in cancer (Barber *et al.* 2008, Solomon *et al.* 2011, 2013, Guo *et al.* 2013, Balbáz-Martinéz *et al.* 2013, Kon *et al.* 2013, Kim *et al.* 2013). In parallel, a substantial number of similar studies identified strikingly frequent mutations in members of mammalian SWI/SNF complexes, including BAF180 (Shain & Pollack 2013). In an effort to to unify these observations we set out to test the following: does BAF180 play a conserved role in sister chromatid cohesion, and if so, does any role of BAF180 in cohesion represent a tumour suppressor function?

Analysis of cohesion in BAF180 -/- mouse embryonic stem cells

To test whether BAF180 functions in sister chromatid cohesion we first utilized mouse embryonic stem cells (mESCs) that were wild-type (+/+) or contained a homozygous BAF180 mutation (-/-) that abolishes all BAF180 expression (Wang *et al.* 2004). We next prepared metaphase chromosome spreads from each genotype and scored chromosomes for sister chromatid cohesion. We based our scoring assay on those

from previously published studies (e.g. Barber *et al.* 2008, Carretero *et al.* 2013), in which a clearly resolved gap between DAPI stained sister chromatids at the centromere represents a centromeric cohesion defect (Fig. 4.1A). Cells were categorized as having defective centromere cohesion when 3 or more chromosomes showed a defect, or as having normal centromere cohesion when less than 3 chromosomes showed a defect. Quantification of 200 spreads from each genotype revealed that there was a statistically significant increase in the number of BAF180 -/- cells with defective centromere cohesion compared to wild-type (Fig. 4.1B; $P<0.001$, Fisher's exact test).

In vertebrate cells the two versions of yeast Scc3, known as SA1 and SA2, differentially regulate arm and centromere cohesion, respectively (Canudas & Smith 2009). To determine if BAF180 also mediates arm cohesion we analysed arm cohesion in the same metaphase mESCs. Chromosomes were described as having a defect in arm cohesion when sister chromatids were clearly separated along the whole length of the arms (Fig. 4.1A). Similarly, cells were categorized as having defective arm cohesion when 3 or more chromosomes showed a defect, or as having normal arm cohesion when less than 3 chromosomes showed a defect. In contrast to cohesion at the centromere, we did not observe a significant difference in the number of BAF180 -/- cells displaying defective arm cohesion (Fig. 4.1C; $P=0.59$, Fisher's exact test). Collectively, these results suggest that BAF180 is important for promoting sister chromatid cohesion specifically at centromeres in mESCs (Brownlee *et al.* 2014)

Fluorescent in situ *hybridization (FISH) analysis on mitotic BAF180-depleted 1BR-hTERT and U2OS cells*

To examine the cohesion defect in BAF180-deficient cells in more detail, and to determine if it is also apparent in human cells, we first depleted BAF180 in 1BR-hTERT cells using siRNA. Western blotting confirmed efficient BAF180 depletion in these cells (Fig. 4.2A). Next, we performed (FISH) on mitotic cells isolated by shake-off from asynchronously growing cultures (performed by Ross Cloney). Using a probe directed against the centromeric region of chromosome 10 (Fig. 4.2B (green)), we found that the siBAF180-treated cells displayed a statistically significant increase in the distribution of distances between the two signals from the sister chromatids compared to siControl cells (Fig. 4.2C and D; $P<0.001$, Kolmogorov-Smirnov test). In contrast, when the distances between the arm signals of chromosome 10 (Fig. 4.3A (red)) were measured, we found no significant shift in the distribution of measurements between siControl- and siBAF180-treated cells (Fig. 4.3B and C; $P=0.586$, Kolomogorov-

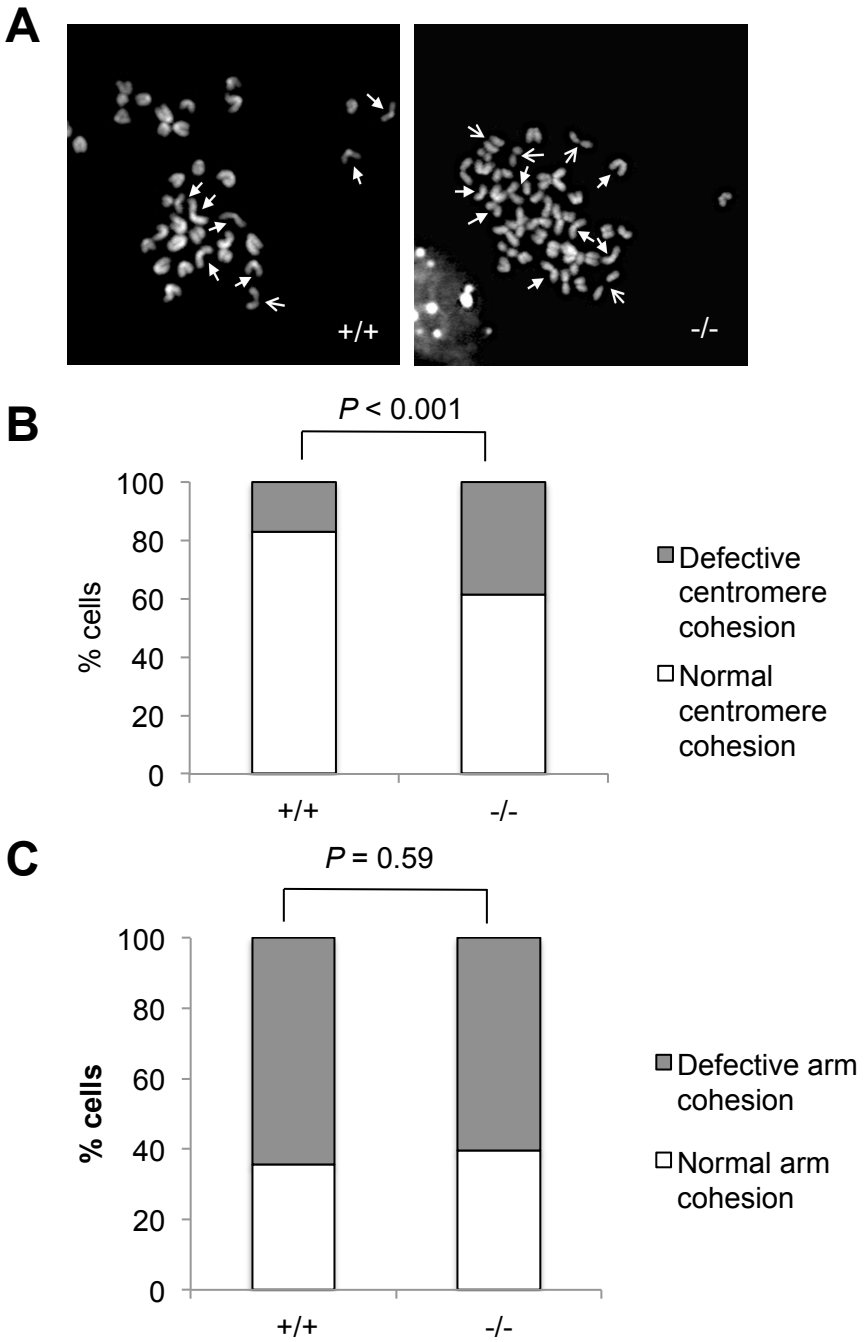

Figure 4.1. BAF180 promotes centromeric sister chromatid cohesion in mESCs (A) Representative WT (+/+) and BAF180 knockout (-/-) mESC metaphase spreads. Cells were analysed according to whether cohesion was defective at centromeres (open arrows) or arms (open and closed arrows). (B) Cells were scored as 'normal' when two or fewer chromosomes showed centromeric cohesion defects, or 'defective' when three or more chromosomes showed a defect (P<0.0001 between +/+ and -/- cells; Fisher's exact test) (C) Cells were scored as 'normal' when two or fewer chromosomes showed arm cohesion defects, or 'defective' when three or more chromosomes showed a defect (P=0.59 between +/+ and -/- cells; Fisher's exact test). 200 cells were scored per genotype from two independent experiments.

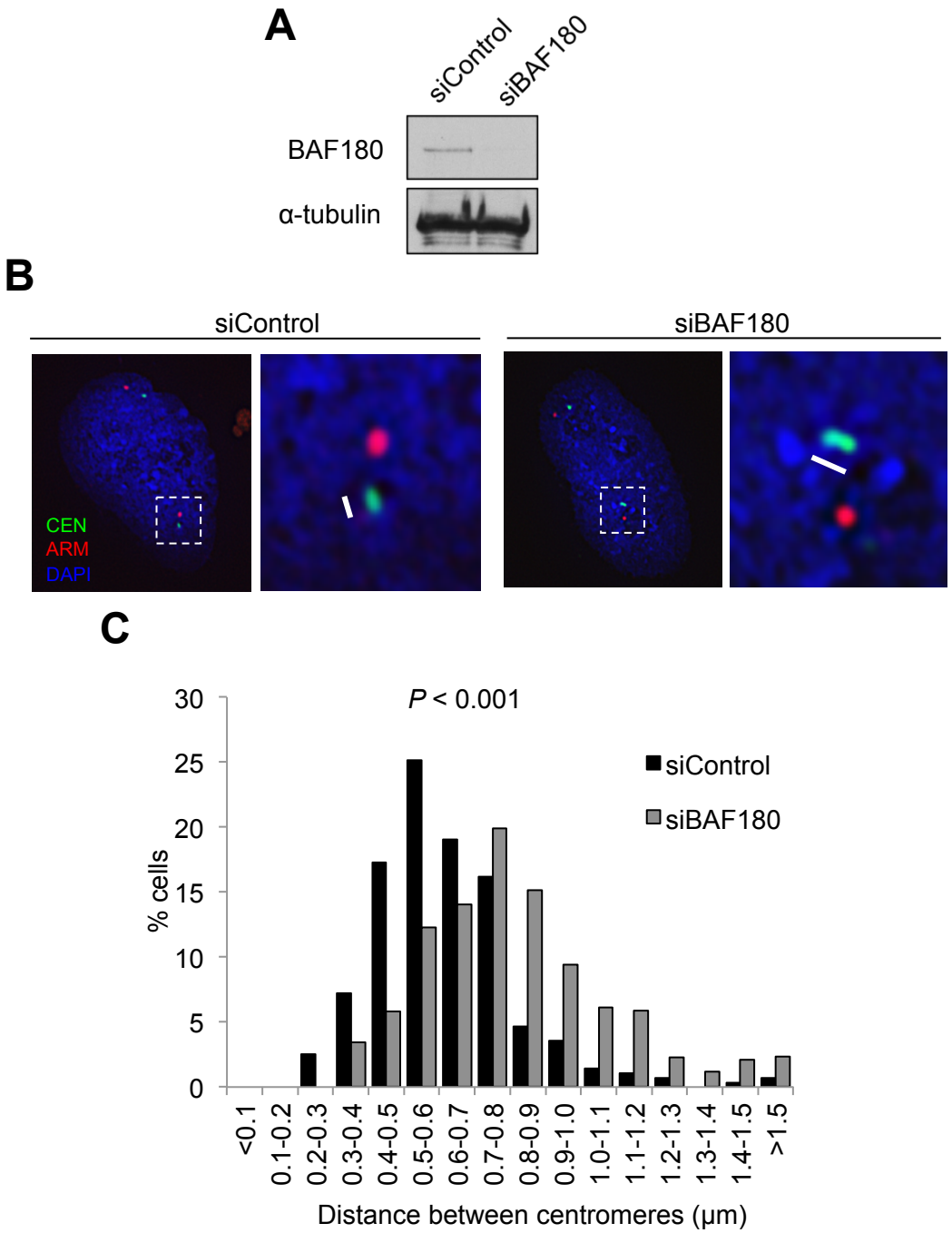
A
siControl
siBAF180
BAF180
α-tubulin
B
siControl
siBAF180
CEN
ARM
DAPI
C
P < 0.001
siControl
siBAF180
% cells
30
25
20
15
10
5
0
<0.1
0.1-0.2
0.2-0.3
0.3-0.4
0.4-0.5
0.5-0.6
0.6-0.7
0.7-0.8
0.8-0.9
0.9-1.0
1.0-1.1
1.1-1.2
1.2-1.3
1.3-1.4
1.4-1.5
>1.5
Distance between centromeres (μm)

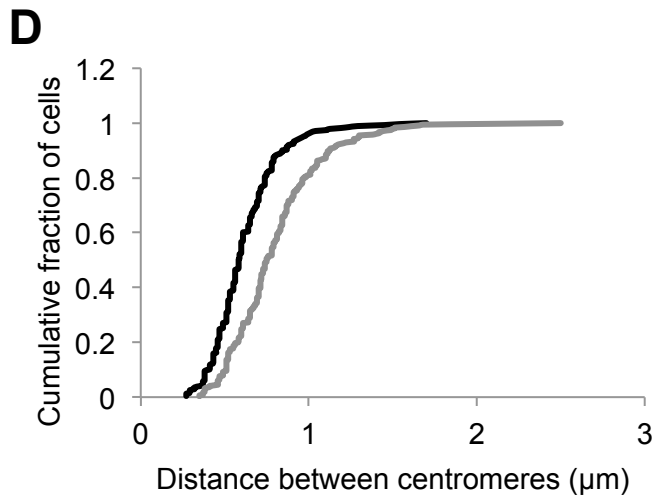

Figure 4.2. siRNA-mediated depletion of BAF180 in 1BR-hTERT cells results in defective centromeric cohesion (A) Analysis of BAF180 depletion efficiency in 1BR-hTERT cells by Western blotting. α-tubulin was used as a loading control. (B) Representative images of siControl- (left panel) and siBAF180-treated (right panel) mitotic cells probed with a mixture of FISH probes directed against the centromere (green) and arm (red) of chromosome 10. (C) FISH analysis on cells from (B). The distances between signals from the sister chromatid centromeres (green) were measured from two independent experiments (>400 measurements in total) and the distributions plotted as a histogram (P<0.001, Kolmogorov-Smirnov test). (D) Data from (C) presented as a cumulative plot.

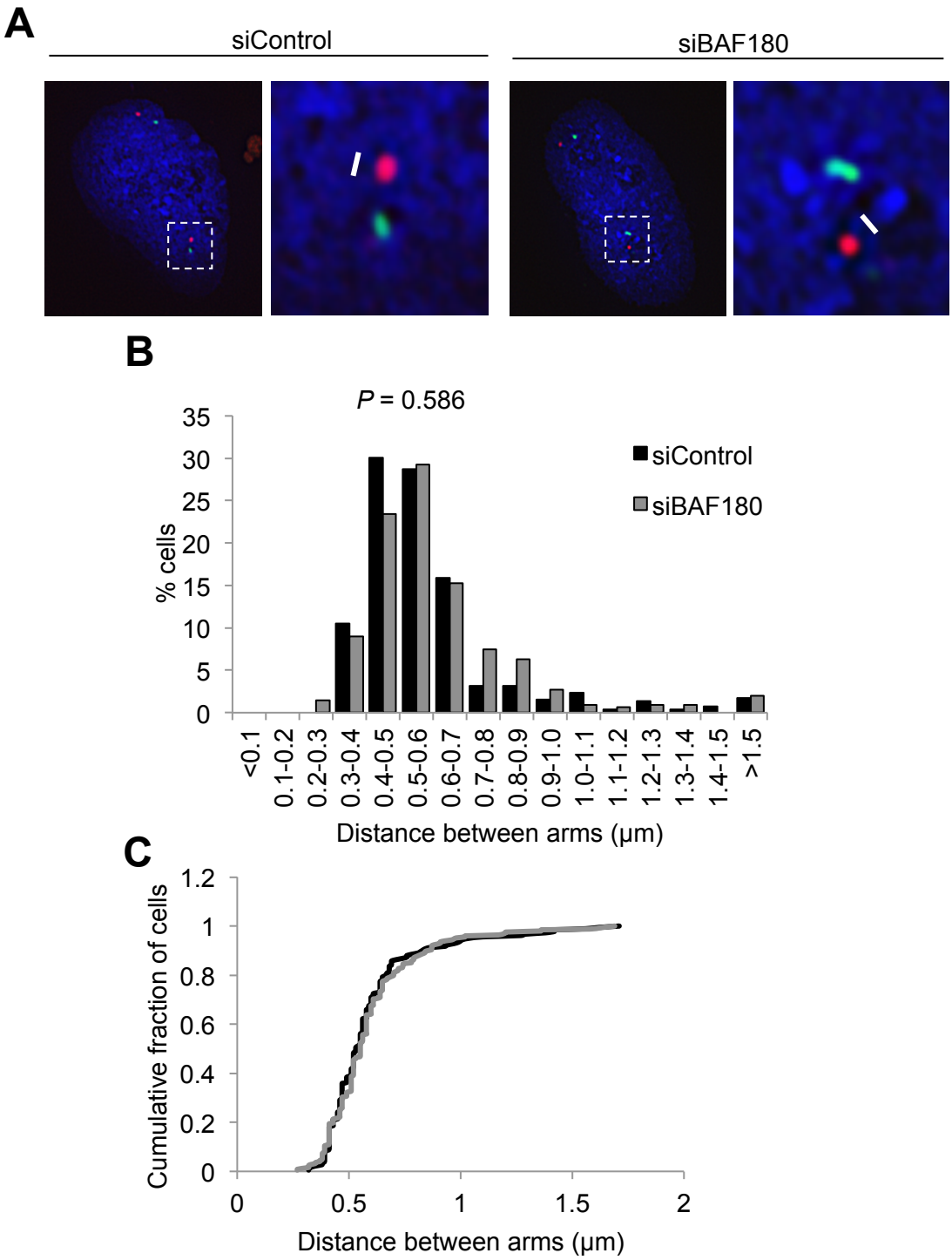

Figure 4.3. siRNA-mediated depletion of BAF180 in 1BR-hTERT cells does not cause defective cohesion at chromosome arms (A) Representative images of siControl- (left panel) and siBAF180-treated (right panel) mitotic cells probed with a mixture of FISH probes directed against the centromere (green) and arm (red) regions of chromosome 10. (B) FISH analysis on cells from (A). The distances between signals from the sister chromatid arms (red) were measured from two independent experiments (>400 measurements in total) and the distributions plotted as a histogram (*P*=0.586, Kolmogorov-Smirnov test).(C) Data from (B) presented as a cumulative plot.

Smirnov test). Similarly, using a probe directed against the subtelomeric region of chromosome 16 (Fig. 4.4A) there was no significant change in the distribution of distances between sister chromatid telomeres following BAF180 depletion (Fig. 4.4B and C; *P*=0.877, Kolmogorov-Smirnov test). Together, these data indicate that depletion of BAF180 in human cells also leads to a cohesion defect that is specific to the centromere, similar to that seen for SA2-depleted cells (Canudas & Smith 2009).

We also created a BAF180 small hairpin RNA (shRNA) stable cell line in U2OS cells and a corresponding control cell line (created by Suzanna Hopkins). Western blotting confirmed efficient BAF180 depletion in these cells (Fig. 4.5A). Mitotic cells isolated by shake-off from asynchronous cells were probed using the centromere 10-specifc FISH probe and the distances between signals from the sister chromatids were measured. Consistent with the data from the 1BR-hTERT cells, BAF180 depletion in the U2OS cells led to a statistically significant increase in the distribution of measurements (Fig. 4.5B and C; *P*<0.001, Kolmogorov-Smirnov test). Therefore, the centromeric cohesion defect in BAF180-depleted cells appears to be a conserved function in mammalian cells (Brownlee *et al.* 2014).

Depletion of BAF180 and SA2 results in a comparable defect in centromeric cohesion

The centromeric cohesion defect that we observe upon BAF180 depletion appears relatively modest compared to the defect observed in SA2-depleted HeLa cells reported by Canudas & Smith (Canudas & Smith 2009). This might be due to differences in cell type, or that SA2 depletion indeed leads to a more severe cohesion defect. In order to compare the SA2 cohesion defect with that of BAF180 more directly we individually depleted SA2 and BAF180 using siRNA in 1BR-hTERTs and analysed centromere separation by FISH as described. We confirmed efficient knockdown of SA2 by Western blot (Fig. 4.6A, Anna L. Chambers). The shift in the distribution of distances between the centromeres was slightly greater in SA2-depleted cells compared to that of BAF180 (Fig. 4.6B and C; *P*=0.001 for BAF180, *P*<0.001 for SA2 compared to siControl cells, Kolmogorov-Smirnov test). Therefore, the cohesion defect following BAF180 depletion is comparable to that in cells lacking SA2 (Brownlee *et al.* 2014).

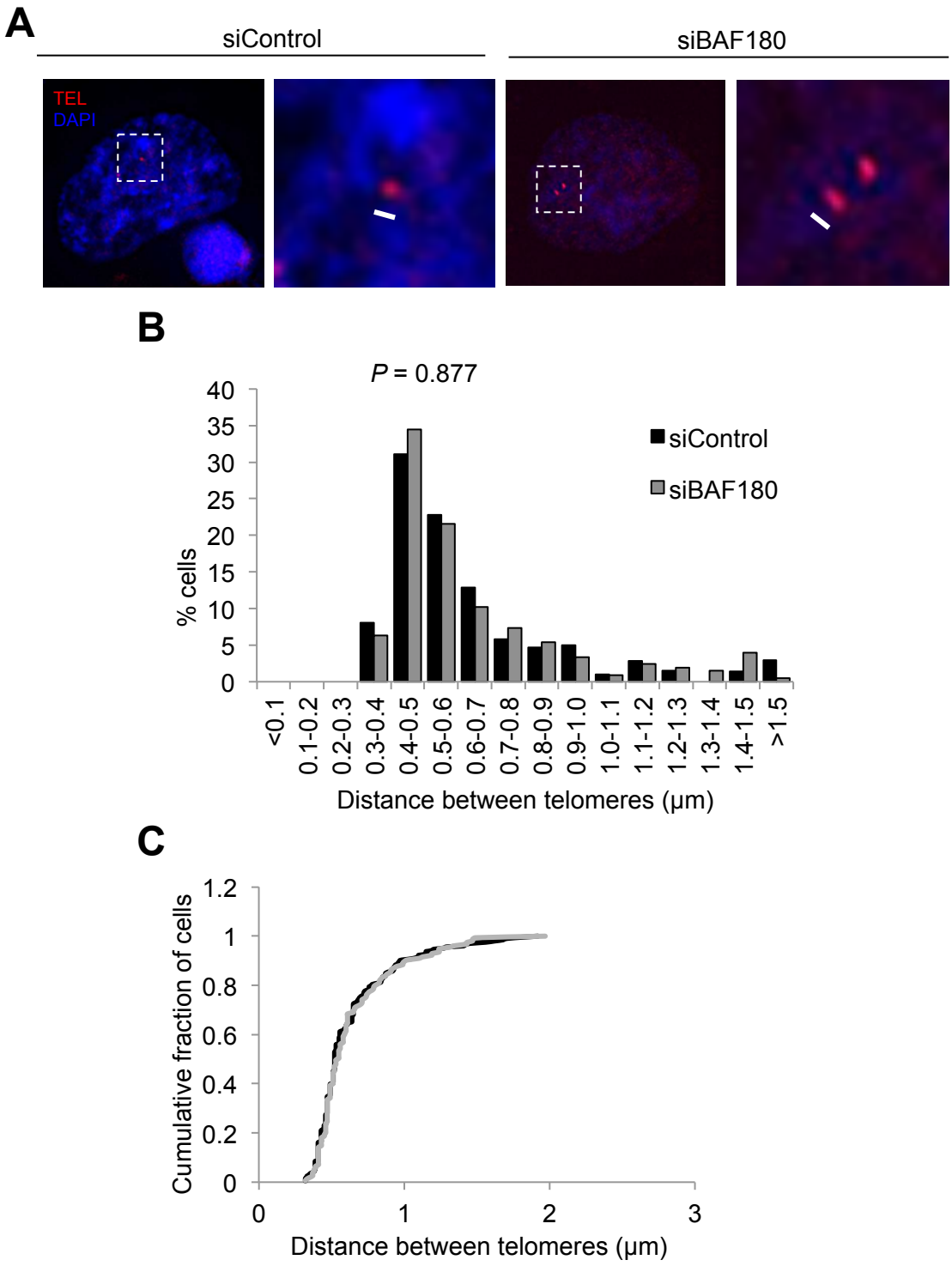

Figure 4.4. siRNA-mediated depletion of BAF180 in 1BR-hTERT cells does not cause defective cohesion at telomeres (A) Representative images of siControl- (left panel) and siBAF180-treated (right panel) mitotic cells probed with a FISH probe directed against the subtelomeric region of chromosome 16 (red). (B) FISH analysis on cells from (A). The distances between signals from the sister chromatid telomeres were measured from two independent experiments (>400 measurements in total) and the distributions plotted as a histogram (*P*=0.877, Kolmogorov-Smirnov test). (C) Data from (B) presented as a cumulative plot.

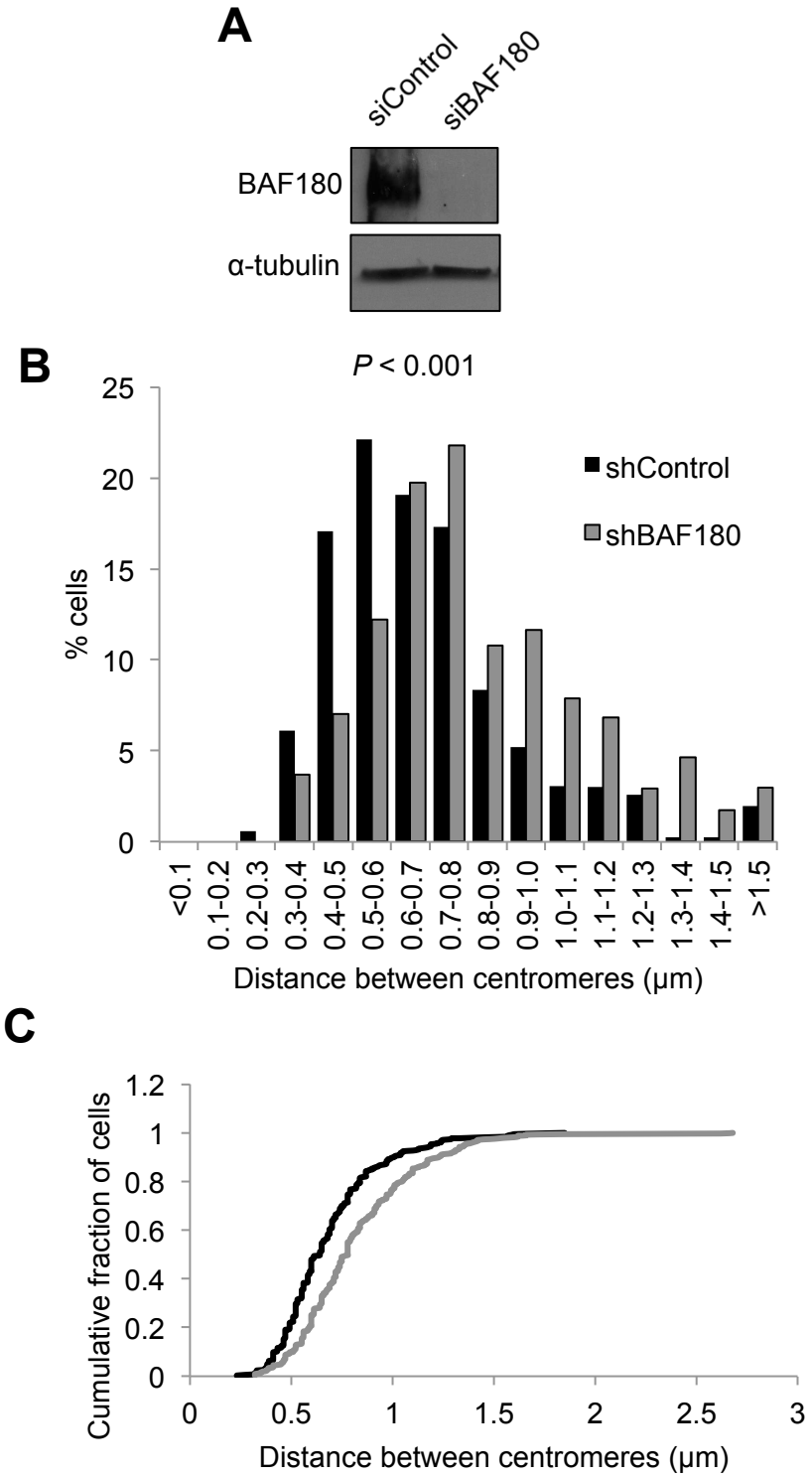

Figure 4.5. Stable shBAF180-depleted U2OS cells show defective centromeric cohesion (A) Western blot analysis of BAF180 depletion in U2OS cells stably expressing BAF180 shRNA and control shRNA. α-tubulin was used as a loading control. (B) FISH analysis on mitotic cells probed with a FISH probe directed against the centromere of chromosome 10. The distances between signals from the sister chromatids were measured from two independent experiments (>400 measurements in total) and the distributions plotted as a histogram (P<0.001, Kolmogorov-Smirnov test). (D) Data from (C) presented as a cumulative plot.

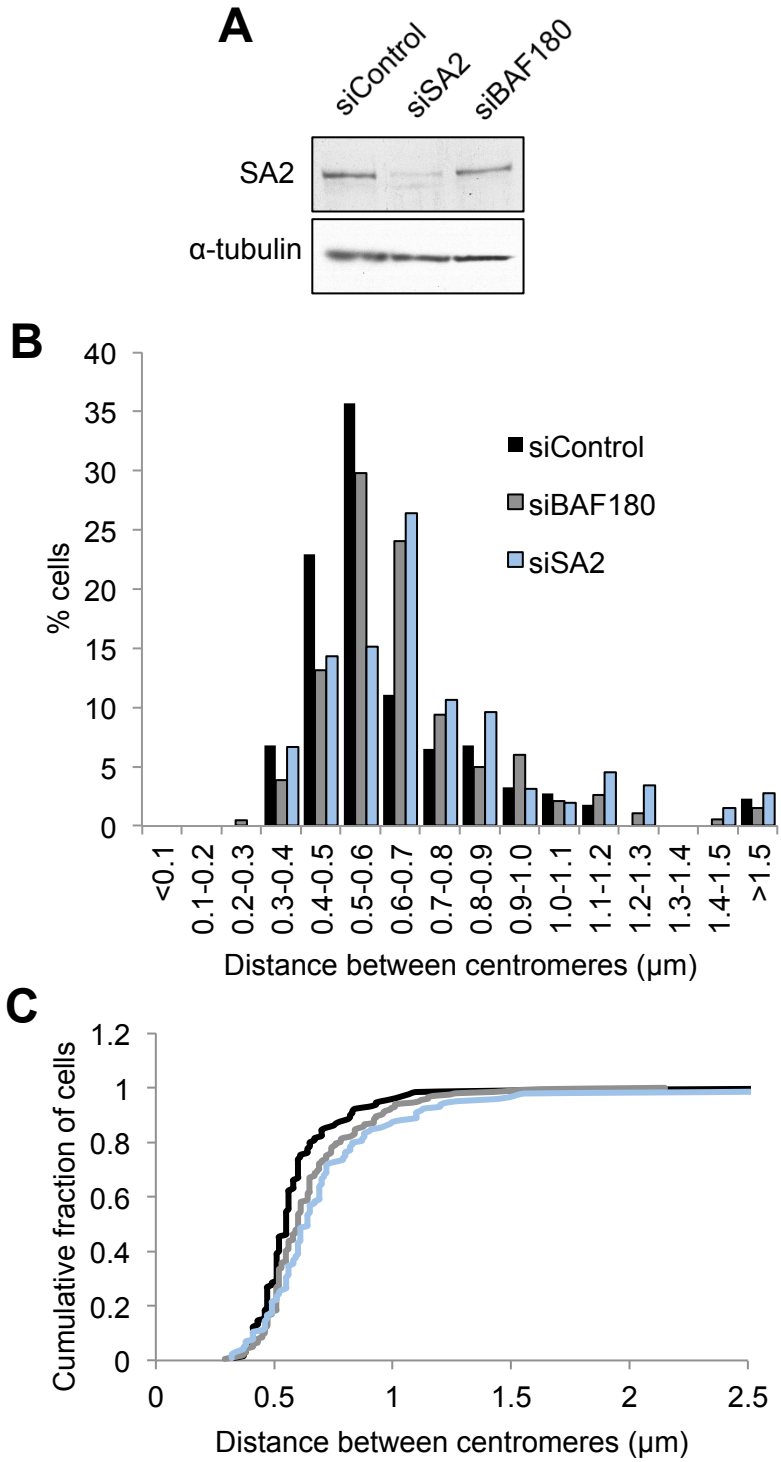

Figure 4.6. Depletion of BAF180 and SA2 results in a comparable defect in centromeric cohesion (A) Western blot analysis of siRNA-treated 1BR-hTERT cells using antibodies directed against SA2 or α-tubulin. (B) FISH analysis on mitotic cells probed with a FISH probe directed against the centromere of chromosome 10. The distances between signals from the sister chromatids were measured from two independent experiments (>200 measurements in total) and the distributions plotted as a histogram (P=0.001 between siControl and siBAF180 cells, P<0.001 between siControl and siSA2 cells; Kolmogorov-Smirnov test). (D) Data from (C) presented as a cumulative plot.

BAF180 is not required for transcription of cohesin genes and has tissue-specific roles in regulating p53-dependent p21 transcription

Defects in cohesion could be caused by a number of different mechanisms, such as lower levels of cohesins, inappropriate loading onto chromatin, or an inability to establish cohesion once loaded. One possible mechanism by which BAF180 mediates cohesion is transcriptional regulation of cohesin genes. In argument against this possibility, microarray data from the report by Varela *et al.* did not identify any significantly misregulated cohesin genes following BAF180 depletion in 3 renal cell carcinoma cell lines (Varela *et al.* 2011). Nevertheless, we first examined the levels of Smc1α*,* Smc3*,* Stag1 and Stag2 proteins from asynchronous BAF180 +/+ and -/- mESC whole-cell extracts by Western blot (Anna L. Chambers). There were no gross changes in the levels of these proteins in BAF180 -/- cells compared to BAF180 +/+ cells, suggesting that these proteins are not grossly downregulated in the absence of BAF180 in these cells (Fig. 4.7A).

We also examined the mRNA levels of the core cohesin genes *SMC1A, SMC3, STAG1, STAG2 and RAD21* in siBAF180-treated 1BR-hTERT cells and the stable shBAF180 U2OS cells, and compared the controls using quantitative RT-PCR (qRT-PCR, Anna L. Chambers). BAF180 depletion did not lead to significantly reduced levels of these transcripts in either cells line (Fig. 4.7B and C). In fact, in the shBAF180 U2OS cells the *RAD21* transcript, and to a lesser extent the *STAG1* and *SMC3* transcripts, were upregulated (Fig. 4.7C). Collectively, these data suggest that the cohesion defect in BAF180-depleted mouse and human cells is unlikely to be due to indirect transcriptional effects.

One mechanism by which BAF180 might function as a tumour suppressor is in positively regulating p53-dependent p21 transcription in response to oncogenic and replicative stresses (Burrows *et al.* 2010, Xia *et al.* 2008). Recently, p21 was implicated in mitotic control by regulating Cyclin B1, and reduction of p21 levels led to an extended mitosis and impaired Aurora B activity in human cells (Kreis *et al.* 2013). Thus, the cohesion defect we observe in BAF180-depleted cells might be a consequence of reduced p21-dependent mitotic activity. We examined p21 transcription levels in BAF180-depleted 1BR-hTERT cells and found that, consistent with previous studies, basal levels of p21 were reduced in siBAF180 cells (Fig. 4.7D). Treatment with the MDM2 inhibitor nutlin-3a, which alleviates p53 inhibition, led to lower p21 levels in siBAF180 cells compared to siControl cells (Fig. 4.7E). In contrast, and of great importance to this study, we found that basal p21 levels in shBAF180 U2OS cells were actually ~3-fold higher than the shControl cells (Fig. 4.7D), suggesting

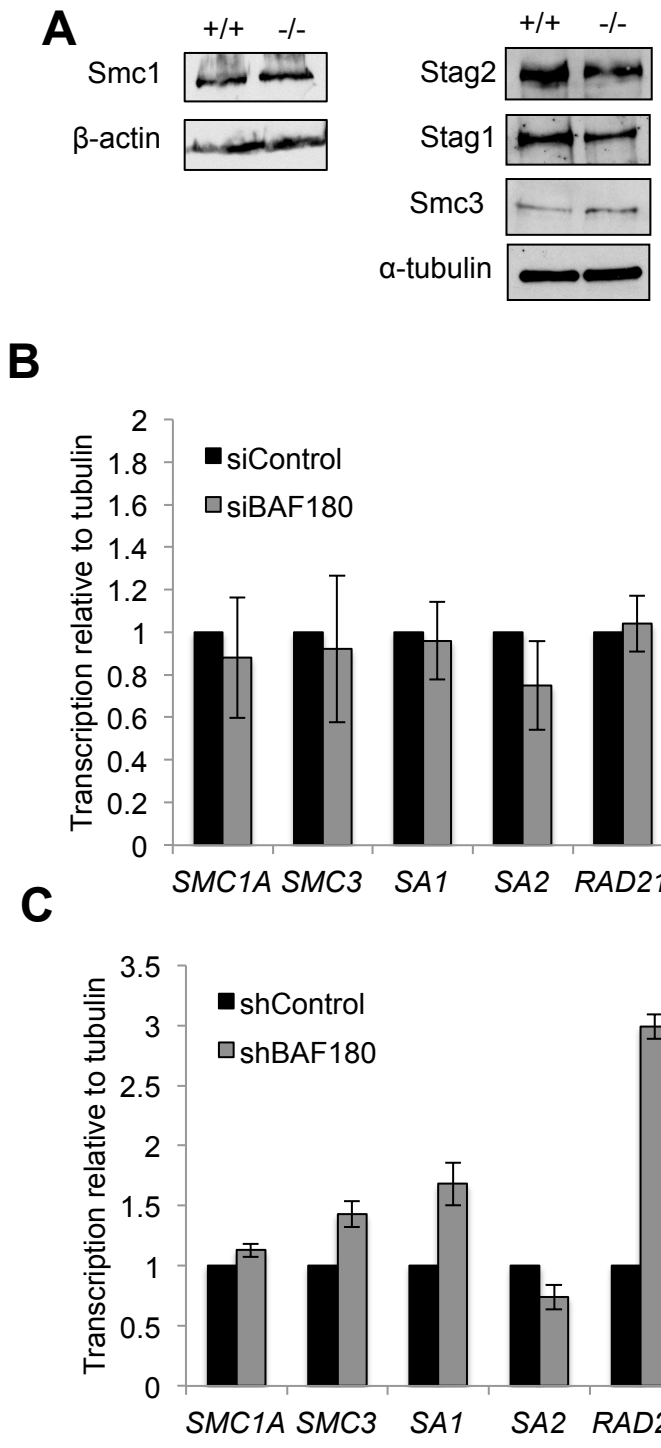
A
+/+
-/-
Smc1
β-actin
+/+
-/-
Stag2
Stag1
Smc3
α-tubulin
B
Transcription relative to tubulin
siControl
siBAF180
SMC1A
SMC3
SA1
SA2
RAD21
C
Transcription relative to tubulin
shControl
shBAF180
SMC1A
SMC3
SA1
SA2
RAD21

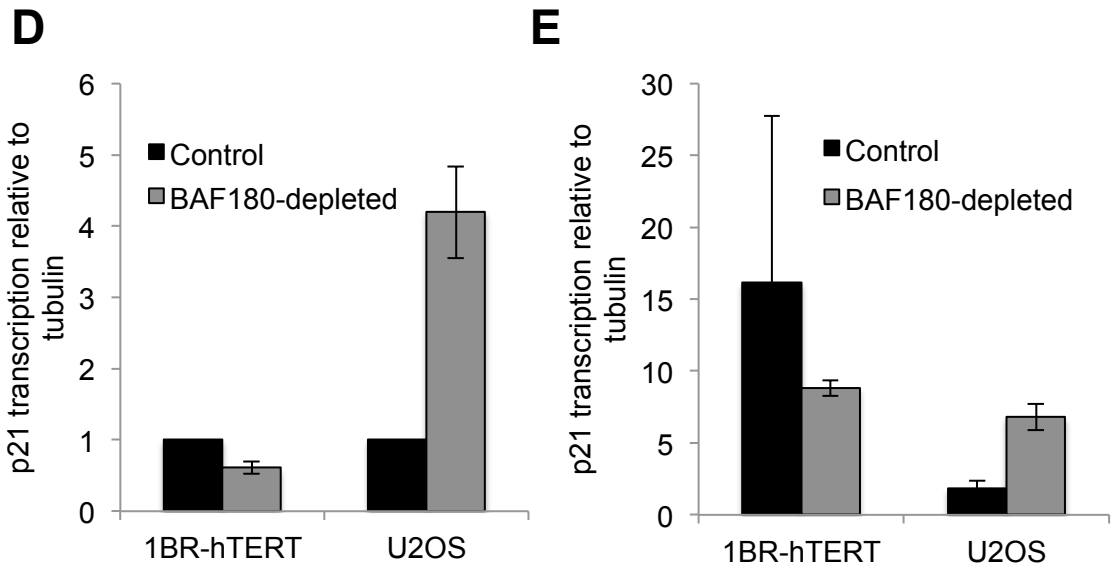

Figure 4.7. BAF180 is not required for transcription of cohesin genes and has tissue-specific roles in regulating p53-dependent p21 transcription (A) Western blot analysis of cohesin subunits in whole-cell extracts (WCE) prepared from WT (+/+) and BAF180 knockout (-/-) mESCs. (B) Transcription of cohesin subunits in BAF180-depleted 1BR-hTERT cells. Transcript levels from three independent experiments were analysed by qPCR and normalized to α-tubulin transcript. Data for BAF180-depleted cells are shown relative to siControl cells. (C) Transcription of cohesin subunits in shBAF180 U2OS cells. Transcript levels levels from three independent experiments were analysed by qPCR and normalized to α-tubulin. Data for shBAF180 cells are shown relative to shControl cells. (D) Transcription of basal p21 in BAF180-depleted 1BR-hTERT and U2OS cells. Transcript levels from three independent experiments were analysed by qPCR and normalized to β-actin. Data for BAF180-depleted cells are shown relative to control cells. (E) Transcription of nutlin-3a-induced p21 in BAF180-depleted 1BR-hTERT and U2OS cells. Transcript levels from three independent experiments were analysed by qPCR and normalized to β-actin.

that p53-dependent transcriptional activation of p21 is BAF180-independent in these cells. A similar increase in p21 transcription in the shBAF180 cells compared to the shControl cells was observed after treatment with nutlin-3a (Fig. 4.7E). Thus, the centromeric cohesion defect in the shBAF180 U2OS cells cannot be attributed to p21-dependent mitotic regulation.

Analysis of cohesin loading dynamics during S-phase in BAF180 depleted U2OS cells

Whilst cohesin is loaded onto chromatin during G1, levels of stably bound cohesin increase concomitantly with replication in S-phase (Gerlich *et al.* 2006). To investigate whether BAF180 depletion leads to a defect in cohesin loading stable shBAF180 U2OS cells were arrested at G1/S using aphidicolin. Cells were harvested for chromatin fractionation 0, 3, and 6hrs after release into fresh media to allow passage into S-phase. We confirmed efficient G1/S arrest and timely progression through S-phase in both shControl and shBAF180 cells by FACS (Fig. 4.8A). At 0hrs, when cells were in G1/S, the levels of chromatin-bound SMC1 were low as expected in the shControl cells (Fig. 4.8B). 6hrs after release a substantial increase in chromatin-bound SMC3 was observed as the bulk of cells were progressing through S-phase. Interestingly, there were increased levels of chromatin-bound SMC1 at 0 and 3hrs in the shBAF180 cells compared to the shControl cells (Figure 4.8B). Nevertheless, after 6hrs the levels of chromatin-bound SMC1 was comparable in the shControl and shBAF180 cells, suggesting that cohesin loading during S-phase is not grossly impaired in the absence of BAF180. However, because centromere-localized cohesin only represents ~10% of all chromatin bound cohesin (Peters *et al.* 2008) reduced loading only at the centromere might not be obvious in this assay. Further investigation is required to determine the molecular basis of the centromeric cohesion defect in cells lacking BAF180.

Abnormal chromosome morphology in BAF180-depleted MRC5CV1 cells

Performing siRNA depletion of BAF180 in MRC5CV1 cells (Fig. 4.5A) reproducibly led to the appearance of short, squat chromosomes with wider chromosome arms compared to control cells (Fig. 4.5B). To quantify this, we measured the length of the longest chromosome in each metaphase spread from siControl and siBAF180 cells. We found a significant reduction in the mean length of the longest chromosome measured in the siBAF180-treated cells compared to the siControl cells (Fig. 4.5C; P=0.002, two-tailed unpaired t-test). This might reflect a role for BAF180 in mediating

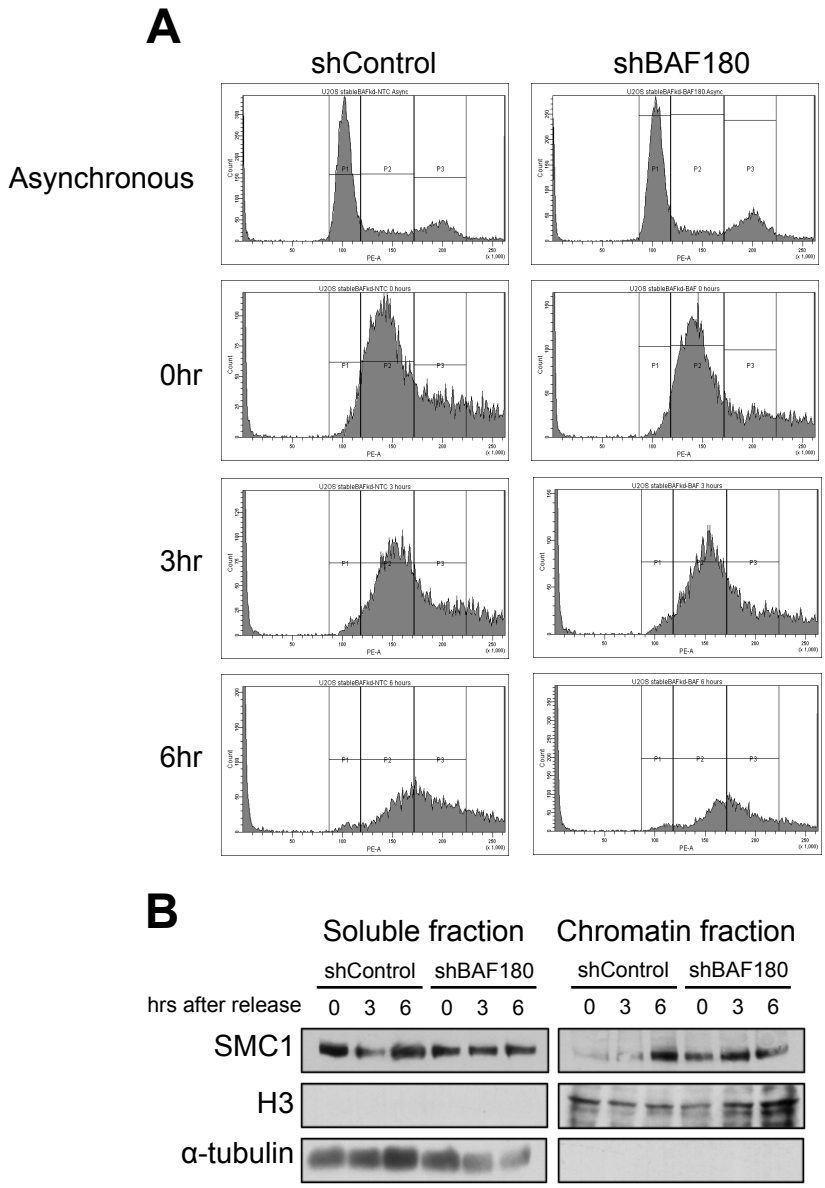

Figure 4.8. The cohesion defect in BAF180-depleted U2OS cells is not due to reduced levels of total chromatin-bound cohesin (A) FACS analysis of shControl and shBAF180 U2OS cells arrested in G1/S using aphidicolin. Samples were collected for FACS 0, 3 and 6hrs after release into fresh media. (B) Samples of the same cells treated as in (A) were collected for chromatin fractionation. The soluble and chromatin fractions were analysed by Western blot using antibodies against SMC1, histone H3 and α-tubulin.

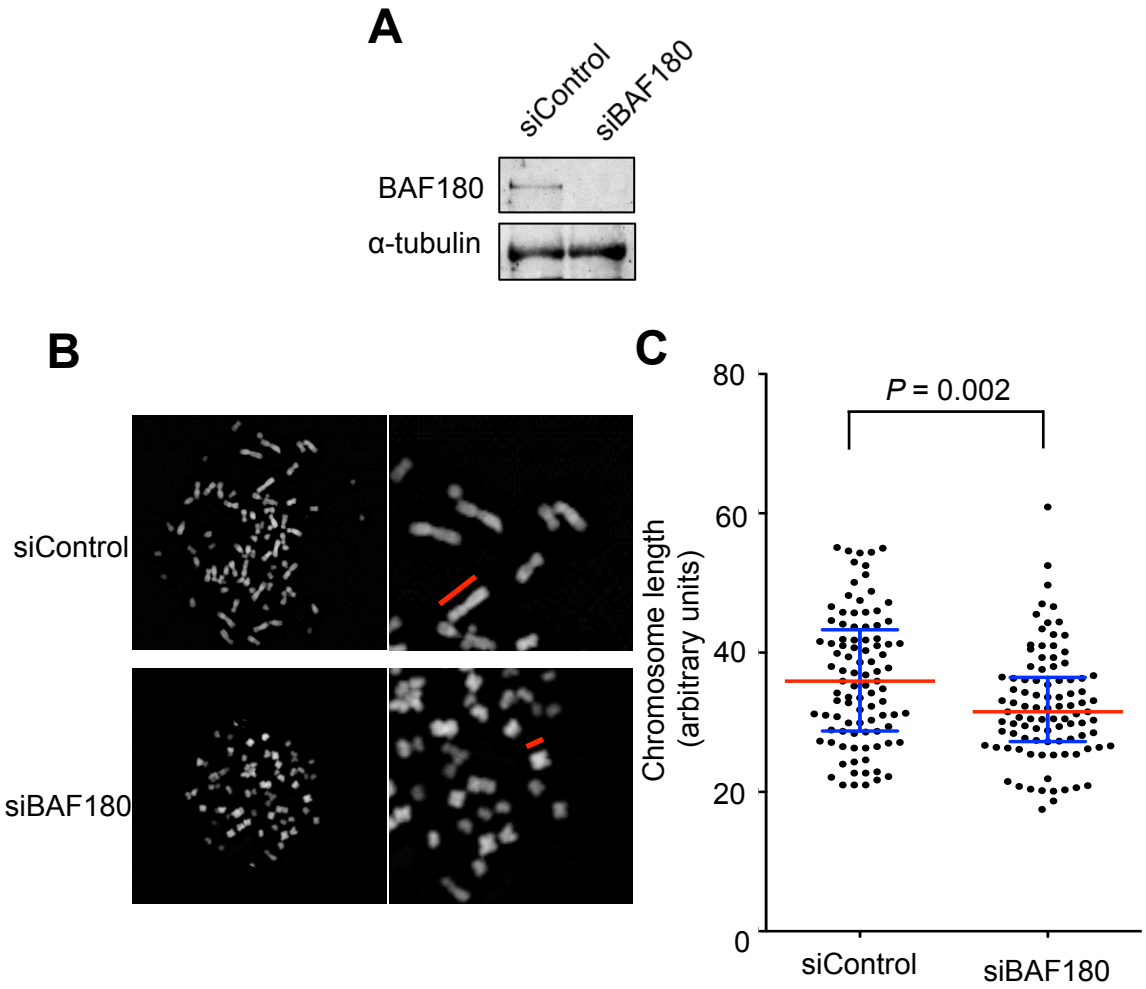

Figure 4.9. siRNA-mediated depletion of BAF180 in MRC5CV1 cells leads to altered chromosome morphology (A) Analysis of BAF180 depletion efficiency in MRC5CV1 cells by Western blotting. α-tubulin was used as a loading control. (B) Representative siControl (top) and siBAF180 (bottom) metaphase chromosome spreads. Red line indicates the length of the longest chromosome in the spread. (C) Dot plot showing the length of the longest chromosomes from 96 siControl and siBAF180 metaphase chromosome spreads. Red line indicates the median chromosome length, upper and lower blue lines represent the upper and lower quartiles. *P* = 0.002, two-tailed unpaired t-test.

the largely unclear chromosome condensation function of cohesin. Indeed, it has been reported that siRNA depletion of ATRX and HDAC3, which, like BAF180, are required for centromeric cohesion, similarly results in chromosomes of this morphology (Ritchie *et al.* 2008, Eot-Hollier *et al.* 2008).

Cells lacking BAF180 are aneuploid and show evidence of chromosome instability (CIN)

Strikingly frequent inactivating mutations and deletions in the gene encoding SA2, as well as other centromere-specific cohesin genes, were recently found in a diverse range of tumour types, suggesting that loss of centromeric cohesion contributes to tumourigenesis (Solomon *et al.* 2011, 2013, Guo *et al.* 2013, Balbáz-Martinéz *et al.* 2013, Kon *et al.* 2013, Kim *et al.* 2013). Furthermore, disruption of centromeric cohesion causes aneuploidy in both normal and cancer cells (Barber *et al.* 2008, Zhang *et al.* 2008, Ritchie *et al.* 2010, Manning *et al.* 2010, Solomon *et al.* 2011, 2013, Guo *et al.* 2013, Carretero *et al.* 2013). We next sought to determine if loss of BAF180 similarly leads to aneuploidy. We found that in metaphase spreads of mESCs lacking BAF180 there is a modal gain of two chromosomes in the cell population compared to wild-type cells (Figure 4.10A), suggesting that loss of BAF180 does indeed cause aneuploidy. Micronuclei can arise in cells as a consequence of chromosome missegregation, which is a prerequisite for the generation of aneuploidy, and are often observed in cells with defective cohesion (e.g. Ritchie *et al.* 2008). We observed a significant increase in the frequency of micronuclei present in asynchronous BAF180 -/- mESCs compared to wild-type cells (Fig. 4.10B, upper panel; *P*=0.03, Fisher's exact test). A similar increase was also observed in 1BR-hTERT cells depleted of BAF180 using siRNA (Fig. 4.10B, middle panel; *P*=0.015, Fisher's exact test) and U2OS cells stably depleted of BAF180 using shRNA (Fig. 4.10B, bottom panel; *P*=0.034, Fisher's exact test). In addition, analysing anaphase cells from BAF180 -/- and wild-type mESCs revealed a significantly higher frequency of abnormal anaphase events in the BAF180 -/- cells (Fig. 4.10C and D; *P*=0.006, Fisher's exact test). These were most commonly lagging chromosomes, which are thought to arise through merotelic kinetochore-microtubule attachments, whilst anaphase bridges were less common. Collectively these data suggest that loss of BAF180 leads to an increased rate of chromosome missegregation and aneuploidy.

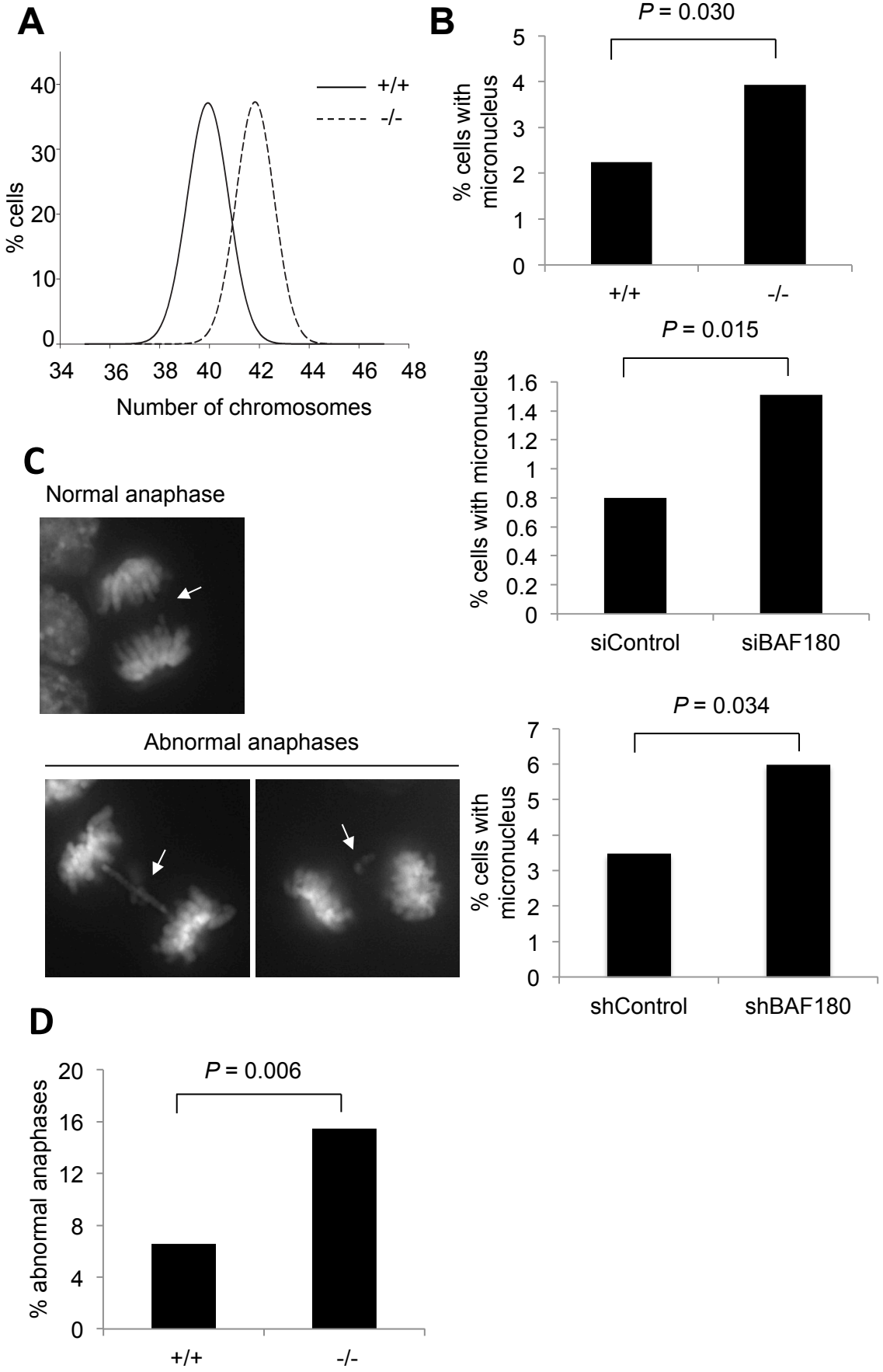
A
40
30
20
10
0
% cells
+/+
-/-
34
36
38
40
42
44
46
48
Number of chromosomes
B
P = 0.030
% cells with micronucleus
5
4
3
2
1
0
+/+
-/-
P = 0.015
% cells with micronucleus
1.6
1.4
1.2
1
0.8
0.6
0.4
0.2
0
siControl
siBAF180
P = 0.034
% cells with micronucleus
7
6
5
4
3
2
1
0
shControl
shBAF180
C
Normal anaphase
Abnormal anaphases
D
P = 0.006
% abnormal anaphases
20
16
12
8
4
0
+/+
-/-

Figure 4.10. Loss of BAF180 results in aneuploidy, increased frequencies of micronuclei and abnormal anaphase events. (A) Chromosome counts from WT (+/+) and BAF180 knockout (-/-) MES cell metaphase spreads plotted as distribution curves. Chromosomes from 100 cells were counted for each genotype. (B) Representative image of a MES cell with a micronucleus (arrowed). (C) Quantification of micronuclei present in wt (+/+) and BAF180 knockout (-/-) MES cells. A minimum of 900 cells from two independent experiments were counted. (D) Quantification of micronuclei present in siControl- and siBAF180-treated 1BR hTERT cells. A minimum of 2600 cells from three independent experiments were counted.

Loss of BAF180 leads to hypersensitivity to DNA damage, increased frequency of chromosome aberrations and dynamic CIN

In addition to a role in preventing chromosome missegregation, cohesion is important for facilitating repair of DNA damage by homologous recombination. Intriguingly, a recent study showed that the enrichment of cohesin surrounding DSBs is specifically regulated by SA2-containing cohesin complexes (Kong *et al.* 2014). Other studies also suggest that components of the centromeric cohesion pathway, including PDS5B, specifically facilitate DNA repair by HR (Brough *et al.* 2012, Carretero *et al.* 2013). To determine if BAF180 is required for DNA repair we performed viability assays with BAF180 -/- and wild-type mESCs using the DNA interstrand crosslinking agent mitomycin C. This drug causes replication fork collapse and generates DSBs in S-phase that are repaired by HR in a cohesin-dependent manner, and cells with defective cohesion are rendered hypersensitive to this drug. The BAF180 -/- cells were substantially more sensitive to MMC than the wild-type cells (Fig. 4.11A), suggesting that BAF180 is required for DNA repair by HR.

It has been reported that aneuploidy can sensitise cells to genotoxic agents, at least in yeast (Sheltzer *et al.* 2011). Because the BAF180 -/- cell line is aneuploid one possibility is that the MMC hypersensitivity we observe is a consequence of aneuploidy. To test this, we depleted BAF180 using siRNA in 1BR-hTERT cells and performed viability assays with MMC. Importantly, we do not see obvious changes in ploidy in this cell line within the timescale of this experiment following BAF180 depletion (data not shown). We find that BAF180-depleted 1BR-hTERT cells were also more sensitive to MMC than the corresponding control cells (Fig. 4.11B), indicating that BAF180 loss, and not aneuploidy, is indeed the cause of MMC sensitivity. We also performed the same viability assay with MMC in the stable shBAF180 U2OS cells. As mentioned previously, p21 levels in these cells are elevated rather than reduced in the absence of BAF180. Because p21 has diverse roles in many cell processes, including DNA repair (Kreis *et al.* 2013), this cell line provides us with an opportunity to measure the effects of BAF180-dependent DNA repair when p21 is not downregulated. We found that the shControl U2OS cells were considerably more resistant to MMC than wild-type mESCs and siControl 1BR-hTERT cells (Fig. 4.11C). Nevertheless, we detected reduced viability at lower doses of MMC in the shBAF180 cells compared to the shControl cells (Fig. 4.11C). Altogether, we find that mESCs, 1BR-hTERT and U2OS cells are more sensitive to MMC in the absence of BAF180, suggesting a conserved role for BAF180 in HR-dependent DNA repair in mammalian cells.

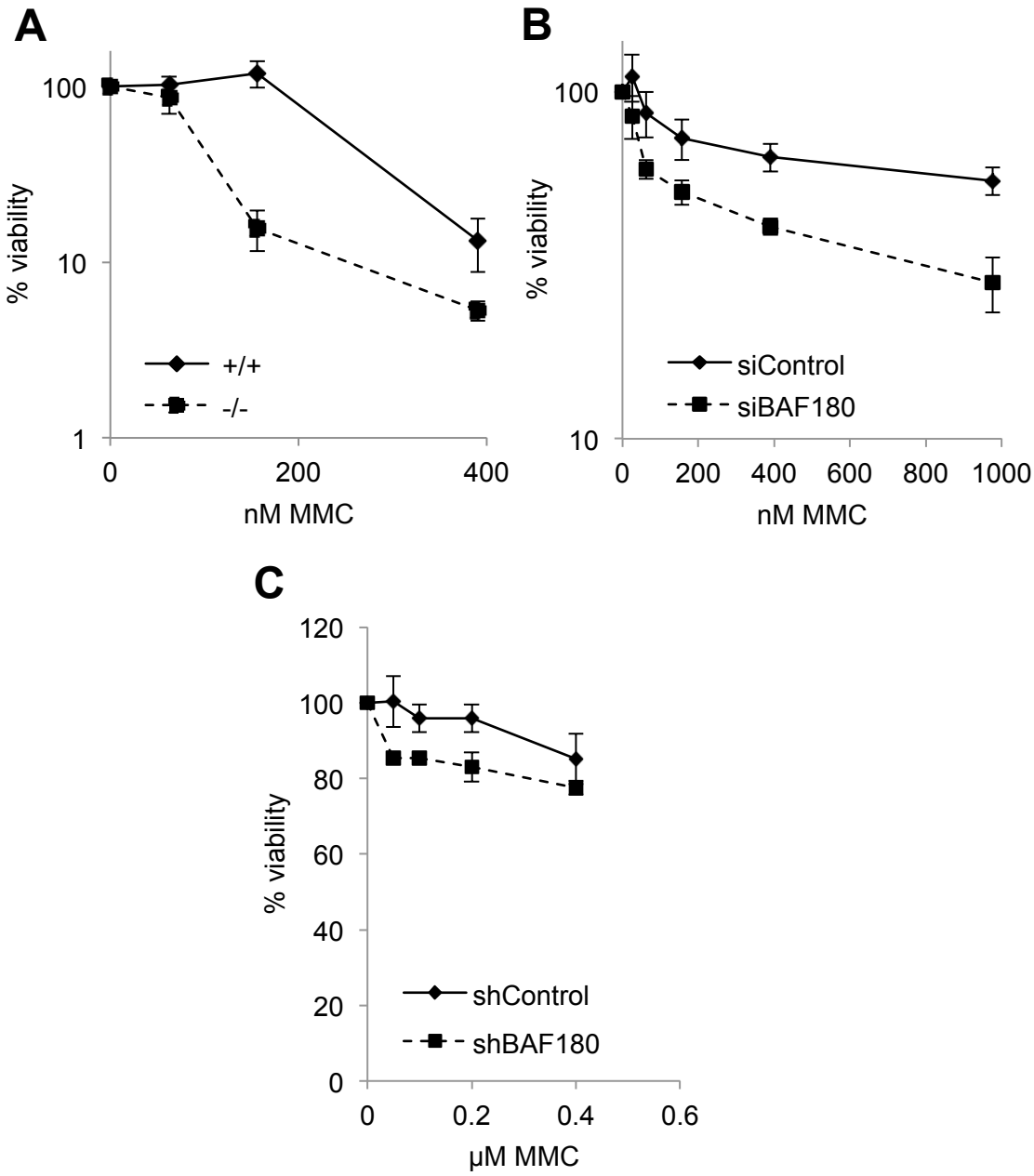

Figure 4.11. Loss of BAF180 leads to hypersensitivity to MMC (A) Viability curves of WT (+/+) or BAF180 knockout (-/-) mESCs (B) control and BAF180-depleted 1BR-hTERT cells and (C) control and BAF180-depleted U2OS cells following exposure to mitomycin C.

Failure to repair DNA double-strand breaks induced by MMC can result in chromosomal instability (CIN) in the form of structural chromosome aberrations, which are a hallmark of cancer cells and thought to contribute to tumourigenesis. Analysis of BAF180 -/- and wild-type mESC metaphase spreads treated with MMC revealed significantly increased frequencies of chromatid and chromosomal unrepaired breaks, as well as chromosomal fusions, in the BAF180 -/- cells (Fig. 4.12A and B and Table 4.1). Interestingly, the most significant difference in aberration frequency between wild-type and BAF180 -/- cells was observed for chromosomal breaks, which predominantly appeared to occur adjacent to or at the centromeres. We did not observe a significant increase in the frequency of radial chromosome structures in the BAF180 -/- cells; however the frequency of these was very low in both genotypes (Fig. 4.12B). We also analysed the prevalence of structural chromosome aberrations in the stable shBAF180 and shControl U2OS cells treated with MMC. Although we did not find significantly increased frequencies of fusion and radial chromosomes in the BAF180-depleted cells we did observe a significant increase in breaks (chromatid and chromosome) (Fig. 4.12C and D). These data suggest that BAF180 is important for the repair of MMC-induced DSBs to prevent the formation of structural chromosome aberrations in both mouse and human cells.

Micronuclei can arise from the missegregation of whole chromosomes or from chromosome fragments. Also, chromosomes harbouring structural aberrations such as fusions and radials in metaphase might be more likely to missegregate than normal chromosomes during anaphase. Consistently, we found a highly significant increase in the frequency of micronuclei in BAF180 -/- cells compared to wild-type after MMC exposure (Fig. 4.13A; $P<0.001$, Fisher's exact test). A significant increase in micronuclei frequency was also observed in shBAF180 U2OS cells compared to shControl cells (Fig. 4.13B; $P=0.005$, Fisher's exact test).

Whilst there was a negligible effect on chromosome number in the wild-type cells (Fig. 4.13B), MMC exposure in the BAF180-/- cells caused in striking effect on aneuploidy manifest as chromosome loss (Fig. 4.13C), providing evidence of dynamic CIN in these cells. The loss of chromosomes in BAF180-/- cells after DNA damage mirrors the increased frequency of micronuclei and might be due to failed segregation of damaged or structurally abnormal chromosomes during anaphase. In conclusion, loss of BAF180 leads to rapid and dynamic chromosomal instability (CIN) after treatment with MMC and this might be related to its role in promoting sister chromatid cohesion.

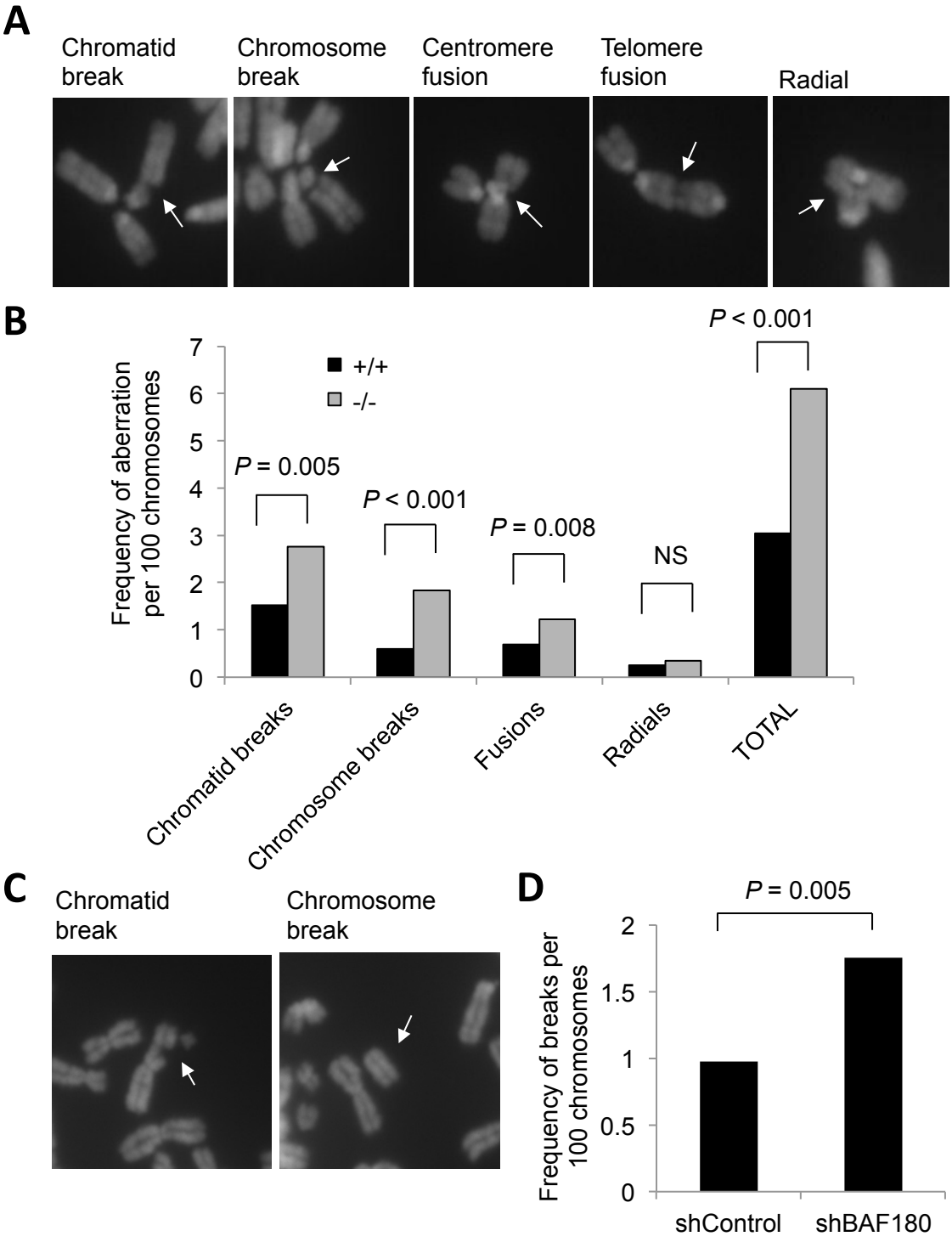

Figure 4.12. BAF180-deficient mESC and U2OS cells show increased frequencies of structural chromosomal aberrations after treatment with MMC (A) Representative images of each category of aberration. B) The presence of structural chromosome aberrations in metaphase spreads prepared from WT (+/+) or BAF180 knockout (-/-) mESCs following exposure to MMC was analysed and presented as frequency of aberrations per 100 chromosomes. (C) Representative images of chromatid and chromosome breaks (acentric fragments) from U2OS cells treated with MMC. (D) Analysis of the total number of breaks (chromatid and chromosome) in control or BAF180-depleted U2OS cells treated with MMC

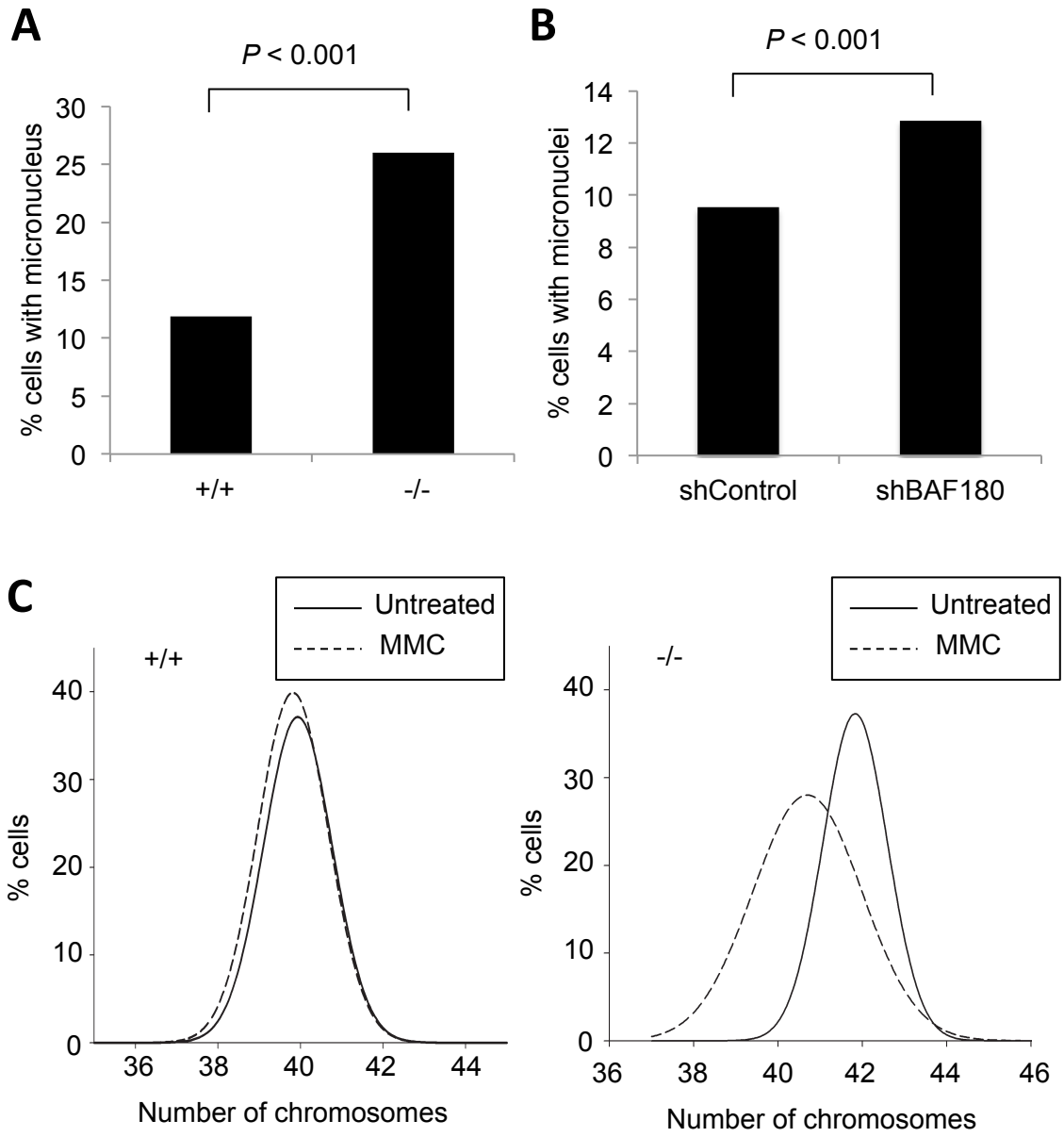

Figure 4.13. BAF180-deficient mESCs show increased frequencies of micronuclei and dynamic chromosomal instability following treatment with MMC. (A) Quantification of micronuclei present in WT (+/+) and BAF180 knockout (-/-) mESCs after treatment with MMC. (B) Quantification of micronuclei present in shControl and shBAF180 U2OS cells after exposure to MMC. (C) Distribution curves showing chromosome numbers from WT (+/+) (left panel) and BAF180 knockout (-/-) (right panel) mESCs following exposure to MMC.

Table 4.1. Average number and range per cell of chromosomal aberrations in mESCs following MMC exposure

Category	+/+	-/-
Chromatid breaks	0.5 (0-3)	2.2 (0-14)
Chromosome breaks	0.3 (0-4)	0.8 (0-10)
Triradial	0.1 (0-2)	0.1 (0-1)
Quadriradial	0 (0-0)	0.02 (0-1)
Fusion	0.3 (0-2)	0.5 (0-8)
Total	2.2 (0-6)	4.6 (0-32)

4.2. Discussion

In this section we identified a novel role of BAF180 in promoting centromeric sister chromatid cohesion. This defect was apparent in BAF180 knockout mouse embryonic stem cells (mESCs), immortilized human fibroblasts depleted of BAF180 using siRNA, and an osteosarcoma cell line stably depleted of BAF180 using shRNA or shRNA. Thus, this function of BAF180 appears to be highly conserved in mammals. Importantly, we showed that the centromeric cohesion defect is not due to transcriptional misregulation of cohesin genes in these cells, and is independent of p21 status.

Disrupted centromeric cohesion is known to compromise mitotic fidelity, and consistent with this we found that BAF180-depleted cells showed significant increases in micronuclei and abnormal mitotic events. Moreover, we found that BAF180 knockout mESCs were aneuploid, which has important implications for its role as a tumour suppressor gene. We also explored the consequences of impaired cohesion in DNA repair. Cells lacking BAF180 were hypersensitive to DNA damage, displayed increased frequencies of structural chromosome aberrations in metaphase, and showed evidence of dynamic chromosomal instability when treated with DNA damaging agents. These phenotypes are all readily explained by a defect in cohesion, which is likely to represent an important tumour suppressor function of BAF180.

Impaired centromeric cohesion in mammalian cells depleted of BAF180

We first analysed cohesion in chromosome spreads from BAF180 knockout mESCs. Although statistically significant differences in the number of cells showing defective centromeric cohesion in the BAF180 -/- cell line were observed, the defect did not appear perhaps as striking as that reported in cells lacking other centromere-specific

cohesion components. In ~65% of Pds5B -/- MEF metaphase cells >5 chromosomes displayed a sister chromatid cohesion defect (Carretero *et al.* 2013). Although not directly comparable because of different scoring criteria, in ~40% of BAF180 -/- mESCs 3 or more chromosomes displayed a sister chromatid cohesion defect in our assay. Thus, the defect appears less severe in the BAF180 -/- cells. Similarly, in 20% of Esco2 -/- two-cell embryo metaphase cells all of the chromosomes exhibited a marked centromeric cohesion defect (Whelan *et al.* 2012). This describes a more severe defect than that observed in BAF180 -/- mESCs. In addition, the Esco2 -/- anaphase cells apparently all showed >5 lagging chromosomes, which is a far greater frequency than we saw in the BAF180 -/- mESCs.

A relatively mild centromeric cohesion defect might actually be fundamental to explaining why BAF180 is such a potent tumour suppressor gene in human cancer. Complete loss of centromeric cohesion defect would have catastrophic consequences for the cells because of overwhelming problems with chromosome segregation. This would in turn severely inhibit the ability of these cells to proliferate. In contrast, a more modest defect is likely to maintain the proliferative capacity of the cells but undermine mitotic fidelity, leading to low levels of aneuploidy that might ultimately lead to a growth advantage (Figure 4.14). Indeed, this has been proposed to be the case with Rb, which has a relatively mild centromeric cohesion defect that is accompanied with lower levels of chromosome missegregation (Manning *et al.* 2010).

The idea that the severity of the cohesion defect might correlate with proliferation appears to be true when comparing proliferation in BAF180-depleted cells with cells lacking Pds5B and Esco2. shRNA-mediated depletion of BAF180 in primary BJ fibroblasts leads to increased proliferation (Burrows *et al.* 2010), and re-expression of BAF180 in a breast cancer cell line harbouring a truncating BAF180 mutation significantly suppressed colony formation (Xia *et al.* 2008). In addition, siRNA-mediated depletion of BAF180 in 4/5 RCC cell lines resulted in significantly increased proliferation, colony formation and cell migration. Therefore, BAF180 depletion appears to actually increase proliferation, at least in human cancer cells. In contrast, Pds5B -/- MEFs showed reduced proliferation compared to wild-type MEFs (Carretero *et al.* 2013), and only 5% of Esco2 -/- homozygous embryos reached the 8-cell stage of development (Whelan *et al.* 2012). This most likely results from the massive chromosome missegregation problems observed in these cells.

There are no reports describing a cohesion defect in Stag2-depleted mouse cells, so we were not able to compare this with our BAF180 -/- mESC cohesion defect. However, we were able to compare the SA2-dependent cohesion defect with that of BAF180 in human cells. We found that the SA2-depleted cells showed a comparable,

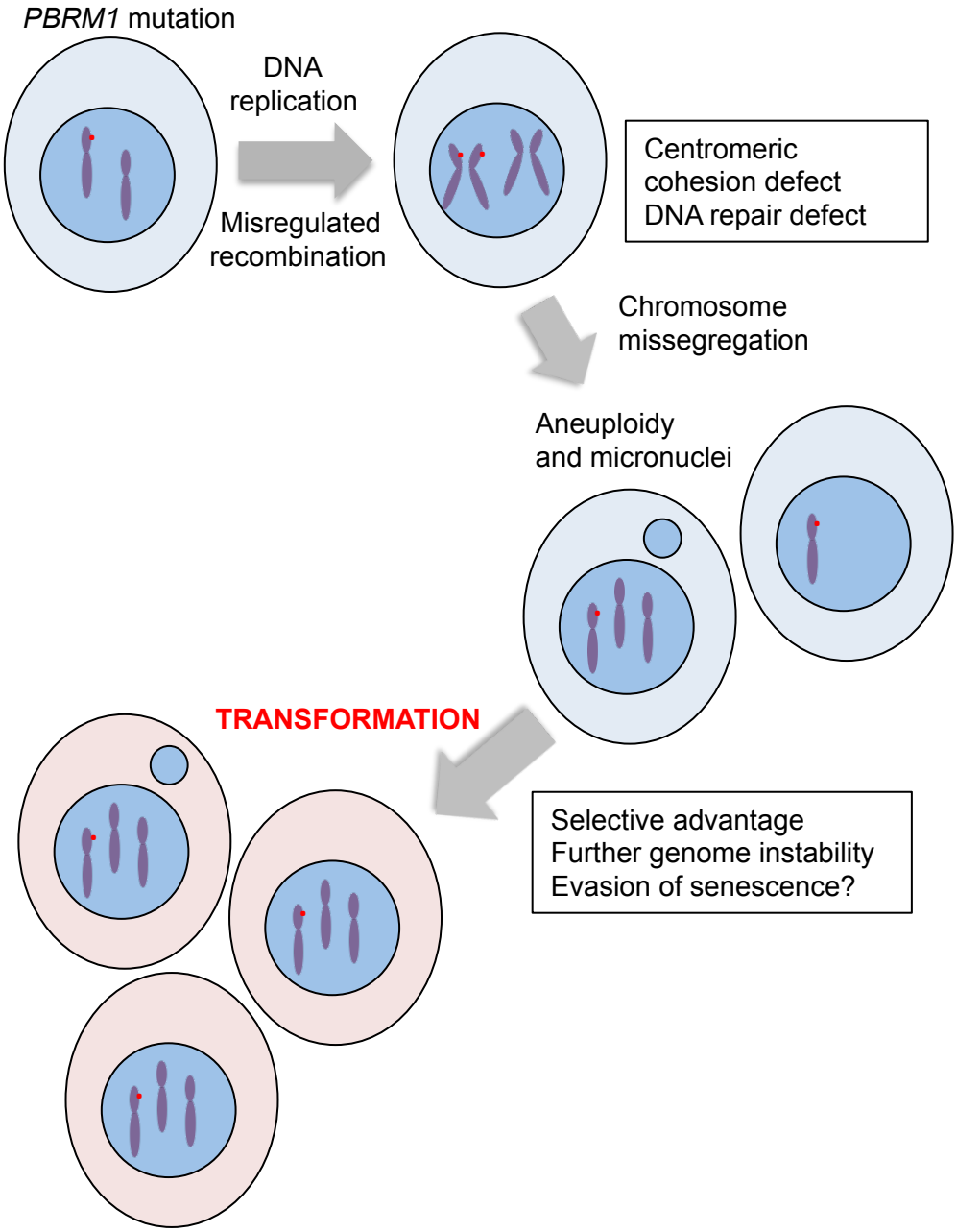

Figure 4.14. Model describing the consequences of BAF180 inactivation and the drive towards tumourigenesis. An early event following mutational inactivation of BAF180 might be chromosome 3p LOH, resulting from misregulation of cohesin-dependent recombination. During DNA replication, the absence of BAF180 leads to a defect in establishing centromeric cohesion. The inability to efficiently repair DNA DSBs arising during replication might contribute to further structural chromosome rearrangements. Chromosome segregation errors occurring during anaphase due to impaired centromeric cohesion generates low levels of aneuploidy and micronuclei. Micronuclei could contribute to further genome instability by re-integrating damaged DNA into the genome. The simultaneous inactivation of tumour suppressor pathways regulating senescence and proliferation, such as p21, might increase the tolerance of aneuploidy in these cells. Ultimately, such cells acquire a selective advantage and undergo transformation.

but slightly more severe defect than the BAF180-depleted cells. Therefore, loss of SA2 might not result in a severe cohesion defect as might be predicted from its physical interaction with the core cohesin ring. However, the molecular function of SA2 is unclear in human cells, and its yeast homologue (Scc3) actually appears to promote anti-establishment. A mild cohesion defect in SA2-depleted cells is also consistent with the findings that SA2 is very frequently mutated in cancer. As described, a mild defect would maintain the proliferative capacity of the cells but compromise mitotic fidelity, leading to low levels of aneuploidy. In contrast, a severe defect is unlikely to be advantageous because it would compromise proliferation from excessive chromosome missegregation. This might also explain why mutational inactivation of the core cohesin subunits, which would probably result in a severe cohesion defect, is observed at a much lower frequency in human cancers (e.g. Kon *et al*. 2013).

Possible mechanisms for BAF180-dependent centromere cohesion

We found that BAF180 -/- mESCs and 1BR-hTERT fibroblasts depleted of BAF180 showed a cohesion defect that was only apparent at the centromere. This is consistent with findings that in mammalian cells centromeric and arm/telomere cohesion are regulated by different versions of proteins in different pathways. Thus, BAF180 might cooperate with components of the centromere-specific cohesion pathway, including SA2, PDS5B and ESCO2. A centromere-specific role for BAF180 is also consistent with previous finding that BAF180 localizes to kinetochores of mitotic chromosomes (Xue *et al.* 2000), and that Brg1 is required for maintaining the structure of pericentromeic heterochromatin (Bourgo *et al.* 2009).

How might BAF180 function mechanistically in promoting centromeric sister chromatid cohesion? One possibility is that BAF180 regulates the recruitment of PBAF to pericentromeric heterochromatin. This seems likely because of the multiple bromodomains present in BAF180, which might bind to acetylated lysines on histones. In addition, the second BAH domain of BAF180 is known to bind to unmodified H3 (Chambers *et al.* 2013). In this scenario, BAF180 would recognise a specific set of histone modifications that would dictate its preferential binding to pericentromeric heterochromatin. The heterochromatin-associated H3K9me3 and H4K20me3 modifications are unlikely to contribute to this binding because in their absence Brg1-dependent heterochromatin structure is normal (Bourgo *et al.* 2009). Once recruited, chromatin remodelling facilitated by BRG1 would create a chromatin environment that favours cohesin loading or establishment.

Alternatively, the bromodomains of BAF180 might bind to other non-histone acetyl-lysine residues. Possible candidates include lysines K105 and K106 in SMC3, perhaps acetylated specifically by ESCO2. In this scenario, a certain BAF180 bromodomain or pair of bromodomains would bind to these acetylated residues. The remaining bromodomains might simultaneously bind to acetylated lysines present on histones. Thus, BAF180 would serve to bridge chromatin and cohesin together. Rigorous testing to identify the true binding targets of the BAF180 bromodomains is crucial for understanding how the protein might function mechanistically.

BAF180 does not exert its effect on cohesion through transcriptional regulation

It is currently thought that SWI/SNF subunits exert their tumour suppressor activity by regulating the transcription of tumour suppressor genes. In this study we made the novel and important finding that BAF180 has a direct structural role in promoting cohesion independently of transcriptional regulation. Whole-cell levels of the core cohesin subunits and the regulatory SA proteins were not grossly reduced in the mESCs lacking BAF180. Similarly, there were no significant reductions in the mRNA levels of these subunits in BAF180-depleted 1BR-hTERT cells and U2OS cells. In fact, we observed increased *SMC3, SA1* and *RAD21* mRNA levels in the U2OS cells stably depleted of BAF180. This was particularly striking for *RAD21*, which displayed a 3-fold increase in transcript levels compared to control cells. Interestingly, a recent report showed that RAD21 is particularly sensitive to depletion of other cohesin subunits in human cells (Kong *et al.* 2014). This adds support to our findings that BAF180 is an important protein involved in cohesion, and suggests that BAF180 functions closely with other cohesin subunits. The transcriptional upregulation of cohesin subunits in BAF180-depleted cells might represent a compensatory mechanism in response to impaired cohesion.

Evidence for tissue-specific roles of BAF180 in controlling p21 transcription

We found that the U2OS cells stably depleted of BAF180 displayed a clear defect in centromeric cohesion that was independent of p21 mitotic activity. Depletion of BAF180 in these cells led to increased rather than decreased basal and induced p21 expression. This is in contrast to our data from BAF180-depelted 1BR-hTERT cells, and previous studies using primary BJ fibroblasts and breast cancer cells, in which BAF180 depletion results in reduced p21 expression (Xia *et al.* 2008, Burrows *et al.* 2010). Interestingly, microarray data from the report by Varela *et al.* did not identify p21

as being significantly misregulated following BAF180 depletion in 3 BAF180-positive renal cell carcinomas (Varela *et al.* 2011). In fact, the gene encoding p21, *CDKN1A,* did not even appear in the top 250 misregulated genes. This further supports the idea of tissue-dependent regulation of p21 transcription by BAF180. Whilst this might be a phenomenon specific to transformed cells, it would be interesting to more comprehensively analyse p21 transcription in other cell types. It would be especially interesting to determine the effect of BAF180 depletion on p21 transcription in non-transformed renal cells. Exome sequencing has shown that this cell type appears to be particularly prone to transformation following BAF180 mutational inactivation. This might shed light on the actual importance of BAF180-dependent p21 transcription in tumourigenesis. Intriguingly, p21 -/- null mice do not show increased aneuploidy or chromatid breaks compared to wild-type cells, but p21 -/- ATM -/- mice exhibit more aneuploidy and chromatid breakage than ATM -/- cells (Shen *et al.* 2005). This suggests that p21 is able to enhance aneuploidy in a genome instability background, and that the aneuploidy we observe in BAF180 -/- cells cannot be due to defective p21 activity alone. We propose that the defect in cohesion provides the genome instability necessary to drive aneuploidy, perhaps in cooperation with impaired p21 activity in the BAF180 -/- cells (Figure 4.14).

Loss of BAF180 impairs mitotic fidelity and leads to aneuploidy and micronuclei

Compromised centromeric cohesion impairs mitotic fidelity, most likely by increasing the chance of merotelic microtubule-kinetochore attachment (Compton *et al.* 2011). The most frequent consequence of merotelic attachment in anaphase is a lagging chromosome. Other abnormal anaphase events such as anaphase bridges have also been reported in cells lacking centromeric cohesin components (e.g. Solomon *et al.* 2011). We observed a modest but statistically significant increase in the frequency of abnormal mitotic events in BAF180 -/- mESCs compared to wild-type cells. This is consistent with a centromeric cohesion defect and the associated increase in chromosome missegregation. In addition, a modest but significant increase in the frequency of spontaneously arising micronuclei was observed in BAF180 -/- mESCs, 1BR-hTERTs depleted of BAF180 using siRNA, and U2OS cells stably depleted of BAF180 using shRNA. Micronuclei are thought to arise from missegregation of whole chromosomes or chromosomal fragments. Recently, chromosomal DNA contained in micronuclei from lagging chromosomes was found to replicative defectively, generating DNA damage, extensive chromosome fragmentation and rearrangements (Crasta *et al.* 2012). Importantly, the damaged chromosomal material inside the micronucleus was

able to re-integrate into the genome. Therefore, the increased micronuclei observed in BAF180-deficient cells could contribute to further genome instability (Figure 4.14).

Strikingly, we found that the BAF180 -/- mESCs were aneuploid, with a modal gain of two chromosomes compared to wild-type cells. Because we did not generate the BAF180 -/- mESCs, we do not know exactly how and over what timescale this aneuploidy developed. However, because the population of cells as a whole had this aneuploidy it suggests that it occurred early and conferred a selective advantage. We also do not know whether all of the BAF180 -/- aneuploid cells have gained the same two chromosomes. Nevertheless, the gain of a small number of chromosomes is very similar to the pattern of aneuploidy observed following SA2 depletion in several cell types. Knockout of SA2 in a colorectal cell line resulted in a modal gain of 1 chromosome (Solomon *et al.* 2011), and shRNA-mediated depletion of SA2 in an urothelial carcinoma cell line similarly led to a modal gain of 1 chromosome (Solomon *et al.* 2013).

The pattern of aneuploidy in BAF180 -/- mESCs is reminiscent of the hyperdiploid karyotype found in a subset of ccRCCs

Concurrent loss of *PBRM1, VHL* and *SETD2* appears to be the major driving mechanism for clear cell renal cell carcinoma (ccRCC) development (Varela *et al.* 2011). Loss of *VHL* leads to HIF accumulation and activation of hypoxia-inducible target genes under normal conditions. *SETD2* is a methyltransferase that specifically methylates H3K36, which is associated with active transcription. All three of these genes reside on chromosome 3p21, and multiple ccRCCs harbour mutations in all three genes, indicating that they provide non-redundant functions. The physical linkage and likely interaction of these genes is thought to be the key driver for the very frequent 3p LOH observed in ccRCCs (Varela *et al.* 2011). Indeed, loss of chromosome 3 or 3p is observed in 80-98% of sporadic ccRCCs (Kovacs 1993, Gunawan *et al.* 2001, H öglund *et al.* 2004).

Subsequent ccRCC progression occurs via at least two distinct genetic pathways that are characterized by a specific pattern of aneuploidy (Höglund *et al.* 2004). The first pathway (80% of ccRCCs) involves losses of whole chromosomes and partial chromosomes through unbalanced translocations to result in a hypodiploid karyotype. Chromosome 3p is often lost in an unbalanced translocation between chromosomes 3 and 5 in this pathway. Interestingly, we found that BAF180 -/- cells treated with MMC rapidly lose chromosomes in a manner reminiscent of this aneuploidy route. The second pathway (18% of ccRCCs) involves gains of whole

chromosomes (commonly chromosomes 7 (18-30%), 16 (11%), 20 (10%), 12 (10-15%), and 2 (9-14%)) to produce a hyperdiploid karyotype. This is very similar to the hyperdiploid karyotype of BAF180 -/- mESCs, which have a modal gain of two chromosomes. It would be very interesting to identify the actual chromosomes gained in these cells, and compare them with those frequently gained in this pathway of ccRCC development. It would also be of interest to see if these cells have 3p LOH. Altogether, our findings strongly suggest that loss of BAF180 alone is sufficient for the development of aneuploidy in mESCs. Furthermore, the patterns of aneuploidy observed in the BAF180 -/- mESCs is very similar to the two common patterns of aneuploidy in ccRCC, suggesting that BAF180 loss alone might be sufficient for causing aneuploidy in ccRCC.

Evidence for a role of BAF180 in cohesin-dependent DNA repair via HR

We found that the BAF180 -/- mESCs, 1BR-hTERT cells depleted of BAF180 using siRNA, and U2OS cells stably depleted of BAF180 using shRNA were hypersensitive to the DNA interstrand crosslinking agent MMC. The repair of an interstrand crosslink (ICL) is initiated when two replication forks converge on the lesion (Raschle *et al.* 2008). The leading strands extend to the crosslink before it is cleaved from one sister strand by dual incisions made by the structure specific endonucleases factors XPF and Mus81. This uncouples the sister strands and generates a DSB. TLS across the adducted lesion initiates extension of the nascent strand beyond the lesion. Ultimately, the adducted lesion is removed by NER and RAD51-depedent HR repair of the DSB (Raschle *et al.* 2008, Long *et al.* 2011).

Therefore, sensitivity to MMC could potentially reflect a role for BAF180 in any of these steps. There have been no reports describing a role for BAF180 or its budding yeast homologues in promoting endonuclease activity or TLS. In contrast, several studies have reported defects in HR-dependent DNA repair in the budding yeast BAF180 homologues Rsc1 and Rsc2 (Chai *et al.* 2005, Oum *et al.* 2012). In addition, the defective sister chromatid HR in *rsc2* cells at DSBs was due to impaired accumulation of DSB-induced cohesin at the DSB site (Oum *et al.* 2012). Although we did not directly explore the role of BAF180 in HR using a specific HR assay, we found that BAF180 is important for promoting cohesion. Therefore it seems most likely that the role of BAF180 in maintaining viability after MMC stems from a function in cohesin-dependent HR. In addition, very recent reports also suggest that members of the centromere-specific cohesion pathway, including PDS5B and SA2, are involved in promoting the enrichment of cohesin at DNA DSBs (Brough *et al.* 2012, Carretero *et al.*

2013, Kong *et al.* 2014). Thus, BAF180 might cooperate with these centromere-specific cohesion factors to facilitate cohesin-dependent HR.

Sensitivity to DNA damage can also result from impaired DNA damage checkpoint activity. We rigorously tested the ability of *rsc1* and *rsc2* null strains to enact G1 and G2/M DNA damage checkpoint activation in response to MMS in the previous chapter, and found that both strains were able to activate these checkpoints. Depletion of BRG1 did not lead to G2/M or intra-S checkpoint defects in response to IR or adriamycin (Park *et al.* 2006). Similarly, depletion of SNF5 did not cause checkpoint defects in response to UV (Ray *et al.* 2009) or IR (McKenna *et al.* 2008). Collectively, data from the BAF180 homologues in yeast and other subunits of the PBAF complex suggest that BAF180 is unlikely to function in checkpoint activation in response to various DNA lesions. However, BRG1 depletion did lead to a defect in the intra-S checkpoint specifically after treatment with cisplatin (Park *et al.* 2006). Therefore we cannot entirely rule out the possibility that BAF180 also has a role in intra-S checkpoint activity in response to certain types of lesion, and that this might underlie the MMC sensitivity seen in BAF180-depleted cells. Intriguingly, a currently held idea is that a major function of the intra-S checkpoint is to protect replication forks from inappropriate recombination (Labib & De Piccoli 2011). Because cohesin is important for preventing inappropriate recombination, a role for BAF180 in the intra-S checkpoint might actually stem from its role in cohesion.

We also found that mESCs lacking BAF180 showed statistically increased frequencies of structural chromosome chromosome aberrations after treatment with MMC. Treatment with MMC also led to significantly increased chromatid and chromosome breaks in BAF180-depleted U2OS cells, and a striking increase in micronuclei after MMC treatment in both cells types. Furthermore, BAF180 -/- mESCs rapidly exhibited further dynamic aneuploidy after MMC treatment. These phenotypes are consistent with the increased MMC sensitivity of these cells, and likely reflect a defect in cohesin-dependent DNA repair by HR. Moreover, a role for BAF180 in HR-dependent DNA repair is likely to represent a novel tumour suppressor function. Such a role could underlie the initiating LOH at 3p observed in *PBRM1*-mutated ccRCCs (Figure 4.14).

CHAPTER 5: MUTATIONS IDENTIFIED IN BAF180 FROM CANCER SAMPLES IMPAIR COHESIN-DEPENDENT FUNCTIONS IN YEAST AND MAMMALS

5.1. Results

Introduction

Whilst the vast majority of mutations found in BAF180 from various cancer types result in a truncated protein product, a number of in-frame deletions and missense mutations that might not result in complete loss of protein have been identified. Intriguingly, 9 out of 11 missense mutations in a cohort of renal cell carcinomas occurred in the bromodomains or BAH domains. Out of an additional 6 homozygous missense mutations subsequently identified from a range of different cancer types, 4 of these occurred in the bromodomains, and one occurred in the second BAH domain (Varela *et al.* 2011). Thus, these mutations might not only provide crucial insight into the roles of BAF180 in tumourigenesis but also the specific roles of these domains. In the previous chapter we identified and characterized a novel role of BAF180 in promoting centromeric sister chromatid cohesion, which likely represents an important tumour suppressor function. BAF180 has also been ascribed with several other tumour suppressor functions that relate to transcriptional regulation. However, the importance of this activity in tumourigenesis has not been demonstrated. In this section we analysed the effects of a set of conserved missense mutations identified in renal cell carcinomas, expressed in both yeast and human cells. By measuring the impact of these mutations on distinct transcription- and cohesion-related processes we might gain insight into the importance of each in tumour suppression.

Predicted consequences of cancer associated BAF180 missense mutations on BAF180 folding and stability

Of the 9 missense mutations identified in the cohort of renal cell carcinomas 3 were previously assessed for having a functional impact using a scoring system calibrated with protein domain alignments from Pfam (Varela *et al.* 2011). All three of these mutations (T232P in BD2, A597D in BD4 and H1204P in BAH2) were predicted to be deleterious, with a significantly lower mean score than a randomly generated set of *in silico* missense mutations occurring in scorable parts of the gene (Varela *et al.* 2011).

We extended this analysis to predict the effects of all the bromodomain and BAH domain missense mutations on the stability of full-length BAF180 using a combination of techniques. These included manual inspection of structures, amino acid sequence threading (Kelley & Sternberg 2009), and use of the publicly available webserver 'Site Directed Mutator' (Worth *et al.* 2011). Of the 10 missense mutations occurring in the bromodomains, 7 were predicted to be slightly destabilizing or highly destabilizing, consistent with a functionally inactivating impact on BAF180 (Brownlee *et al.* 2012). Potentially more interesting are the 3 bromodomain mutations that were predicted to be neutral in terms of BAF180 folding and stability. These included M523I and R540S in BD4, and F840L in BD6. Intriguingly, the R540S mutation is located in the acetyl-lysine-binding ZA loop of the bromodomain. Thus, mutation of this residue might affect the acetyl-lysine binding affinity or substrate specificity of this bromodomain (Brownlee *et al.* 2012).

Cancer associated mutations of BAF180 are conserved in the yeast homologues

For further analysis we focused on 3 of these BAF180 missense cancer mutations that had different predicted effects on the stability of full length BAF180, and were conserved in the homologous *S. cerevisiae* RSC proteins (Table 5.1). The first mutation, T232P, occurs in the αA helix of BAF180 BD2 and is equivalent to T67P in BD1 of Rsc2 (Fig. 5.1A and B). This mutation was predicted to be slightly destabilizing in the context of full-length BAF180 (Table 5.1). The second mutation, M523I (M538I in BAF180 isoform 8; used herein), occurs in the αZ helix of BAF180 BD4 and corresponds to M280I in BD2 of Rsc2 (Fig. 5.1A and B). This mutation was predicted to be neutral in terms of BAF180 stability (Table 5.1). The third mutation, H1204P, resides in BAH2 of BAF180 and corresponds to H458P in the BAH domain of Rsc2 (Fig 5.1A and C). This mutation was predicted to have a destabilizing effect when expressed in BAF180 (Table 5.1).

Table 5.1. Analysis of cancer-associated in-frame missense mutations found in *PBRM1*

COSMIC	Mutation	Secondary structure element	BAF180 domain	Predicted effect of mutation*	Rsc2 residue	Rsc2 domain	Comments
52807	T232P	αA	BD2	Slightly destabilizing[1]	T67P	BD1	Mutation is likely to disrupt αA helix and protein fold
52844	M538I	αZ	BD4	Neutral[2]	M280I	BD2	Mutation places a hydrophobic residue into solvent, likely to be tolerated in terms of protein stability
52780	H1204P		BAH2	Highly destabilizing[2]	H458P	BAH	Mutation occurs in hydrophobic core of BAH domain, likely to affect/disrupt protein fold

*SDM analysis

[1]PDB code 3LJW (Charlop-Powers *et al.* 2011)

[2]Phyre model

Two of these mutations (T232P and H1204P) were also conserved in Rsc1 (Figure 5.1B and C). However, Rsc2 has a greater effect on DNA damage responses and cohesion (Chambers *et al.* 2013, Baetz *et al.* 2004, see also Chapter 3), so we created the equivalent mutations solely in the conserved residues of Rsc2 using site-directed mutagenesis. We first analysed the effect of these mutations on Rsc2 protein stability. Wild-type and mutant Rsc2 myc-tagged expression constructs were transformed into *rsc2* null yeast and Western blotting was performed on whole-cell extracts. The Rsc2-T67P mutation slightly reduces protein levels, consistent with a slightly destabilizing effect as predicted by the SDM analysis (Figure. 5.1D). Interestingly, expression of the Rsc2-M280I mutation appears to result in slightly higher levels of Rsc2 compared to wild-type, suggesting that it might be a stabilizing mutation (Figure. 5.1D). Levels of Rsc2 expression were severely reduced when the Rsc2-H458P mutation was expressed, consistent with a highly destabilizing effect (Figure. 5.1D).

BAF180 missense cancer mutations expressed in yeast do not compromise a transcription-related subset of Rsc2 functions

Cells lacking *RSC2* are hypersensitive to a number of agents that cause DNA damage, replication stress, and microtubule destabilization, reflecting the widespread roles of the protein in DNA repair, replication and mitotic spindle function. *rsc2* null cells are also temperature sensitive and hypersensitive to DMSO, which likely reflects transcriptional misregulation of cell wall biosynthesis genes (Angus-Hill *et al.* 2001). To determine whether BAF180 cancer mutations impair the ability of Rsc2 to regulate transcriptional activity we performed spot tests with DMSO. The Rsc2-H458P mutation severely sensitizes cells to both agents to levels comparable to the *rsc2* null, consistent

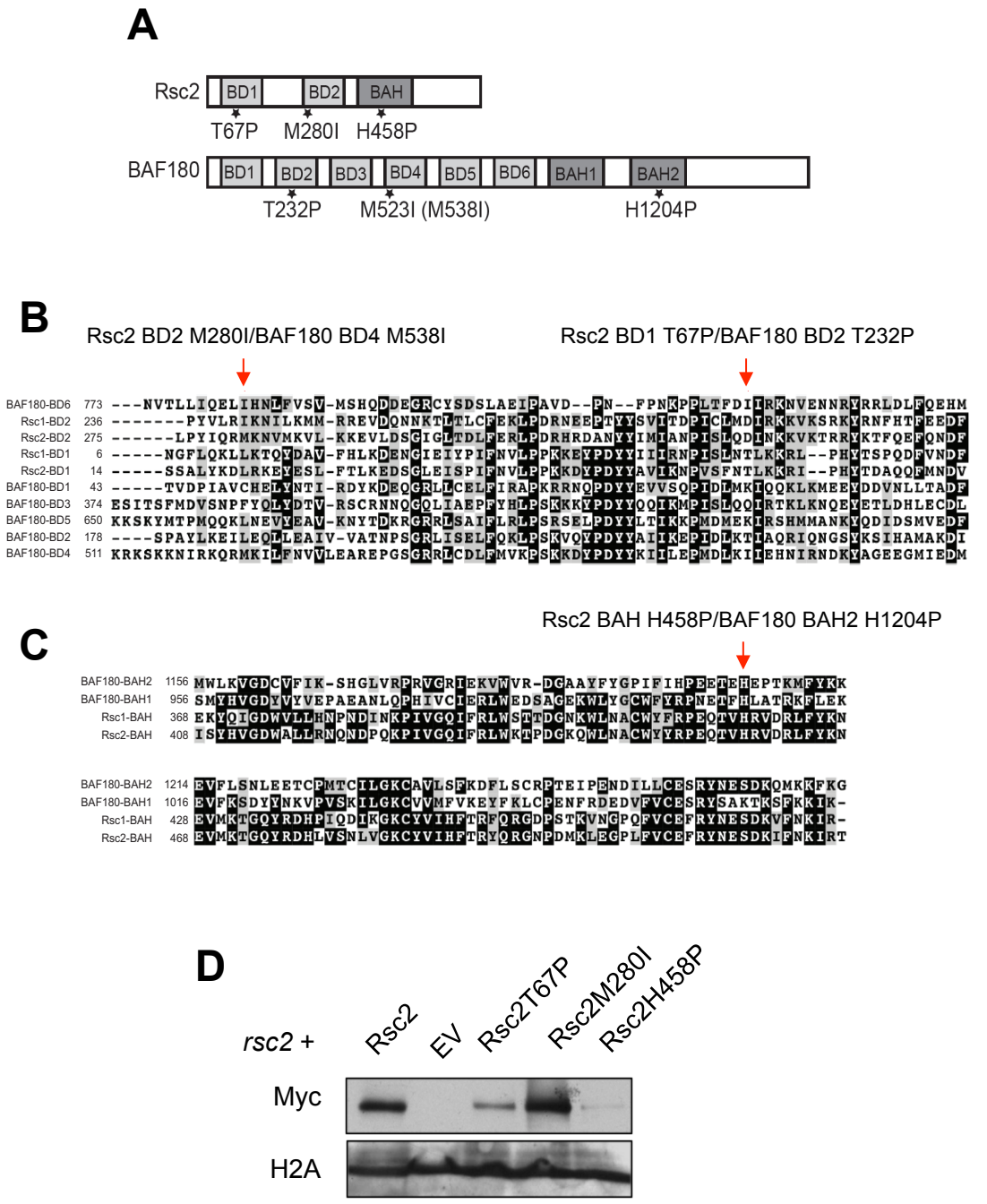

Figure 5.1. Conservation and expression of BAF180 renal cell carcinoma missense mutations in yeast Rsc2. (A) Illustration of domain organization and relative position of cancer-associated mutations in Rsc2 and BAF180. BDs and BAH domains are numbers sequentially. (B) Pileup of all six bromodomains of BAF180 with the bromodomains of Rsc1 and Rsc2. The cancer associated mutations of BAF180 are indicated (M523 corresponds to M538 of BAF180 isoform 8, used in our assays). (C) Pileup of the two BAH domains of BAF180 with the BAH domains from Rsc1 and Rsc2. The cancer associated H1204P mutation is indicated. (D) Analysis of WT and mutant Rsc2 expression levels in total protein preparations by Western blotting. Loading control: H2A

with greatly reduced protein levels (Figure. 5.2A). Neither the Rsc2-T67P nor the Rsc2-M280I mutations had any obvious sensitizing effect on DMSO, suggesting that these mutations are at least partly functional *in vivo* (Figure. 5.2A). To quantify these observations, we next performed survival assays with DMSO. We found that expression of the Rsc2-T67P and Rsc2-M280I mutations did not cause a significant decrease in survival on DMSO, whilst the Rsc2-H458P significantly reduced survival (Figure. 5.2B).

We also quantified the levels of survival of the mutant Rsc2 plasmids at the non-permissive temperature of 37°C, which may reflect Rsc2-dependent transcriptional activity, and found that neither the Rsc2-T67P or Rsc2-M280I mutations led to reduced survival (Figure 5.2C). In contrast, the Rsc2-H458P mutation actually led to a more severe growth defect at 37°C compared to the *rsc2* strain carrying an empty vector. This suggests that this mutation might have a dominant-negative effect in this context. Rsc2 facilitates the transcriptional activation and repression of many genes, including genes involved in nitrogen and carbon metabolism (Du *et al.* 1998, Angus-Hill *et al.* 2001). Next, we assessed the ability of the cancer-associated mutations to repress the Rsc2-dependent transcription of the high-affinity glucose transporter gene *HXT7*. Using RT-qPCR we found that the *rsc2* strain carrying the wild-type Rsc2 plasmid significantly reduced *HXT7* transcript levels as expected (Figure 5.2D). Both the Rsc2-T67P and Rsc2-M280I mutant plasmids were also able to repress *HXT7* transcription to the same level as wild-type, whilst the H458P mutation showed levels comparable to the empty-vector cells (Figure 5.2D). Collectively, these results suggest that two of the cancer-associated mutations do not compromise a transcription-related subset of Rsc2 functions *in vivo.*

BAF180 missense cancer mutations expressed in yeast result in impaired cohesin-dependent Rsc2 functions

In contrast to the results obtained with DMSO, the Rsc2-T67P mutation reproducibly appeared to slightly sensitize cells to MMS, whilst the M280I reproducibly seemed to exhibit slight MMS resistance compared to wild-type (Figure. 5.3A). We found that these changes in survival in response to MMS were statistically significant when quantified using survival assays (Figure 5.3B). Although the MMS resistance in the Rsc2-M280I construct was unexpected, these results suggest that both the T67P and M280I cancer mutations affect the function of Rsc2 in the response to MMS-induced DNA damage. In the previous section we showed that cells lacking *RSC2* display elevated rates of marker loss by unequal sister chromatid exchange and direct-repeat

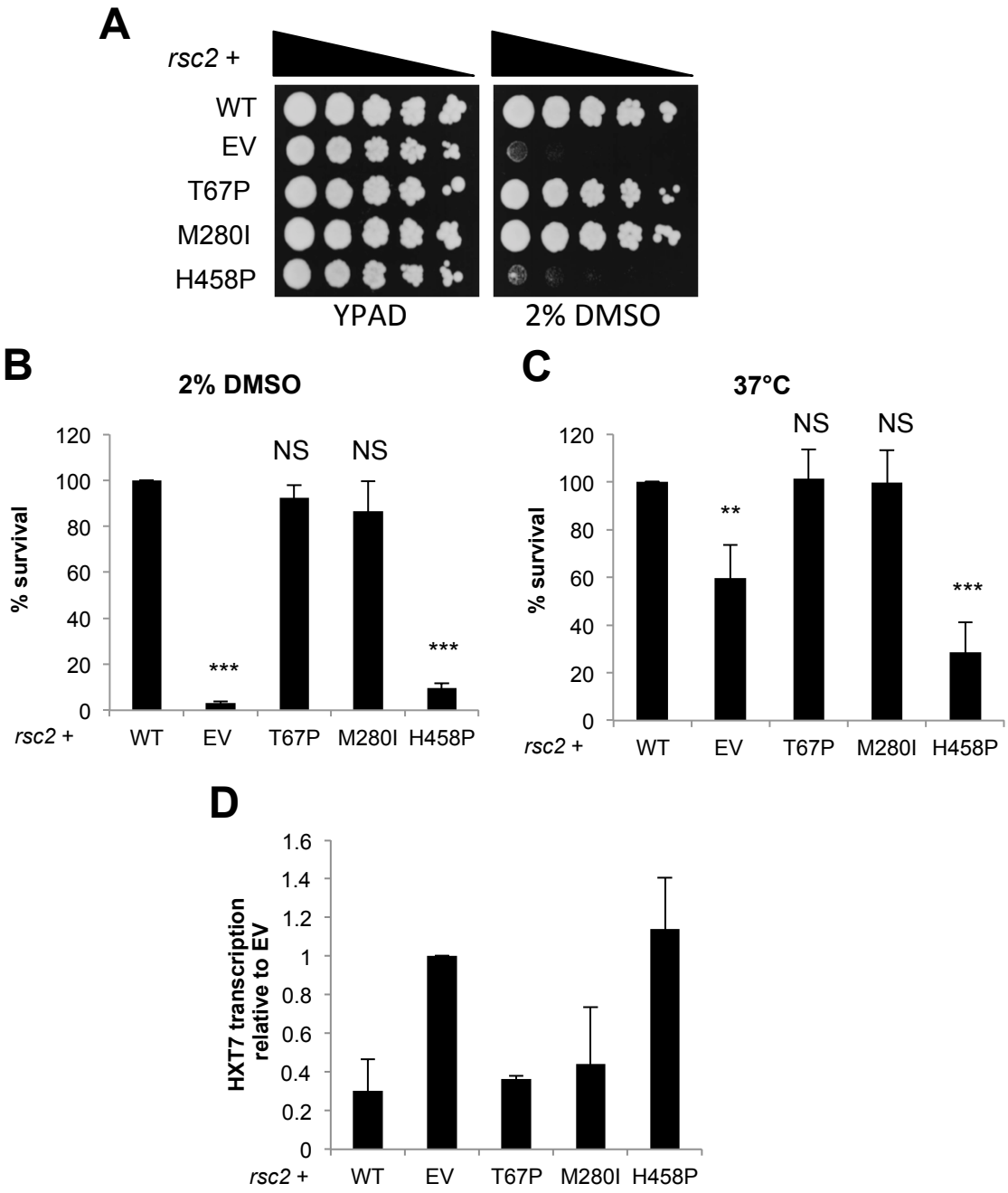

Figure 5.2. BAF180 missense cancer mutations expressed in yeast do not compromise a transcription-related subset of Rsc2 functions (A) Serial dilutions of mid-log cultures of *rsc2* cells containing the indicated Rsc2 expression constructs were plated onto YPAD media with and without DMSO. (B) Hypersensitivity to DMSO as a readout of Rsc2-dependent transcriptional activity was quantified by plating serial dilutions of the indicated mid-log cultures from (A) onto YPAD media with or without 2% DMSO. (C) Hypersensitivity to 37°C (ts phenotype) was analysed by plating serial dilutions of the indicated mid-log cultures onto YPAD media and incubating at 30°C or 37°C. Wild-type survival levels are set to 100% and mutant strains are shown relative to wild-type. Data are means ± s.d., n=3; statistical significance was indicated as $^{*}P < 0.05$, $^{**}P < 0.01$, $^{***}P < 0.001$, unpaired two-tailed t test. (D) Quantitative RT-PCR analysis of *HXT7* transcription in *rsc2* cells transformed with the indicated plasmids.

recombination (see Chapter 3). This reflects decreased DNA repeat stability and is characteristic of cells with compromised cohesion (Huang *et al.* 2006, Smith & Rothstein 1999). Importantly, misregulation of homologous recombination pathways because of defective cohesion might be responsible for genomic instability, which is associated with tumourigenesis (Xu *et al.* 2011). We therefore tested the cancer-associated mutations using the unequal sister chromatid exchange assay. Strikingly, *ADE2* marker loss at the rDNA was significantly higher than wild-type when all three of the mutations were expressed (Figure 5.3C). This suggests that these mutations impair the ability of Rsc2 to repress spontaneous recombination at the rDNA repeats. In addition, none of the cancer-associated mutations were able to fully complement the growth defect associated with *rsc2* null cells (Figure 5.3D). This growth defect might reflect the known defects in cohesion and chromosome segregation in cells lacking *RSC2.* Collectively, these data are consistent with the idea that some cancer-associated mutations do not compromise all functions of Rsc2, but do compromise the cohesion-related functions of Rsc2 and result in genome instability (Brownlee *et al.* 2014).

BAF180 missense cancer mutations expressed in human cells result in defective centromeric cohesion

We next sought to determine whether these cancer mutations have an effect on centromeric sister chromatid cohesion in mammalian cells, as shown in cells lacking BAF180 in the previous chapter. Because expression of the H458P mutation (H1204P in BAF180) in Rsc2 severely reduced protein levels, we chose not to include it and concentrated on the two mutations that were expressed at reasonable levels. We first created siRNA resistant wild-type EGFP-tagged BAF180 construct and constructs containing either the T232P or M538I mutations. We next depleted BAF180 using siRNA in U2OS cells, synchronised the cells in G2 using double thymidine block, and transiently transfected with -EGFP, wild-type BAF180-EGFP, T232P BAF180-EGFP or M538I BAF180-EGFP constructs (Figure. 5.4A). BAF180 depletion by siRNA was confirmed by Western blotting (Figure. 5.4B). We found that expression of the mutants was comparable to that of the wild-type construct, as measured by quantifying GFP immunofluorescence (Figures 5.4C and 5.5C). Successful synchronization in G2 was confirmed by immunostaining for CENPF, a marker for G2 (Figure. 5.4D).

Cells were immunostained for GFP and probed using the same FISH probe as in Chapter 4 (Figure. 4.2B), directed against the centromeric region of chromosome 10. As expected, the siBAF180 cells transfected with the -EGFP construct displayed a

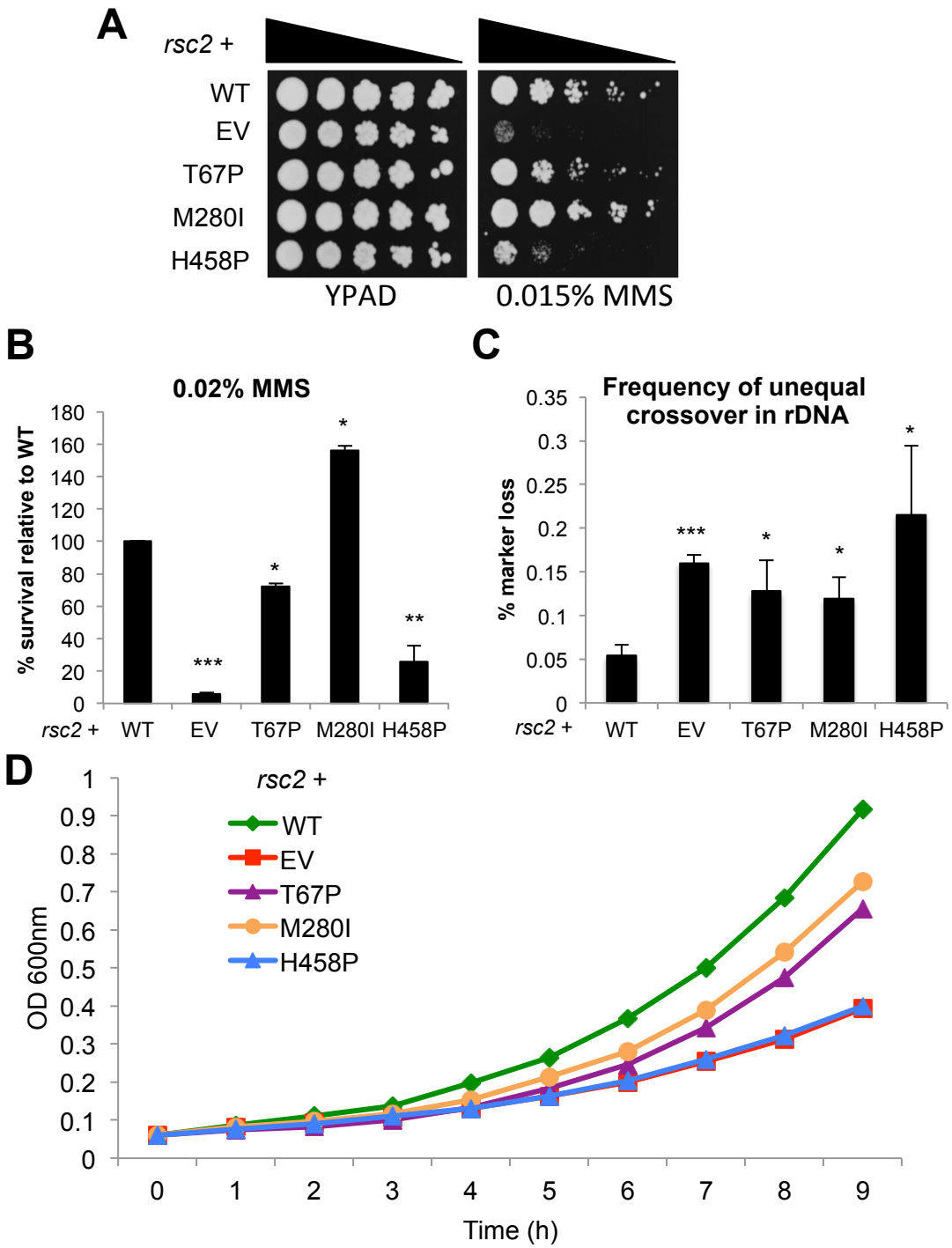

Figure 5.3. BAF180 missense cancer mutations expressed in yeast result in impaired cohesin-dependent Rsc2 functions (A) Serial dilutions of mid-log cultures of *rsc2* cells containing the indicated Rsc2 expression constructs were plated onto YPAD media with and without 0.015% MMS. (B) Hypersensitivity to MMS was quantified by plating serial dilutions of the indicated mid-log cultures from (A) onto YPAD media with or without 0.02% MMS. (C) Frequency of unequal rDNA crossover events in *rsc2* yeast strains containing the indicated Rsc2 expression construct. Data are means ± s.d., n=3; statistical significance was indicated as $^{*}P < 0.05$, $^{**}P < 0.01$, $^{***}P < 0.001$, unpaired two-tailed t test. (D) Growth curves of *rsc2* yeast strains containing the indicated Rsc2 expression construct.

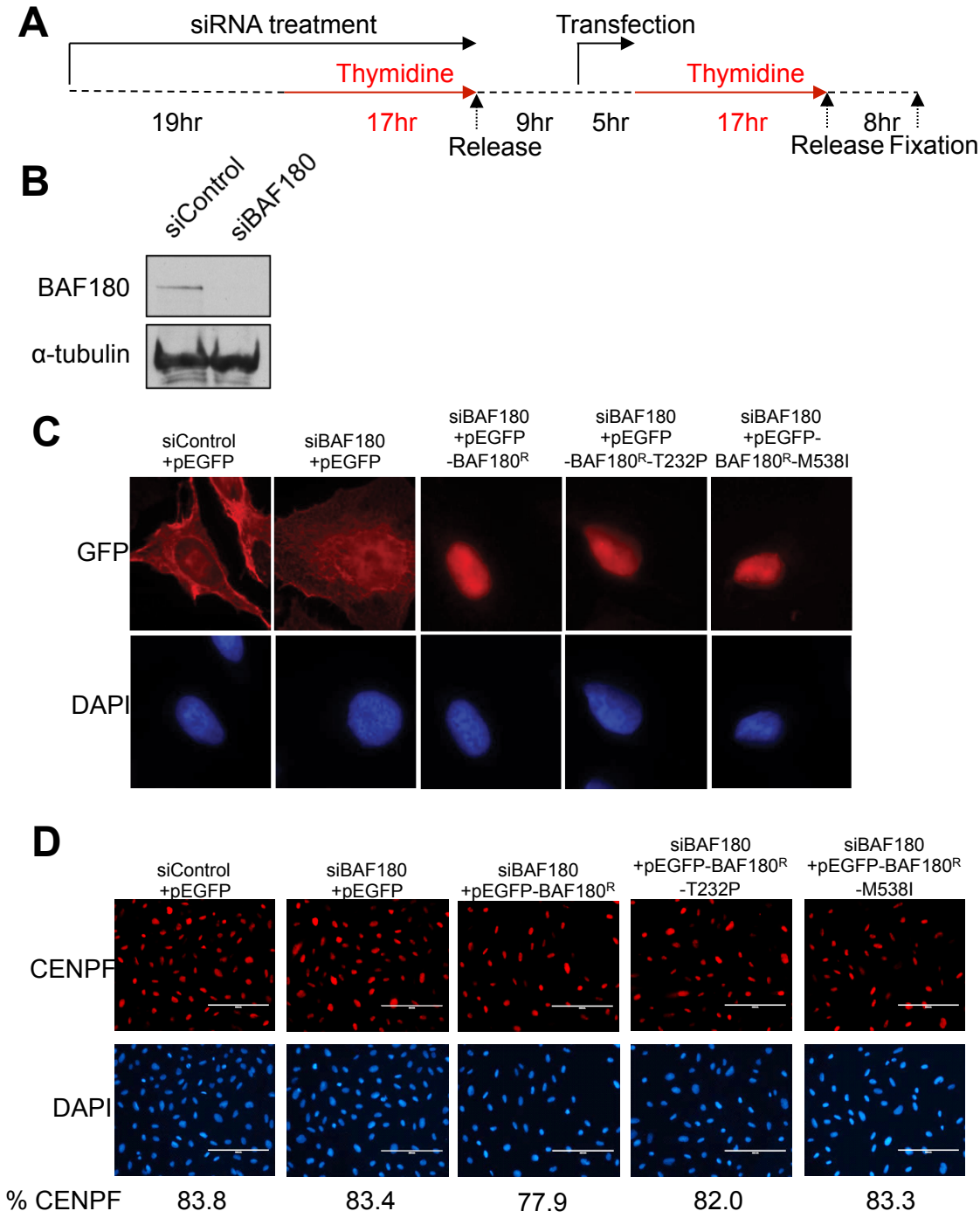

Figure 5.4. Complementation of BAF180-depleted U2OS cells with BAF180 missense cancer mutations. (A) Schematic of protocol used to deplete BAF180 using siRNA, transfect with –pEGFP or –pEGFP-BAF180^R expression plasmids and synchronize cells in G2. (B) Analysis of BAF180 depletion efficiency in U2OS cells by Western blotting. α-tubulin was used as a loading control. (C) Expression of –pEGFP and pEGFP-BAF180^R constructs in siBAF180 U2OS cells. Cells were treated as in (A) and processed for IF-FISH using a probe directed against the centromere of chromosome 10. IF using anti-GFP antibody shows GFP or GFP-BAF180 in the red channel. (D) Cells treated as in (A) were immunostained with CENPF as a marker of G2 and % CENPF-positive cells is shown underneath images.

significant increase in the distribution of distances between the two signals from the sister chromatids compared to siControl cells (Figure 5.5A; compare green and black bars, and B). Importantly, siBAF180-treated cells transfected with the wild-type BAF180-EGFP construct showed clear rescue of the cohesion defect to levels very similar to the siControl cells transfected with the -EGFP construct (Figure 5.5A; compare grey and black bars, and B). Strikingly, both the T232P BAF180-EGFP and M538I BAF180-EGFP constructs are unable to even partially rescue the cohesion defect, showing distributions of distances between signals comparable to the siBAF180 cells transfected with -GFP (Figure 5.5A; compare green, red and blue bars, and B). Interestingly, the T232P BAF180-GFP construct actually appeared to show a greater defect than the –GFP construct in siBAF180-depleted cells (Figure 5.5A; compare red and green bars, and B). These data indicate that both the T232P and M538I cancer mutations completely impair the ability of BAF180 to promote centromeric sister chromatid cohesion. Furthermore, this strongly suggests that this function of BAF180 is important in tumour suppression.

5.2. Discussion

In this section we analysed the effects of three conserved BAF180 missense mutations identified in ccRCCs, expressed in the budding yeast Rsc2 homologue and in human cells. This study is the first to our knowledge that has explored the cellular consequences of BAF180 cancer mutations. We found that Rsc2 protein levels correlated well with the predicted effects of these mutations on BAF180 stability. Interestingly, we showed that the two mutations that maintained relatively high Rsc2 protein levels did not compromise a subset of Rsc2-dependent phenotypes, including regulation of transcriptional activity. In contrast, these mutations consistently impaired or altered the activity of Rsc2 in processes relating to cohesion. This provides strong evidence that these cancer-associated mutations impair a subset of Rsc2-depedent activities that relates specifically to cohesion. Furthermore, we showed that expression of these two cancer mutations in human cells completely impairs the ability of BAF180 to promote centromeric sister chromatid cohesion, identifying a novel, cancer-relevant tumour suppressor function.

BAF180 missense cancer mutations expressed in yeast do not impair Rsc2-dependent transcriptional activity

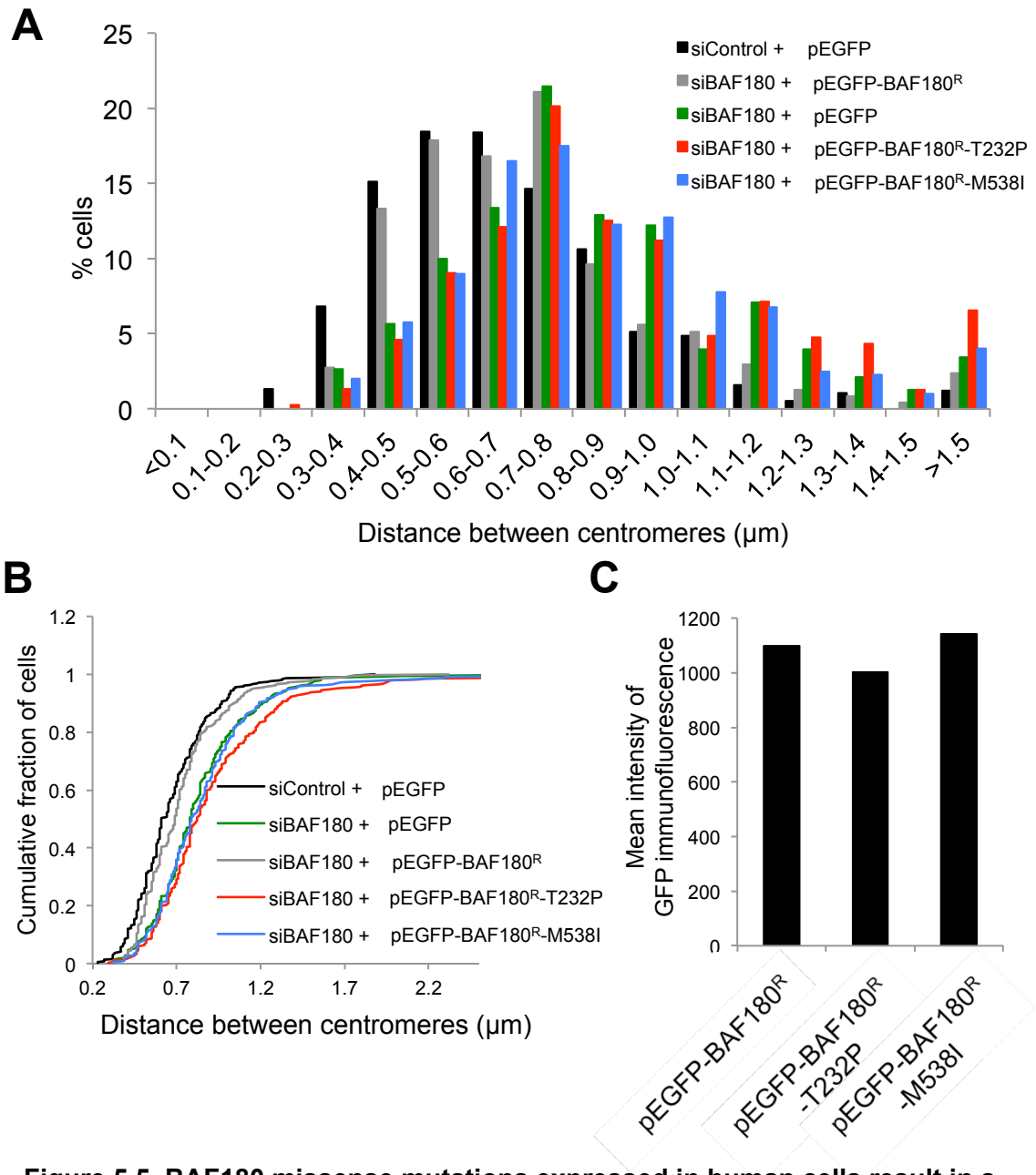

Figure 5.5. BAF180 missense mutations expressed in human cells result in a defect in centromeric cohesion. (A) FISH analysis of G2 phase U2OS cells transfected with the indicated BAF180 expression construct using a probe directed against the centromere of chromosome 10. The distances between the signals between sister chromatids was measured and the distribution of measurements was plotted as a histogram. (B) The data in (A) are presented as a cumulative plot to further illustrate the defect in cohesion in cells transfected with cancer-associated mutants. Statistical analysis of the data presented in (A) and (B) showed that rescue of the cohesion defect by reintroduction of WT BAF180 (siBAF180 + GFP-BAF180) was significant ($P < 0.001$, Kolmogorov-Smirnov test). In contrast, centromeric cohesion in cells expressing the cancer mutants was not significantly different from that in BAF180-depleted cells containing empty vector (siBAF180 + GFP; $P = 0.06$ for T232P and $P = 0.37$ for M538I), but was significantly different from that in cells with WT BAF180 reintroduced ($P < 0.001$ for both mutants compared with WT)

We showed that the T67P and M280I mutations expressed in Rsc2 did not sensitise cells to DMSO or non-permissive temperature, and did not impair the ability of Rsc2 to repress transcription of the *HXT7* gene. These results strongly suggest that these mutations do not impair a transcriptional subset of Rsc2-related functions. This has very important implications for the role of BAF180 as a tumour suppressor, because BAF180 (and other SWI/SNF subunits) are widely believed to exert their tumour suppressor activity through transcriptional regulation. Taken with our other observations that p21 transcription does not appear to be strictly controlled by BAF180 in all cell types, these data argue for additional, more important roles of BAF180 in tumour suppression. Evidence from another study examining the effect of SWI/SNF cancer-associated mutations supports the idea that additional functions of SWI/SNF exist in tumour suppression. The study by Vries *et al.* showed that a selection of cancer-derived SNF5 mutations were able to initiate $p16^{INK4A}$-depedent G1 arrest, senescence and apoptosis (Vries *et al.* 2005). Therefore, other processes other than transcriptional regulation of proliferation might underlie the cancer association of these mutations.

BAF180 missense cancer mutations have different effects on protein stability but completely impair cohesion in mammalian cells

The T67P mutation expressed in budding yeast Rsc2 destabilized the protein, suggesting that limiting amounts of BAF180 in human cells might underlie its tumourigenic effect. In support of this idea, the majority of BAF180 mutations in various cancers result in a truncated protein product. However, we found that when this mutation was overexpressed in human cells, in which protein levels were comparable to wild-type BAF180-expressing cells, the T232P mutation completely impaired the ability of BAF180 to restore centromere cohesion. In addition, the rate of unequal sister chromatid exchange when this mutation was expressed in Rsc2 was very similar to *rsc2* null cells. These findings suggest that the T232 residue and BD2 of BAF180 are critically important for cohesion, and that changes in protein levels are perhaps a secondary consequence of its mutation to proline. The T232 residue occurs in the αA helix of BD2, and therefore might be directly involved in acetyl-lysine binding or regulating the architecture of this bromodomain.

Expression of the M538I mutation in BAF180 was also completely unable to rescue the cohesion defect, and expression of the equivalent M280I mutation in Rsc2 led to a very similar increase in unequal sister chromatid exchange. This mutation resides in the αZ helix of BAF180 BD4 and did not compromise the stability of Rsc2.

Therefore this residue and BAF180 BD4 also appear to be critical for BAF180-dependent cohesion. Although we did not examine the effect of the H1204P mutation on cohesion in human cells, we found that it increased levels of unequal sister chromatid exchange to rates comparable to *rsc2* null cells and cells expressing T67P and M280I. Moreover, this mutation appeared to impair all functions of Rsc2 to levels comparable to an *rsc2* null, which is consistent with its highly destabilizing effect. Therefore, we predict that expression of this mutation in human cells is also very likely to severely disrupt centromeric cohesion.

Distinct effects of BAF180 missense cancer mutations suggest different functions for individual bromodomains

Although the three BAF180 cancer mutations had very similar effects in some assays, they were also seen to behave very differently in others. Firstly, expression of the M280I mutation in Rsc2 reproducibly led to increased resistance to the alkylating agent MMS. Because this mutation appeared to slightly stabilize the Rsc2 protein, this resistance might simply represent limiting amounts of Rsc2 in wild-type cells. An alternative explanation comes from a report showing that whilst *rad53* null cells rapidly lose viability after MMS, due to the inability to activate the DNA damage checkpoint, reduced levels of Rad53 results in resistance to MMS (Cordón-Preciado *et al.* 2006). An explanation follows that cells with reduced amounts of Rad53 are able to maintain fork stability, but cannot initiate an intra-S phase checkpoint (Cordón-Preciado *et al.* 2006). The finding that the M280I mutation in Rsc2 has a similar effect suggests a previously undiscovered role for Rsc2 in the intra-S checkpoint. However, this possibility is difficult to reconcile with findings by us and from other labs showing that Rsc2 is not required for G1 or G2/M DNA damage checkpoint activation (See chapter 3, Chambers *et al.* 2012, Oum *et al.* 2011). Nevertheless, this does not necessarily rule out a specific function of Rsc2 in the intra-S checkpoint, which has not been specifically tested. The H548P mutation also behaved in a manner that was not entirely expected. Expression of this mutation, which led to a severe reduction in levels of Rsc2 protein, actually led to worse survival than the *rsc2* null strain when grown at the non-permissive temperature. This suggests that this mutation somehow functions in a dominant negative manner under certain conditions. Because haploid yeast was used in these assays (in which the only Rsc2 present is the mutant form), one possibility is that the small amount of Rsc2 expressing this mutation inhibits the activity of Rsc1. This is conceivable because *rsc1* null cells are also temperature sensitive, but to a lesser extent than *rsc2* cells (Oum *et al.* 2011). In addition, the BAH domains of Rsc1

and Rsc2 both bind to H3 (Chambers *et al.* 2013). Therefore, alteration of the structure of the Rsc2 BAH domain could conceivably interfere with the binding of the Rsc1 BAH domain to chromatin. Such an effect on the conserved BAF180 BAH domains is likely to further compromise the normal function of the protein and might have relevance in tumourigenesis.

CHAPTER 6: NOVEL HDAC INHIBITORS SENSITIZE CELLS LACKING BAF180

6.1. Results

Introduction

The high-throughout screening technology known as heterozygote diploid-based synthetic lethality analysis with microarrays (dSLAM) is often used to identify synthetic lethal interactions in budding yeast. dSLAM essentially examines genome-wide synthetic lethality using a query mutation, which is introduced into a large scale population of ~6000 haploid-convertible heterozygote diploid yeast knockout mutants via integrative transformation (Pan *et al.* 2007). The resulting heterozygous diploid double mutants are sporulated to generate single and double mutant haploid strains, which are examined for synthetic growth defects. Using this technique, Lin *et al.* examined 38 query genes involved in histone (de)acetylation, and identified synthetic lethal interactions between Rsc2 and components of the Hda1 and Rpd3 HDAC complexes (Lin *et al.* 2008). This finding promoted us to address whether loss of BAF180, which is the mammalian homologue of Rsc2, also results in synthetic lethality with loss of HDACs. Moreover, because BAF180 is frequently mutated in cancer, a conserved synthetic lethal interaction with HDAC loss could be exploited as a potential therapeutic strategy using HDAC inhibitors.

BAF180 protein expression is lost or reduced in 50% of a panel of breast cancer cell lines

It is now well established that BAF180 is an important tumour suppressor gene, given its frequency of mutation in cancer as described in previous sections. However, the full scale of BAF180 involvement in cancer is likely to be underappreciated because relatively few whole-exome sequencing studies have been performed. In order to further examine the involvement of BAF180 in cancer we screened a panel of 16 breast cancer cells lines for BAF180 protein levels using Western blotting. Strikingly, we found that 8 out of 16 cell lines showed severely reduced or completely absent BAF180 expression (Figure 6.1). Intriguingly, two of the cell lines that have had their genomes fully sequenced and lacked BAF180 expression (red asterisks) did not contain mutations in *PBRM1*. These findings suggest that BAF180 expression might

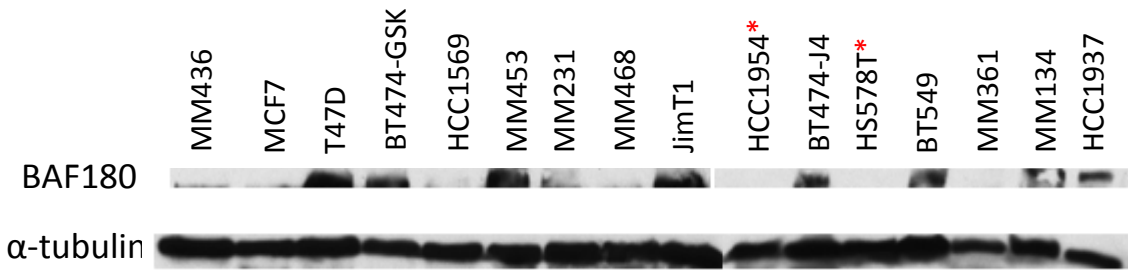

Figure 6.1. BAF180 protein expression is lost or reduced at high frequency in breast cancer cells. Analysis of BAF180 expression in a panel of 16 breast cancer cell lines by Western blotting. α-tubulin was used as a loading control. Red asterisks indicate genome-sequenced cell lines that do not contain a mutation in the gene encoding BAF180

be lost at an unappreciated frequency via mechanisms other than mutation of the *PBRM1* gene.

Screening a panel of novel and commercially available HDAC inhibitors for synthetic lethality in BAF180 -/- mESCs

Our observation that BAF180 expression can be lost via mutation-independent mechanisms suggests that BAF180 mutation spectrums underrepresent the true frequency of BAF180 loss in cancer. We realized that exploiting BAF180 loss could provide an important means to develop treatments for BAF180-deficient cancers. Because Rsc2 is synthetic lethal with HDACs in budding yeast, and HDAC inhibitors are a very promising class of small molecules for cancer therapy, we set out to test whether HDAC inhibitors would specifically sensitize mammalian cells lacking BAF180.

We first procured a panel of 7 commercially available and 10 novel HDAC inhibitors, the latter of which were synthesized by the John Spencer lab. The novel HDAC inhibitors are structurally similar to SAHA, which consists of an aryl cap, a flexible linker and a zinc-binding motif (Figure 6.2A). Originally these compounds were synthesized using 'click' chemistry, which alters the zinc-binding motif and the conformational restriction of the linker region (Spencer *et al.* 2012). The resulting set of structurally distinct HDAC inhibitors display varied entropy upon enzyme binding, altered enzyme selectivity, and pharmacokinetics (Spencer *et al.* 2012). An example of the chemical structure of two ferrocene-based HDAC inhibitors, JAHA and JA125, which were produced using SAHA 'click' chemistry, are shown in Figure 6.2A.

Next, we performed viability assays on wild type (+/+) and BAF180 knockout (-/-) mESCs using these 17 HDAC inhibitors. The full list of HDAC inhibitors is shown in Table 6.3. The BAF180 -/- cells were no more sensitive to SAHA than the wild-type cells (Figure 6.2B). The ferrocene-based SAHA analogue JAHA also did not lead to increased sensitivity in the BAF180 -/- cells. In contrast, JA125 reproducibly led to substantially reduced viability in the BAF180 -/- cells compared to WT (Figure 6.2B). The complete viability assay dataset for all of the HDAC inhibitors is shown in Appendix I. The inhibitors JA234 and Scriptaid, and to a lesser extent JA224 and KD5170 also reproducibly sensitized the BAF180 -/- cells (Appendix I and Table 6.1).

We calculated the IC50 viability ratio for BAF180 +/+ and BAF180 -/- cells for each drug as a measure of the BAF180 -/- fold-sensitivity (Table 6.1). JA125, JA234 and Scriptaid sensitized the BAF180 -/- mESCs 3.1-, 2.3-, and 1.8-fold, respectively.

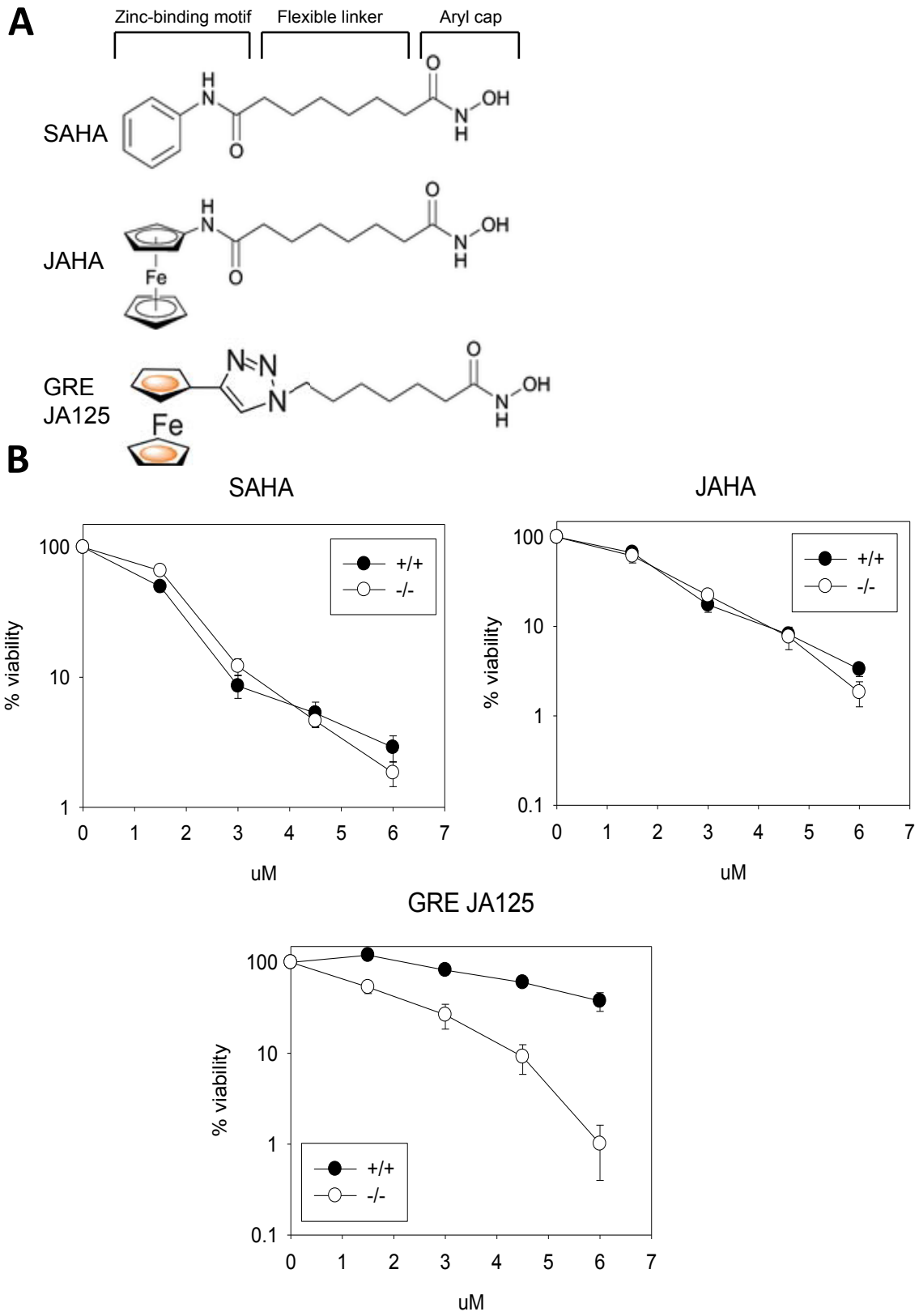

Figure 6.2. Novel HDAC inhibitors specifically sensitize BAF180 -/- mESCs (A) Chemical structures of SAHA and its analogues JAHA and JA125 generated by click chemistry. (B) Viability curves of WT (+/+) or BAF180 knockout (-/-) mESCs following exposure to SAHA, JAHA and JA125.

The remaining drugs all showed fold-sensitivities of less than 1.4 (Table 6.1 and Appendix I). Where available, the activity of each HDAC inhibitor (IC50, μM) against the 11 human HDAC enzymes is shown in Table 6.1 and colour coded by efficacy. Intriguingly, JA125, JA234 and Scriptaid, which sensitize the BAF180 -/- cells to the greatest extent, differ from the other drugs in that that they strongly inhibit HDACs 1, 2, 6, and also show the strongest inhibition of HDAC8 (Table 6.1). Furthermore, JA125 and JA234 are the only two drugs that show strong inhibition of HDAC3. Collectively, these results suggest that properties unique to the novel HDAC inhibitors JA125 JA234 confer an ability to induce synthetic lethality in mESCs lacking BAF180.

6.2. Discussion

In this section we extended our findings from previous chapters to consider a possible therapeutic option for the treatment of BAF180-deficient cancers. We first screened a set of breast cancer cell lines for BAF180 protein expression and found that an unexpected number showed loss of or reduced BAF180. This suggests that BAF180 loss might be much more widespread in cancer than is currently realised. Furthermore, it suggests that successfully exploiting BAF180 deficiency in cancer could be particularly fruitful as a therapeutic strategy. To this end, we evaluated whether HDAC inhibitors could be of potential use to specifically sensitize BAF180-deficient cells. Tantalizingly, two novel HDAC inhibitors with unique pharmacophore properties substantially sensitized mESCs lacking BAF180 compared to wild-type mESCs. Further research using these inhibitors is necessary to assess their full potential for the treatment of BAF180-deficient cancers.

Mutation-independent mechanisms contribute to loss of BAF180 expression in breast cancer

We found that in 8 out of 16 breast cancer cell lines BAF180 protein expression was reduced or lost, and 2 of these 8 cell lines that have had their genomes fully sequenced did not contain mutations in *PBRM1.* Thus, alternative mechanisms might contribute to reduced BAF180 protein expression in breast cancer. Xia *et al.* reported *PBRM1* LOH in 25 out of 52 (48.1%) primary breast tumours, and only one of these tumours contained a *PBRM1* mutation (Xia *et al.* 2008). Although BAF180 protein levels were not assessed in these cases, *PBRM1* LOH could conceivably reduce

HDAC inhibitor	BAF180 sensitivity	1	2	3	4	5	6	7	8	9	10	11
JA125[1]	3.1	4.5×10^{-3}	9.5×10^{-3}	7.2×10^{-3}	IA	IA	2.6×10^{-3}	IA	0.18	IA	NT	NT
JA234[1]	2.3	2.2×10^{-3}	3.7×10^{-3}	4.1×10^{-3}	IA	IA	1.4×10^{-3}	IA	0.8	IA	NT	NT
Scriptaid[4]	1.8	6.4×10^{-4}	1.4×10^{3}	0.6	14	IA	3.4×10^{-2}	2.25	1.5×10^{-2}	IA	?	?
JA224[1]	1.3	0.22	0.27	0.2	IA	IA	0.17	IA	2.4	IA	NT	NT
KD5170[3]	1.3	2.0×10^{-2}	2	8.0×10^{-2}	3.0×10^{-2}	0.95	1.4×10^{-2}	8.5×10^{-2}	2.5	0.15	1.8×10^{-2}	?
SBHA[2]	1.2	0.25	?	0.3	?	?	?	?	?	?	?	?
JA249[1]	1.1	5.2	IA	5.9	IA	IA	0.16	IA	3.1	IA	NT	NT
MC1568[5]	1	IA	IA	IA	IA	IA	?	?	?	?	?	?
JA219[1]	1	?	?	?	?	?	?	?	?	?	?	?
JA245[1]	1	0.19	0.39	0.34	IA	IA	0.13	IA	4.2	IA	?	?
JA246[1]	1	6.9	IA	6.6	IA	IA	0.38	IA	4.8	IA	?	?
NSC3852	1	?	?	?	?	?	?	?	?	?	?	?
ISC2-057-1	1	?	?	?	?	?	?	?	?	?	?	?
JAHA[1]	1	1.1×10^{-2}	1.1×10^{-2}	1.4×10^{-2}	IA	IA	8.0×10^{-4}	IA	1.36	IA	?	?
SAHA[1]	0.9	5.0×10^{-2}	9.0×10^{-2}	6.7×10^{-2}	IA	IA	1.9×10^{-2}	IA	1.35	IA	?	?
TC-H 106[2]	0.8	0.15	0.76	0.37	IA	IA	IA	IA	5	IA	?	?
TSA[3]	0.6	1.2×10^{-2}	2.0×10^{-2}	1.0×10^{-2}	2.2×10^{-2}	1.6×10^{-2}	2.0×10^{-3}	8.1×10^{-2}	0.12	8.0×10^{-2}	2.8×10^{-2}	?

[1]Spencer *et al.* 2012
[2]Richon *et al.* 1998
[3]Hassig *et al.* 2008
[4]Huber *et al.* 2011
[5]Duong *et al.* 2008

Table 6.1. Profile of HDAC inhibitors and their effects on BAF180 +/+ and BAF180 -/- mESCs. BAF180 sensitivity values are calculated as the IC50 ratio of IC50 BAF180 +/+ and BAF180 -/- cells. A value greater than 1 indicates that BAF180 -/- cells are inhibited more effectively that BAF180 +/+ cells. Activity of each inhibitor against the 11 human HDAC enzymes (IC50, μM) is provided and colour coded by efficacy (dark red is very strong inhibition (<1 x 10^{-3} μM), red is strong inhibition (<1 x 10^{-2} μM), orange is moderate inhibition (<1 x 10^{-1} μM), yellow is weak inhibition (<1.0 μM), pale green is very weak inhibition (<20 μM), IA is inactive, and ? Means the data is unavailable

BAF180 protein levels by at least 50%. Therefore, *PBRM1* LOH could underlie the reduced BAF180 expression we observe in the non-mutated breast cancer cell lines.

Alternatively, the *PBRM1* gene could be epigenetically silenced. In support of this possibility, Brough *et al.* reported that reduced PDS5B expression in 75 out of 160 (46.9%) breast tumours was correlated with promoter methylation status rather than genomic loss (Brough *et al.* 2013). Again, the PDS5B protein loss frequency of 46.9% is remarkably similar to that which we observe for BAF180. In addition, the loss of STAG2 expression in 27% of gastric cancers, 23% of colorectal carcinomas, and 30% of prostate carcinomas was not associated with mutations in the *STAG2* gene (Kim *et al.* 2012). Therefore, the expression of proteins that regulate centromeric cohesion, including BAF180, appears to be reduced or lost in cancer at a far higher frequency than that represented by their mutation frequency. Moreover, these findings add further weight to the notion that disruption of centromere cohesion contributes to tumourigenesis.

mESCs lacking BAF180 are hypersensitive to novel HDAC inhibitors

We utilized a panel of commercially available and novel HDAC inhibitors to broadly test the hypothesis that loss of BAF180 is synthetic lethal with loss of HDACs, as is the case with its yeast homologue, Rsc2. This approach has advantages and limitations over using alternative synthetic screening techniques such as siRNA library screens. Because the panel HDAC inhibitors used generally displayed broad HDAC specificity, we were unable to firmly identify whether BAF180 is synthetic lethal with a single HDAC or a combination of HDACs. However, because some HDAC inhibitors already represent a very promising class of small molecule for cancer therapy, this approach potentially allows us to bypass the drug development process.

We found that two novel HDAC inhibitors, JA125 and JA234, were particularly effective at reducing viability in mESCs lacking BAF180, suggesting that loss of BAF180 is indeed synthetic lethal with HDAC inhibition. These two inhibitors display pharmacological activity that is distinct from all of the other HDAC inhibitors tested. Essentially, they target HDACs 1, 2, 3, 6 and 8 with the same relative activity as SAHA, but with ~10-fold higher efficacy. Because SAHA did not sensitize the BAF180 -/- mESCs, it seems that the improved inhibition of these particular HDACs is a critical property of these HDAC inhibitors.

A limited group of HDACs might be responsible for the synthetic lethality with BAF180 loss

The subtle differences in activity of some of the other inhibitors might shed light on which HDACs are particularly relevant for the synthetic lethality with loss of BAF180. For example, JAHA displays the same inhibition as SAHA for HDACs 1, 2, 3 and 8, but inhibits HDAC6 with ~24-fold greater efficiency. However, JAHA does not sensitize the BAF180 -/- mESCs any better than SAHA. Therefore, HDAC6 inhibition alone can perhaps be ruled out as being responsible for the synthetic lethality with loss of BAF180. HDAC6 is a cytoplasmic deacetylase that regulates cellular motility, adhesion and chaperone function through its targeting of tubulin, cortactin and HSP90 (Valenzuela-Fernandez *et al.* 2008). To date, BAF180 has not been directly implicated in these processes, suggesting that a synthetic lethal interaction with HDAC6 is unlikely. A second example is with Scriptaid, which sensitized the BAF180 -/- mESCs, but to a lesser extent than JA125 and JA234. The main difference between Scriptaid and these two inhibitors is that it displays ~150-fold weaker inhibition of HDAC3. Therefore, inhibiting HDAC3 might be important for inducing synthetic lethality with loss of BAF180. Intriguingly, both of these proteins are required for centromeric cohesion (Brownlee *et al.* 2014, Eot-Hollier *et al.* 2008), thus it is conceivable that simultaneous loss of BAF180 and HDAC3 reduces viability by severely disrupting chromosome segregation.

Synthetic lethality with loss of BAF180 and inhibition of HDACs 1, 2 and 8 can also be interpreted in the context of our results from previous chapters. HDACs 1 and 2 are involved in DNA repair via NHEJ, and to a lesser extend via HR, by deacetylating H3K56 (Miller *et al.* 2010). We showed that BAF180 is important for maintaining viability and promoting DNA repair after treatment with MMC, which likely reflects a function in cohesion-dependent DNA repair by HR. Although we did not directly test the involvement of BAF180 in NHEJ, a role for BAF180 in this pathway seems likely because both of its budding yeast homologues, Rsc1 and Rsc2, are required for NHEJ (Chambers *et al.* 2012). Therefore, simultaneous inhibition of HDACs 1 and 2 with loss of BAF180 might lead to synthetic lethality because the repair of endogenous DNA damage is severely compromised.

Finally, JA125, JA234 and Scriptaid were further distinguished from the other HDAC inhibitors in that they most strongly inhibited HDAC8. In the absence of HDAC8, SMC3 is not deacetylated, ultimately leading to reduced cohesin loading (Deardorff *et al.* 2012). Thus, in a manner that might be similar to inhibiting HDAC3,

inhibition of HDAC8 in cells lacking BAF180 might lead to synthetic lethality because of a severe cohesion defect and overwhelming chromosome segregation errors. In summary, these findings suggest that strongly inhibiting a discrete combination of HDACs preferentially leads to synthetic lethality in cells lacking BAF180. It is compelling that the two drugs, namely JA125 and JA234, which bring about the greatest synthetic lethal effect, most strongly inhibit a combination of four HDACs that function in the same pathway as BAF180 relating to cohesion. In order to explore the full potential of these HDAC inhibitors testing will need to extend to relevant human cancer cell lines.

Appendix I. HDAC inhibitors viability assays

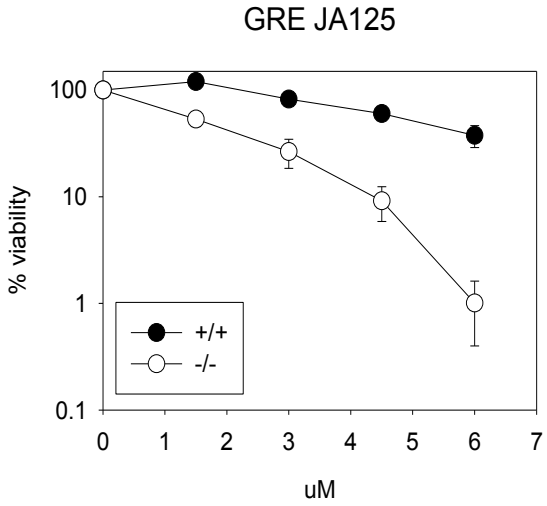

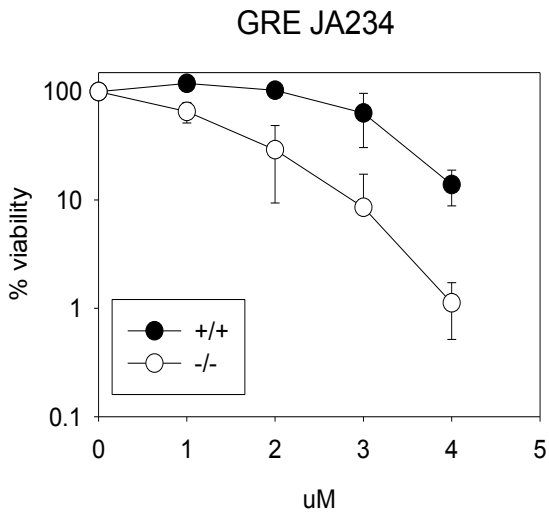

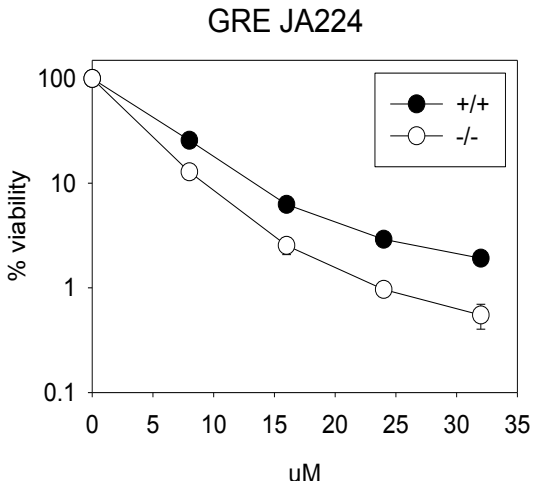

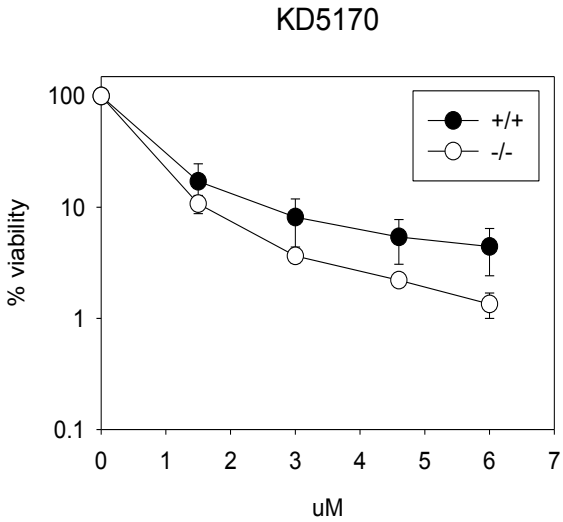

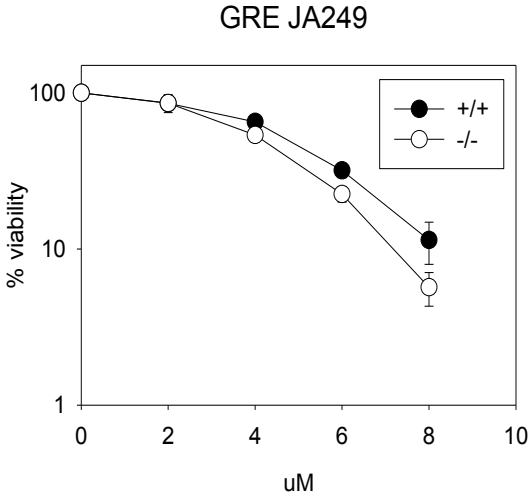

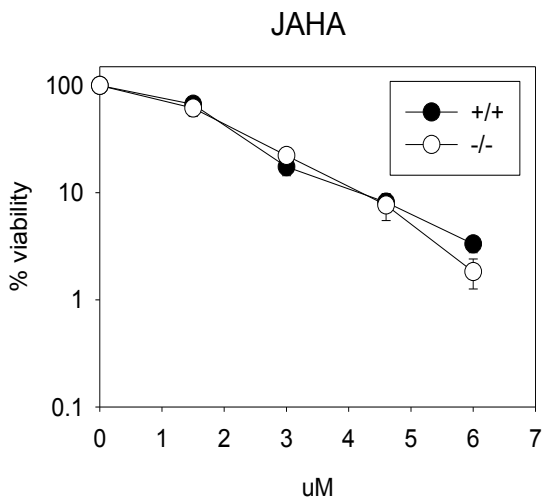
JAHA
100
10
1
0.1
% viability
0 1 2 3 4 5 6 7
uM
+/+
-/-

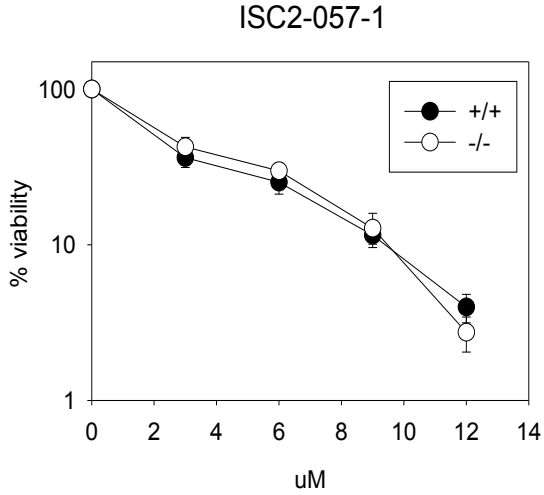
ISC2-057-1
100
10
1
% viability
0 2 4 6 8 10 12 14
uM
+/+
-/-

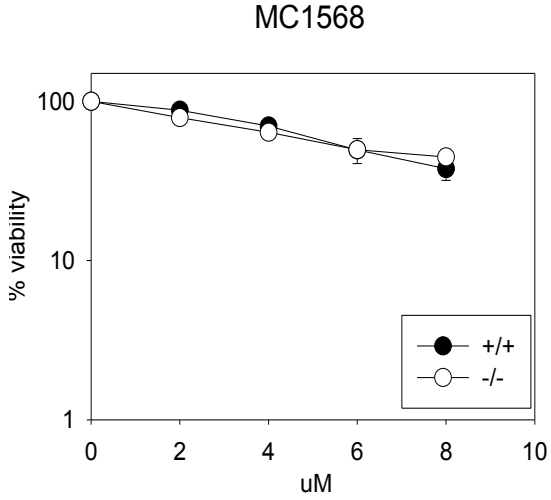
MC1568
100
10
1
% viability
0 2 4 6 8 10
uM
+/+
-/-

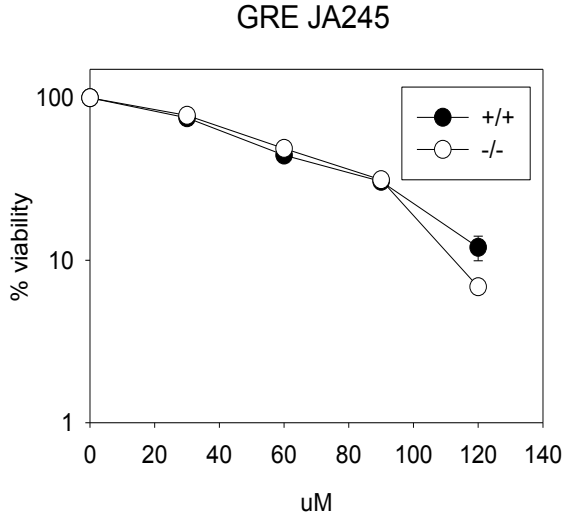
GRE JA245
100
10
1
% viability
0 20 40 60 80 100 120 140
uM
+/+
-/-

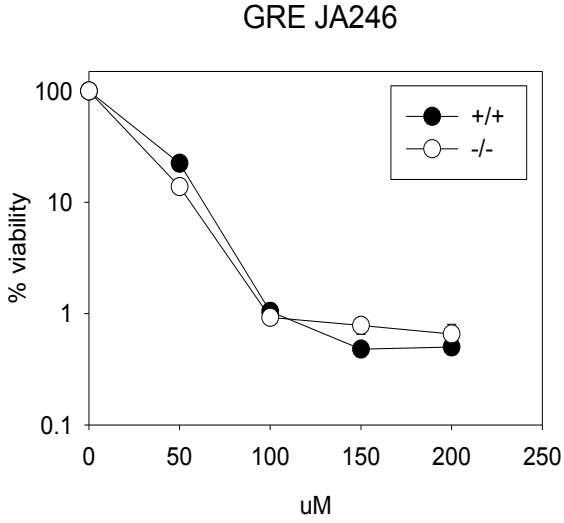
GRE JA246
100
10
1
0.1
% viability
0 50 100 150 200 250
uM
+/+
-/-

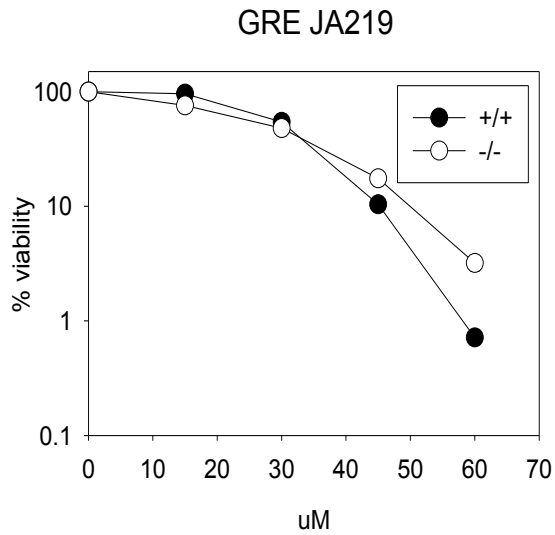
GRE JA219
100
10
1
0.1
% viability
0 10 20 30 40 50 60 70
uM
+/+
-/-

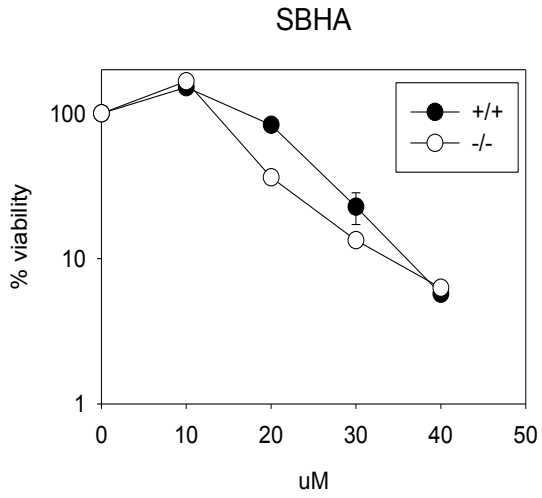
SBHA
% viability
100
10
1
0
10
20
30
40
50
uM
+/+
-/-

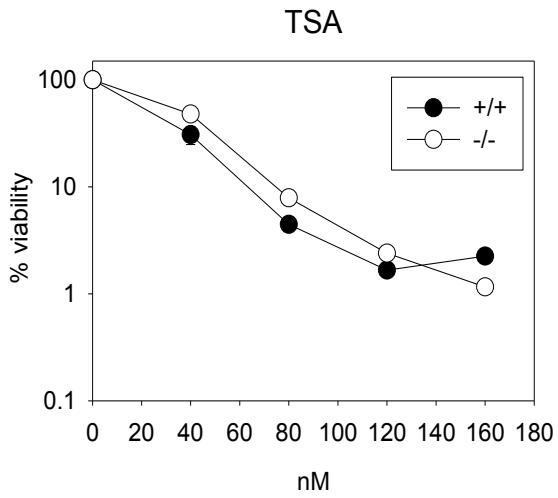
TSA
% viability
100
10
1
0.1
0
20
40
60
80
100
120
140
160
180
nM
+/+
-/-

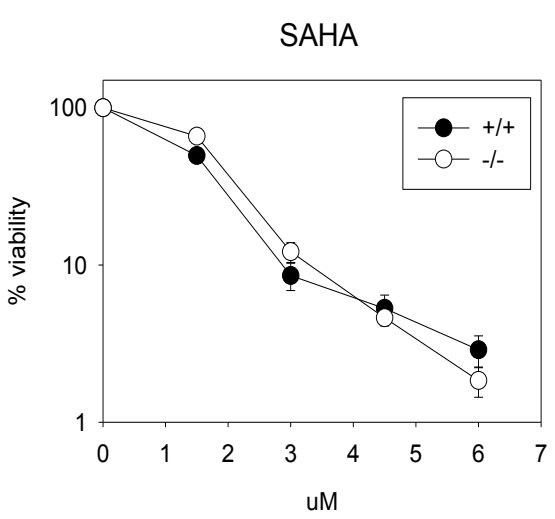
SAHA
% viability
100
10
1
0
1
2
3
4
5
6
7
uM
+/+
-/-

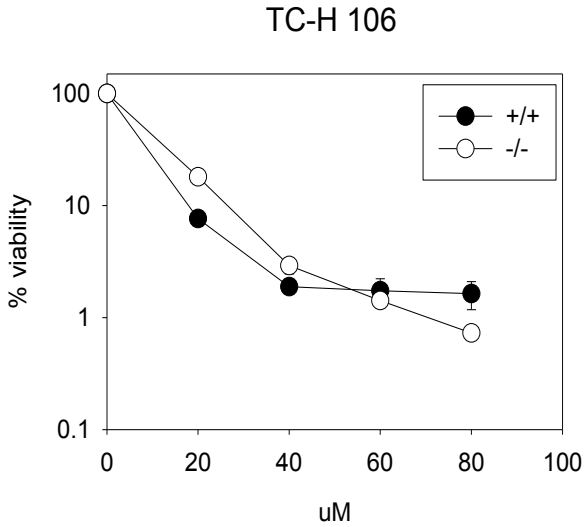
TC-H 106
% viability
100
10
1
0.1
0
20
40
60
80
100
uM
+/+
-/-

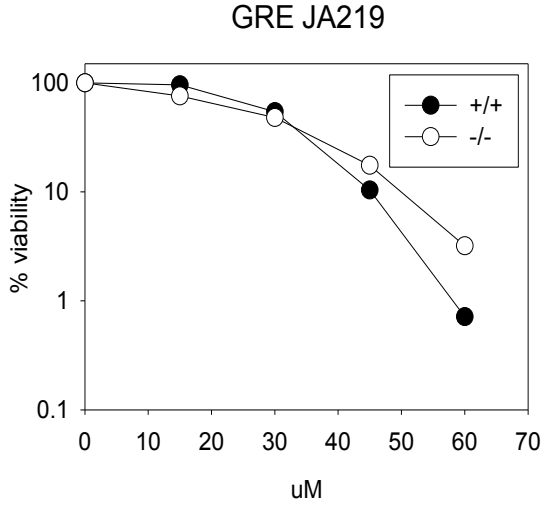
GRE JA219
% viability
100
10
1
0.1
0
10
20
30
40
50
60
70
uM
+/+
-/-

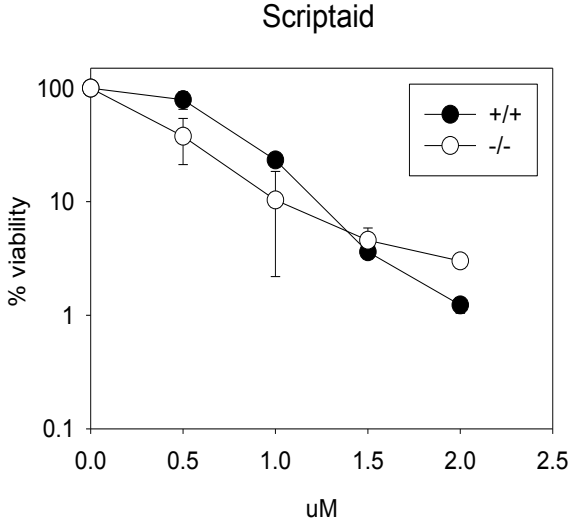
Scriptaid
% viability
100
10
1
0.1
0.0
0.5
1.0
1.5
2.0
2.5
uM
+/+
-/-

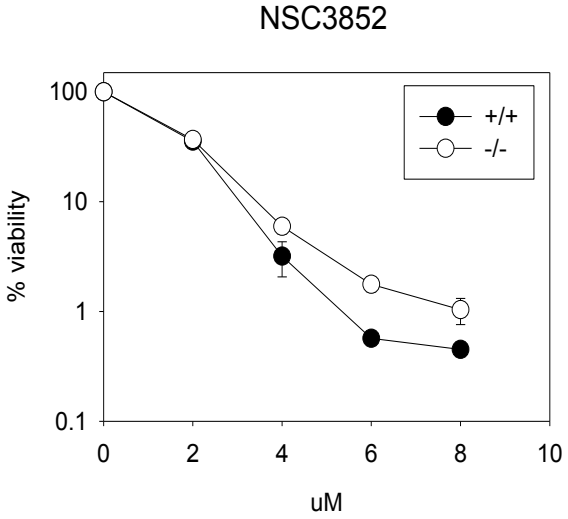
NSC3852
100
10
1
0.1
% viability
0
2
4
6
8
10
uM
+/+
-/-

References

Aboussekhra, A., *et al*. *RADH*, a gene of *Saccharomyces cerevisiae* encoding a putative DNA helicase involved in DNA repair. Characteristics of *radH* mutants and sequence of the gene. *Nucleic Acids Res.* **17**: 7211–7219 (1989)

Aboussekhra, A., *et al.* Semidominant suppressors of Srs2 helicase mutations of *Saccharomyces cerevisiae* map in the *RAD51* gene, whose sequence predicts a protein with similarities to procaryotic RecA proteins. *Mol. Cell Biol.* **12**: 3224–3234 (1992)

Acs, K., *et al*. The AAA-ATPase VCP/p97 promotes 53BP1 recruitment by removing L3MBTL1 from DNA double-strand breaks. *Nature Struct. Mol. Biol.* **18**: 1345–1350 (2011)

Adimoolam, S., *et al.* HDAC inhibitor PCI-24781 decreases RAD51 expression and inhibits homologous recombination. *PNAS* **104**: 19482–19487 (2007)

Agrawal, N., *et al.* Exome sequencing of head and neck squamous cell carcinoma reveals inactivating mutations in NOTCH1. *Science* **333**: 1154–1157 (2011)

Aguilera, A., and Klein, H. L. Genetic control of intrachromosomal recombination in *Saccharomyces cerevisiae*. I. Isolation and genetic characterization of hyper-recombination mutations. *Genetics.* **119**: 779–790 (1988)

Ahel, I., *et al.* The neurodegenerative disease protein aprataxin resolves abortive DNA ligation intermediates. *Nature* **443**: 713–716 (2006)

Ahmad, F., and Stewart, E. The N-terminal region of the *Schizosaccharomyces pombe* RecQ helicase, Rqh1p, physically interacts with Topoisomerase III andis required for Rqh1p function. *Mol. Genet. Genomics* **273**: 102-114 (2005)

Alarcon-Vargas, D., *et al*. Targeting cyclin D1, a downstream effector of INI1/hSNF5, in rhabdoid tumors. *Oncogene* **25**: 722–734 (2006)

Albulescu, L. O., *et al.* A quantitative, high-throughput reverse genetic screen reveals novel connections between pre-mRNA splicing and 5′- and 3′-end transcript determinants. *PLoS Genet.* **8**: e1002530 (2012)

Amato, A., *et al.* RNAi mediated acute depletion of retinoblastoma protein (pRb) promotes aneuploidy in human primary cells via micronuclei formation. *BMC Cell Biol.* **2**: 79

Ancelin, K., *et al.* Targeting assay to study the cis functions of human telomeric proteins: evidence for inhibition of telomerase by TRF1 and for activation of telomere degradation by TRF2. *Mol. Cell Biol.* **22**: 3474-3487 (2002)

Andres, S. N., *et al.* A human XRCC4-XLF complex bridges DNA. *Nucleic Acids Res.* **40**: 1868–1878 (2012)

Angus-Hill, M. L., *et al.* A Rsc3/Rsc30 zinc cluster dimer reveals novel roles for the chromatin remodeler RSC in gene expression and cell cycle control. *Mol. Cell* **7**: 741–751 (2001)

Antúnez de Mayolo, A., *et al.* Multiple start codons and phosphorylation result in discrete Rad52 protein species. *Nucleic Acids Res.* **34**: 2587-2597 (2006)

Aravind, L., and Koonin, E. V. SAP - a putative DNA-binding motif involved in chromosomal organization. *Trends Biochem. Sci.* **25**: 112–114

Armache, K. J., *et al.* Structural basis of silencing: Sir3 BAH domain in complex with a nucleosome at 3.0 A resolution. *Science* **334**: 977–982 (2011)

Arumugam, P., *et al.* ATP hydrolysis is required for cohesin's association with chromosomes. *Curr. Biol.* **13**: 1941-1953 (2003)

Asp, P., *et al.* Expression of BRG1, a human SWI/SNF component, affects the organisation of actin filaments through the RhoA signalling pathway. *J. Cell Sci.* **115**: 2735–2746 (2002)

Asturias, F. J,. *et al.* Structural analysis of the RSC chromatin-remodeling complex. *PNAS* **99:** 13477–13480 (2002)

Ayoub, N., *et al.* The carboxyl terminus of Brca2 links the disassembly of Rad51 complexes to mitotic entry. *Curr. Biol.* **19**: 1075-1085 (2009)

Badie, S., *et al.* RAD51C facilitates checkpoint signaling by promoting CHK2 phosphorylation. *J. Cell Biol.* **185**: 587-600 (2009)

Baetz, K. K., *et al*. The *ctf13-30/CTF13* genomic haploinsufficiency modifier screen identifies the yeast chromatin remodelling complex RSC, which is required for the establishment of sister chromatid cohesion. *Mol. Cell Biol.* **24:** 1232-1244 (2004)

Balbáz-Martinéz, C., *et al.* Recurrent inactivation of *STAG2* in bladder cancer is not associated with aneuploidy. *Nature Genet.* **45**: 1464-1469 (2013)

Bannister, A. J., *et al.* Spatial distribution of di- and trimethyl lysine 36 of histone H3 at active genes. *J. Biol. Chem.* **280**: 17732–17736 (2005)

Barber, L. J., *et al.* SPAR1/RTEL1 maintains genomic stability by suppressing homologous recombination. *Cell* **135**: 261-271 (2008)

Barber, T. D., *et al.* 2008. Chromatid cohesion defects may underlie chromosome instability in human colorectal cancers. *PNAS* **105:** 3443-3448

Barnhart, M. C., *et al.* HJURP is a CENP-A chromatin assembly factor sufficient to form a functional de novo kinetochore. *J. Cell Biol.* **194**: 229–243 (2011)

Bauerschmidt, C., *et al*. Cohesin promotes the repair of ionizing radiation-induced DNA double-strand breaks in replicated chromatin. *Nucleic Acids Res.* **38**: 477-487 (2010)

Becker, E., *et al.* Detection of a tandem BRCT in Nbs1 and Xrs2 with functional implications in the DNA damage response. *Bioinformatics* **22**: 1289-1292 (2006)

Bennett, C. B., *et al.* Genes required for ionizing radiation resistance in yeast. *Nature Genet.* **29**: 426–434 (2001)

Bernstein, B. E., *et al.* Methylation of histone H3 Lys 4 in coding regions of active genes. *PNAS* **99**: 8695–8700 (2002)

Bernstein, B. E., *et al.* The mammalian epigenome. *Cell* **128**: 669–681 (2007)

Bernstein, N. K., *et al.* The molecular architecture of the mammalian DNA repair enzyme, polynucleotide kinase. *Mol. Cell* **17**: 657–670 (2005)

Bertocci, B., *et al.* Nonoverlapping functions of DNA polymerases mu, lambda, and terminal deoxynucleotidyltransferase during immunoglobulin V(D)J recombination in vivo. *Immunity* **25**: 31-41 (2006)

Beroukhim, R., *et al.* The landscape of somatic copy-number alteration across human cancers. *Nature* **463**: 899–905 (2010)

Beucher, J., *et al.* ATM and Artemis promote homologous recombination of radiation-induced DNA double-strand breaks in G2. *EMBO J.* **28**: 3413–3427

Bewersdorf, J., *et al.* H2AX chromatin structures and their response to DNA damage revealed by 4Pi microscopy. *PNAS* **103**: 18137-18142. (2006)

Bienko, M., *et al.* Ubiquitin-binding domains in translesion synthesis polymerases. *Science* **310**: 1821–1824 (2005)

Birkenbihl, R. P., and Subramani, S. Cloning and characterization of rad21 an essential gene of *Schizosaccharomyces pombe* involved in DNA double-strand-break repair. *Nucleic Acids Res.* **20**: 6605-6611 (1992)

Birrell, G. W., *et al.* Transcriptional response of *Saccharomyces cerevisiae* to DNA-damaging agents does not identify the genes that protect against these agents. *PNAS* **99**: 8778–8783 (2002)

Bishop, A. J., and Schiestl, R. H. Role of homologous recombination in carcinogenesis. *Exp. Mol. Pathol.* **74**: 94-105 (2003)

Black, B. E., *et al.* Structural determinants for generating centromeric chromatin. *Nature.* **430**: 578–582 (2004)

Black, B. E., *et al.* Centromere identity maintained by nucleosomes assembled with histone H3 containing the CENP-A targeting domain. *Mol. Cell.* **25**: 309–322 (2007)

Blier, P. R., *et al.* Binding of Ku protein to DNA. Measurement of affinity for ends and demonstration of binding to nicks. *J. Biol. Chem.* **268**: 7594–7601 (1993)

Blower, M. D., *et al.* Conserved organization of centromeric chromatin in flies and humans. *Dev. Cell* **2**: 319–330 (2002)

Boeckmann, L., *et al.* Phosphorylation of centromeric histone H3 variant regulates chromosome segregation in *Saccharomyces cerevisiae*. *Mol. Biol. Cell* **24**: 2034–2044 (2013)

Bolden, J. E., *et al.* Anticancer activities of histone deacetylase inhibitors. *Nat. Rev. Drug Discov.* **5**: 769–784 (2006)

Bommi-Reddy, A., *et al.* Kinase requirements in human cells: III. Altered kinase requirements in *VHL−/−* cancer cells detected in a pilot synthetic lethal screen. *PNAS* **105**: 16484–16489 (2008)

Bönisch, C., and Hake, S. B. Histone H2A variants in nucleosomes and chromatin: more or less stable? *Nucleic Acids Res.* **40**: 10719-10741 (2012)

Botuyan, M. V., *et al*. Structural basis for the methylation state-specific recognition of histone H4-K20 by 53BP1 and Crb2 in DNA repair. *Cell* **127**: 1361–1373 (2006)

Boulton, S. J., and Jackson, S. P. Identification of a Saccharomyces cerevisiae Ku80 homologue: roles in DNA double strand break rejoining and in telomeric maintenance. *Nucleic Acids Res.* **24**: 4639-4648 (1996)

Bourgo, R. J., *et al.* SWI/SNF Deficiency Results in Aberrant Chromatin Organization, Mitotic Failure, and Diminished Proliferative Capacity. *Mol. Biol. Cell* **20**: 3192-3199 (2009)

Boyer, L. A., *et al.* Functional delineation of three groups of the ATP-dependent family of chromatin remodeling enzymes. *J. Biol. Chem.* **275:** 18864–18870 (2000)

Brough, R., *et al*. APRIN is a cell cycle specific BRCA2-interacting protein required for genome integrity and a predictor of outcome after chemotherapy in breast cancer. *EMBO J.* **31**: 1160-1176 (2012)

Brownlee, P. M., *et al.* Cancer and the bromodomains of BAF180. *Biochem. Soc. Trans.* **40**: 364-369 (2012)

Brownlee, P. M., *et al.* BAF180 promotes cohesion and prevents genome instability and aneuploidy. *Cell Rep.* **6**: 1-9 (2014)

Bryant, H. E., *et al.* Specific killing of BRCA2-deficient tumours with inhibitors of poly(ADP-ribose) polymerase. *Nature* **434**: 913–917 (2005)

Bugreev, D. V., *et al.* Novel pro-and anti-recombination activities of the Bloom's syndrome helicase. *Genes Dev.* **21**: 3085-3094 (2007)

Bui, M., *et al.* Cell-cycle-dependent structural transitions in the human CENP-A nucleosome in vivo. *Cell* **150**: 317–326 (2012)

Bultman, S., *et al*. A Brg1 null mutation in the mouse reveals functional differences among mammalian SWI/SNF complexes. *Mol. Cell* **6**: 1287–1295 (2000)

Burgess, R. C., *et al.* The Slx5-Slx8-complex affects sumoylation of DNA repair proteins and negatively regulates recombination. *Mol. Cell Biol.* **27**: 6153-6162 (2007)

Burkhart, D. L., and Sage, J. Cellular mechanisms of tumour suppression by the retinoblastoma gene. *Nat. Rev. Cancer* **8**: 671-82 (2008)

Burrows, A. E., *et al.* 2010. Polybromo-associated BRG1-associated factor components BRD7 and BAF180 are critical regulators of p53 required for induction of replicative senescence. *PNAS* **107:** 14280-14285

Cairns, B. R., *et al.* RSC, an essential, abundant chromatin-remodeling complex. *Cell* **87**: 1249-1260 (1996)

Cairns, B. R., *et al.* Two functionally distinct forms of the RSC nucleosome-remodeling complex, containing essential AT hook, BAH, and bromodomains. *Mol. Cell* **4**: 715-723 (1999)

Callebaut, I., *et al.* The BAH (bromo-adjacent homology) domain: a link between DNA methylation, replication and transcriptional regulation. *FEBS Lett.* **446**: 189-93 (1999)

Campsteijn, C., *et al.* Reverse genetic analysis of the yeast RSC chromatin remodeler reveals a role for RSC3 and SNF5 homolog 1 in ploidy maintenance. *PLoS Genet.* **3**: e92 (2007)

Canudas, S., *et al.* Protein requirements for sister telomere association in human cells. *EMBO J.* **26**: 4867-4878 (2007)

Canudas, S., and Smith, S. Differential regulation of telomere and centromere cohesion by the Scc3 homologues SA1 and SA2, respectively, in human cells. *J. Cell Biol.* **187**: 165-173 (2009)

Canzio, D., *et al.* Chromodomain-mediated oligomerization of HP1 suggests a nucleosome-bridging mechanism for heterochromatin assembly. *Mol. Cell* **41**: 67–81 (2011)

Cao, R., and Zhang, Y. The functions of E(Z)/EZH2-mediated methylation of lysine 27 in histone H3. *Curr. Opin. Genet. Dev.* **14**: 155–164 (2004)

Caramel, J., *et al.* RhoA-dependent regulation of cell migration by the tumor suppressor hSNF5/INI1. *Cancer Res.* **68**: 6154–6161 (2008)

Carr, A. M., *et al.* Analysis of a histone H2A variant from fission yeast: evidence for a role in chromosome stability. *Mol. Gen. Genet.* **245**: 628–635 (1994)

Carreira, A., *et al.* The BRC repeats of BRCA2 modulate the DNA-binding selectivity of RAD51. *Cell* **136**: 1032-1043 (2009)

Carreira, A., and Kowalczykowski, S. C. Two classes of BRC repeats in BRCA2 promote RAD51 nucleoprotein filament function by distinct mechanisms. *PNAS* **108**: 10448-10453 (2011)

Carretero, M., *et al.* Cohesin ties up the genome. *Curr. Opin. Cell Biol.* **22**: 781-787 (2010)

Carretero, M., *et al.* Pds5B is required for cohesion establishment and Aurora B accumulation at centromeres. *EMBO J.* **32**: 2938-2949 (2013)

Carroll, C. W., *et al.* Centromere assembly requires the direct recognition of CENP-A nucleosomes by CENP-N. *Nat. Cell Biol.* **11**: 896–902 (2009)

Carroll, C. W., *et al.* Dual recognition of CENP-A nucleosomes is required for centromere assembly. *J. Cell Biol.* **189**: 1143–1155 (2010)

Carrozza, M. J., *et al.* Histone H3 methylation by Set2 directs deacetylation of coding regions by Rpd3S to suppress spurious intragenic transcription. *Cell* **123**: 581–592 (2005)

Carter, S. L., *et al.* A signature of chromosomal instability inferred from gene expression profiles predicts clinical outcome in multiple human cancers. *Nat. Genet.* **38**: 1043-1048 (2006)

Cary, R. B., *et al.* DNA looping by Ku and the DNA-dependent protein kinase. *PNAS* 4267–4272 (1997)

Casey, G., *et al.* Functional evidence for a breast cancer growth suppressor gene on chromosome 17. *Hum. Mol. Genet.* **2**: 1921–1927 (1993)

Catania, S., and Allshire, R. C. Anarchic centromeres: deciphering order from apparent chaos. *Curr. Opin. Cell Biol.* **26**: 41-50 (2014)

Cejka, P., *et al.* Rmi1 stimulates decatenation of double Holliday junctions during dissolution by Sgs1-Top3. *Nat. Struc. Mol. Biol.* **17**: 1377-1382 (2010)

Celeste, A., *et al.* Genomic instability in mice lacking histone H2AX. *Science* **296**: 922-927 (2002)

Chaban, Y., *et al.* Structure of a RSC-nucleosome complex and insights into chromatin remodeling. *Nat. Struct. Mol. Biol.* **15**: 1272–1277 (2008)

Chai, B., *et al.* Distinct roles for the RSC and Swi/Snf ATP-dependent chromatin remodelers in DNA double-strand break repair. *Genes Dev.* **19**: 1656–1661 (2005)

Chakraborty, S., *et al.* Identification of genes associated with tumorigenesis of retinoblastoma by microarray analysis. *Genomics* **90**: 344–353 (2007)

Chambers, A. L., and Downs, J. A. The RSC and INO80 chromatin-remodeling complexes in DNA double-strand break repair. *Prog. Mol. Biol. Trans. Sci.* **110**: 230-261 (2012)

Chambers, A. L., *et al.* The BAH domain of Rsc2 is a H3 binding domain. *Nucleic Acids Res.* **41**: 9168-9182 (2013)

Chan, D.A, and Giaccia, A. J. Harnessing synthetic lethal interactions in anticancer drug discovery. *Nat. Rev. Drug Discov.* **10**: 351-364 (2011)

Chan, K. L., *et al.* Cohesin's DNA exit gate is distinct from its entrance gate and is regulated by acetylation. *Cell* **150**: 961-974 (2012)

Chan, K. L., *et al.* Pds5 promotes and protects cohesin acetylation. *PNAS* **110**: 13020-13025

Chandrasekaran, R., and Thompson, M. Polybromo-1-bromodomains bind histone H3 at specific acetyl-lysine positions. *Biochem. Biophys. Res. Commun.* **355**: 661-666 (2007)

Chang, M., *et al.* RMI1/NCE4, a suppressor of genome instability, encodes a member of the RecQ helicase/Topo III complex. *EMBO J.* **24**: 2024-2033 (2005)

Chapman, J. R., and Jackson, S. P. Phospho-dependent interactions between NBS1 and MDC1 mediate chromatin retention of the MRN complex at sites of DNA damage. *EMBO Rep.* **9**: 795-801 (2008)

Chapman, J. R., *et al*. RIF1 is essential for 53BP1-dependent nonhomologous end joining and suppression of DNA double-strand break resection. *Mol. Cell* **49**: 858–871 (2013)

Chapman, M. A., *et al.* Initial genome sequencing and analysis of multiple myeloma. *Nature* **471**: 467–472 (2011)

Charles, G. M., *et al.* Site-specific acetylation mark on an essential chromatin-remodeling complex promotes resistance to replication stress. *PNAS* **108**: 10620-10625 (2011)

Charlop-Powers, Z., *et al.* Structural insights into selective histone H3 recognition by the human Polybromo bromodomain 2. *Cell Res.* **20**: 529-538 (2011)

Chaumeil, J., *et al.* Combined immunofluorescence, RNA fluorescent in situ hybridization, and DNA fluorescent in situ hybridization to study chromatin changes, transcriptional activity, nuclear organization, and X-chromosome inactivation. *Methods Mol. Biol.* **463**: 297-308 (2008)

Chen, J., and Archer, T. K. Regulating SWI/SNF subunit levels via protein-protein interactions and proteasomal degradation: BAF155 and BAF170 limit expression of BAF57. *Mol. Cell Biol.* **25**: 9016–9027 (2005)

Chen, L., *et al.* Promotion of Dnl4-catalyzed DNA end-joining by the Rad50/Mre11/Xrs2 and Hdf1/Hdf2 complexes. *Mol. Cell* **8**:1105-1115 (2001)

Chen, S. H., *et al.* A proteome-wide analysis of kinase-substrate network in the DNA damage response. *J. Biol. Chem.* **285**: 12803-12812 (2010)

Chen, X., *et al.* The Fun30 nucleosome remodeler promotes resection of DNA double-strand break ends. *Nature* **489:** 576-580 (2012)

Cheng, S. W., *et al*. c-MYC interacts with INI1/hSNF5 and requires the SWI/SNF complex for transactivation function. *Nature Genet.* **22**: 102–105 (1999)

Chiang, T., *et al.* Evidence that weakened centromere cohesion is a leading cause of age-related aneuploidy in oocytes. *Curr. Biol.* **20**: 1522-1528 (2010)

Cimini, D., *et al.* Merotelic kinetochore orientation is a major mechanism of aneuploidy in mitotic mammalian tissue cells. *J. Cell Biol.* **153**: 517-527 (2001)

Cimini, D., *et al.* Merotelic kinetochore orientation occurs frequently during early mitosis in mammalian tissue cells and error correction is achieved by two different mechanisms. *J. Cell Sci.* **116**: 4213–4225 (2003)

Ciosk, R., *et al.* Cohesin's binding to chromosomes depends on a separate complex consisting of Scc2 and Scc4 proteins. *Mol. Cell* **5**: 243-254 (2000)

Clapier, C. R., and Cairns, B. R. The biology of chromatin remodeling complexes. *Annu. Rev. Biochem.* **78**: 273-304 (2009)

Clements, P. M., *et al.* The ataxia-oculomotor apraxia 1 gene product has a role distinct from ATM and interacts with the DNA strand break repair proteins XRCC1 and XRCC4. *DNA Repair* **3**: 1493–1502 (2004)

Cohen, R. L., *et al.* Structural and functional dissection of Mif2p, a conserved DNA-binding kinetochore protein. *Mol. Biol. Cell* **19**: 4480-4491 (2008)

Colavito, S., *et al.* Functional significance of the Rad51-Srs2 complex in Rad51 presynaptic filament disruption. *Nucleic Acids Res.* **37**: 6754-6764 (2009)

Collins, N, *et al.* An ACF1-ISWI chromatin-remodeling complex is required for DNA replication through heterochromatin. *Nat. Genet.* **32**: 627–632 (2002)

Compton, D. A. Mechanisms of aneuploidy. *Curr. Opin. Cell Biol.* **23**: 109-113 (2011)

Conde e Silva, N., *et al.* CENP-A-containing nucleosomes: easier disassembly versus exclusive centromeric localization. *J. Mol. Biol.* **370**: 555–573 (2007)

Cook, P. J., *et al.* Tyrosine dephosphorylation of H2AX modulates apoptosis and survival decisions. *Nature* **458**: 591-596 (2009)

Cooper, M. P., *et al.* Ku complex interacts with and stimulates the Werner protein. *Genes Dev.* **14**: 907–912 (2000)

Cordón-Preciado, V., *et al.* Limiting amounts of budding yeast Rad53 S-phase checkpoint activity results in increased resistance to DNA alkylation damage. *Nucleic Acids Res.* **34**: 5852-5862 (2006)

Costantini, S., *et al.* Interaction of the Ku heterodimer with the DNA ligase IV/Xrcc4 complex and its regulation by DNA-PK. *DNA Repair* **6**: 712–722 (2007)

Costello, T., *et al.* The yeast Fun30 and human SMARCAD1 chromatin remodelers promote DNA end resection. *Nature* **489**: 581-584 (2012)

Covo, S., *et al.* Cohesin is limiting for the suppression of DNA damage-induced recombination between homologous chromosomes. *PLoS Genet.* **6**: e1001006 (2010)

Crasta, K., *et al.* DNA breaks and chromosome pulverization from errors in mitosis. *Nature* **482**: 53-58 (2012)

Dalal, Y., *et al.* Structure, dynamics, and evolution of centromeric nucleosomes. *PNAS* **104**: 15974–15981 (2007)

Daley, J. M., *et al.* Nonhomologous end joining in yeast. *Annu. Rev. Genet.* **39**: 431-451 (2005)

Davis, A. P., and Symington, L. S. The yeast recombinatorial repair protein Rad59 interacts with Rad52 and stimulates single-strand annealing. *Genetics* **159**: 515-525 (2001)

Davis, B. J., *et al.* End-bridging is required for pol mu to efficiently promote repair of noncomplementary ends by nonhomologous end joining. *Nucleic Acids Res.* **36**: 3085-3094 (2008)

Davies, A. A., *et al.* Activation of ubiquitin-dependent DNA damage bypass is mediated by replication protein A. *Mol. Cell* **29**: 625–636 (2008)

Davies, O. R., and Pellegrini, L. Interaction with the BRCA2 C terminus protects RAD51-DNA filaments from disassembly by BRC repeats. *Nat. Struct. Mol. Biol.* **14**: 475-483 (2007)

Davis, J. A., and Chen, D. J. DNA double-strand break repair by non-homologous end-joining. *Transl. Cancer Res.* **2**: 130-143 (2013)

De Antoni, A., *et al.* A small-molecule inhibitor of Haspin alters the kinetochore functions of Aurora B. *J. Cell Biol.* **199**: 269-284 (2012)

Deardorff, M. A., *et al.* HDAC8 mutations in Cornelia de Lange syndrome affect the cohesin acetylation cycle. *Nature* **489**: 313-317 (2012)

Deem, A. K., *et al.* Epigenetic regulation of genomic integrity. *Chromosoma* **121**: 131-151 (2012)

DelBove, J., *et al.* Identification of a core member of the SWI/SNF complex, BAF155/SMARCC1, as a human tumor suppressor gene. *Epigenetics* **6**: 1444–1453 (2011)

Dimitriadis, E. K., *et al.* Tetrameric organization of vertebrate centromeric nucleosomes. *PNAS* **107**: 20317–20322 (2010)

Di Virgilio, M., *et al*. rif1 prevents resection of DNA breaks and promotes immunoglobulin class switching. *Science* **399**: 711–715 (2013)

Doheny, K. F., *et al.* Identification of essential components of the *S. cerevisiae* kinetochore. *Cell* **73**: 761-74 (1993)

Doll, E., *et al.* Cohesin and recombination proteins influence G1-to-S transition in azygotic meiosis in *Schizosaccharomyces pombe. Genetics* **180**: 727-740 (2008)

Dou, H., *et al.* Regulation of DNA repair through deSUMOylation and SUMOylation of replication protein A complex. *Mol. Cell* **39**: 333-345 (2010)

Downs, J. A., and Jackson, S. P. A means to a DNA end: the many roles of Ku. *Nat. Rev. Mol. Cell Biol.* **5**: 367–378 (2004)

Draviam, V. M., *et al.* Misorientation and reduced stretching of aligned sister kinetochores promote chromosome missegregation in EB1- or APC-depleted cells. *EMBO J.* **25**: 2814–2827 (2006)

Dreier, M. R., *et al.* Regulation of Sororin by Cdk1-mediated phosphorylation. *J. Cell Sci.* **124**: 2976-2987 (2011)

Druker, B. J., *et al.* Perspectives on the development of a molecularly targeted agent. *Cancer Cell* **1**:31–36 (2002)

Du, J., *et al.* Sth1p, a Saccharomyces cerevisiae Snf2p/Swi2p homolog, is an essential ATPase in RSC and differs from Snf/Swi in its interactions with histones and chromatin-associated proteins. *Genetics* **150**: 987‑1005 (1998)

Duelli, D., and Lazebnik, Y. Cell-to-cell fusion as a link between viruses and cancer. *Nat. Rev. Cancer* **7**: 968-976 (2007)

Duncker, B. P., *et al.* The origin recognition complex protein family. *Genome Biol.* **10**: 214 (2009)

Dunleavy, E., *et al.* Centromeric chromatin makes its mark. *Trends Biochem. Sci.* **30**:172-175 (2005)

Dunleavy, E. M., *et al.* HJURP is a cell-cycle-dependent maintenance and deposition factor of CENP-A at centromeres. *Cell* **137**: 485–497 (2009)

Duong, V., *et al.* Specific activity of class II histone deacetylases in human breast cancer cells. *Mol. Cancer Res.* **6**: 1908-1919 (2008)

Dynek, J. N., and Smith, S. Resolution of sister telomere association is required for progression through mitosis. *Science* **304**: 97-100 (2004)

Eggler, A. L., *et al.* The Rad51-dependent pairing of long DNA substrates is stabilized by replication protein A. *J. Biol. Chem.* **277**: 39280-39288 (2002)

Eot-Houllier, G., *et al.* Histone deacetylase 3 is required for centromeric H3K4 deacetylation and sister chromatid cohesion. *Genes Dev.* **22**: 2639-2644 (2008)

Esashi, F., *et al.* Stabilization of RAD51 nucleoprotein filaments by the C-terminal region of BRCA2. *Nat. Struct. Mol. Biol.* **14**: 468-474 (2007)

Escribano-Diaz, C., *et al*. A cell cycle-dependent regulatory circuit composed of 53BP1–RIF1 and BRCA1–CtIP controls DNA repair pathway choice. *Mol. Cell* **49**: 872–883 (2013)

Euskirchen, G. M., *et al.* Diverse roles and interactions of the SWI/SNF chromatin remodeling complex revealed using global approaches. *PLoS Genet.* **7**: e1002008 (2011)

Fachinetti, D., *et al.* A two-step mechanism for epigenetic specification of centromere identity and function. *Nat. Cell Biol.* **15**: 1056–1066 (2013)

Falck, J., *et al.* Conserved modes of recruitment of ATM, ATR and DNA-PKcs to sites of DNA damage. *Nature* **434**: 605–611 (2005)

Fan, J. Y., *et al.* H2A.Z alters the nucleosome surface to promote HP1alpha-mediated chromatin fiber folding. *Mol. Cell* **16**: 655–661 (2004)

Farcas, A. M., *et al.* Cohesin's concatenation of sister DNAs maintains their intertwining. *Mol. Cell* **44**: 97-107 (2011)

Farmer, H., *et al.* Targeting the DNA repair defect in *BRCA* mutant cells as a therapeutic strategy. *Nature* **434**: 917–921 (2005)

Faucher, D., and Wellinger, R. J. Methylated H3K4, a transcription-associated histone modification, is involved in the DNA damage response pathway. *PLoS Genet.* **6**: e1001082 (2010)

Fay, A., *et al.* Cohesin selectively binds and regulates genes with paused RNA polymerase. *Curr. Biol.* **11**: 1624-1634 (2011)

Feng, L., *et al.* RIF1 counteracts BRCA1-mediated end resection during DNA repair. *J. Biol. Chem.* **288**: 11135–11143 (2013)

Feng, Z., *et al.* Rad52 inactivation is synthetically lethal with BRCA2 deficiency. *PNAS* **108**: 686-691 (2011)

Ferreira, H., *et al.* Histone modifications influence the action of Snf2 family remodelling enzymes by different mechanisms. *J. Mol. Biol.* **374**: 563–579

(2007)

Feytout, A., *et al.* Psm3 acetylation on conserved lysine residues is dispensable for viability in fission yeast but contributes to Eso1-mediated sister chromatid cohesion by antagonizing Wapl. *Mol. Cell Biol.* **31**: 1771-1786 (2011)

Filippova, G. N. Genetics and epigenetics of the multifunctional protein CTCF. *Curr. Top. Dev. Biol.* **80**: 337-360 (2008)

Fischle, W., *et al.* Molecular basis for the discrimination of repressive methyllysine marks in histone H3 by Polycomb and HP1 chromodomains. *Genes Dev.* **17**: 1870–1881 (2003)

Fischle, W., *et al.* Regulation of HP1–chromatin binding by histone H3 methylation and phosphorylation. *Nature* **438**: 1116–1122 (2005)

Floer, M., *et al.* A RSC/nucleosome complex determines chromatin architecture and facilitates activator binding. *Cell* **141:** 407–418 (2010)

Florio, C., *et al.* A study of biochemical and functional interactions of Htl1p, a putative component of the Saccharomyces cerevisiae, Rsc chromatin-remodeling complex. *Gene* **395**: 72–85 (2007)

Flott, S., *et al.* Regulation of Rad51 function by phosphorylation. *EMBO Rep.* **12**: 833-839 (2011)

Folco, H. D., *et al.* Heterochromatin and RNAi are required to establish CENP-A chromatin at centromeres. *Science* **319**: 94–97 (2008)

Foltz, D. R., *et al.* Centromere-specific assembly of CENP-A nucleosomes is mediated by HJURP. *Cell* **137**: 472–484 (2009)

Fong, P. C., *et al.* Inhibition of poly(ADP-ribose) polymerase in tumors from BRCA mutation carriers. *N. Engl. J. Med.* **361**: 123–134 (2009)

Fradet-Turcotte, A., *et al*. 53BP1 is a reader of the DNA-damage-induced H2A Lys 15 ubiquitin mark. *Nature* **499**: 50–54 (2013)

Fraga, M. F., *et al.* Loss of acetylation at Lys16 and trimethylation at Lys20 of histone H4 is a common hallmark of human cancer. *Nat Genet.* **37**: 391–400 (2005)

Furuyama, S., and Biggins, S. Centromere identity is specified by a single centromeric nucleosome in budding yeast. *PNAS* **104**: 14706–14711 (2007)

Gadd, S., *et al.* Rhabdoid tumor: gene expression clues to pathogenesis and potential therapeutic targets. *Lab. Invest.* **90**: 724–738 (2010)

Galanty, Y., *et al.* Mammalian SUMO E3-ligases PIAS1 and PIAS4 promote responses to DNA double-strand breaks. *Nature* **462**: 935-939 (2009)

Gandhi, R., *et al.* Human Wapl is a cohesin-binding protein that promotes sister chromatid resolution in mitotic prophase. *Curr. Biol.* **16**: 2406-2417 (2006)

Ganem, N. J., *et al.* Tetraploidy, aneuploidy and cancer. *Curr. Opin. Genet. Dev.* **17**: 157-162 (2007)

Gao, X,. *et al*. ES cell pluripotency and germ-layer formation require the SWI/SNF chromatin remodeling component BAF250a. *PNAS* **105**: 6656–6661 (2008)

Garabedian, M. V., *et al.* The double-bromodomain proteins Bdf1 and Bdf2 modulate chromatin structure to regulate S-phase stress response in *Schizosaccharomyces pombe*. *Genetics* **190**: 487–500 (2012)

Gari, K., *et al.* The Fanconi anemia protein FANCM can promote branch migration of Holliday junctions and replication forks. *Mol. Cell* **29**: 141-148 (2008)

Gassmann, R., *et al.* An inverse relationship to germline transcription defines centromeric chromatin in *C. elegans*. *Nature* **484:** 534-357 (2012)

Gartenberg, M. R. The Sir proteins of Saccharomyces cerevisiae: mediators of transcriptional silencing and much more. *Curr. Opin. Microbiol.* **3**: 132-137 (2000)

Gatti, M., *et al*. A novel ubiquitin mark at the N-terminal tail of histone H2As targeted by RNF168 ubiquitin ligase. *Cell Cycle* **11**: 2538–2544 (2012)

Gerlich, D., *et al.* Live-cell imaging reveals a stable cohesin-chromatin interaction after but not before DNA replication. *Curr. Biol.* **16**: 1571-1578 (2006)

Ghiselli, G., and Iozzo, R. V. Overexpression of bamacan/SMC3 causes transformation. *J. Biol. Chem.* **275**: 20235-20238 (2000)

Ghiselli, G., *et al.* The cohesin SMC3 is a target for the beta-catenin/TCF4 transactivation pathway. *J. Biol. Chem.* **278**: 20259-20267 (2003)

Gnarra, J. R., *et al.* Mutations of the *VHL* tumour suppressor gene in renal carcinoma. *Nature Genet.* **7**: 85–90 (1994)

Gonzalo, S., *et al.* Role of the RB1 family in stabilizing histone methylation at constitutive heterochromatin. *Nat. Cell Biol.* **7**: 420–428 (2005)

Goodwin, G. H., and Nicolas, R. H. The BAH domain, polybromo and the RSC chromatin remodelling complex. *Gene* **268**: 1-7 (2001)

Gordon, D. J., *et al.* Causes and consequences of aneuploidy in cancer. *Nat. Rev. Genet.* **13**: 189-203 (2012)

Gottlieb, S., and Esposito, R. E. A new role for a yeast transcriptional silencer gene, SIR2, in regulation of recombination in ribosomal DNA. *Cell* **56**: 771-776 (1989)

Gottlieb, T. M., and Jackson, S. P. The DNA-dependent protein kinase: requirement for DNA ends and association with Ku antigen. *Cell* **72**: 131–142 (1993)

Goutte-Gattat, D., *et al.* Phosphorylation of the CENP-A amino-terminus in mitotic centromeric chromatin is required for kinetochore function. *PNAS* **110**: 8579–8584 (2013)

Gravel, S., *et al.* DNA helicases Sgs1 and BLM promote DNA double-strand break resection. *Genes Dev.* **22**: 2767-2772 (2008)

Greaves, I. K., *et al.* H2A.Z contributes to the unique 3D structure of the centromere. *PNAS* **104**: 525–530

(2007)

Grewal, S. I. RNAi-dependent formation of heterochromatin and its diverse functions. *Curr. Opin. Genet. Dev.* **20**: 134–141 (2010)

Gruber, S., *et al.* Chromosomal cohesin forms a ring. *Cell* **112**: 765-777 (2003)

Gruber, S., *et al.* Evidence that loading of cohesin onto chromosomes involves opening of its SMC hinge. *Cell* **127**: 523-537 (2006)

Grundy, G. J., *et al.* APLF promotes the assembly and activity of non-homologous end joining protein complexes. *EMBO J.* **32**: 112–125 (2013)

Gu, J., *et al.* XRCC4:DNA ligase IV can ligate incompatible DNA ends and can ligate across gaps. *EMBO J.* **26**: 1010–1023 (2007)

Guacci, V., and Koshland, D. Cohesin-independent segregation of sister chromatids in budding yeast. *Mol. Biol. Cell* **23**: 729-739 (2012)

Guan, B., *et al.* ARID1A, a factor that promotes formation of SWI/SNF-mediated chromatin remodeling, is a tumor suppressor in gynecologic cancers. *Cancer Res.* **71**: 6718–6727 (2011)

Guarente, L. Synthetic enhancement in gene interaction: a genetic tool come of age. *Trends Genet.* **9**: 362–366 (1993)

Guidi, C. J., *et al*. Disruption of Ini1 leads to peri-implantation lethality and tumorigenesis in mice. *Mol. Cell Biol.* **21**: 3598–3603 (2001)

Guidi, C. J., *et al*. Functional interaction of the retinoblastoma and Ini1/Snf5 tumor suppressors in cell growth and pituitary tumorigenesis. *Cancer Res.* **66**: 8076-8082 (2006)

Guillou, E., *et al.* Cohesin organizes chromatin loops at DNA replication factories. *Genes Dev.* **24**: 2812-2822 (2010)

Gunawan, B., *et al.* Prognostic impacts of cytogenetic findings in clear cell renal cell carcinoma: gain of 5q31-qter predicts a distinct clinical phenotype with favorable prognosis. *Cancer Res.* **61**: 7731-7738 (2001)

Guo, G., *et al.* Whole-genome and whole-exome sequencing of bladder cancer identifies frequent alterations in genes involved in sister chromatid cohesion and segregation. *Nature Genet.* **45**: 1459-1463 (2013)

Gupta, A., *et al.* Involvement of human MOF in ATM function. *Mol. Cell Biol.* **25**: 5292-5305 (2005)

Guse, A., *et al.* In vitro centromere and kinetochore assembly on defined chromatin templates. *Nature* **477**: 354–358 (2011)

Gutiérrez-Caballero, C., *et al.* Shugoshins: from protectors of cohesion to versatile adaptors at the centromere. *Trends Genet.* **28**: 351-360 (2012)

Haber, J. E. Mating-type gene switching in *Saccharomyces cerevisiae. Annu. Rev. Genet.* **32**: 561-599. (1998)

Haering, C. H., *et al.* Molecular architecture of SMC proteins and the yeast cohesin complex. *Mol. Cell* **9**: 773-88 (2002)

Hagemann, C., *et al.* The cohesin-interacting protein, precocious dissociation of sisters 5A/sister chromatid cohesion protein 112, is up-regulated in human astrocytic tumors. *Int. J. Mol. Med.* **27**: 39-51 (2011)

Haigis, M. C., and Sinclair, D. A. Mammalian sirtuins: biological insights and disease relevance. *Annu. Rev. Pathol.* **5**: 253-295 (2010)

Hajdu, I., *et al*. Wolf–Hirschhorn syndrome candidate 1 is involved in the cellular response to DNA damage. *PNAS* **108**: 13130–13134 (2011)

Hajra, S., *et al.* The centromere-specific histone variant Cse4p (CENP-A) is essential for functional chromatin architecture at the yeast 2μm circle partitioning locus and promotes equal plasmid segregation. *J. Cell Biol.* **174**: 779–790 (2006)

Hall, J. M., *et al.* Linkage of early-onset familial breast cancer to chromosome 17q21. *Science* **250**: 1684-1689 (1990)

Hall J, M., *et al.* Closing in on a breast cancer gene on chromosome 17q. *Am. J. Hum. Genet.* **50**: 1235–1242 (1992)

Hallson, G., *et al.* The Drosophila cohesin subunit Rad21 is a trithorax group (trxG) protein. *PNAS* **105**: 12405-12410 (2008)

Hammel, M., *et al.* Ku and DNA-dependent protein kinase dynamic conformations and assembly regulate DNA binding and the initial non-homologous end joining complex. *J. Biol. Chem.* **285**: 1414–1423 (2010)

Harrison, J. C., and Haber, J. E. Surviving the breakup: the DNA damage checkpoint. *Annu. Rev. Genet.* **40**: 209-235 (2006)

Hartley, K. O., *et al.* DNA-dependent protein kinase catalytic subunit: a relative of phosphatidylinositol 3-kinase and the ataxia telangiectasia gene product. *Cell* 1995 **82**: 849–856 (1995)

Hartman, J. L., *et al.* Principles for the buffering of genetic variation. *Science* **291**: 1001–1004 (2001)

Hartman, T., *et al.* Pds5 is an essential chromosomal protein required for both sister chromatid cohesion and condensation in *Saccharomyces cerevisiae. J. Cell Biol.* **151**: 613-626 (2000)

Hassig, C. A., *et al.* KD5170, a novel mercaptoketone-based histone deacetylase inhibitor that exhibits broad spectrum antitumor activity in vitro and in vivo. *Mol. Cancer Ther.* **7**: 1054-1065 (2008)

Hassold, T., and Hunt, P. To err (meiotically) is human: the genesis of human aneuploidy. *Nat. Rev. Genet.* **2**: 280-291 (2001)

Hasson, D., *et al.* The octamer is the major form of CENP-A nucleosomes at human centromeres. *Nat. Struct. Mol. Biol.* **20**: 687–695 (2013)

Haughtaling, B. R., *et al.* A dynamic molecular link between the telomere length regulator TRF1 and the chromosome end protector TRF2. *Curr. Biol.* **14**: 1621-1631 (2004)

Hays, S. L., *et al.* Complex formation in yeast double-strand break repair: participation of Rad51, Rad52, Rad55, and Rad57 proteins. *PNAS* **92**: 6925-6929 (1995)

Hellman, S., and Vokes, E. E. Advancing current treatments for cancer. *Sci. Am.* **275** :118–123 (1996)

Hemmerich, P., *et al.* Interaction of yeast kinetochore proteins with centromere-protein/transcription factor Cbf1. *PNAS* **97**: 12583-12588 (2000)

Henry-Mowatt, J., *et al.* XRCC3 and Rad51 modulate replication fork progression on damaged vertebrate chromosomes. *Mol. Cell.* **11**: 1109-1117 (2003)

Herman, J. G., *et al.* Silencing of the *VHL* tumor-suppressor gene by DNA methylation in renal carcinoma. *PNAS* **91**: 9700–9704 (1994)

Hernando, E., *et al.* Rb inactivation promotes genomic instability by uncoupling cell cycle progression from mitotic control. *Nature* **430**: 797-802 (2004)

Herzberg, K., *et al.* Phosphorylation of Rad55 on serines 2, 8, and 14 is required for efficient homologous recombination in the recovery of stalled replication forks. *Mol. Cell Biol.* **26**: 8396-8409 (2006)

Hickman, M. A., and Rusche, L. N. Transcriptional silencing functions of the yeast protein Orc1/Sir3 subfunctionalized after gene duplication. *PNAS* **107**: 19384–19389 (2010)

Hirota, T., *et al.* Histone H3 serine 10 phosphorylation by Aurora B causes HP1 dissociation from heterochromatin. *Nature* **438:** 1176–1180 (2005)

Ho, L., *et al.* An embryonic stem cell chromatin remodeling complex, esBAF, is an essential component of the core pluripotency transcriptional network. *PNAS* **106**: 5187–5191 (2009)

Hoege, C., *et al. RAD6*-dependent DNA repair is linked to modification of PCNA by ubiquitin and SUMO. *Nature* **419**: 135–141 (2002)

Höglund, M., *et al.*Dissecting karyotypic patterns in renal cell carcinoma: an analysis of the accumulated cytogenetic data. *Cancer Genet. Cytogenet.* **153**: 1-9 (2004)

Honda, M., *et al.* Tyrosine phosphorylation enhances RAD52-mediated annealing by modulating its DNA binding. *EMBO J.* **30**: 3368-3382 (2011)

Hopfner, K. P., *et al.* Structural biochemistry and interaction architecture of the DNA double-strand break repair Mre11 nuclease and Rad50-ATPase. *Cell* **105**: 473-85 (2001)

Hopfner, K. P., *et al.* The Rad50 zinc-hook is a structure joining Mre11 complexes in DNA recombination and repair. *Nature* **418**: 562-6 (2002)

Horikawa, I., and Barrett, J. C. cDNA cloning of the human polybromo-1 gene on chromosome 3p21. *DNA Seq.* 13: 211-215 (2002)

Horn, P. J., and Peterson, C. L. Molecular biology. Chromatin higher order folding--wrapping up transcription. *Science* **297**: 1824-1827 (2002)

Hou, C., *et al.* Cell type specificity of chromatin organization mediated by CTCF and cohesin. *PNAS* **107**: 3651-3656 (2010)

Hou, F. J., and Zou, H. Two human orthologues of Eco1/Ctf7 acetyltransferases are both required for proper sister chromatid cohesion. *Mol. Biol. Cell* **16**: 3908-3918 (2005)

Hsiao, K. Y., and Mizzen, C. A. Histone H4 deacetylation facilitates 53BP1 DNA damage signaling and double-strand break repair. *J. Mol. Cell Biol.* **5**: 157–165 (2013)

Hsiao, S. J., and Smith, S. Sister telomeres rendered dysfunctional by persistent cohesion are fused by NHEJ. *J. Cell Biol.* **184**: 515-526 (2009)

Hsu, H. C., *et al*. Structural basis for origin recognition complex 1 protein-silence information regulator 1 protein interaction in epigenetic silencing. *PNAS* **102**: 8519-24 (2005)

Hsu, H. L., *et al.* Defining interactions between DNA-PK and ligase IV/XRCC4. *DNA Repair* **1**: 225–235 (2001)

Hsu, J. M., *et al.* The yeast RSC chromatin-remodeling complex is required for kinetochore function in chromosome segregation. *Mol. Cell Biol.* **23**: 3202-3215 (2003)

Hu, B., *et al.* ATP hydrolysis is required for relocating cohesin from sites occupied by its Scc2/4 loading complex. *Curr. Biol.* **21**: 12-24 (2011)

Huang, J., *et al.* The RSC nucleosome-remodeling complex is required for cohesin's association with chromosome arms. *Mol. Cell* **23:** 739-750 (2004)

Huang, J. *et al.* Inhibition of homologous recombination by a cohesin-associated clamp complex recruited to the rDNA recombination enhancer. *Genes Dev.* **20**: 2887-2901 (2006)

Huang, J., *et al.* SOSS complexes participate in the maintenance of genomic stability. *Mol. Cell* **35**: 384-393 (2009)

Huber, K., *et al.* Inhibitors of histone deacetylases: correlation between isoform specificity and reactivation of HIV type 1 (HIV-1) from latently infected cells. *J. Biol. Chem.* **286**: 22211-22218 (2011)

Hudson, B. P., *et al.* Solution structure and acetyl-lysine binding activity of the GCN5 bromodomain. *J. Mol. Biol.* **304**: 355-370 (2000)

Huen, M. S. Y., *et al*. RNF8 transduces the DNA-damage signal via histone ubiquitylation and checkpoint protein assembly. *Cell* **131**: 901–914 (2007)

Hutchinson, L., *et al.* Targeted therapies: PARP inhibitor olaparib is safe and effective in patients with BRCA1 and BRCA2 mutations. *Nature Rev. Clin. Oncol.* **7**: 549 (2010)

Huyen, Y., *et al*. Methylated lysine 79 of histone H3 targets 53BP1 to DNA double-strand breaks. *Nature* **432**: 406–411 (2004)

Iles, N., *et al.* APLF (C2orf13) is a novel human protein involved in the cellular response to

chromosomal DNA strand breaks. *Mol. Cell Biol.* **27**: 3793–3803 (2007)

Iovino, F., *et al.* RB acute loss induces centrosome amplification and aneuploidy in murine primary fibroblasts. *Mol. Cancer* **5**: 38 (2006)

Ira, G., *et al.* Srs2 and Sgs1-Top3 suppress crossovers during double-strand break repair in yeast. *Cell* **115**: 401-411 (2003)

Isaac, C. E., *et al.* The retinoblastoma protein regulates pericentric heterochromatin. *Mol. Cell. Biol.* **26**: 3659-3671 (2006)

Isakoff, M. S., *et al.* Inactivation of the Snf5 tumor suppressor stimulates cell cycle progression and cooperates with p53 loss in oncogenic transformation. *PNAS* **102**: 17745-17750 (2005)

Jackson, J. D., and Gorovsky, M. A. Histone H2A.Z has a conserved function that is distinct from that of the major H2A sequence variants. *Nucleic Acids Res.* **28**: 3811–3816 (2000)

Jacobs, S. A., *et al.* Structure of HP1 chromodomain bound to a lysine 9–methylated histone H3 tail. *Science* **295**: 2080–2083 (2002)

Jacobson, R. H., *et al.* Structure and function of a human TAFII250 double bromodomain module. *Science* **288**: 1422–1425 (2000)

Jagani, Z., *et al*. Loss of the tumor suppressor Snf5 leads to aberrant activation of the Hedgehog-Gli pathway. *Nature Med.* **16**: 1429–1433 (2010)

Jansen, L. E., *et al.* Propagation of centromeric chromatin requires exit from mitosis. *J. Cell Biol.* **176**: 795–805 (2007)

Javaheri, A., *et al.* Yeast G1 DNA damage checkpoint regulation by H2A phosphorylation is independent of chromatin remodeling. *PNAS* **103**: 13771-13776 (2006)

Jazayeri, A., *et al.* ATM- and cell cycle-dependent regulation of ATR in response to DNA double-strand breaks. *Nat. Cell Biol.* **8**: 37-45 (2006)

Jeggo, P. A., *et al.* The role of homologous recombination in radiation-induced double-strand break repair. *Radiother. Oncol.* **101**: 7–12 (2011)

Jenuwein, T., and Allis, C. D. Translating the histone code. *Science* **293**: 1074–1080 (2001)

Jeong, K. W., *et al.* Recognition of enhancer element-specific histone methylation by TIP60 in transcriptional activation. *Nat. Struct. Mol. Biol.* **18**: 1358–1365 (2011)

Jeyaprakash, A. A., *et al.* Structural basis for the recognition of phosphorylated histone H3 by the survivin subunit of the chromosomal passenger complex. *Structure* **19**: 1625–1634 (2011)

Jiao, Y., *et al.* Exome sequencing identifies frequent inactivating mutations in BAP1, ARID1A and PBRM1 in intrahepatic cholangiocarcinomas. *Nat. Genet.* **45**: 1470-3 (2013)

Johnson, R. D., and Symington, L. S. Functional differences and interactions among the putative RecA homologs Rad51, Rad55, and Rad57. *Mol. Cell Biol.* **15**: 4843-4850 (1995)

Jones, S., *et al.* Core signaling pathways in human pancreatic cancers revealed by global genomic analyses. *Science* **321**: 1801–1806 (2008)

Joshi, A. A., *et al.* Eaf3 chromodomain interaction with methylated H3–K36 links histone deacetylation to Pol II elongation. *Mol. Cell* **20**: 971–978 (2005)

Jungmichel, S., and Stucki, M. MDC1: The art of keeping things in focus. *Chromosoma* **119**: 337-349 (2010)

Junop, M. S., *et al.* Crystal structure of the Xrcc4 DNA repair protein and implications for end joining. *EMBO J.* **19**: 5962–5970

Kaeser, M. D., *et al.* BRD7, a novel PBAF-specific SWI/SNF subunit, is required for target gene activation and repression in embryonic stem cells. *J. Biol. Chem.* **283**: 32254–32263 (2008)

Kagansky, A., *et al.* Synthetic heterochromatin bypasses RNAi and centromeric repeats to establish functional centromeres. *Science* **324**: 1716–1719 (2009)

Kagey, M. H., *et al.* Mediator and cohesin connect gene expression and chromatin architecture. *Nature* **467**: 430-435 (2010)

Kaidi, A., and Jackson, S. P. KAT5 tyrosine phosphorylation couples chromatin sensing to ATM signalling. *Nature* **498**: 70-74 (2013)

Kanno, S., *et al.* A novel human AP endonuclease with conserved zinc-finger-like motifs involved in DNA strand break responses. *EMBO J.* **26**: 2094–2103 (2007)

Kannouche, P. L., *et al.* Interaction of human DNA polymerase η with monoubiquitinated PCNA; a possible mechanism for the polymerase switch in response to DNA damage. *Mol. Cell* **14**: 491–500 (2004)

Kapoor, T. M., *et al.* Probing spindle assembly mechanisms with monastrol, a small molecule inhibitor of the mitotic kinesin, Eg5. *J. Cell Biol.* **150**: 975-988 (2000)

Karagiannis, T. C., *et al.* Disparity of histone deacetylase inhibition on repair of radiation-induced DNA damage on euchromatin and constitutive heterochromatin compartments. *Oncogene* **26**: 3963–3971 (2007)

Karlsson, R., *et al.* Rho GTPase function in tumorigenesis. *Biochim. Biophys. Acta* **1796**: 91–98 (2009)

Karmakar, P., *et al.* Ku heterodimer binds to both ends of the Werner protein and functional interaction occurs at the Werner N-terminus. *Nucleic Acids Res.* **30**: 3583–3591 (2002)

Kato, H., *et al.* A conserved mechanism for centromeric nucleosome recognition by centromere protein CENP-C. *Science* **340**: 1110–1113 (2013)

Kawauchi, S., *et al.* Multiple organ system defects and transcriptional dysregulation in the Nipbl(+/-) mouse, a model of Cornelia de Lange Syndrome. *PLoS Genet.* **5**: e1000650

Kelly, A. E., *et al.* Survivin reads phosphorylated histone H3 threonine 3 to activate the mitotic kinase Aurora B. *Science* **330**: 235-239 (2010)

Kelley, L. A., and Sternberg, M. J. Protein structure prediction on the Web: a case study using the Phyre server. *Nat. Protoc.* **4**: 363-371 (2009)

Kennison, J. A., and Tamkun, J. W. Dosage-dependent modifiers of polycomb and antennapedia mutations in *Drosophila*. *PNAS* **85**: 8136–8140 (1988)

Kennison, J. A. The Polycomb and trithorax group proteins of *Drosophila*: trans-regulators of homeotic gene function. *Annu. Rev. Genet.* **29**: 289–303 (1995)

Kent, N. A., *et al.* Dual chromatin remodeling roles for RSC during DNA double strand break induction and repair at the yeast MAT locus. *J. Biol. Chem.* **282**: 27693–27701 (2007)

Keogh, M. C., *et al.* Cotranscriptional Set2 methylation of histone H3 lysine 36 recruits a repressive Rpd3 complex. *Cell* **123**: 593–605 (2005)

Khanna, K. K., and Jackson, S. P. DNA double-strand breaks: signaling, repair and the cancer connection. *Nat. Genet.* **27**:247–254 (2001)

Kia, S. K., *et al.* SWI/SNF mediates polycomb eviction and epigenetic reprogramming of the INK4b-ARF-INK4a locus. *Mol. Cell Biol.* **28**: 3457–3464 (2008)

Kidder, B. L., *et al.* SWI/SNF-Brg1 regulates self-renewal and occupies core pluripotency-related genes in embryonic stem cells. *Stem Cells* **27**: 317–328 (2009)

Kim, B. J., *et al.* Genome-wide reinforcement of cohesin binding at pre-existing cohesin sites in response to ionizing radiation in human cells. *J. Biol. Chem.* **285**: 22784-22792 (2010)

Kim, J. A., *et al.* Heterochromatin is refractory to gamma-H2AX modification in yeast and mammals. *J. Biol. Chem.* **178**: 209-218 (2007)

Kim, M. S., *et al.* Histone deacetylases induce angiogenesis by negative regulation of tumor suppressor genes. *Nat. Med.* **7**: 437–443 (2001)

Kim, M. S., *et al.* Frameshift mutations of chromosome cohesion-related genes *SGOL1* and *PDS5B* in gastric and colorectal cancers with high microsatellite instability. *Hum. Pathol.* **44:** 2234-2240 (2013)

Kim, S. H., *et al.* TIN2, a new regulator of telomere length in human cells. *Nat. Genetics* **23**: 405-412 (1999)

Kim, S. T., *et al.* Specific recruitment of human cohesin to laser-induced DNA damage. *J. Biol. Chem.* **277**: 45149-45153 (2002)

Kim, S. T., *et al.* Involvement of the cohesin protein, Smc1, in Atm-dependent and independent responses to DNA damage. *Genes Dev.* **16**: 560-570 (2002)

Kitagawa, R., *et al.* Phosphorylation of SMC1 is a critical downstream event in the ATM-NBS1-BRCA1 pathway. *Genes Dev.* **18**: 1423-1438 (2004)

Kitamura, E., *et al.* Kinetochore microtubule interaction during S phase in *Saccharomyces cerevisiae*. *Genes Dev.* **21**: 3319-3330 (2007)

Kitano, H., and Yuan, Z. M. Regulation of ionizing radiation-induced Rad52 nuclear foci formation by c-Abl-mediated phosphorylation. *J. Biol. Chem.* **277**: 48944-48948 (2002)

Klein, F., *et al.* A central role for cohesins in sister chromatid cohesion, formation of axial elements, and recombination during yeast meiosis. *Cell* **98**: 91-103 (1999)

Klochendler-Yeivin, A,. *et al*. The murine SNF5/INI1 chromatin remodeling factor is essential for embryonic development and tumor suppression. *EMBO Rep.* **1**: 500–506 (2000)

Koch, C. A., *et al.* Xrcc4 physically links DNA end processing by polynucleotide kinase to DNA ligation by DNA ligase IV. *EMBO J.* **23**: 3874–3885 (2004)

Koerber, R. T., *et al.* Interaction of transcriptional regulators with specific nucleosomes across the *Saccharomyces* genome. Mol. Cell **35**: 889–902 (2009)

Kogut, I., *et al.* The Scc2/Scc4 cohesin loader determines the distribution of cohesin on budding yeast chromosomes. *Genes Dev.* **23**: 2345-2357 (2009)

Kolas, N. K., *et al*. Orchestration of the DNA-damage response by the RNF8 ubiquitin ligase. *Science* **318**: 1637–1640 (2007)

Kolodner, R. D., *et al.* Aneuploidy drives a mutator phenotype in cancer. *Science* **333**: 942-943 (2011)

Kon, A., *et al.* Recurrent mutations in multiple components of the cohesin complex in myeloid neoplasms. *Nature Genet.* **45**: 1232-1237 (2013)

Kong, X., *et al.* Distinct functions of human cohesin-SA1 and cohesin-SA2 in DSB repair. *Mol. Cell Biol.* **34**: 685-698 (2014)

Kops, G. J. The kinetochore and spindle checkpoint in mammals. *Front. Biosci.* **13**: 3606-3620 (2008)

Kovacs, G., *et al.* Molecular cytogenetics of renal cell tumors. *Adv. Cancer Res.* **62**: 89-124 (1993)

Koyama, H., *et al.* Abundance of the RSC nucleosome-remodeling complex is important for the cells to tolerate DNA damage in Saccharomyces cerevisiae. *FEBS Lett.* **531**: 215–221 (2002)

Kreis, N. N., *et al.* p21Waf1/Cip1 deficiency causes multiple mitotic defects in tumor cells. *Oncogene* (in press) (2013)

Krejci, L., *et al.* Interaction with Rad51 is indispensable for recombination mediator function of Rad52. *J. Biol. Chem.* **277**: 40132-40141 (2002)

Krejci, L., *et al*. DNA helicase Srs2 disrupts the Rad51 presynaptic filament. *Nature* **423**: 305–309 (2003)

Krejci, L., *et al.* Role of ATP hydrolysis in the antirecombinase function of *Saccharomyces cerevisiae* Srs2 protein. *J. Biol. Chem.* **279**: 23193-23199 (2004)

Krejci, L., *et al.* Homologous recombination and its regulation. *Nucleic Acids Res.* **40**: 5795-5818 (2012)

Kueng, S., *et al.* Wapl controls the dynamic association of cohesin with chromatin. *Cell* **127**: 955-967 (2006)

Kuo, A. J., *et al.* The BAH domain of ORC1 links H4K20me2 to DNA replication licensing and Meier-Gorlin syndrome. *Nature* **484**: 115–119 (2012)

Kusumoto, R., *et al.* Werner protein cooperates with the XRCC4-DNA ligase IV complex in end-processing. *Biochemistry* **47**: 7548–7556 (2008)

Kuznetsov, S., *et al.* RAD51C deficiency in mice results in early prophase I arrest in males and sister chromatid separation at metaphase II in females. *J. Cell Biol.* **176**: 581-592 (2007)

Kwon, S. J., *et al.* ATM-mediated phosphorylation of the chromatin remodeling enzyme BRG1 modulates DNA double-strand break repair. *Oncogene* (in press) (2014)

Labib, K., and De Piccoli, G. Surviving chromosome replication: the many roles of the S-phase checkpoint pathway. *Philos. Trans. R. Soc. Lond. B. Biol. Sci.* **366**: 3554-3561 (2011)

Lachner, M., *et al.* Methylation of histone H3 lysine 9 creates a binding site for HP1 proteins. *Nature* **410**: 116–120 (2001)

Lampson, M. A., and Cheeseman, I. M. Sensing centromere tension: Aurora B and the regulation of kinetochore function. *Trends Cell Biol.* **21**: 133-140 (2011)

Lange, M., *et al.* Regulation of muscle development by DPF3, a novel histone acetylation and methylation reader of the BAF chromatin remodeling complex. *Genes Dev.* **22**: 2370–2384 (2008)

Lara-Gonzalez, P., *et al.* The spindle assembly checkpoint. *Curr. Biol.* **22**: 966-980 (2012)

Lechner, J., and Carbon, J. A 240 kd multisubunit protein complex, CBF3, is a major component of the budding yeast centromere. *Cell* **64**: 717-725 (1991)

Lee, H. S. *et al.* A cooperative activation loop among SWI/SNF, gamma-H2AX and H3 acetylation for DNA double-strand break repair. *EMBO J.* **29**: 1434-1445 (2010)

Lee, J. H., and Paull, T. T. Activation and regulation of ATM kinase activity in response to DNA double-strand breaks. *Oncogene* 2007 **26**: 7741-7748 (2007)

Lee, J. W., *et al.* Implication of DNA polymerase lambda in alignment-based gap filling for nonhomologous DNA end joining in human nuclear extracts. *J. Biol. Chem.* **279**: 805-811 (2004)

Lee, S. K., *et al.* Requirement of yeast *SGS1* and *SRS2* genes for replication and transcription. *Science.* **286**: 2339–2342 (1999)

Lehmann, A. R., *et al.* Translesion synthesis: Y-family polymerases and the polymerase switch. *DNA Repair.* **6**: 891–899 (2007)

Lemon, B., *et al.* Selectivity of chromatin-remodelling cofactors for ligand-activated transcription. *Nature* **414**: 924–928 (2001)

Lengauer, C., *et al.* Genetic instability in colorectal cancers. *Nature* **386**: 623-627 (1997)

Leschziner, A. E., *et al.* Conformational flexibility in the chromatin remodeler RSC observed by electron microscopy and the orthogonal tilt reconstruction method. *PNAS* **104:** 4913–4918 (2007)

Lessard, J., *et al.* An essential switch in subunit composition of a chromatin remodeling complex during neural development. *Neuron* **55**: 201–215 (2007)

Li, S., *et al.* Polynucleotide kinase and aprataxin-like forkhead-associated protein (PALF) acts as both a single-stranded DNA endonuclease and a single-stranded DNA 3′ exonuclease and can participate in DNA end joining in a biochemical system. *J. Biol. Chem.* **286**: 36368–36377 (2011)

Li, X., *et al.* MOF and H4 K16 acetylation play important roles in DNA damage repair by modulating recruitment of DNA damage repair protein Mdc1. *Mol. Cell Biol.* **30**: 5335-5347 (2010)

Li, Y., *et al.* HSSB1 and hSSB2 form similar multiprotein complexes that participate in DNA damage response. *J. Biol. Chem.* **284**: 23525-23531 (2009)

Lia, G., *et al.* Direct observation of DNA distortion by the RSC complex. *Mol. Cell* **21**: 417–425 (2006)

Liang, B., *et al.* RSC Functions as an early double-strand-break sensor in the cell's response to DNA damage. *Curr. Biol.* **17**: 1432–1437 (2007)

Liang, G., *et al.* Distinct localization of histone H3 acetylation and H3–K4 methylation to the transcription start sites in the human genome. *PNAS* **101**: 7357–7362 (2004)

Lickert, H. *et al.* Baf60c is essential for function of BAF chromatin remodelling complexes in heart development. *Nature* **432**: 107–112 (2004)

Lieber, M. R. The mechanism of double-strand DNA break repair by the nonhomologous DNA end joining pathway. *Annu. Rev. Biochem.* **79**: 181-211 (2010)

Lim, H. S., *et al.* Crystal structure of the Mre11-Rad50-ATPγS complex: understanding the interplay between Mre11 and Rad50. *Genes Dev.* **25**: 1091-1104 (2011)

Lin, Y. Y., *et al.* A comprehensive synthetic genetic interaction network governing yeast histone acetylation and deacetylation. *Genes Dev.* **22**: 2062-2074 (2008)

Liu, H., *et al.* Promoter methylation inhibits BRD7 expression in human nasopharyngeal carcinoma cells. *BMC Cancer* **8**: 253 (2008)

Liu, H., *et al.* Phosphorylation-enabled binding of SGO1-PP2A to cohesin protects Sororin and centromeric cohesion during mitosis. *Nat. Cell Biol.* **15**: 40-49 (2013)

Liu, J., *et al.* Rad51 paralogues Rad55-Rad57 balance the antirecombinase Srs2 in Rad51 filament formation. *Nature* **479**: 245-248 (2011)

Liu, Y., *et al.* Role of RAD51C and XRCC3 in genetic recombination and DNA repair. *J. Biol. Chem.* **282**: 1973-1979 (2007)

Loeb, L. A. A mutator phenotype in cancer. *Cancer Res.* **61**: 3230-3239 (2001)

Lohr, J. G., *et al.* Discovery and prioritization of somatic mutations in diffuse large B-cell lymphoma (DLBCL) by whole-exome sequencing. *PNAS* **109**: 3879–3884 (2012)

Long, D. T., *et al.* Mechanism of RAD51-dependent DNA interstrand cross-link repair. *Science* **333**: 84-7 (2011)

Lorch, Y., *et al.* Activated RSC-nucleosome complex and persistently altered form of the nucleosome. *Cell* **94:** 29–34 (1998)

Lorch, Y., *et al*. Histone octamer transfer by a chromatin-remodeling complex. *Cell* **96:** 389–392 (1999)

Lorch, Y., *et al.* Chromatin remodeling by nucleosome disassembly in vitro. *PNAS* **103**: 3090–3093 (2006)

Lorch, Y., *et al.* Mechanism of chromatin remodeling. *PNAS* **107**: 3458–3462 (2010)

Losada, A., *et al.* Identification and characterization of SA/Scc3p subunits in the *Xenopus* and human cohesion complexes. *J. Cell Biol.* **7**: 405-416 (2000)

Losada, A., *et al.* Functional contribution of Pds5 to cohesin-mediated cohesion in human cells and *Xenopus* egg extracts. *J. Cell Sci.* **118**: 2133-2141 (2005)

Lou, Z., *et al.* MDC1 maintains genomic stability by participating in the amplification of ATM-dependent DNA damage signals. *Mol. Cell* **21**: 187-200 (2006)

Lowe, S. W., and Sherr, C. J. 2003. Tumor suppression by Ink4a-Arf: Progress and puzzles. *Curr. Opin. Genet. Dev.* **13:** 77-83 (2003)

Lu, C. Y., *et al.* Sumoylation of the BLM ortholog, Sgs1, promotes telomere-telomere recombination in budding yeast. *Nucleic Acids Res.* **38**: 488-498 (2010)

Lu, C., *et al*. Regulation of tumor angiogenesis by EZH2. *Cancer Cell* **18**: 185–197 (2010)

Luger, K., *et al.* Crystal structure of the nucleosome core particle at 2.8 A resolution. *Nature* **389**: 251–260 (1997)

Luk, E., *et al.* Stepwise histone replacement by SWR1 requires dual activation with histone H2A.Z and canonical nucleosome. *Cell* **143**: 725–736 (2010)

Lunenburger, H., *et al.* Systematic analysis of the antiproliferative effects of novel and standard anticancer agents in rhabdoid tumor cell lines. *Anticancer Drugs* **21**: 514–522 (2010)

Luo, H., *et al.* Regulation of intra-S phase checkpoint by IR-dependent and IR-independent phosphorylation of SMC3. *J. Biol. Chem.* **283**: 19176-19183 (2008)

Lydeard, J. R., *et al.* Break-induced replication and telomerase-independent telomere maintenance require Pol32. *Nature* **448**: 820-823 (2007)

Ma, Y., *et al.* Hairpin opening and overhang processing by an Artemis/DNA-dependent protein kinase complex in nonhomologous end joining and V(D)J recombination. *Cell* **108**: 781–794 (2002)

Ma, Y., *et al.* The DNA-dependent protein kinase catalytic subunit phosphorylation sites in human Artemis. *J. Biol. Chem.* **280**: 33839–33846 (2005)

MacAlpine, H. K., *et al.* Drosophila ORC localizes to open chromatin and marks sites of cohesin complex loading. *Genome Res.* **20**: 201-211 (2010)

Macrae, C. J., *et al.* APLF (C2orf13) facilitates nonhomologous end-joining and undergoes ATM-dependent hyperphosphorylation following ionizing radiation. *DNA Repair* **7**: 292–302 (2008)

Mahajan, K. N., *et al.* Association of terminal deoxynucleotidyl transferase with Ku. *PNAS* **96**: 13926–13931 (1999)

Mailand, N., *et al*. RNF8 ubiquitylates histones at DNA double-strand breaks and promotes assembly of repair proteins. *Cell* **131**: 887–900 (2007)

Malik, H. S., *et al.* A Hitchhiker's guide to survival finally makes CENs. *J. Cell Biol.* **174:** 747-749 (2006)

Mallette, F. A., *et al.* Myc down-regulation as a mechanism to activate the Rb pathway in STAT5A-induced senescence. *J. Biol. Chem.* 2007 **282**: 34938-34944 (2007)

Mallette, F. A., *et al*. RNF8- and RNF168-dependent degradation of KDM4A/JMJD2A triggers 53BP1 recruitment to DNA damage sites. *EMBO J.* **31**: 1865–1878 (2012)

Mankouri, H. W., *et al.* SGS1 is a multicopy suppressor of srs2: functional overlap between DNA helicases. *Nucleic Acids Res.* **30**: 1103-1113 (2002)

Mankouri, H. W., *et al.* Shu proteins promote the formation of homologous recombination intermediates that are processed by Sgs1-Rmi1-Top3. *Mol. Biol. Cell* **18**: 4062-4073 (2007)

Manning, A. L., *et al.* Loss of pRB causes centromere dysfunction and chromosomal instability. *Genes Dev.* **24**: 1364-1376 (2010)

Manning, A. L., and Dyson, N. J. RB: mitotic implications of a tumour suppressor. *Nat. Rev. Cancer* **12**: 220-226 (2012)

Maradeo, M. E., and Skibbens, R. V. The Elg1-RFC clamp-loading complex performs a role in sister chromatid cohesion. *PLoS One* **4**: e4707 (2009)

Maradeo, M. E., and Skibbens, R. V. Replication factor C complexes play unique pro-and anti-establishment roles in sister chromatid cohesion. *PLoS One* **5**: e15381 (2010)

Martin, M., *et al.* Class IIa histone deacetylases: regulating the regulators. *Oncogene* **26**: 5450-5467 (2007)

Mari, P. O., *et al.* Dynamic assembly of end-joining complexes requires interaction between Ku70/80 and XRCC4. PNAS **103**: 18597–18602 (2006)

Martin, S. A., *et al.* DNA polymerases as potential therapeutic targets for cancers deficient in the DNA mismatch repair proteins MSH2 or MLH1. *Cancer Cell* **17**: 235–248 (2010)

Martin, S. A., *et al.* Parallel high throughput RNA interference screens identify PINK1 as a potential therapeutic target for the treatment of DNA mismatch repair deficient cancers. *Cancer Res.* **71**: 1836–1848 (2011)

Masson, J. Y, *et al.* Identification and purification of two distinct complexes containing the five RAD51 paralogs. *Genes Dev.* **15**: 3296-3307 (2001)

Matangkasombut, O., and Buratowski, S. Different sensitivities of bromodomain factors 1 and 2 to histone H4 acetylation. *Mol. Cell* **11**: 353–363 (2003)

Matsuoka, S., *et al.* ATM and ATR substrate analysis reveals extensive protein networks responsive to DNA damage. *Science* **316**: 1160-1166

Matsuzaki, K., *et al.* Forkhead-associated domain of yeast Xrs2, a homolog of human Nbs1, promotes nonhomologous end joining through interaction with a ligase IV partner protein, Lif1. *Genetics* 2008 **179**: 213-225 (2008)

Mattiroli, F., *et al*. RNF168 ubiquitinates K13-15 on H2A/H2AX to drive DNA damage signaling. *Cell* **150**: 1182–1195 (2012)

Mayhew, C. N., *et al.* RB loss abrogates cell cycle control and genome integrity to promote liver tumourigenesis. *Gastroenterology* **133**: 976-984 (2007)

McAinsh, A. D., *et al.* Structure, function, and regulation of budding yeast kinetochores. *Annu. Rev. Cell Dev. Biol.* **19**:519-539 (2003)

McCarroll, R. M., and Fangman, W. L. Time of replication of yeast centromeres and telomeres. *Cell* **54**: 505-513 (1988)

McIlwraith, M. J., and West, S. C. DNA repair synthesis facilitates RAD52-mediated second-end capture during DSB repair. *Mol. Cell* **29**: 510-516 (2008)

McIntyre, J., *et al. In vivo* analysis of cohesin architecture using FRET in the budding yeast *Saccharomyces cerevisiae. EMBO J.* **26**: 3783-3793 (2007)

McKenna, E. S., *et al.* Loss of the epigenetic tumor suppressor SNF5 leads to cancer without genomic instability. *Mol. Cell Biol.* **28**: 6223-6233 (2008)

Melander, F., *et al.* Phosphorylation of SDT repeats in the MDC1 N terminus triggers retention of NBS1 at the DNA damage-modified chromatin. *J. Cell Biol.* **181**: 213-226 (2008)

Mendiburo, M. J., *et al. Drosophila* CENH3 is sufficient for centromere formation. *Science* **334**: 686–690 (2011)

Meyer, R., *et al.* Overexpression and mislocalization of the chromosomal segregation protein separase in multiple human cancers. *Clin. Cancer Res.* **15**: 2703-2710 (2009)

Michaelis, C., *et al.* Cohesins: chromosomal proteins that prevent premature separation of sister chromatids. *Cell* **91**: 35-45

Miele, A., and Dekker, J. Long-range chromosomal interactions and gene regulation. *Mol. Biosyst.* **4**: 1046-57 (2008)

Miell, M. D. D., *et al.* CENP-A confers a reduction in height on octameric nucleosomes. *Nat. Struct. Mol. Biol.* **20**: 763–765 (2013)

Migliori, V., *et al.* Symmetric dimethylation of H3R2 is a newly identified histone mark that supports euchromatin maintenance. *Nat. Struct. Mol. Biol.* **19:** 136–144 (2012)

Miller, K. M., *et al*. Human HDAC1 and HDAC2 function in the DNA-damage response to promote DNA nonhomologous end-joining. *Nature Struct. Mol. Biol.* **17**: 1144–1151 (2010)

Mimitou, E. P., and Symington, L. S. Sae2, Exo1 and Sgs1 collaborate in DNA double-strand break processing. *Nature* **455**: 770-4 (2008)

Mimitou, E. P., and Symington, L. S. Ku prevents Exo1 and Sgs1-dependent resection of DNA ends in the absence of a functional MRX complex or Sae2. *EMBO J.* **29**: 3358-3369 (2010)

Mimori, T., *et al.* Characterization of the DNA-binding protein antigen Ku recognized by autoantibodies from patients with rheumatic disorders. *J. Biol. Chem.* **261**: 2274–2278

Min, J., *et al.* Structural basis for specific binding of Polycomb chromodomain to histone H3 methylated at Lys 27. *Genes Dev.* **17**: 1823–1828 (2003)

Misulovin, Z., *et al.* Association of cohesin and Nipped-B with transcriptionally active regions of the *Drosophila melanogaster* genome. *Chromosoma* **117**: 89-102 (2008)

Minucci, S., and Pelicci, P. G. Histone deacetylase inhibitors and the promise ofepigenetic (and more) treatments for cancer. *Nat. Rev. Cancer* **6**: 38–51 (2006)

Miyanari, Y., and Torres-Padilla, M. E. Control of ground-state pluripotency by allelic regulation of Nanog. *Nature* **483**: 470-473 (2012)

Mohrmann, L., and Verrijzer, C. P. Composition and functional specificity of SWI2/SNF2 class chromatin remodeling complexes. *Biochim. Biophys. Acta.* **1681**: 59-73 (2005)

Moon, A. F., *et al.* The X family portrait: structural insights into biological functions of X family polymerases. *DNA Repair* **6**: 1709–1725 (2007)

Moore, J. K., and Haber, J. E. Cell cycle and genetic requirements of two pathways of nonhomologous end-joining repair of double-strand breaks in *Saccharomyces cerevisiae. Mol. Cell Biol.* **16**: 2164-2173 (1996)

Moree, B., *et al.* CENP-C recruits M18BP1 to centromeres to promote CENP-A chromatin assembly. *J. Cell Biol.* **194**: 855–871 (2011)

Morin, R. D., *et al.* Frequent mutation of histone-modifying genes in non-Hodgkin lymphoma. *Nature* **476**: 298–303 (2011)

Morinière, J., *et al.* Cooperative binding of two acetylation marks on a histone tail by a single bromodomain. *Nature* **461**:664–668 (2009)

Morris, J. R., *et al.* The SUMO modification pathway is involved in the BRCA1 response to genotoxic stress. *Nature* **462**: 886-890 (2009)

Mortensen, U. H., *et al.* DNA strand annealing is promoted by the yeast Rad52 protein. *PNAS* **93**: 10729-10734 (1996)

Moscariello, M., *et al.* Accurate repair of non-cohesive, double strand breaks in Saccharomyces cerevisiae: enhancement by homology-assisted end-joining. *Yeast* **27:** 837–848 (2010)

Moynahan, M E., and Yasin, M. Mitotic homologous recombination maintains genomic stability and suppresses tumourigenesis. *Nature Rev. Mol. Cell Biol.* **11**: 196-207 (2010)

Mujtaba, S., *et al.* Structural basis of lysine-acetylated HIV-1 Tat recognition by PCAF bromodomain. *Mol. Cell* **9**: 575-86 (2002)

Muller, P., *et al.* The conserved bromo-adjacent homology domain of yeast Orc1 functions in the selection of DNA replication origins within chromatin. *Genes Dev.* **24**: 1418–1433 (2010)

Munoz, I. M., *et al.* Phospho-epitope binding by the BRCT domains of hPTIP controls multiple aspects of the cellular response to DNA damage. *Nucleic Acids Res.* **35**: 5312–5322 (2007)

Murayama, Y., and Uhlmann, F. Biochemical reconstitution of topological DNA binding by the cohesin ring. *Nature* **505**: 367-371 (2014)

Murr, R., *et al.* Histone acetylation by Trrap-Tip60 modulates loading of repair proteins and repair of DNA double-strand breaks. *Nat. Cell Biol.* **8**: 91-99 (2006)

Musacchio, A., and Salmon, E. D. The spindle-assembly checkpoint in space and time. *Nat. Rev. Mol. Cell Biol.* **8**: 379-393 (2007)

Musselman, C. A., *et al.* Perceiving the epigenetic landscape through histone readers. *Nat. Struct. Mol. Biol.* **19**: 1218-1227 (2012)

Nagao, K., *et al.* Separase-mediated cleavage of cohesin at interphase is required for DNA repair. *Nature* **430**: 1044-1048 (2004)

Nagl, N. G., *et al.* The c-myc gene is a direct target of mammalian SWI/SNF-related complexes during differentiation-associated cell cycle arrest. *Cancer Res.* **66**: 1289–1293 (2006)

Nagl, N. G., Distinct mammalian SWI/SNF chromatin remodeling complexes with opposing roles in cell-cycle control. *EMBO J.* **26**: 752–763 (2007)

Nakada, D., *et al.* ATM-related Tel1 associates with double-strand breaks through an Xrs2-dependent mechanism. *Genes Dev.* **17**: 1957-1962 (2003)

Nasmyth, K. Disseminating the genome: joining, resolving, and separating sister chromatids during mitosis and meiosis. *Annu. Rev. Genet.* **35**: 673-745 (2001)

Neshat, M. S., *et al.* Enhanced sensitivity of PTEN-deficient tumors to inhibition of FRAP/mTOR. *PNAS* **98**: 10314–10319 (2001)

Nezi, L., and Musacchio, A. Sister chromatid tension and the spindle assembly checkpoint. *Curr. Opin. Cell Biol.* **21**: 785-795

Ng, H. H., *et al.* Genome-wide location and regulated recruitment of the RSC nucleosome-remodeling complex. *Genes Dev.* **16:** 806–819 (2002)

Nick McElhinny, S. A., and Ramsden, D. A. Polymerase mu is a DNA-directed DNA/RNA polymerase. *Mol. Cell Biol.* **23**: 2309-2315 (2003)

Nick McElhinny, S. A., *et al.* A gradient of template dependence defines distinct biological roles for family X polymerases in nonhomologous end joining. *Mol. Cell* **19**: 357–366 (2005)

Niimi, A., *et al.* A role for chromatin remodellers in replication of damaged DNA. *Nucleic Acids Res.* **40**: 7393-7403 (2012)

Nikolaev, L. G., *et al.* Vertebrate Protein CTCF and its Multiple Roles in a Large-Scale Regulation of Genome Activity. *Curr. Genomics* **10**: 294-302 (2009)

Nimonkar, A. V., *et al.* Rad52 promotes second-end DNA capture in double-stranded break repair to form complement-stabilized joint molecules. *PNAS* **106**: 3077-3082 (2009)

Nishiyama, T., *et al.* Sororin mediates sister chromatid cohesion by antagonizing Wapl. *Cell* **143**: 737-749 (2010)

Niu, H., *et al.* Mechanism of the ATP-dependent DNA end-resection machinery from Saccharomyces cerevisiae. *Nature* **467**:108-111 (2010)

Noguchi, K., *et al.* The BAH domain facilitates the ability of human Orc1 protein to activate replication origins *in vivo*. *EMBO J.* **25:** 5372–5382 (2006)

Nonaka, N., *et al.* Recruitment of cohesin to heterochromatic regions by Swi6/HP1 in fission yeast. *Nat. Cell Biol.* **4**: 89-93. (2002)

Norris, A., and Boeke, J. D. Silent information regulator 3: the Goldilocks of the silencing complex. *Genes Dev.* **24**: 115-22 (2010)

Norris, A., *et al.* Compensatory interactions between Sir3p and the nucleosomal LRS surface imply their direct interaction. *PLoS Genet.* **4**: e1000301 (2008)

Ocampo-Hafalla, M. T., and Uhlmann, F. Cohesin loading and sliding. *J. Cell Sci.* **124**: 685-691 (2011)

Ocker, M. Deacetylase inhibitors – focus on non-histone targets and effects. *World J. Biol. Chem.* **1**: 55–61 (2010)

Oda, H., *et al*. Regulation of the histone H4 monomethylase PR-Set7 by $CRL4^{Cdt2}$-mediated PCNA-dependent degradation during DNA damage. *Mol. Cell* **40**: 364–376 (2010)

Ogiwara, H., *et al.* Histone acetylation by CBP and p300 at double-strand break sites facilitates SWI/SNF chromatin remodeling and the recruitment of non-homologous end joining factors. *Oncogene* **30**: 2135-

2146 (2011)

Oh, S. D., *et al.* BLM ortholog, Sgs1, prevents aberrant crossing-over by suppressing formation of multichromatid joint molecules. *Cell* **130**: 259-272 (2007)

Oh, S. D., *et al.* RecQ helicase, Sgs1, and XPF family endonuclease, Mus81-Mms4, resolve aberrant joint molecules during meiotic recombination. *Mol. Cell* **31**: 324-336 (2008)

Ohuchi, T., *et al.* Rad52 sumoylation and its involvement in the efficient induction of homologous recombination. *DNA Repair* **7**: 879-889 (2008)

Ohuchi, T., *et al.* Accumulation of sumoylated Rad52 in checkpoint mutants perturbed in DNA replication. *DNA repair* **8**: 690-696 (2009)

Oikawa, K., *et al.* Expression of a novel human gene, human wings apart-like (hWAPL), is associated with cervical carcinogenesis and tumor progression. *Cancer Res.* **64**: 3545-3549 (2004)

Oliveira, R. A., and Nasmyth, K. Getting through anaphase: splitting the sisters and beyond. *Biochem. Soc. Trans.* **38**: 1639-1644 (2010)

Oliver, A. W., *et al.* Crystal structure of the proximal BAH domain of the polybromo protein. *Biochem. J.* **389**: 657-664 (2005)

Olszak A.M., Heterochromatin boundaries are hotspots for de novo kinetochore formation. *Nat. Cell Biol.* **13**: 799–808 (2011)

Onishi, M., *et al.* Role of the conserved Sir3-BAH domain in nucleosome binding and silent chromatin assembly. *Mol. Cell* **28**: 1015–1028 (2007)

Onn, I., *et al.* Sister chromatid cohesion: a simple concept with a complex reality. *Annu. Rev. Cell Dev. Biol.* **24**: 105-129 (2008)

Oruetxebarria, I., *et al.* P16INK4a is required for hSNF5 chromatin remodeler-induced cellular senescence in malignant rhabdoid tumor cells. *J. Biol. Chem.* **279**: 3807-3816 (2004)

Oum, J. H., *et al.* RSC facilitates Rad59-dependent homologous recombination between sister chromatids by promoting cohesin loading at DNA double-strand breaks. *Mol. Cell Biol.* **31**:3924-3937 (2011)

Ouyang, K. J., *et al.* SUMO modification regulates BLM and RAD51 interaction at damaged replication forks. *PLoS Biol.* **7**: e1000252 (2009)

Padeganeh, A., *et al.* Octameric CENP-A nucleosomes are present at human centromeres throughout the cell cycle. *Curr. Biol.* **23**: 764–769 (2013)

Palmbos, P. L., *et al.* Recruitment of Saccharomyces cerevisiae Dnl4-Lif1 complex to a double-strand break requires interactions with Yku80 and the Xrs2 FHA domain. *Genetics* **180**:1809-1819 (2008)

Pan, X., *et al.* dSLAM analysis of genome-wide genetic interactions in Saccharomyces cerevisiae. *Methods* **41**: 206-221 (2007)

Pang, D., *et al.* Ku proteins join DNA fragments as shown by atomic force microscopy. *Cancer Res.* **57**: 1412–1415 (1997)

Panier, S., and Boulton, S. J. Double-strand break repair: 53BP1 comes into focus. *Nature Rev. Mol. Cell Biol.* **15**: 7-18 (2014)

Panizza, S., *et al.* Pds5 cooperates with cohesin in maintaining sister chromatid cohesion. *Curr. Biol.* **10**: 1557-1564 (2000)

Parikh, B., and Advani, S. Pattern of second primary neoplasms following breast cancer. *J. Surg. Oncol.* **63**: 179–182 (1996)

Parisi, S., *et al.* Rec8p, a meitotic recombination and sister chromatid cohesion phosphoprotein of the Rad21p family conserved from fission yeast to humans. *Mol. Cell Biol.* **19:** 3515-3528 (1999)

Park, J. H., *et al.* Mammalian SWI/SNF complexes facilitate DNA double-strand break repair by promoting gamma-H2AX induction. *EMBO J.* **25**: 3986-3997 (2006)

Parnas, O., *et al.* The ELG1 clamp loader plays a role in sister chromatid cohesion. *PLoS One* **4**: e5497 (2009)

Pasqualucci, L., *et al.* Analysis of the coding genome of diffuse large B-cell lymphoma. *Nat. Genet.* **43**: 830–837 (2011)

Paull, T. T., and Gellert, M. The 3' to 5' exonuclease activity of Mre 11 facilitates repair of DNA double-strand breaks. *Mol. Cell* **1**:969-979 (1998)

Pei, H., *et al*. MMSET regulates histone H4K20 methylation and 53BP1 accumulation at DNA damage sites. *Nature* **470**: 124–128 (2011)

Pellegrini, L., *et al.* Insights into DNA recombination from the structure of a RAD51-BRCA2 complex. *Nature* **420**: 287-293 (2002)

Peng, C., *et al.* The transcriptional regulation role of BRD7 by binding to acetylated histone through bromodomain. *J. Cell Biochem.* **97**: 882–892 (2006)

Peng, G., *et al.* BRIT1/MCPH1 links chromatin remodelling to DNA damage response. *Nat. Cell Biol.* **11**: 865-872 (2009)

Perry, J. J., *et al.* WRN exonuclease structure and molecular mechanism imply an editing role in DNA end processing. *Nat. Struct. Mol. Biol.* **13**: 414-422 (2006)

Petermann, E., *et al.* Importance of poly(ADP-ribose) polymerases in the regulation of DNA-dependent processes. *Cell. Mol. Life Sci.* **62**: 731–738 (2005)

Petermann, E., *et al.* Hydroxyurea-stalled replication forks become progressively inactivated and require two different RAD51-mediated pathways for restart and repair. *Mol. Cell* **37**: 492-502 (2010)

Peters, A. H., *et al.* Loss of the Suv39h histone methyltransferases impairs mammalian heterochromatin and genome stability. *Cell* **107**: 323–337 (2001)

Peters, A. H, *et al.* Partitioning and plasticity of repressive histone methylation states in mammalian chromatin. *Mol. Cell* **12**: 1577–1589 (2003)

Peters, J. M., *et al.* The cohesin complex and its roles in chromosome biology. *Genes Dev.* **22**: 3089–3114 (2008)

Pinto, D. M., and Flaus, A. Structure and function of histone H2AX. *Subcell. Biochem.* **50**:55-78 (2010)

Plate, I., *et al.* Interaction with RPA is necessary for Rad52 repair center formation and for its mediator activity. *J. Biol. Chem.* **283**: 29077-29085 (2008)

Plosky, B. S., *et al.* Controlling the subcellular localization of DNA polymerases iota and eta via interactions with ubiquitin. *EMBO J.* **25**: 2847–2855 (2006)

Podsypanina, K., *et al.* An inhibitor of mTOR reduces neoplasia and normalizes p70/S6 kinase activity in *Pten*+/− mice. *PNAS* **98**: 10320–10325 (2001)

Porkka, K. P., *et al.* RAD21 and KIAA0196 at 8q24 are amplified and overexpressed in prostate cancer. *Genes Chromosomes Cancer*. **39**: 1-10 (2004)

Pottier, N., *et al*. The SWI/SNF chromatin-remodeling complex and glucocorticoid resistance in acute lymphoblastic leukemia. *J. Natl. Cancer Inst.* **100**: 1792–1803 (2008)

Potts, P. R., *et al.* SMC5/6 complex promotes sister chromatid homologous recombination by recruiting the SMC1/3 cohesin complex to double-strand breaks. *EMBO J.* **25**: 3377-3388 (2006)

Puyol, M., *et al.* A synthetic lethal interaction between K-RAS oncogenes and Cdk4 unveils a therapeutic strategy for non-small cell lung carcinoma. *Cancer Cell* **18**: 63–73 (2010)

Quesada, V., *et al.* Exome sequencing identifies recurrent mutations of the splicing factor SF3B1 gene in chronic lymphocytic leukemia. *Nat. Genet.* **44**: 47–52 (2011)

Prakash, R., *et al.* Yeast Mph1 helicase dissociates Rad51-made D-loops: implications for crossover control in mitotic recombination. *Genes Dev.* **23**: 67-79 (2009)

Rai, R., *et al.* BRIT1 regulates early DNA damage response, chromosomal integrity, and cancer. *Cancer Cell* **10**: 145-157 (2006)

Ramadan, K., *et al.* The DNA-polymerase-X family: controllers of DNA quality? *Nat. Rev. Mol. Cell Biol.* **5**: 1038-1043 (2004)

Rancati, G., *et al.* Aneuploidy underlies rapid adaptive evolution of yeast cells deprived of a conserved cytokinesis motor. *Cell.* **135**: 879-93 (2008)

Rando, O. J., and Chang, H. Y. Genome-wide views of chromatin structure. *Annu. Rev. Biochem.* **78**: 245-271 (2009)

Räschle, M., *et al.* Mechanism of replication-coupled DNA interstrand crosslink repair. *Cell* **134**: 969-980 (2008)

Ray, A., *et al.* Human SNF5/INI1, a component of the human SWI/SNF chromatin remodeling complex, promotes nucleotide excision repair by influencing ATM recruitment and downstream H2AX phosphorylation. *Mol. Cell Biol.* **29**: 6206-6219 (2009)

Reisman, D. N., *et al*. Concomitant down-regulation of BRM and BRG1 in human tumor cell lines: differential effects on RB-mediated growth arrest vs CD44 expression. *Oncogene* **21**: 1196–1207 (2002)

Reliene, R., *et al.* Involvement of homologous recombination in carcinogenesis. *Adv. Genet.* **58**: 67-87 (2007)

Remeseiro, S., *et al.* Cohesin-SA1 deficiency drives aneuploidy and tumourigenesis in mice due to impaired replication of telomeres. *EMBO J.* **31**: 2076-2089 (2012)

Remeseiro, S., *et al.* A unique role for cohesin-SA1 in gene regulation and development. *EMBO J.* **31**: 2090-2102 (2012)

Remeseiro, S., and Losada, A. Cohesin, a chromatin engagement ring. *Curr. Opin. Cell Biol.* **25**: 63-71 (2013)

Rhodes, D. R., *et al.* Large-scale meta-analysis of cancer microarray data identifies common transcriptional profiles of neoplastic transformation and progression. *PNAS* **101**: 9309-9314 (2004)

Rice, J. C., *et al.* Histone methyltransferases direct different degrees of methylation to define distinct chromatin domains. *Mol. Cell* **12**: 1591–1598 (2003)

Richard, D. J., *et al.* Single-stranded DNA-binding protein hSSB1 is critical for genomic stability. *Nature* **453**: 677-681 (2008)

Richard, D. J., *et al.* hSSB1 interacts directly with the MRN complex stimulating its recruitment to DNA double-strand breaks and its endo-nuclease activity. *Nucleic Acids Res.* **39**: 3643-3651 (2011)

Richmond, T. J., and Davey, C. A. The structure of DNA in the nucleosome core. *Nature* **423**: 145-150 (2003)

Richon, V. M., *et al.* A class of hybrid polar inducers of transformed cell differentiation inhibits histone deacetylases. *PNAS* **95**: 3003-3007 (1998)

Richon, V. M., *et al.* Histone deacetylase inhibitor selectively induces p21WAF1 expression and gene-associated histone acetylation. *PNAS* **97**: 10014–10019 (2000)

Riley, T., *et al.* Transcriptional control of human p53-regulated genes. *Nat. Rev. Mol. Cell Biol.* **9**: 402–412 (2008)

Ritchie, A. W., and Chisholm, G. D. The natural history of renal carcinoma. *Semin. Oncol.* **10**: 390–400 (1983)

Ritchie, K., *et al.* Loss of ATRX leads to chromosome cohesion and congression defects. *J. Cell Biol.* **180**: 315-324 (2010)

Roberts, C. W., *et al.* Haploinsufficiency of Snf5 (integrase interactor 1) predisposes to malignant rhabdoid tumors in mice. *PNAS* **97**: 13796–13800 (2000)

Roe, O. D., *et al.* Malignant pleural mesothelioma: genome-wide expression patterns reflecting general resistance mechanisms and a proposal of novel targets. *Lung Cancer* **67**: 57-68 (2009)

Rogakou, E. P., *et al.* DNA double-stranded breaks induce histone H2AX phosphorylation on serine 139. *J. Biol. Chem.* **273**: 5858-5868 (1998)

Rogakou, E. P., *et al.* Megabase chromatin domains involved in DNA double-strand breaks in vivo. *J. Cell Biol.* **146**: 905-916 (1999)

Rolef Ben-Shahar, T., *et al.* Eco1-dependent cohesin acetylation during establishment of sister chromatid cohesion. *Science* **321**: 563-566 (2008)

Rossio, V., *et al.* The RSC chromatin-remodeling complex influences mitotic exit and adaptation to the spindle assembly checkpoint by controlling the Cdc14 phosphatase. *J. Cell Biol.* **191**: 981-997 (2010)

Rosson, G. B., *et al.* BRG1 loss in MiaPaCa2 cells induces an altered cellular morphology and disruption in the organization of the actin cytoskeleton. *J. Cell Physiol.* **205**: 286–294 (2005)

Rothkamm, K., *et al.* Pathways of DNA double-strand break repair During the mammalian cell cycle. *Mol. Cell. Biol.* **23:** 5706–5715 (2003)

Rouleau, M., *et al.* PARP inhibition: PARP1 and beyond. *Nature Rev. Cancer* **10**: 293–301 (2010)

Rowland, B. D., *et al.* Building sister chromatid cohesion: Smc3 acetylation counteracts an antiestablishment activity. *Mol. Cell* **33**: 763-774 (2009)

Rudra, S., and Skibbens, R. Cohesin codes – interpreting chromatin architecture and the many facets of cohesin function. *J. Cell Sci.* **126**: 31-41 (2013)

Rufini, A., *et al.* Senescence and aging: the critical roles of p53. *Oncogene* **32**: 5129-5143 (2013)

Ryu, B.,*et al.* Comprehensive expression profiling of tumor cell lines identifies molecular signatures of melanoma progression. *PLoS One* **4**: e594 (2007)

Saha, A., *et al.* Chromatin remodeling by RSC involves ATP-dependent DNA translocation. *Genes Dev.* **16**: 2120–2134 (2002)

Saha, A., *et al.* Chromatin remodeling through directional DNA translocation from an internal nucleosomal site. *Nat. Struct. Mol. Biol.* **12**: 747–755 (2005)

Saitoh, H., *et al.* Perturbation of SUMOylation enzyme Ubc9 by distinct domain within necleoporin RanBP2/Nup358. *J. Biol. Chem.* **277**: 4755-4763 (2002)
Saitoh, K., *et al.* The putative nuclear localization signal of the human RAD52 protein is a potential sumoylation site. *J. Biochem.* **147**: 833-842 (2010)

Sakai, A., *et al.* Condensin but not cohesin SMC heterodimer induces DNA reannealing through protein-protein assembly. *EMBO J.* **22**: 2764-2775 (2003)

Salehi, F., *et al.* Pituitary tumor-transforming gene in endocrine and other neoplasms: a review and update. *Endocr. Relat. Cancer.* **15**: 721-743 (2008)

Samel, A., *et al.* Methylation of CenH3 arginine 37 regulates kinetochore integrity and chromosome segregation. *PNAS* **109**: 9029–9034 (2012)

Sandor, V., *et al.* P21-dependent g(1)arrest with downregulation of cyclin D1 and upregulation of cyclin E by the histone deacetylase inhibitor FR901228. *Br. J. Cancer* **83**: 817–825 (2000)

San Filippo, J., *et al.* Mechanism of eukaryotic homologous recombination. *Annu. Rev. Biochem.* **77**: 229-5 (2008)

Saponaro, M., *et al.* Cdk1 targets Srs2 to complete synthesis-dependent strand annealing and to promote recombinatorial repair. *PLoS Genet.* **6**: e1000858 (2010)

Sarthy, A. V., *et al.* Survivin depletion preferentially reduces the survival of activated K-RAS-transformed cells. *Mol. Cancer Ther.* **6**: 269–276 (2007)

Sato, H., *et al.* Epigenetic inactivation and subsequent heterochromatinization of a centromere stabilize dicentric chromosomes. *Curr. Biol.* **22**: 658–667 (2012)

Schlacher, K., *et al.* Double-strand break repair-independent role for BRCA2 in blocking stalled replication fork degradation by MRE11. *Cell* **145:** 529–542 (2011)

Schmidt, D., *et al.* A CTCF-independent role for cohesin in tissue-specific transcription. *Genome Res.* **20**: 578-588 (2010)

Sebesta, M., *et al.* Reconstitution of DNA repair synthesis *in vitro* and the role of polymerase and helicase activities. *DNA repair* **10**: 567-576 (2011)

Sekulic, N., *et al.* The structure of (CENP-A–H4)2 reveals physical features that mark centromeres. *Nature* **467**: 347–351 (2010)

Seong, C., *et al.* Molecular anatomy of the recombination mediator function of *Saccharomyces cerevisiae* Rad52. *J. Biol. Chem.* **283**: 12166-12174 (2008)

Seong, C., *et al.* Regulation of Rad51 recombinase presynaptic filament assembly via interactions with the Rad52 mediator and the Srs2 anti-recombinase. *J. Biol. Chem.* **284**: 24363-24371 (2009)

Shain, A. H., *et al.* Convergent structural alterations define SWItch/Sucrose NonFermentable (SWI/SNF) chromatin remodeler as a central tumor suppressive complex in pancreatic cancer. *PNAS* **109**: 252–259 (2012)

Shain, A. H., and Pollack, J. R. The spectrum of SWI/SNF mutations, ubiquitous in human cancers. *PLoS One* **8**: e55119 (2013)

Shamu, C. E., and Murray, A. W. Sister chromatid separation in frog egg extracts requires DNA topoisomerase II activity during anaphase. *J. Cell Biol.* **117**: 921-934 (1992)

Shang, W. -H., *et al.* Chromosome engineering allows the efficient isolation of vertebrate neocentromeres. *Dev. Cell* **24**: 635–648 (2013)

Shen, K. C., *et al.* ATM and p21 cooperate to suppress aneuploidy and subsequent tumor development. *Cancer Res.* **65**: 8747-8753 (2005)

Sherwood, R., *et al.* Sister acts: coordinating DNA replication and cohesion establishment. *Genes Dev.* **24**: 2723-2731 (2010)

Shete, S., *et al.* Genome-wide association study identifies five susceptibility loci for glioma. *Nature Genet.* **41**: 899-904 (2009)

Shi, W., *et al.* The role of RPA2 phosphorylation in homologous recombination in response to replication arrest. *Carcinogenesis* **31**: 994-1002 (2010)

Shi, X., *et al.* ING2 PHD domain links histone H3 lysine 4 methylation to active gene repression. *Nature* **442**: 96–99 (2006)

Shibata, A., *et al.* Role of ATM and the Damage Response Mediator Proteins 53BP1 and MDC1 in the Maintenance of G2/M Checkpoint Arrest. *Mol. Cell Biol.* **30:** 3371-3383 (2010)

Shibata, A., *et al.* Factors determining DNA double-strand break repair pathway choice in G2 phase. *EMBO J.* **30**: 1079–1092 (2011)

Shibata, A., *et al.* DNA double-strand break repair pathway choice is directed by distinct MRE11 nuclease activities. *Mol Cell.* **53**: 7-18 (2014)

Shim, E. Y., *et al.* The yeast chromatin remodeler RSC complex facilitates end joining repair of DNA double-strand breaks. *Mol. Cell Biol.* **25**: 3934–3944 (2005)

Shim, E. Y., *et al.* RSC mobilizes nucleosomes to improve accessibility of repair machinery to the damaged chromatin. *Mol. Cell Biol.* **27:** 1602–1613 (2007)

Shinohara, A., *et al.* Rad51 protein involved in repair and recombination in *S. cerevisiae* is a RecA-like protein. *Cell* **69**: 457-470 (1992)

Shinohara, A., and Ogawa, T. Stimulation by Rad52 of yeast Rad51-mediated recombination. *Nature* **391**: 404-407 (1998)

Shintomi, K., and Hirano, T. Releasing cohesin from chromosome arms in early mitosis: opposing actions of Wapl-Pds5 and Sgo1. *Genes Dev.* **23**: 2224-2236 (2009)

Shintomi, K., and Hirano, T. Sister chromatid resolution: a cohesin releasing network and beyond. *Chromosoma* **119**: 459-467 (2010)

Shim, E. Y., *et al.* Saccharomyces cerevisiae Mre11/Rad50/Xrs2 and Ku proteins regulate association of Exo1 and Dna2 with DNA breaks. *EMBO J.* **29:** 3370-3380 (2010)

Shivji, M. K., *et al.* The BRC repeats of human BRCA2 differentially regulate RAD51 binding on single- versus double-stranded DNA to stimulate strand exchange. *PNAS* **106**: 13254-13259 (2009)

Schneider, R., *et al.* Histone H3 lysine 4 methylation patterns in higher eukaryotic genes. *Nat. Cell Biol.* **6**: 73–77 (2004)

Shogren-Knaak, M., *et al.* Histone H4-K16 acetylation controls chromatin structure and protein interactions. *Science* **311**: 844-847 (2006)

Shroff, R., *et al.* Distribution and dynamics of chromatin modification induced by a defined DNA double-strand break. *Curr. Biol.* **14**: 1703-1711 (2004)

Sibanda, B. L., *et al.* Crystal structure of an Xrcc4-DNA ligase IV complex. *Nat. Struct. Biol.* **8**: 1015–1019 (2001)

Simon, J. A., and Lange, C. A. Roles of the EZH2 histone methyltransferase in cancer epigenetics. *Mutat. Res.* **647**: 21–29 (2008)

Singhal, N., *et al*. Chromatin-remodeling components of the BAF complex facilitate reprogramming. *Cell* **141**: 943–955 (2010)

Singleton, M. R., *et al.* Structure of the single-strand annealing domain of human RAD52 protein. *PNAS* **99**: 13492-13497 (2002)

Sirinakis, G., *et al.* The RSC chromatin remodelling ATPase translocates DNA with high force and small step size. *EMBO J.* 2011 **30**: 2364-2372 (2011)

Sjogren, C., and Nasmyth, K. Sister chromatid cohesion is required for postreplicative double-strand break repair in *Saccharomyces cerevisiae*. *Curr. Biol.* **11**: 991-995 (2001)

Skibbens, R. V., *et al.* Ctf7p is essential for sister chromatid cohesion and links mitotic chromosome structure to the DNA replication machinery. *Genes. Dev.* **13**: 307-319 (1999)

Skibbens, R. V. Holding your own: establishing sister chromatid cohesion. *Genome Res.* **10**: 1664-1671 (2000)

Skibbens, R. V. Sticking a fork in cohesion – it's not done yet! *Trends Genet.* **27**: 499-506 (2011)

Skiniotis, G., *et al.* Acetylated histone tail peptides induce structural rearrangements in the RSC chromatin remodeling complex. *J. Biol. Chem.* **282:** 20804–20808 (2007)

Slupianek, A., *et al.* Targeting RAD51 phosphotyrosine-315 to prevent unfaithful recombination repair in BCR-ABL1 leukemia. *Blood* **118**: 1062-1068 (2011)

Smith, B. C., Denu, J. M. Chemical mechanisms of histone lysine and arginine modifications. *Biochim. Biophys. Acta.* **1789**: 45–57 (2009)

Smith, J., and Rothstein, R. An allele of RFA1 suppresses RAD52-dependent double-strand break repair in Saccharomyces cerevisiae. *Genetics* 1999 **151**: 447-458 (1999)

Smith, M. E., *et al*. Therapeutically targeting cyclin D1 in primary tumors arising from loss of Ini1. *PNAS* **108**: 319–324 (2011)

Smith, S., *et al.* Tankyrase, a poly(ADP-ribose) polymerase at human telomeres. *Science* **282**: 1484-1487 (1998)

Smith, S., and de Lange, T. Tankyrase promotes telomere elongation in human cells. *Curr. Biol.* **10**: 1299-1302 (2000)

Solomon, D. A., *et al.* Mutational inactivation of *STAG2* causes aneuploidy in human cancer. *Science* **333**: 1039-1043 (2011)

Solomon, D. A., *et al.* Frequent truncating mutations of *STAG2* in bladder cancer. *Nature Genet.* **45**: 1428-1430 (2013)

Song, B., and Sung, P. Functional interactions among yeast Rad51 recombinase, Rad52 mediator, and replication protein A in strand exchange. *J. Biol. Chem.* **275**: 15895-15904 (2000)

Song, J., *et al.* Cohesin acetylation promotes sister chromatid cohesion only in association with the replication machinery. *J. Biol. Chem.* **287**: 34325-34336 (2012)

Sonoda, E., *et al.* Rad51-deficient vertebrate cells accumulate chromosomal breaks prior to cell death. *EMBO J.* **17**: 598-608 (1998)

Sonoda, E., *et al.* Scc1/Rad21/Mcd1 is required for sister chromatid cohesion and kinetochore function in vertebrate cells. *Dev. Cell* **1**: 759-770 (2001)

Sotillo, R., *et al.* Mad2 overexpression promotes aneuploidy and tumorigenesis in mice. *Cancer Cell* **11**: 9–23 (2007)

Soutoglou, E., *et al.* Positional stability of single double-strand breaks in mammalian cells. *Nat. Cell Biol.* **9**: 675–682 (2007)

Soutourina, J., *et al.* Rsc4 connects the chromatin remodeler RSC to RNA polymerases. *Mol. Cell Biol.* **26**: 4920–4933 (2006)

Spencer, F., *et al.* Mitotic chromosome transmission fidelity mutants in *Saccharomyces cerevisiae. Genetics* **124**: 237-249 (1990)

Spencer, J., *et al.* Click JAHAs: conformationally restricted ferrocene-based histone deacetylase inhibitors. *Med. Chem. Commun.* **3**: 61-64 (2012)

Spycher, C., *et al.* Constitutive phosphorylation of MDC1 physically links the MRE11-RAD50-NBS1 complex to damaged chromatin. *J. Cell Biol.* **181**: 227-240 (2008)

Srinivasen, S. V., *et al.* RB loss promotes aberrant ploidy by deregulating levels and activity of DNA replication factors. *J. Biol. Chem.* **282**: 23867-23877 (2007)

Stevaux, O., and Dyson, N. J. A revised picture of the E2F transcriptional network and RB function. *Curr. Op. Cell Biol.* **14:** 684-691 (2002)

Stracker, T. H., and Petrini, J. H. The MRE11 complex: starting from the ends *Nat. Rev. Mol. Cell Biol.* **12:** 90–103 (2011)

Strahl, B. D., and Allis, C. D. The language of covalent histone modifications. *Nature* **403**: 41–45 (2000)

Stransky, N., *et al.* The mutational landscape of head and neck squamous cell carcinoma. *Science* **333**: 1157–1160 (2011)

Strobeck, M. W., *et al*. The BRG-1 subunit of the SWI/SNF complex regulates CD44 expression. *J. Biol. Chem.* **276**: 9273–9278 (2001)

Strubbe, G., *et al.* Polycomb purification by *in vivo* biotinylation tagging reveals cohesin and Trithorax group proteins as interaction partners. *PNAS* **108**: 5572-5577 (2011)

Strunnikov, A. V., *et al.* CEP3 encodes a centromere protein of Saccharomyces cerevisiae. *J. Cell Biol.* **128**: 749-760 (1995)

Stucki, M., *et al.* MDC1 directly binds phosphorylated histone H2AX to regulate cellular responses to DNA double-strand breaks. *Cell* **123**: 1213-1226 (2005)

Su, D., *et al.* Structural basis for recognition of H3K56-acetylated histone H3–H4 by the chaperone Rtt106. *Nature* **483**: 104–107 (2012)

Sugiyama, T., *et al.* DNA annealing by RAD52 protein is stimulated by specific interaction with the complex of replication protein A and single-stranded DNA. *PNAS* **95**: 6049-6054 (1998)

Sullivan, B. A., and Karpen, G. H. Centromeric chromatin exhibits a histone modification pattern that is distinct from both euchromatin and heterochromatin. *Nat. Struct. Mol. Biol.* 2004 **11**: 1076-1083 (2004)

Sumara, I., *et al.* Characterization of vertebrate cohesin complexes and their regulation in prophase. *J. Cell Biol.* **151**: 749-762 (2000)

Sun, W., *et al.* The FANCM ortholog Fml1 promotes recombination at stalled replication forks and limits crossing over during DNA double-strand break repair. *Mol. Cell* **32**: 118-128 (2008)

Sun, Y., *et al.* A role for the Tip60 histone acetyltransferase in the acetylation and activation of ATM. *PNAS* **102**: 13182-13187 (2005)

Sun, Y., *et al.* Histone H3 methylation links DNA damage detection to activation of the tumour suppressor Tip60. *Nat. Cell Biol.* **11**: 1376-1382 (2009)

Sun, Z., *et al.* Rad53 FHA domain associated with phosphorylated Rad9 in the DNA damage checkpoint. *Science* **281**: 272-274 (1998)

Sung, P. Yeast Rad55 and Rad57 proteins form a heterodimer that functions with replication protein A to promote DNA strand exchange by Rad51 recombinase. *Genes Dev.* **11**: 1111-1121 (1997)

Sung, P., *et al.* Rad51 recombinase and recombination mediators. *J. Biol. Chem.* **278**: 42729-42732 (2003)

Sutani, T., *et al.* Budding yeast Wpl1 (Rad61)-Pds5 complex counteracts sister chromatid cohesion-establishing reaction. *Curr. Biol.* **19**: 492-497

Sy, S. M., *et al.* PALB2 regulates recombinatorial repair through chromatin association and oligomerization. *J. Biol. Chem.* **284**: 18302-18310 (2009)

Symington, L. S., and Gautier, J. Double-strand break end resection and repair pathway choice. *Annu. Rev. Genet.* **45**: 247-271 (2011)

Takahashi, T. S., *et al.* Recruitment of *Xenopus* Scc2 and cohesin to chromatin requires the pre-replication complex. *Nat. Cell Biol.* **6**: 991-996 (2004)

Tamkun, J. W., *et al*. brahma: a regulator of *Drosophila* homeotic genes structurally related to the yeast transcriptional activator SNF2/SWI2. *Cell* **68**: 561–572 (1992)

Tanaka, K., *et al.* Establishment and maintenance of sister chromatid cohesion in fission yeast by a unique mechanism. *EMBO J.* **20**: 5779-5790 (2001)

Tang, J., *et al*. Acetylation limits 53BP1 association with damaged chromatin to promote homologous recombination. *Nature Struct. Mol. Biol.* **20**: 317–325 (2013)

Tedeschi, A., *et al.* Wapl is an essential regulator of chromatin structure and chromosome segregation. *Nature* **501**: 564-568 (2013)

Terret, M. E., *et al.* Cohesin acetylation speeds the replication fork. *Nature* **462**: 231-234 (2009)

Thomas, G. V., *et al.* Hypoxia-inducible factor determines sensitivity to inhibitors of mTOR in kidney cancer. *Nature Med.* **12**: 122–127 (2006)

Thompson, S. L., and Compton, D. A. Examining the link between chromosomal instability and aneuploidy in human cells. *J. Cell Biol.* **180**: 665-672 (2008)

Thorslund, T., and West, S. C. BRCA2: a universal recombinase regulator. *Oncogene* **26**: 7720-7730 (2007)

Titus, L. C., *et al.* Members of the RSC chromatin-remodeling complex are required for maintaining proper nuclear envelope structure and pore complex localization. *Mol. Biol. Cell* **21**: 1072-1087 (2010)

Torrance, C. J., *et al.* Use of isogenic human cancer cells for high-throughput screening and drug discovery. *Nature Biotech.* **19**: 940–945 (2001)

Torres, E. M., *et al.* Effects of aneuploidy on cellular physiology and cell division in haploid yeast. *Science* **317**: 916-924 (2007)

Torres, E. M., *et al.* Aneuploidy: cells losing their balance. *Genetics* **179**: 737-746 (2008)

Torres, E. M., *et al.* Thoughts on aneuploidy. *Cold Spring Harb. Symp. Quant. Biol.* **75:** 445-451 (2010)

Tóth, A., *et al.* Yeast cohesin complex requires a conserved protein, Eco1p (Ctf7), to establish cohesion between sister chromatids during DNA replication. *Genes Dev.* **13**: 320-333 (1999)

Toyoda, Y., and Yanagida, M. Coordinated requirements of human Topo II and cohesin for metaphase centromere alignment under Mad2-dependent spindle checkpoint surveillance. *Mol. Biol. Cell* **17**: 2287-2302 (2006)

Trickey, M., *et al.* The anaphase-promoting complex/cyclosome controls repair and recombination by ubiquitylating Rhp54 in fission yeast. *Mol Cell Biol.* **28**: 3905-3916 (2008)

Trotter, K. W., and Archer, T. K. Reconstitution of glucocorticoid receptor-dependent transcription in vivo. *Mol. Cell Biol.* **24**: 3347–3358 (2004)

Trotter, K. W., and Archer, T. K. The BRG1 transcriptional coregulator. *Nucl. Recept. Signal.* **6**: e004 (2008)

Trouche, D., *et al.* RB and hbrm cooperate to repress the activation functions of E2F1. *PNAS* **94**: 11268-73 (1997)

Trujillo, K. M., *et al.* Nuclease activities in a complex of human recombination and DNA repair factors Rad50, Mre11, and p95. *J. Biol. Chem.* **273**: 21447-21450 (1998)

Trujillo, K. M., and Sung, P. DNA structure-specific nuclease activities in the Saccharomyces cerevisiae Rad50*Mre11 complex. *J. Biol. Chem.* **276**: 35458-35464 (2001)

Trujillo, K. M., *et al.* Yeast xrs2 binds DNA and helps target rad50 and mre11 to DNA ends. *J. Biol. Chem.* **278**: 48957-48964 (2003)

Tsaber, M., and Haber, J. E. Chromatin modifications and chromatin remodeling during DNA repair in budding yeast. *Curr. Opin. Genet. Dev.* **23**: 166-173 (2013)

Tsikitis, M., *et al.* Genetic ablation of Cyclin D1 abrogates genesis of rhabdoid tumors resulting from Ini1 loss. *PNAS* **102**: 12129–12134 (2005)

Tsuchiya, E., *et al.* The *Saccharomyces cerevisiae* NPS1 gene, a novel CDC gene which encodes a 160 kDa nuclear protein involved in G2 phase control. *EMBO J.* **11:** 4017–4026 (1992)

Turcotte, S., *et al.* A molecule targeting VHL-deficient renal cell carcinoma that induces autophagy. *Cancer Cell* **14**: 90–102 (2008)

Tutt, A., *et al.* Oral poly(ADP-ribose) polymerase inhibitor olaparib in patients with BRCA1 or BRCA2 mutations and advanced breast cancer: a proof-of-concept trial. *Lancet* **376**: 235–244 (2010)

Unal, E., *et al.* DNA damage response pathway uses histone modification to assemble a double-strand break-specific cohesin domain. *Mol. Cell* **16**: 991-1002 (2004)

Unal, E., *et al.* A molecular determinant for the establishment of sister chromatid cohesion. *Science* **321**: 566-569 (2008)

Uringa, E. J., *et al.* RTEL1 contributes to DNA replication and repair and telomere maintenance. *Mol. Biol. Cell* **23**: 2782–2792 (2012)

Valenzuela-Fernández, A., *et al.* HDAC6: a key regulator of cytoskeleton, cell migration and cell-cell interactions. *Trends Cell Biol.* **18**: 291-297 (2008)

VanDemark, A. P., *et al.* Autoregulation of the rsc4 tandem bromodomain by gcn5 acetylation. *Mol. Cell* **27**: 817-28 (2007)

Van Dyck, E., *et al.* Visualization of recombination intermediates produced by RAD52-mediated single-strand annealing. *EMBO Rep.* **2**: 905-909 (2001)

Van Hooser, A. A., *et al.* Specification of kinetochore-forming chromatin by the histone H3 variant CENP-A. J. Cell Sci. **114**: 3529–3542 (2001)

Van Kome, S., *et al.* Functional cross-talk among Rad51, Rad54, and replication protein A in heteroduplex DNA joint formation. *J. Biol. Chem.* **277**: 43578-43587 (2002)

Vannier, J-B., *et al.* RTEL1 dismantles T loops and counteracts telomeric G4-DNA to maintain telomere integrity. *Cell* **149**: 795–806 (2012)

Vannier, J-B., *et al.* RTEL1 is a replisome-associated helicase that promotes telomere and genome-wide replication. *Science* **342:** 239–242 (2013)

Vannier, J-B., *et al.* RTEL1: functions of a disease-associated helicase. *Trends Cell Biol.* (in press) (2014)

van Steensel, B., and de Lange, T. Control of telomere length by the human telomeric protein TRF1. *Nature* **385**: 740-743

van t' Veer, L. J., *et al.* Gene expression profiling predicts clinical outcome of breast cancer. *Nature* **415**: 530-536 (2002)

Varela, I., *et al.* Exome sequencing identifies frequent mutation of the SWI/SNF complex gene *PBRM1* in renal carcinoma. *Nature* **469:** 539-542 (2011)

Vaur, S., *et al.* Pds5 promotes cohesin acetylation and stable cohesin-chromosome interaction. *EMBO Rep.* **13**: 645-652 (2012)

Veaute, X., *et al.* The Srs2 helicase prevents recombination by disrupting Rad51 nucleoprotein filaments. *Nature* **423**: 309–312 (2003)

Venkatesh, S., *et al.* Set2-mediated histone H3 lysine36 methylation suppresses histone exchange on transcribed genes. *Nature* **489**: 452-455 (2012)

Verdaasdonk, J. S., and Bloom, K. Centromeres: unique chromatin structures that drive chromosome segregation. *Nat. Rev. Mol. Cell Biol.* **12**: 320-332 (2011)

Vermeulen, M., *et al.* Selective anchoring of TFIID to nucleosomes by trimethylation of histone H3 lysine 4. *Cell* **131**: 58–69 (2007)

Versteege, I., *et al.* A key role of the hSNF5/INI1 tumour suppressor in the control of the G1-S transition of the cell cycle. *Oncogene* **21**: 6403-6412 (2002)

Ververis, K., *et al.* Histone deacetylase inhibitors (HDACIs): multitargeted anticancer agents. *Biologics* **7**: 47-60 (2013)

Vries, R.G., *et al*. Snf5 tumor suppressor couples chromatin remodelling, checkpoint control, and chromosomal stability. *Genes Dev.* **19:** 665-670 (2005)

Wagener, N., *et al*. The enhancer of zeste homolog 2 gene contributes to cell proliferation and apoptosis resistance in renal cell carcinoma cells. *Int. J. Cancer* **123**: 1545–1550 (2008)

Wagner, J. M., and Karnitz, L. M. Cisplatin-induced DNA damage activates replication checkpoint signaling components that differentially affect tumor cell survival. *Mol. Pharmacol.* **76**: 208-214 (2009)

Walter, W., *et al.* 14-3-3 interaction with histone H3 involves a dual modification pattern of phosphoacetylation. *Mol. Cell Biol.* **28**: 2840–2849 (2008)

Wang, F., *et al.* Histone H3 Thr-3 phosphorylation by Haspin positions Aurora B at centromeres in mitosis. *Science* **330**: 231–235 (2010)

Wang, F., *et al.* A positive feedback loop involving Haspin and Aurora B promotes CPC accumulation at centromeres in mitosis. *Curr. Biol.* **21**: 1061-1069 (2010)

Wang, F., *et al.* Haspin inhibitors reveal centromeric functions of Aurora B in chromosome segregation. *J. Cell Biol.* **199**: 251-268 (2012)

Wang, K., *et al.* Exome sequencing identifies frequent mutation of ARID1A in molecular subtypes of gastric cancer. *Nat. Genet.* **43**: 1219–1223 (2011)

Wang, L., *et al.* SF3B1 and other novel cancer genes in chronic lymphocytic leukemia. *N. Engl. J. Med.* **365**: 2497–2506 (2011)

Wang, S. W., *et al.* Involvement of *Schizosaccharomyces pombe* Srs2 in cellular responses to DNA damage. *Nucleic Acids Res.* **29**: 2963–2972 (2001)

Wang, Z., *et al.* Polybromo protein BAF180 functions in mammalian cardiac chamber maturation. *Genes Dev.* **18**: 3106-3116 (2004)

Walker, J. R., *et al.* Structure of the Ku heterodimer bound to DNA and its implications for double-strand break repair. *Nature* **412**: 607–614

Walter, M. J., *et al.* Acquired copy number alterations in adult acute myeloid leukemia genomes. *PNAS* **106**: 12950-12952 (2009)

Watrin, E., and Peters, J. M. The cohesin complex is required for the DNA damage-induced G2/M checkpoint in mammalian cells. *EMBO J.* **28**: 2625-2635 (2009)

Weaver, B. A., *et al.* Aneuploidy acts both oncogenically and as a tumor suppressor. *Cancer Cell.* **11**: 25-36 (2007)

Weitzer, S., *et al.* A model for ATP hydrolysis-dependent binding of cohesin to DNA. *Curr. Biol.* **13**: 1930-1940 (2003)

Welch, J. S., *et al.* The origin and evolution of mutations in acute myeloid leukemia. *Cell* **150**: 264-278 (2012)

Wendt, K. S., and Peters, J. M. How cohesin and CTCF cooperate in regulating gene expression. *Chromosome Res.* **17**: 201-214 (2009)

Weterings, E., and van Gent, D. C. The mechanism of non-homologous end-joining: a synopsis of synapsis. *DNA Repair* **3**: 1425–1435 (2004)

Whelan, G., *et al.* Cohesin acetyltransferase Esco2 is a cell viability factor and is required for cohesion in pericentric heterochromatin. *EMBO J.* **31**: 71-82 (2012)

Wiegand, K. C., *et al.* ARID1A mutations in endometriosis-associated ovarian carcinomas. *N. Engl. J. Med.* **363**: 1532–1543 (2010)

Williams, B. R., *et al.* Aneuploidy affects proliferation and spontaneous immortalization in mammalian cells. *Science* **322**: 703-709 (2008)

Williams, G. J., *et al.* Structural insights into NHEJ: Building up an integrated picture of the dynamic DSB repair super complex, one component and interaction at a time. *DNA Repair* (in press) (2014)

Williams, R. S., *et al.* Mre11-Rad50-Nbs1 is a keystone complex connecting DNA repair machinery, double-strand break signaling, and the chromatin template *Biochem. Cell Biol.* **85**: 509–520 (2007)

Wilson, B., *et al.* The RSC chromatin remodeling complex bears an essential fungal-specific protein module with broad functional roles. *Genetics* **172**: 795-809 (2006)

Wilson, B. G, *et al.* Epigenetic antagonism between polycomb and SWI/SNF complexes during oncogenic transformation. *Cancer Cell* **18**: 316–328 (2010)

Wilson, B. G., and Roberts, C. W. SWI/SNF nucleosome remodellers and cancer. *Nat. Rev. Cancer* **11**: 481-92 (2011)

Wilson, T. E., *et al.* Yeast DNA ligase IV mediates non-homologous DNA end joining. *Nature* **388**: 495-498 (1997)

Winter, S., *et al.* 14-3-3 proteins recognize a histone code at histone H3 and are required for transcriptional activation. *EMBO J.* **27**: 88–99 (2008)

Wong, M. C., *et al. RSC2*, encoding a component of the RSC nucleosome remodeling complex, is essential for 2 micron plasmid maintenance in *Saccharomyces cerevisiae. Mol. Cell Biol.* **22:** 4218-4219 (2002)

Wooster, R., *et al.* Localization of a breast cancer susceptibility gene, *BRCA2,* to chromosome 13q12-13. *Science* **265**: 2088-2090 (1994)

Worth, C. L., *et al.* SDM: a server for predicting effects of mutations on protein stability and malfunction. *Nucleic Acids Res.* **39**: W215-W222 (2011)

Wrensch, M., *et al.* Variants in the CDKN2B and RTEL1 regions are associated with high-grade glioma susceptibility. *Nature Genet.* **41**: 905-908 (2009)

Wu, J. I., *et al.* Understanding the words of chromatin regulation. *Cell* **136**: 200–206 (2009)

Wu, L., and Hickson, I. D. The Bloom's syndrome helicase suppresses crossing over during homologous recombination. *Nature* **426**: 870-874 (2003)

Wu, L., *et al.* MDC1 regulates intra-S-phase checkpoint by targeting NBS1 to DNA double-strand breaks. *PNAS* **105:** Proc Natl Acad Sci U S A. 2008 Aug 12;105(32):11200-5 (2008)

Wu, P. Y., *et al.* Structural and functional interaction between the human DNA repair proteins DNA ligase IV and XRCC4. *Mol. Cell Biol.* **29**: 3163–3172 (2009)

Wu, X., *et al.* Microcephalin regulates BRCA2 and Rad51-associated DNA double-strand break repair. *Cancer Res.* **69**: 5531-5536 (2009)

Wyman, C., and Kanaar, R. DNA double-strand break repair: all's well that ends well. *Annu. Rev. Genet.* **40**: 363-383 (2006)

Xia, B., *et al.* Control of BRCA2 cellular and clinical functions by a nuclear partner, PALB2. *Mol. Cell* **22**: 719-729 (2006)

Xia, W. *et al.* 2008. BAF180 Is a Critical Regulator of p21 Induction and a Tumor Suppressor Mutated in Breast Cancer. *Cancer Res.* **68:** 1667-1674

Xiao, A., *et al.* WSTF regulates the H2A.X DNA damage response via a novel tyrosine kinase activity. *Nature* **457**: 57-62 (2009)

Xu, H., *et al.* Rad21-cohesin haploinsufficiency impedes DNA repair and enhances gastrointestinal radiosensitivity in mice. *PLoS One* **5**: e12112 (2010)

Xu, H., *et al.* Can corruption of chromosome cohesion create a conduit to cancer? *Nat. Rev. Cancer* **11**: 199-210 (2011)

Xue, Y., *et al.* The Human SWI/SNF-B chromatin-remodeling complex is related to yeast Rsc and localizes to kinetochores of mitotic chromosomes. *PNAS* **97:** 13015-13020 (2000)

Yan, Z., *et al*. BAF250B-associated SWI/SNF chromatin-remodeling complex is required to maintain undifferentiated mouse embryonic stem cells. *Stem Cells* **26**: 1155–1165 (2008)

Yang, H., *et al.* BRCA2 function in DNA binding and recombination from a BRCA2-DSS1-ssDNA structure. *Science* **297**: 1837-1848 (2002)

Yang, W., and Woodgate, R. What a difference a decade makes: insights into translesion DNA synthesis. *PNAS* **104**: 15591–15598 (2007)

Yang, X. J., and Seto, E. The Rpd3/Hda1 family of lysine deacetylases: from bacteria and yeast to mice and men. *Nat. Rev. Mol. Cell Biol.* **9**: 206-18 (2008)

Yang, Y., *et al.* TDRD3 is an effector molecule for arginine-methylated histone marks. *Mol. Cell* **40**: 1016–1023 (2010)

Yannone, S. M., *et al.* Coordinate 5' and 3' endonucleolytic trimming of terminally blocked blunt DNA double-strand break ends by Artemis nuclease and DNA-dependent protein kinase. *Nucleic Acids Res*. **36**: 3354-3365 (2008)

Yano, K., *et al.* Ku recruits XLF to DNA double-strand breaks. *EMBO Rep*. **9**: 91–96 (2008)

Yano, K., *et al.* Molecular mechanism of protein assembly on DNA double-strand breaks in the non-homologous end-joining pathway. *J. Radiat. Res.* **50**: 97–108 (2009)

Yano, K., *et al.* Functional significance of the interaction with Ku in DNA double-strand break recognition of XLF. *FEBS Lett.* **585**: 841–846 (2011)

Yasui, Y., *et al.* Autophosphorylation of a newly identified site of Aurora-B is indispensable for cytokinesis. *J. Biol. Chem.* **279**: 12997-13003 (2004)

Yata, K., *et al.* Plk1 and CK2 act in concert to regulate rad51 during DNA double strand break repair. *Mol. Cell* **45**: 371-383 (2012)

Yazdi, P. T., *et al.* SMC1 is a downstream effector in the ATM/NBS1 branch of the human S-phase checkpoint. *Genes Dev.* **16**: 571-582 (2002)

Yokoyama, H., *et al.* Preferential binding to branched DNA strands and strand-annealing activity of the human Rad51B, Rad51C, Rad51D and Xrcc2 protein complex. *Nucleic Acids Res.* **32**: 2556-2565 (2004)

Young, A. C., *et al.* Analysis of *VHL* gene alterations and their relationship to clinical parameters in sporadic conventional renal cell carcinoma. *Clin. Cancer Res.* **15**: 7582–7592 (2009)

Yuan, Z. M., *et al.* Regulation of Rad51 function by c-Abl in response to DNA damage. *J. Biol. Chem.* **273**: 3799-3802 (1998)

Yuen, K. W. Y., *et al.* Rapid de novo centromere formation occurs independently of heterochromatin protein 1 in *C. elegans* embryos. Curr. Biol. **21**: 1800–1807 (2011)

Zeitlin, S. G., *et al.* CENP-A is phosphorylated by Aurora B kinase and plays an unexpected role in completion of cytokinesis. *J. Cell Biol.* **155**: 1147–1157 (2001)

Zeng, L., *et al.* Mechanism and regulation of acetylated histone binding by the tandem PHD finger of DPF3b. *Nature* **466**: 258–262 (2010)

Zhang, B., *et al.* Mice lacking sister chromatid cohesion protein PDS5B exhibit developmental abnormalities reminiscent of Cornelia de Lange syndrome. *Development* **134**: 3191-3201 (2007)

Zhang, B., *et al.* Dosage effects of cohesin regulatory factor PDS5 on mammalian development: implications for cohesinopathies. *PLoS One* **4**: e5232

Zhang, J., *et al.* Acetylation of Smc3 by Eco1 is required for S-phase sister chromatid cohesion in both human and yeast. *Mol. Cell* **31**: 143-151

Zhang, J. L., *et al.* Acetylation of Smc3 by Eco1 is required for S phase sister chromatid cohesion in both human and yeast. *Mol. Cell* **31**: 143-151 (2008)

Zhang, N., *et al.* Overexpression of separase induces aneuploidy and mammary tumourigenesis. *PNAS* **105**: 13033-13038 (2008)

Zhang, Q., *et al.* Biochemical profiling of histone binding selectivity of the yeast bromodomain family. *PLoS ONE* **5**: e8903 (2010)

Zhang, W., *et al.* Assembly of drosophila centromeric nucleosomes requires CID dimerization. *Mol. Cell* **45**: 263–269 (2012)

Zhang, Y., *et al.* DNA translocation and loop formation mechanism of chromatin remodeling by SWI/SNF and RSC. *Mol. Cell* **24**: 559–568 (2006)

Zhang, Y., *et al.* Attenuated DNA damage repair by trichostatin A through BRCA1 suppression. *Radiat. Res.* **168**: 115–124 (2007)

Zhang, Z., *et al.* The three-dimensional structure of the C-terminal DNA-binding domain of human Ku70. *J. Biol. Chem.* **276**: 38231–38236

Zhang, Z., *et al.* Solution structure of the C-terminal domain of Ku80 suggests important sites for protein-protein interactions. *Structure* **12**: 495–502

Zhang, Z. K., *et al*. Cell cycle arrest and repression of cyclin D1 transcription by INI1/hSNF5. *Mol. Cell Biol.* **22**: 5975–5988 (2002)

Zhao, Q., *et al.* PRMT5-mediated methylation of histone H4R3 recruits DNMT3A, coupling histone and DNA methylation in gene silencing. *Nat. Struct. Mol. Biol.* **16**: 304–311 (2009)

Zhao, Y., *et al.* Inhibitors of histone deacetylases target the Rb-E2F1 pathway for apoptosis induction through activation of proapoptotic protein Bim. *PNAS* **102**: 16090–16095 (2005)

Zheng, X. F., *et al.* Processing of DNA structures via DNA unwinding and branch migration by the *S. cerevisiae* Mph1 protein. *DNA repair* **10**: 1034-1043 (2011)

Zhu, Z., *et al.* Sgs1 helicase and two nucleases Dna2 and Exo1 resect DNA double-strand break ends. *Cell* **134**: 981-994 (2008)

Zimmermann, M., *et al.* 53BP1 regulates repair using rif1 to control 5′ end resection. *Science* **399**: 700–704 (2013)

Zlatanova, J., and Thakar, A. H2A.Z: view from the top. *Structure* **16**: 166–179 (2008)

Zou, L., and Elledge, S. J. Sensing DNA damage through ATRIP recognition of RPA-ssDNA complexes. *Science* **300**: 1542-1548 (2003)